# Immobilization of Microorganisms in Suitable Matrices for the Sequestration of Chromium from Industrial Effluents

## THESIS

Submitted in partial fulfillment of

the requirements for the degree of

**DOCTOR OF PHILOSOPHY**

by

**SATHVIKA T**

**ID. No: 2013PHXF0406H**

Under the Supervision of

**Prof. N. RAJESH**

Department of Chemistry

&

**Prof. VIDYA RAJESH**

Department of Biological Sciences


**BIRLA INSTITUTE OF TECHNOLOGY AND SCIENCE, PILANI**

**Hyderabad Campus, Hyderabad, INDIA**

**2018**

**BIRLA INSTITUTE OF TECHNOLOGY & SCIENCE, PILANI**
**Hyderabad Campus, Hyderabad, Telangana**

# CERTIFICATE

This is to certify that the thesis entitled **"Immobilization of Microorganisms in Suitable Matrices for the Sequestration of Chromium from Industrial Effluents"** submitted by **Sathvika .T, ID.No. 2013PHXF0406H** for the award of Ph. D. degree of the Institute embodies the original work done by her under our supervision.

Signature in full of the supervisor : _____

Name in capital block letters : **N. RAJESH**

Designation : **Professor**

**Department of Chemistry**

Date : _____

Signature in full of the co-supervisor : _____

Name in capital block letters : **VIDYA RAJESH**

Designation : **Professor**

**Department of Biological Sciences**

Date : _____

# Acknowledgements

The endless thanks and love goes to the **Supreme divine couple Sri Sri Radha Krishna** for all the mercy and blessings they bestowed onto me, which has enabled me to write this note in my research work.

I owe my sincere gratitude to **Prof. B. N. Jain**, Ex-Vice Chancellor (BITS), **Prof. V.S.Rao**, Ex-Director (BITS-Pilani, Hyderabad Campus), **Prof. Souvik Bhattacharya** (Vice Chancellor (BITS) and **Prof. G Sundar** (Director BITS Pilani Hyderabad Campus) for permitting me to carry out my doctoral work in this campus.

I would like to express my gratitude to my supervisor **Prof. N. Rajesh,** co-Supervisor and **Prof. Vidya Rajesh** for their sincere guidance, encouragement, suggestion and very constructive criticism that has contributed immensely to the evolution of ideas on the subject. This thesis would not have been possible without their support. Under their supervision, it has been a period of intense learning for me not only in scientific arena, but also on a personal level.

I sincerely acknowledge my DAC (doctoral advisory committee) members, **Prof. Ramakrishnan Ganesan** and **Prof. Sankar Ganesh** for their support and valuable scientific suggestions from time to time.

My sincere regards to **Prof. K. Sumithra** and **Prof. Anupam Bhattacharya** (Former Head, Department of Chemistry), **Prof. Manab Chakravarthy** (Head, Department of Chemistry), BITS-Pilani, Hyderabad Campus for providing me the laboratory facilities and valuable suggestions.

I express thanks to **Prof. K.V.G. Chandrasekhar, Dr. Balaji Gopalan** former DRC (Doctoral Research committee) conveners and **Prof. Jayanty Subbalakshmi ,** present

DRC convener , and to all the faculty members of Chemistry Department, BITS Pilani, Hyderabad campus for their help and encouragement in carrying out my research work.

I express thanks to my colleagues **Dr. Santhana Krishna kumar, Dr. Manasi, Jagadeesh Kodali, Arunraj B and Rolly kumari** for their support and maintaining a healthy and cordial environment. I am also thankful to all the **technicians** in Chemistry Department and Central Analytical Laboratory for their co-operation.

Financial assistance from funding sources **Department of Science and Technology (DST-SERB)** New Delhi, India and **BITS Pilani, Hyderabad** is gratefully acknowledged.

Thanks to **Dr. G. Ravi Chandra** Scientist F and Team Leader at CMCT in International Advanced Research Centre for powder metallurgy and new materials (**ARCI), Hyderabad**, **Vimta labs**, **India**, **Surface characterization lab, IIT Kanpur and Sprint testing solutions India,** for their valuable assistance in characterization of the samples.

A special thanks to my family for all their love and encouragement. Words cannot express how grateful I am to my parents **Sri. Mallika** and **Sri. Murali Krishna** and my adorable loving little sister **Susmitha** for all the sacrifices they made on my behalf and who longed to see this achievement come true. My wholehearted thanks to my dearest friend **Puneet Chandran**, Senior research fellow ARCI was the main reason I am into research who provided me moral and emotional support in life and also being outstandingly supportive throughout my research. I would like to thank my well-wishers and dear friends **B.Varalakshmi** and **B.Subramanyam** for their excellent support during my stay at BITS Hyderabad. I would also like to thank all of my friends who supported me in writing, and incented me to strive towards my goal.

**Date:** **SATHVIKA .T**

# Abstract

The rising concern for pollution due to heavy metals has led to the search for improved methods and materials for their detoxification. Chromium, one of the major industrial pollutants is not an exception. Conventional methods such as precipitation, solvent extraction, reverse osmosis etc., are known for the removal of toxic chromium. However, due to their various disadvantages such as sludge formation, solvent disposal and cost factor there is a need to develop newer, cost effective and also environment friendly adsorbents with appropriate modifications so as to increase the adsorption capacity of the metal ions. Natural materials that are available in large quantities or certain waste from agricultural operations have good potential to be used as low cost adsorbents, because of accessibility and environment friendly nature. In this context, the use of microbial cells immobilized in various matrices (such as *Saccharomyces cerevisiae* (Yeast)-cellulose, *Aspergillus*-clay, *Rhizobium*-MWCNT, *Nitrosomonas*-MOF etc.,) offers a viable and cost effective alternative compared to conventional methods of heavy metal decontamination from a variety of industrial effluents. The interdisciplinary approach involving chemistry and biotechnology offers greener solutions to mitigate heavy metal pollution originating from wastewaters.

The thesis begins with an overview of the chromium chemistry which includes its history, occurrence, characteristics, and toxicity. It mainly focuses on recent literature review on the removal of the toxic metal.

The **chapter two** presents the materials and methods used for the work.

The **chapter three** focuses on the developed yeast-matrix combinations divided into two parts :

The **first part** of the work presented in this chapter highlights the convergence of chemistry and biotechnology through the microwave assisted preparation of baker's yeast *(Saccharomyces cerevisiae)* immobilized in glutaraldehyde cross linked cellulose as a novel and green adsorbent for the removal of toxic Cr(VI). Microwave assisted preparation is a new approach to immobilize a microorganism and it ensured that just 200 s was enough for the incorporation of yeast in the biopolymer matrix. The yeast immobilized biopolymer acts as a good host to accommodate the Cr(VI) oxy anion. The hexavalent chromium could be adsorbed effectively at pH 2.5 and the

functional groups present in the microbe and cellulose play a dominant role in the interaction. The proof of concept was established through analytical characterization techniques.

Thermodynamic feasibility, second order kinetics and Langmuir isotherm model authenticates the experimental biosorption data. The yeast impregnated cellulose adsorbent could be regenerated using sodium hydroxide. Yeast and cellulose are non-toxic, inexpensive and easily obtainable and this lucid methodology provides a sustainable alternative for chromium remediation.

The **second part** deals with the immobilization of the same eukaryote (*Saccharomyces cerevisiae* i.e., baker's yeast) in multiwalled carbon nanotubes (MWCNTs) for the effective adsorption of hexavalent chromium. The carboxylic groups were introduced into the MWCNTs during oxidation using potassium permanganate and were subjected to EDC-HOBT coupling to bind with microbial cell surface. The elaborate investigative techniques were used to characterize the developed biosorbents. Experimental variables such as pH, adsorbent dosage, kinetics, isotherms and thermodynamics were investigated and it was observed that the system follows pseudo second order kinetics with a best fit for Langmuir isotherm. Electrostatic interactions between the functional groups in the microbial cell wall and hydrochromate anion at pH 2.0 propel the adsorption mechanism. The lab scale column studies were performed with higher volumes of the Cr(VI) contaminated water. Sodium hydroxide was used as the desorbing agent for reuse of the biosorbents. The sustainable biosorbents show prospects to treat chromium contaminated water.

The **fourth chapter** focuses on fungi immobilized in various matrices.

The **first part** illustrates the isolation of *Aspergillus* species (fungi) from bread and its immobilization in sodium montmorillonite (an inorganic clay material). This biosorbent has good ability to remove toxic Cr(VI) from acidic medium. FTIR, SEM-EDAX, optical imaging and TGA techniques were used to explore the characteristics of the biosorbent before and after Cr(VI) adsorption. Optimum pH and temperature for Cr(VI) biosorption were 2.0 and 30°C, respectively and the kinetics followed the pseudo second order model. The biosorbent

regeneration was accomplished using sodium hydroxide. As a proof of concept, the method was validated in an industrial effluent wastewater sample BCR-715 a certified reference material and an electroplating industry effluent.

The aim of the **second part** in chapter 4 was to investigate the removal of hexavalent chromium from aqueous solution through batch and fixed bed column experiments using a dead biomass of isolated *Aspergillus* fungal species immobilized in epichlorohydrin crosslinked cellulose. Parameters such as pH, isotherms, kinetics and temperature effect were studied with a view to understand the adsorption efficiency. Biomass as low as 0.4 g could adsorb a Cr(VI) concentration of 5 mg $L^{-1}$ completely within 3 hours from an aqueous volume of 30 mL. Optimum pH and temperature for Cr(VI) biosorption were 2.0 and 30°C, respectively. Kinetic studies favour the pseudo second order model. The biosorbent–Cr(VI) interactions were corroborated by FTIR, SEM, EDAX and XPS analysis. Emphasis is laid on various column modelling studies at different bed heights, flowrates, and concentrations of Cr(VI) and the experimental data obtained was in good agreement with Bed Depth Service Time (BDST) model. The synergism of *Aspergillus* and cellulose as a potential biosorbent was also validated in a synthetic mixture of diverse ions and a certified industrial effluent wastewater sample (BCR-715).

**Chapter five** deals with another interesting combination that can be very useful to alleviate heavy metal toxicity. Towards this direction, the potential of endomycorrizhal fungal spores in conjunction with a clay mineral as a novel approach was explored for chromium (VI) adsorption. The immobilization of AMF *(Arbuscular Mycorrhizal fungus)* spores in montmorillonite (in its $Na^+$ form) provides a good platform to adsorb hexavalent chromium. The adsorption was observed at pH 2.0-3.0 involving the electrostatic interaction between the functional groups present in the fungi-clay biosorbent surface and tetraoxohydrochromate (VI) anion. Diverse characterization techniques such as FT-IR, XPS, SEM, confocal microscopy and XRF were used to observe the interaction of chromium with the biosorbent. Batch adsorption studies involving the experimental variables such as pH variation, kinetics, isotherms and thermodynamics were performed. The system followed pseudo second order kinetics obeying monolayer adsorption.

The biosorbent was stable and regenerated for three adsorption-desorption cycles using sodium hydroxide.

**Chapter six** is divided into two parts:

The **first part** deals with the immobilization of a prokaryote (*Rhizobium*) in multiwalled carbon nanotubes (MWCNTs) for the effective removal of hexavalent chromium. The COOH functionalization of MWCNTs was achieved by covalent method using potassium permanganate as the oxidant. The interaction between microbe and MWCNTs was attained using EDC-HOBT coupling. The analytical characterization techniques were used to characterize the developed biosorbent. The batch parameters such as pH, adsorbent dosage, kinetics, isotherms and thermodynamics were optimized. The developed system follows pseudo second order kinetics with a best fit for Langmuir isotherm. The lab scale column studies were conducted to treat higher volumes of the Cr(VI) contaminated water with sodium hydroxide as the desorbing agent for the regeneration of the biosorbent.

The method developed in the **second part** of chapter 6 demonstrates immobilization of *Rhizobium* (isolated from soil) in sodium montmorillonite provides a conducive environment to capture hexavalent chromium. Additionally, various characterization techniques were done to observe the impact of sequestration. The batch parameters such as pH variation, kinetics, isotherms, thermodynamics etc., were studied. Pseudo second order kinetics coupled with a higher regression coefficient value for Freundlich isotherm and a Langmuir adsorption capacity of 22.22 mg $g^{-1}$ was observed for the adsorption process. The adsorption rate was enriched by charge interactions between protonated clay-rhizobium surface and hexavalent chromium ions in acidic medium. The biosorbent was stable and easily recovered using sodium hydroxide. Preliminary column studies were done to test the efficiency of the developed biosorbent at larger volumes in laboratory scale.

Another interesting application was developed in the final part, **chapter seven** of the thesis. In this work a novel biosorbent, *Nitrosomonas* modified Zirconium metal organic framework (MOF) biosorbent is proposed as a sustainable approach for the effective remediation of toxic

hexavalent chromium. Detailed analytical characterization of the synthesized biosorbent was performed using various techniques such as Powder X-ray Diffraction (PXRD), Fourier Transform Infrared (FTIR), X-ray Photoelectron Spectroscopy (XPS), Thermo Gravimetric analysis (TGA), Optical microscopy, Field Emission Scanning Electron Microscopy (FESEM), High Resolution Transmission Electron Microscopy (HRTEM) , surface area and porosity measurements. The developed biosorbent has a surface area of 921 $m^2g^{-1}$. Important batch adsorption parameters such as pH variation, adsorbent dosage, kinetics, isotherms and temperature variation were studied. A multilayer Freundlich adsorption and pseudo second order kinetics drive the exothermic biosorption process. The electrostatic interactions between the biosorbent surface and metal ions aid towards understanding the adsorption mechanism. Laboratory scale column studies were conducted and the regeneration of the biosorbent was done using sodium hydroxide. The validity of the method was tested in a certified reference material BCR-032 (Moroccan rock phosphate) for the removal of total chromium.

**Keywords:** Chromium(VI), *Saccharomyces cerevisiae*, Cellulose, Immobilization, Microwave, Biosorption, *Aspergillus*, Sodium montmorillonite, Ultrasonication, AMF spores, *Rhizobium sp*, MWCNTs, *Nitrosomonas sp*, Zr- Metal Organic Framework (MOF), Analytical characterization, DNA isolation, Polymerase chain reaction, Phylogenetic tree, Adsorption kinetics, isotherms and thermodynamics, column studies, column modeling studies.

# TABLE OF CONTENTS

## Chapter 6

**Chapter 7**



**Chapter 8**

# LIST OF ABBREVIATIONS

| | |
|---|---|
| AAS | Atomic absorption spectrophotometer |
| AER | Adsorbent Exhaustion Rate |
| AMF | Arbuscular Mycorrhizal fungus |
| b | Langmuir constant |
| BCR-032 | Certified reference material (Moroccan phosphate rock) |
| BCR-715 | Certified reference material (Industrial effluent wastewater) |
| BET | Brunauer-Emmett-Teller |
| BJH | Barrett-Joyner-Halenda |
| CEC | Cation Exchange Capacity |
| DMF | Dimethyl Formamide |
| DNA | Deoxyribonucleic Acid |
| EBRT | Empty Bed Residence time |
| EDAX | Energy-dispersive X-ray spectroscopy |
| EDC | 1-Ethyl-3-(3-dimethylaminopropyl)carbodiimide |
| EDS | Energy Dispersive Spectroscopy |
| FESEM | Field emission Scanning Electronic Microscope |
| FT-IR | Fourier transform infrared spectroscopy |
| GO | Graphene oxide |
| HSAB | Hard-Soft Acid Base |
| HOBT | Hydroxybenzotriazole |
| HRTEM | High Resolution Transmission Electron Microscopy |
| IC | Ion Chromatography |
| JCPDS | Joint Committee of Powder Diffraction Standards |
| $K_F$ | Freundlich constant (adsorption capacity) |
| $K_c$ | Equilibrium Constant |

| | |
|---|---|
| $k_{int}$ | Intra-particle diffusion constant |
| MALDI-TOF | Matrix assisted laser desorption ionization time of flight |
| MWCNT | Multiwalled Carbon nanotube |
| n | Adsorption Intensity |
| NaMMT | Sodium Montmorillonite |
| NCIM | National Collection of Industrial microorganisms |
| PCR | Polymerase Chain Reaction |
| PXRD | Powder X-Ray Diffraction |
| PZC | Point of Zero charge |
| $q_o$ | Maximum Adsorption capacity |
| R | Universal Gas Constant |
| $R_L$ | Dimensionless Constant |
| RBH | Rodamine B hydrazide |
| RF | Rhodamine Furfural complex |
| SEM | Scanning Electronic Microscope |
| SPE | Solid Phase Extraction |
| TE | Tris-EDTA |
| TES | Tris-EDTA-sodium dodecyl sulphate |
| TGA | Thermo Gravimetric Analysis |
| USEPA | United States Environmental protection agency |
| Uio-66 | University of Oslo – 66 |
| UV-Vis | Ultraviolet visible |
| XPS | X-Ray Photoelectron Spectroscopy |
| XRF | X-Ray fluorescence Spectroscopy |
| YMA | Yeast Mannitol Agar |
| YEPD | Yeast Extract Peptone Dextrose |
| Zr-MOF | Zr-Metal Organic Framework |

## LIST OF FIGURES

## LIST OF TABLES

# Chapter – 1

# Introduction

The global water crisis is a major issue of this century. Earth, the blue planet is covered largely with water sources of which the potable water sources are quite minimal. [1] The presence of heavy metals such as Cd, Cr, Hg, Cu, Pb, Ni, Zn etc., in the water bodies beyond the tolerance limit is a serious environmental concern.[2,3] In a world-wide environmental quantitative assessment given by Nriagu and Pachyna [4] it was established that human activities play a major role in heavy metal pollution which lead to deleterious effects in the ecological food chain. Complexation of heavy metals with the ligands containing S, N and O donor atoms results in the structural changes of proteins coupled with enzyme inhibition and hydrogen bond breakage, thereby altering the biological mechanisms. [5] Amidst the toxic heavy metals, chromium (Cr) is a major concern because of its varied industrial applications causing harmful effects when released into the environment. [6] Out of the several conventional techniques such as ion exchange, precipitation, liquid-liquid extraction, and membrane based techniques, solid phase extraction (SPE) has been utilized extensively for the removal of various metals[7,8] including chromium. Considering the multiple drawbacks such as higher operational capital costs, use of organic solvents and sludge disposal problems, adsorption techniques provide a more viable and sustainable option for treating wastewaters containing heavy metals. Adsorption can be performed using batch and column methods. The ease of regeneration of the adsorbent and relative cost effectiveness are some of the inherent advantages associated with the process.[9,10] An overview of chromium chemistry and the remediation techniques for chromium sequestration is presented in the following pages.

## 1.1.Chromium Chemistry

### 1.1.1. History, Occurrence and Characteristics of Chromium

Around 200 years ago the French chemist Nicholas-Louis Vanquelin discovered an interesting element in the crocoite ore also known as Siberian red lead, which reflects different colors such as red, yellow, green in its compounds and named as 'Chromium' according to Greek word '*chroma*' meaning colour. [11] With an atomic number 24 chromium is a silvery, shiny, brittle hard metal with a high melting and boiling points as 1857 $^{o}$C and 2672 $^{o}$C respectively. Chromium exists in various oxidation states in the range -2 to + 6 but the trivalent and hexavalent forms are

more predominant. [12] The existence of chromium in earth and universe varies as 15 ppm by mass is found in universe, 20ppm in the sun, 140ppm in the rocks on the earth, 0.6 ppb in sea water, 1ppb in water streams and 30 ppb by mass in humans. The principal ore from which the Cr is extracted is known as chromite ore ($FeCr_2O_4$) which is a blackish silvery white metal and weakly magnetic.[11] The trivalent chromium upon hydrolysis produces various cationic species as $CrOH^{2+}$, $Cr(OH)_2^{+}$, $Cr(OH)_4^{-}$ which are mononuclear, neutral species such as $Cr(OH)_3$, poly nuclear species as $Cr_2(OH)_2$ and $Cr_3(OH)_4^{5-}$ respectively. At pH values less than the $pK_a$ (5.8) of $HCrO_4^{-}$ anion, the hexavalent chromium is present as dichromate and hydrogen chromate oxy anion ($HCrO_4^{-}$). Although the hydrogen chromate oxy anion can exist in equilibrium with dichromate, ($2HCrO_4^{-} \rightleftharpoons Cr_2O_7^{2-} + H_2O$) it is only at pH<2 and high Cr(VI) concentrations, the existence of dichromate anion would be more probable. [13] According to Hard soft acid base (HSAB) principle Cr is a hard acid and it interacts strongly with the hard bases such as nitrogen and oxygen donor ligands.

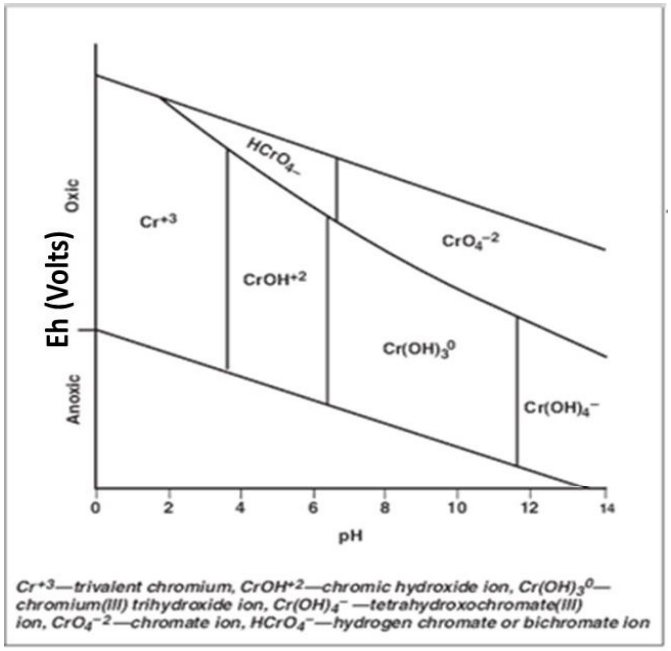


**Figure 1.1** Chromium speciation at varying pH[13]

### 1.1.2. Toxicity of Cr

The appealing orange colour dichromate anion finds extensive application in electroplating, [14] catalyst production, cement industries and the radiant green Cr(III) salts are known for their utility in leather tanning. [15] Chromium alloy coatings (CrAlSiN) are used in high speed machining applications as it enhances the metal resistant properties by encountering oxidation and corrosion.[16] Minimal amount of Cr (III) is required for glucose metabolism in the body which is available in foods such as broccoli, yeast, cheese, cereals etc. Cr(III) has low mobility and solubility whereas most of the Cr(VI) is a man-made carcinogen and its contamination is in limelight because of its high mobility and solubility causing cytotoxicity and genotoxicity.[17] Intracellularly, Cr(VI) undergoes reduction by producing various reaction intermediates such as Cr(V), Cr(IV), reactive oxygen species(ROS), peroxides, radicals and finally to Cr(III) which causes oxidative damage to DNA, proteins and lipids.[18] The chronic exposure to Cr(VI) could also lead to renal, respiratory, gastrointestinal, cardiovascular and haematological ailments.[19] Prolonged exposure causes lung cancer usually observed as an occupational hazard.[20]

As a potent environmental pollutant causing deleterious effects on humans the International Agency for Research on Cancer (IARC) classified Cr(VI) as type I carcinogen.[21] Hence, the United States Environmental Protection Act (USEPA) [22] has stipulated the maximum tolerable level of Cr in drinking water to be 0.05 mg $L^{-1}$ and it is imperative to develop environmentally benign methods to detoxify chromium that is discharged from the industrial effluents.

## 1.2. Remediation methods for Cr(VI)

Common heavy metal contaminated water treatment technologies include ion exchange, adsorption, precipitation, chelation, reverse osmosis, solvent extraction, membrane separation etc..[7,8] The conventional methodology of reducing Cr(VI) to the less hazardous Cr(III) and subsequent precipitation as the green $Cr(OH)_3$ is associated with the problem of sludge handling and further safe disposal. Hence, there is a need to shift the focus towards green and cost effective methods as viable strategies. It is noteworthy to mention here that, in comparison to the chemical adsorbents, biomass immobilized sorbents are more environment friendly. Hence, bio-sorption is regarded as an effective proposition for heavy metal removal as they are cost effective

and further the ample availability of biomass could be utilized to treat larger volume of the liquid waste effluents. [23] Microorganisms possess a high surface area-to-volume ratio and hence offer a good contact interface for heavy metal interaction. [24] Most of the fungi, bacteria and algae have good potential to adsorb heavy metals [25-28] and the ease with which they tolerate higher concentrations renders them metal resistant. [29]

### 1.2.1. Biosorption of heavy metals

Biosorption encompasses the use of living as well as non-living microorganisms. The removal of pollutants by living microorganisms involves principally a metabolism dependent active bioaccumulation process.[30] The bioaccumulation depends on the extra and intracellular processes. The extracellular polysaccharides generated by the microorganism plays an important role in the biosorption using living cells. The utility of living microorganisms is more significant in metabolism dependent processes such as sewage treatment, anaerobic digestion etc. However, there are practical limitations in the application of living organisms for heavy metal removal. This is due to the fact that at higher metal ion concentrations and when requisite amount of metal ions are tolerated by the microorganisms, the metabolism is disturbed leading to the death of the microbes.[31] Hence, with living cells, the biosorption processes are prone to the pH variation and also dependent on the stress response generated by the toxic metal ion. These shortcomings are overcome when non-living microorganisms are used for the removal of metal ions. [31]

The removal of metal ions by non-living microorganisms involves a metabolism independent, passive biosorption mechanism. The binding of metals involves the coordination with the various active chelating functional groups in the cell surface. There are considerable advantages of using dead cells for biosorption over the living cells. In the case of dead cells, the growth of microbe and its application for metal removal are two distinct processes. These can be controlled more effectively thereby increasing the removal of metal ion by the biosorbent. Dead cells can be stored and used over a longer time period and are not affected by the metal toxicity and furthermore an uninterrupted nutrient supply to preserve the microbe is not required. With dead cells, the adsorption parameters such as isotherms, kinetics etc can be studied easily by taking a known weight of the biosorbent. Living cells in the wet condition have larger water content and

are prone to decay over a time period.[32] Hence, non-living microorganisms are easily amenable for surface modification using appropriate matrix support. Therefore, the immobilization of dead microbes onto a suitable support gives higher rigidity and is also effective for column operations to treat a large sample volume, thereby enhancing the ease of regeneration of the biosorbent. [33] The metal microbe interactions in bioremediation is summarized schematically in Fig 1.2.

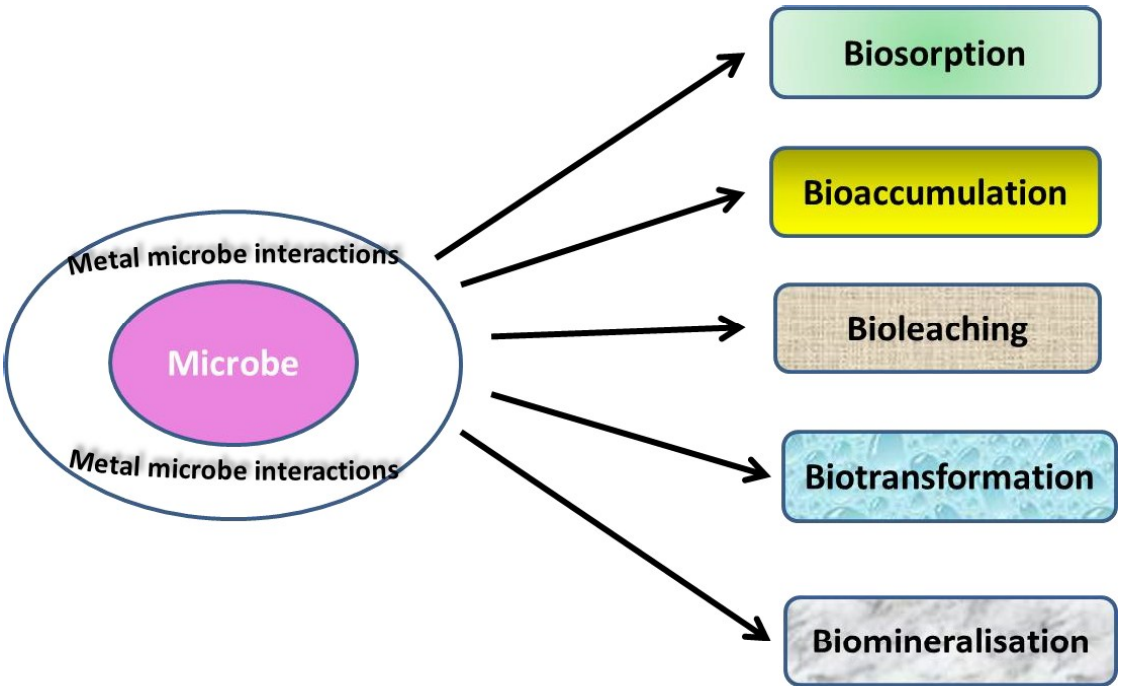


**Figure 1.2** Metal–microbe interactions during bioremediation[34]

### 1.3. Recent literature review on the use of microbes for sequestration of Cr(VI)

Literature reports have suggested that there has been extensive research for the heavy metal removal using microbes. Several organisms are still being tested to remove heavy metals from industrial wastes with higher adsorption capacity. The following microbes in combination with suitable matrices were explored for the removal of Cr(VI) in the current study.

### 1.3.1. *Saccharomyces cerevisiae*

*Saccharomyces cerevisiae* (*S.cerevisiae*) is a eukaryotic unicellular microbe commonly known as baker's yeast is easily available and is known to have broad applications in food industry[35] such as wine making, brewing, baking etc., As *S. cerevisiae* is classified under Generally Recognized as Safe (GRAS) product, it is widely used in industrial water treatment[36] Immobilized yeast cells in a microporous hollow fiber fermenter have been utilized to generate ethanol.[37] Yeast immobilized in delignified cellulose has been used in wine making.[38] Since yeast can be cultivated on a large scale in an inexpensive growth media and the yield obtained would also be very high, yeast is chosen as biosorbent for removal of several heavy metals. Also, it is available in large quantities as a byproduct in many food industries. Krauter et al. studied the removal of Cr(VI) from the ground water by using baker's yeast under aerobic and anaerobic conditions.[39] Ksheminska et al. made a comparative study on sensitivity of the yeast *Pichia guilliermondii*, towards the accumulation of Cr(III) and Cr(VI).[40] The removal of Uranium (VI) by the living and heat killed cells of *S.cerevisiae* was studied by Lu et al. where the adsorption of the metal ions is high in dead cells. [41] Machado et al. have reported the removal of heavy metals by yeast and the competitive effect of inorganic ligands and metal ions present in the electroplating effluents. [42]

### 1.3.2. *Aspergillus sp*

Fungal species are known to have good potential in removing toxic metals such as cadmium, lead, copper, chromium etc. from aqueous medium. *Aspergillus* species finds applications in biotechnological processes such as citric acid production, transformations of progesterone, citral etc. *Aspergillus* is also used to synthesize extracellular enzymes such as amylase, lipase and pectinase and the Food and Drug Administration (FDA) has recognised these enzymes to be safe and non-toxic.[33] The lipase enzymes secreted by *Aspergillus* finds applications as a biocatalyst in various industrial processes such as additives to detergents, synthesis of enantiopure drugs and food ingredients.[43,44] The xylanase enzyme produced by *Aspergillus* is also used for biobleaching. [45]

Filamentous fungi such as *Aspergillus sp* are known for their excellent potential to remediate hexavalent chromium.[46] Pre-treatment of *Aspergillus niger* with CTAB followed by immobilization in a polysulfone matrix[47] gives a biosorption capacity of 3.1 mg $g^{-1}$. A removal efficiency of 29% has been reported using dead mass of the same fungal species.[48] Das et al [49] reported the interaction of chromium with *Aspergillus versicolor* using Atomic force microscopy (AFM), FTIR and Transmission electron microscopy (TEM). The XPS studies revealed that bound Cr was in the form Cr(III) involving adsorption coupled reduction. Mungasavalli et al.[47] reported that the pre-treated *Aspergillus niger* could adsorb chromium effectively with 15.2 mg $g^{-1}$ Langmuir adsorption capacity. It has been reported that the live *Aspergillus niger* shows adsorption capacity for heavy metals such as Pb, Cu and Cd in the range 0.75-2.3 mg $g^{-1}$, while pre-treated and immobilized *Aspergillus niger* in matrices such as polyurethane matrix [50,51] shows adsorption capacities greater than 20 mg $g^{-1}$ indicating it is easy to modify the inactive surface of microbes which enhances the adsorption capacity.

### 1.3.3. Arbuscular Mycorrhal Fungus (AMF) spores

The synergistic association between phycomycetes fungi and plant roots results in the formation of arbuscular mycorrhiza and the spores produced by these fungi are mainly located in the rhizosphere soil. [52,53] Arbuscular mycorrhiza (AMF) is also known to regulate the heavy metal uptake by soya bean (*Glycine max*) depending on the concentration of the heavy metals in the soil. [54] Arbuscular mycorrhizae present in sunflower plants increases the tolerance towards higher chromium concentrations.[55] Gil-Cardesa et al. reported [56] that *Ricinus communis* and *Conium maculatum* used Cr- mycorrhizal stabilisation mechanism for the removal of Cr from soil near an industrial site. During unfavourable conditions, the vegetative cells of the microbes enter the dormant stage of their life cycle as spores and preserve the genetic material. To encounter the environmental stress and to provide mechanical strength, the outer hyaline layer of AMF spore wall is composed of chitin, cellulose and mannan polysaccharides. [57]

### 1.3.4. *Rhizobium sp*

The prokaryotic nitrogen fixing bacteria *Rhizobium* is a symbiotic, rod shaped, gram negative bacteria which is a potential biofertilizer for plants and also helps in biological nitrogen fixation

thereby influencing the agricultural productivity and is used in controlling root rot infections caused by fungi.[58,59] The legumes inoculated with *Rhizobium* inoculants is a common agriculture practice, which is a cost effective process to provide nutrients to the bacteria. Sludge generated from the agro based industries are rich in carbon and nitrogen sources and augments the growth of *Rhizobium* thereby offering a green alternative to treat waste water as well as reducing the cost of inoculant preparation.[60] As per the reports the activated biomass of *Rhizobium leguminosarum* could remove upto 77.3±4.3 % Cr(III) at 35$^{o}$C at pH 7.0.[61] An ND2 *Rhizobium* isolate from the root nodules of *Phaseolus vulgaris* turned out to be a potential biosorbent for Cr(VI) removal as well as promoting the growth properties of plant thereby increasing the agricultural productivity.[62]

### 1.3.5. *Nitrosomonas sp*

Nitrogen is an important and essential component of life on earth and microbial transformations play a major role in its availability to plants through nitrogen cycle. The nitrifying bacteria such as *Nitrosomonas* and *Nitrobacter* play a major role in nitrogen cycle.[63] *Nitrosomonas* is a rod shaped gram negative chemolithotroph which derives its energy by converting ammonia to nitrite. [63] The conversion of ammonia by *Nitrosomonas* is a two-step nitrification process mediated by the enzymes ammonia mono oxygenase (AMO) and hydroxylamine oxido reductase (HAO). Initially AMO converts ammonia to hydroxylamine and subsequently gets converted to nitrite by HAO respectively. *Nitrosomonas* has potential applications in biotechnology such as bioremediation and degradation of halogenated aliphatic hydrocarbons and aromatic compounds.[64]

## 1.4. Recent literature review on the proposed matrices for sequestration of hexavalent chromium

### 1.4.1. Biopolymer based adsorbents

Biopolymers are bio degradable, environment friendly, non-petroleum based materials and serve as excellent solid supports for the heavy metal removal.[65] Cellulose, chitin, chitosan, lignin and lignocellulose are the commonly used biopolymers for the metal ion adsorption. Cellulose is a

natural polysaccharide $(C_6H_{10}O_5)_n$ with inter and intra molecular hydrogen bonding having good stability. It is made up of linear chains of several β(1-4) linked D-glucose units. (Fig 1.3) $I_\alpha$ and $I_\beta$ are the two crystalline forms of native cellulose. The algal and bacterial cellulose is rich in $I_\alpha$ whereas $I_\beta$ is largely present in plants. The hydrophobic nature of cellulose is attributed to the glycosidic bonds. Unmodified or native cellulose has low ability to absorb metals due to the less availability of adsorption sites. Therefore modifications of cellulose such as functionalization or direct immobilization were studied for metal removal. [66,67]

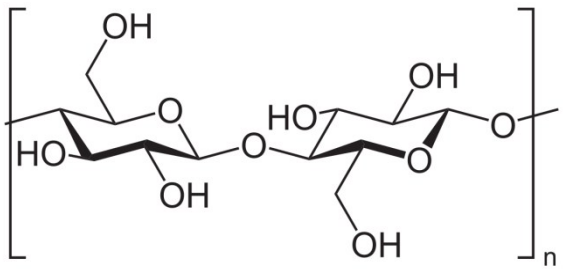


**Figure 1.3.** Structure of Cellulose

The modifications in cellulose can be achieved (i) by altering the backbone of the cellulose by incorporation of metal binding or chelating agents (ii) grafting the polymers chains with chelating ligands. Various metal ions such as Cu(II), Cr(VI), Hg(II), Pd(II) are efficiently adsorbed using chemically modified cellulose by graft copolymerization method using acrylamide, acrylic acid and glycidylmethacrylate . [68,69] The immobilization of ionic liquids onto cellulose is also an interesting application towards the metal detoxification. The metal ions are trapped in the cellulosic layers owing to the interactions between ionic liquid and cellulose.[70,71] Kalidasan et al. developed ionic liquid immobilized in cellulose adsorbents such as the Aliquot 336-cellulose polymer blend[72] and also tertabutylammonium iodide[73] with cellulose to study its potential application in Cr(VI) removal with adsorption capacities 38.94 mg $g^{-1}$ and 16.67 mg $g^{-1}$ respectively.

Chitosan, a nitrogenous polysaccharide is a modified biopolymer synthesized from chitin. It is mainly composed of poly(β-1-4)-2amino-2deoxy-D-glucopyranose (Fig 1.4).[74] Chitosan is produced by the alkaline N-deacetylation of chitin which is widely preset in exoskeleton of crustaceans. Due to the growing need for the new sources of low cost adsorbents, problems on

waste disposal, increasing cost of other adsorbents make chitosan one of the best materials which is biodegradable, abundantly available and of relatively low cost. The presence of functional groups such as amines and hydroxyl groups on the chitosan helps in adsorption/chelation of metal ions and the modifications of chitosan enhanced the metal adsorption capacity.[75] The modifications such as grafting/ crosslinking through crosslinking agents such as glutaraldehyde, epichlorohydrin, enhance the adsorption efficiency of chitosan.[76] The n-butylacrylate grafted chitosan was prepared using microwave by Kumar et al. [77] with a Cr(VI) adsorption capacity of 17.16 mg $g^{-1}$. The crosslinked chitosan was protonated using HCl and was treated to remove Cr(VI) efficiently (191.4 mg $g^{-1}$). [78] Several chitosan based composites such as crosslinked chitosan-bentonite complex,[79] Fe loaded chitosan-carbonized rick husk composite,[80] $Fe_2O_3$ Nanoparticles Encapsulated chitosan beads[81] could remove Cr(VI) and the adsorption capacities were reported to be in the range 88-153 mg $g^{-1}$.

.

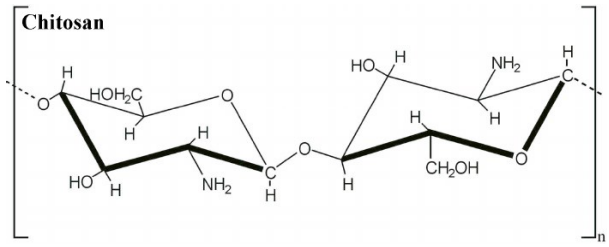


**Figure 1.4.** Structure of chitosan

Some of the recently reported cellulose and chitosan modified adsorbents for Cr(VI) ion removal are tabulated in Table 1.1

**Table 1.1** Cellulose and chitosan based adsorbents for Cr(VI) removal

| Type of adsorbent | pH | Adsorption capacity ($mg\ g^{-1}$) | Reference |
|---|---|---|---|
| n-butylacrylate grafted chitosan | 3.5 | 17.16 | 77 |
| Protonated crosslinked chitosan | 5.0 | 191.4 | 78 |
| $Fe_2O_3$ Nanoparticles Encapsulated chitosan beads | 4.0 | 153.85 | 81 |
| Cellulose-sodium montmorillonite | 3.8-5.5 | 22.2 | 82 |
| Cellulose-magnetite composites | 4.0 | 11.56 | 83 |
| Reticulated chitosan micro/nanoparticles | 2.0 | 124 | 84 |
| Polyethylenimine (PEI) grafted cellulose | 2.0 | 229.1 | 85 |
| Chitosan/MWCNT/$Fe_3O_4$ composite | 2.0 | 335-360.1 | 86 |
| Beta-cyclodextrin–chitosan modified walnut shell biochars | 5.0 | 206 | 87 |
| Heterocyclic modified chitosan | 3.0 | 85.0 | 88 |

### 1.4.2. Clay based adsorbents

Clays are the natural scavengers on earth for many of the pollutants (either anions or cations) involving mechanisms such as ion exchange, adsorption and intercalation. They belong to the class of hydrous aluminosilicates which dominantly compose the colloid fraction of soils, rocks, sediments and water. The perceivable ions present on the clay surface are $Ca^{2+}$, $Mg^{2+}$, $Na^{+}$, $H^{+}$, $K^{+}$, $NH_4^{+}$ and $SO_4^{2-}$, $Cl^{-}$, $PO_4^{3-}$ and $NO_3^{-}$. The ion exchange occurs without affecting the clay structure and the advantages such as large surface area, high cation exchange capacity, layered structure, mechanical and chemical stability to make them as excellent adsorbent materials.[89] Majorly clays are classified under the types 2:1 or 1:1 respectively.

#### (i)1:1 Type clays

These 1:1 clays are composed of single sheets each of aluminium octahedron and silicon tetrahedron such as kaolinite. (Fig 1.5) The absence of isomorphic substitution in either of the sheets leads to chargeless surfaces. Therefore, substitution of cations or anions cannot take place between the sheets except for the water molecules. The two layers are held intact due to the hydrogen bonding between the hydroxyl groups in octahedral sheets and the oxygen in tetrahedral sheets of adjacent layers.

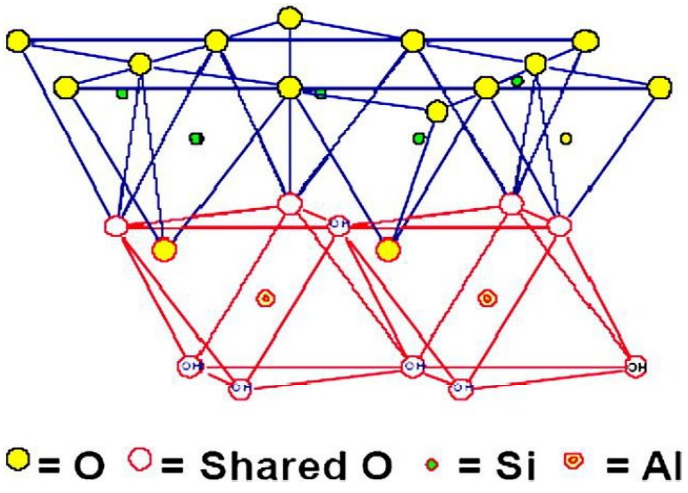


**Figure 1.5.** Structure of kaolinite [89]

**(ii)2:1 Type clays**

These are smectite type of 2:1 clays such as montmorillonite which essentially has two silica tetrahedral sheets and an alumina octahedral sheet. In view of stacking of the layers, Vander Waals gap is evident between the layers and the isomorphic substitution of ions among the tetrahedron and octahedron sheets gives the entire three sheet layer an overall negative charge which is counterbalanced by metal cations such as Na, Mg, Ca, Fe, Li present in the interlayer spacing. [89,90]

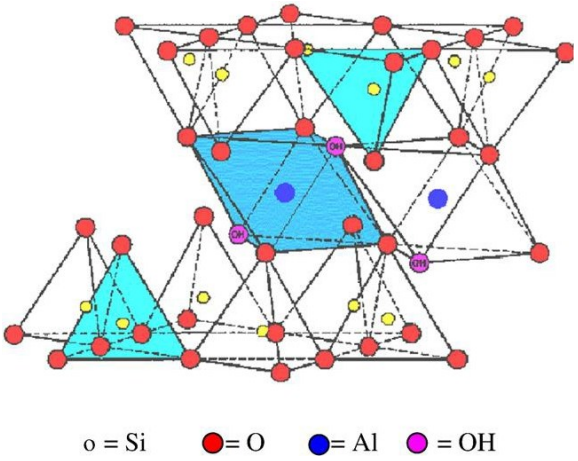


**Figure 1.6.** Structure of Montmorillonite [89]

**Montmorillonite**

Montmorillonite is a 2:1 type of clay with an aluminum tetrahedron sheet sandwiched between two silica octahedral sheets with exchangeable cations which counteract the negative charge produced in the isomorphic substitution. (Fig 1.6) The mechanism of metal removal occurs by ion exchange as well as adsorption. In view of outer sphere complexes by cations such as $Ca^{+2}$, $Na^{+}$, the solute ions are easily exchanged leading to fast kinetics. pH also plays an important role in cation exchange and with increasing pH precipitation of metal ions may occur. The swelling of the interlayers occur when exposed to water where the procedure depends on valences and atomic radii of the exchangeable cations. Due to their large surface area, high cation exchange capacity (CEC), swelling abilities it is widely used in water treatment. The surface modifications of clays and clay composites have received major attention due to diverse applications.[89,90] Chen

et al.[91] developed Chitosan/montmorillonite–$Fe_3O_4$ microspheres by micro emulsion process which has a particle size of 100 μm which has a Cr(VI) removal capacity of 58.82 mg $g^{-1}$. A blend of cellulose-sodium montmorillonite developed by Kumar et al.[82] could remove good amount of Cr(VI). The montmorillonite modified with cetylpyridinium bromide[97] effectively adsorbs Cr(VI) anions over a wide pH range from 3.0 to 6.0. Mg-Al hydrotalcite modified kaolinite clay[92] and a nano composite film of Chitosan/halloysite clay[94] were developed which could remove good amount of Cr(VI). Recently reported literature for the removal of hexavalent chromium from aqueous phase using clay based supports is tabulated below in Table 1.2.

**Table 1.2.** Clay based adsorbents for Cr(VI) removal

| **Adsorbent** | **pH** | **Langmuir adsorption capacity (mg $g^{-1}$)** | **Reference** |
|---|---|---|---|
| Chitosan – sodium montmorillonite –$Fe_3O_4$ microspheres | 5.0 | 58.82 | 91 |
| Cellulose-sodium montmorillonite | 3.8-5.5 | 22.2 | 82 |
| Mg-Al hydrotalcite modified kaolinite clay | 2.5-11.5 | 15.85 | 92 |
| Bentonite clay | 2.0 | 5.9 | 93 |
| Chitosan/halloysite clay Nanocomposite | 3.0 | 142 | 94 |
| Micelle clay complex | 2.0 | 9.43 | 95 |
| Montmorillonite-supported magnetite nanoparticles | 2.0-2.5 | 15.3 | 96 |
| Cetylpyridinium bromide (CPB) modified clay | 3.0-6.0 | 18.05 | 97 |

### 1.4.3. Carbonaceous materials

Several carbonaceous materials such as activated carbon, carbon nanotubes, graphene oxide and their modifications are used in the sequestration of various pollutants. Owing to the excellent properties such as great adsorption capacity, large surface area, low cost, abundant availability, activated carbons (from various sources) are in demand globally mainly because of their use in applications related to their environmental mitigation. The main sources of the commercially activated carbon are coal and agricultural by products.[98] Few recently reported activated carbon and its modification as adsorbents for Cr(VI) are prepared from mango kernel and modified using phosphoric acid could adsorb 7.8 mg $g^{-1}$ of Cr(VI). [99] Labied et al. developed activated carbon from the waste lignocellulosic material which absorbs 62% of hexavalent chromium.[100] As high as 99% of Cr(VI) adsorption was attained by the carbon produced from the *Terminalia* nuts activated with $ZnCl_2$. [98]

Nano- sized materials with their outstanding properties have attracted the attention of scientists and could efficiently be utilized for varied applications. The $sp^2$ hybridized carbon nano tubes (CNT) are one of the interesting forms of elemental carbon categorized into two varieties. The first type is multiwalled carbon nanotubes (MWCNTs) which has concentric rings with a definite spacing between the layers and the second form is single walled carbon nanotubes (SWCNTs) which has a cylindrical single layer. To overcome the hydrophobicity and to improve the hydrophilicity of the surface of CNTs covalent or noncovalent methods are often employed. [101] In covalent surface modification the hydrophilic groups are incorporated exterior to the CNTs sidewalls causing little or more damage. The noncovalent modification is performed by adsorption of surfactants in which there is no damage to the structure and properties of CNTs. The covalent modification is achieved by wet chemical treatment of CNTs with different oxidants such as HCl, $HNO_3$, $H_2SO_4$, $H_2O_2$ and potassium permanganate.[101] The modification enhanced the significant progress properties in the utilization of CNTs for the efficient removal of metal ions and pollutants as they possess large surface area, high mechanical strength, and excellent thermal, electrical properties. [102] Several MWCNTs as adsorbents were developed for the treatment of aqueous solutions contaminated with Cr(VI). Lu et al.[103] developed magnetic $Fe_2O_3$ nanoparticle-MWCNTs composite and was checked for the efficient removal of Cr(VI) at

different temperatures with a $q_{max}$ of 42.02 mg $g^{-1}$ at 35°C. Fe-Ag/functionalized-MWCNT/PES Nanostructured-Hybrid Membranes developed by Machine et al. could remove 94.8% of Cr(VI) from aqueous solution.[104] Chitosan immobilized in nanoparticles and carbon nanotubes by forming a nanocomposite could efficiently remove Cr(VI) up to 84% within a short contact time.[105] Modified magnetic carbon nanotubes developed by Wu et al. could remove hexavalent chromium upto 90% under acidic conditions. [106]

Yet another interesting carbonaceous material, graphene is a layered form of graphite with two dimensional nano structure possessing excellent thermal, mechanical, electrical and chemical properties. Graphene oxide (GO) synthesized from graphite and its modifications were widely for heavy metal sequestration. A novel magnetic graphene oxide-based material DCTA/E/MGO, synthesized by Guo et al. had a high Cr(VI) removal efficiency of 92.27 mg $g^{-1}$. [107] He et al. functionalized GO using 3-aminopropyltriethoxysilane which has a good absorption capacity of 215.2 mg $g^{-1}$ for Cr(VI).[108] $MoS_2$ –rGO composites developed by Jiang et al. have a Langmuir adsorption capacity of 268.82 mg $g^{-1}$ for the metal adsorption.[109] Ethylene diamine-reduced graphene oxide reduced Cr(VI) to Cr(III) was developed by Ma et al. [110] A novel GO- Aliquat-336 developed by Kumar et al.[111] was explored to adsorb Cr(VI) efficiently with a high Langmuir adorption capcity of 287.51 mg $g^{-1}$.

### 1.4.4. Metal Organic Frameworks

Acclaimed for the highly ordered crystalline structure with porous nature, metal organic frameworks (MOF) have emerged as the hybrid class of metal ions and organic ligands in diverse fields. Most of the studies demonstrated that MOFs have overcome the drawbacks involving traditional porous materials such as zeolites, carbonaceous materials in various fields.[112] However the reverse nature of coordination bonds in MOFs lead to lower stability is an important concern. There has been considerable effort to improve the stability of MOFs and in this direction the discovery of Uio-66 (University of Oslo) by Cavka et al. in the year 2008 was remarkable.[113] This Zr based MOF is a cubical framework $Zr_6O_4(OH)_4$ cluster with terephthalic acid as organic linker. The zirconium based MOFs are used widely in several applications due to their good aqueous, acid and thermal stabilities. They have outstanding tunable properties such

as large surface area, high porosity, thermal and chemical stabilities with potential applications in gas storage, drug delivery, sensing, catalysis, ion exchange and separation. [114]

The remediation of pollutants using MOFs reported in the recent times are a fast removal of 2-methyl-4-chlorophenoxy acetic acid (MCPA)[115] by UiO-66-$NH_2$ was achieved in 3 min with an adsorption capacity of 303.3 mg $g^{-1}$. Yin et al. reported the rapid microwave synthesis of Zr-MOF in 3 min and was successfully used for the removal of Pb(II). [116] Nandi et al. developed an ultra-microporous Ni-(4-pyridylcarboxylate)$_2$ MOF with a cubic framework for the selective capture of carbon dioxide and purification of hydrogen.[117] Vellingiri et al.[118] studied the sorption behavior of a mixture of 14 semi volatile and volatile compounds composed of benzene, styrene, toluene, p-xylene, six volatile fatty acids, two indoles and two phenols and concluded that the selected MOFs exhibited strong affinity towards semi volatile compounds. Peng et al. developed a EDTA incorporated MOF trap for the capture of a total of 22 metal ions with 99% removal efficiency. [119] Mehelmy et al. constructed a Uio 66 $NH_2$ and silica gel composite for efficient removal of Cr(VI) with an adsorption efficiency of 277.4 mg $g^{-1}$, [120] IL-MIL-100(Fe) an ionic liquid and iron nano particle modified MOF developed by Nasrollahpur et al. could efficiently remediate Cr (VI) with a 285.71 mg $g^{-1}$ adsorption capacity . [121]

### 1.5. Scope and Objectives of the Work

The foregoing brief review reveals that convergence of biotechnology and chemistry offers greener alternatives in environmental remediation. A systematic literature survey was conducted to understand the latest trends in bio- absorbents. The microbes such as *Saccharomyces cerevisiae*, *Aspergillus sp*, Arbuscular mycorrhizae, *Rhizobium sp*, *Nitrosomonas sp* could either be isolated or procured from the culture collection centers. The isolated biomass was evaluated with respect to the morphological, biochemical and molecular biology techniques which involves morphology, gram staining, motility, 16S rRNA sequencing etc. Suitable quantities of the biomass were grown in appropriate culture media to yield the lyophilized biomass. The immobilization of the above mentioned microbes in solid support matrices such as cellulose, clay, MWCNTs, MOF was achieved by dispersing them in appropriate medium.

The above mentioned microbe-solid support combinations have not been reported for the effective adsorption of hexavalent chromium. The preparation of the biosorbents was carried out using microwave, ultra-sonication and conventional methods. Hexavalent chromium being a hard acid interacts with the functional groups such as amines, hydroxyl and carboxyl groups present on the biosorbent surface thereby effectively fostering electrostatic interaction with hydrochromate anions. The work presented in the following chapters deals with the development of biosorbent using the following steps:

- Isolation and identification of microbes such as yeast, *Aspergillus*, AMF, *Rhizobium* and *Nitrosomonas* from its sources or procuring from the culture collection centers.
- Immobilization of the isolated or procured microbes in matrices such as cellulose, clay, MWCNTs and MOFs using microwave assisted, ultrasonication and conventional methods.
- The developed biosorbents were subjected to characterization and tested for the efficient removal of hexavalent chromium.
- The desorption studies were carried out to check the regeneration ability of the developed biosorbents.

The analytical characterization techniques such as FTIR, FESEM, EDAX, HRTEM, XPS, BET, Optical and Confocal microscopy were used to characterize the biosorbents. Various batch parameters such as pH, adsorbent dosage, kinetics, isotherms, and thermodynamics were investigated and optimized. Lab scale column studies were performed to treat higher volumes of the metal contaminated solution and were also tested in a certified industrial waste water effluent.

**Chapter 3** deals with the immobilization of *Saccharomyces cerevisae* (yeast) in the biopolymer and carbon based adsorbents such as cellulose and MWCNTs for the chromium removal. The biosorbent preparation method, characterization, mechanism, application studies are discussed in detail.

**Chapter 4** provides an insight to the immobilization of filamentous fungus, *Aspergillus* in sodium montmorillonite and cellulose for adsorption of chromium. The fungal isolation from

the bread and its complete characterization was discussed in detail. A detailed insight into various column modeling studies are explained.

**Chapter 5** presents a novel combination of fungal spores immobilized in clay for the removal of chromium. The isolation of Arbuscular Mycorrhizal Fungal spores from the soil was carried out and the analytical characterization of the developed biosorbent is discussed.

**Chapter 6** explores in detail about the immobilization of nitrogen fixing bacteria, *Rhizobium* in MWCNTs and sodium montmorillonite for chromium sequestration. The bacterial isolation from soil of legumes and its characterization is discussed in detail.

**Chapter 7** discusses the *Nitrosomonas* modified Zr-Metal Organic Framework for the effective removal of Cr(VI) and its extensive characterization.

**Chapter 8** presents the overall summary and conclusions.

The corresponding procedures, materials and methods are listed in the next chapter.

**References**


1. Mauter, M.S.; Zucker, I.; Perreault, F.; Werber, J.R.; Kim, J.H.; Elimelech, M. *Nature Sustainability*, **2018**, 1 , 166-175.
2. Spasojevic, P.M.; Panic, V.V.; Jovic, M.D.; Markovic, J.; van Roost, C.; Popovic, I.G.; Velickovic, S.J. *J. Mater. Chem. A*, **2016,**4, 1680-1693.
3. Su, R.; Hussain, J.; Guo, J.; Guan, J.; He, Q.; Yan, X.; Li, D.; Guo, Z. ACS Sustainable Chem. Eng., 2015 , 3, 2084–2091.
4. Nriagu, J.O.; Pacynar, J.M.; *Nature,* **1988**, 333, 134-139.
5. Aragay, G.; Pons, J.; Merkoc, A. *Chem. Rev*. **2011**, 111, 3433–3458.
6. Kumar, A.S.K.; Jiang, S.J.; Tseng, W.L. *J. Mater. Chem. A*, **2015**, 3, 7044-7057.
7. Kalidhasan, S.; Sricharan, S.; Ganesh, M.; Rajesh, N. *J. Chem. Eng. Data*, **2010**, 55, 5627–5633.
8. Yuan, L.; Zhi, W.; Xie, Q.; Chen, X.; Liu, Y. *Environ. Sci.: Water Res. Technol.,* **2015**, 1, 814-822.
9. Camel, V. *Spectrochim. Acta*, *B*, **2003**, 58, 1177-1233.
10. Lalley, J.; Han, C.; Mohan, G.R.; Dionysiou, D.D.; Speth, T.F.; Garland, J.; Nadagouda, M.N. *Environ. Sci.: Water Res. Technol.*, **2015**, 1, 96-107.
11. Jacobs, J.; Testa, S.M. *CRC Press* , 2004.
12. Escudero, C.; Fiol, N.; Poch, J.; Villaescusa, I. J. Hazard.Mater., **2009**, 170, 286-291.
13. McNeill, S; Laurie & Mclean, Joan & Parks, Jeffrey & Edwards, Marc. (2012). Hexavalent chromium review, part 2: Chemistry, occurrence, and treatment. Journal - American Water Works Association. 104. E395-E405.10.5942/jawwa.2012.104.0092.
14. Lennartson, A. *Nat. Chem*. **2014**, 6, 942-942.
15. Ali, S. J.; Rao, J. R.; Nair, B. U. *Green Chem*. **2000**, 2, 298-302.
16. Puneet,C.; Krishna,V.; Venu Gopal,A.; Joshi,S.V. *Mater.Manuf.Process.* **2017** doi: 10.1080/10426914 .2017.1303157.
17. Kalidhasan, S.; Kumar, A.S.K.; Rajesh, V.; Rajesh, N. *Coord. Chem. Rev.* **2016,** 317, 157–166.

18. Gutierrez-Corona, J.F.; Romo-Rodríguez, P.; Santos-Escobar, F.; Espino-Saldana, A.E.; Hernández-Escoto, H. *World J.Microbiol.Biotechnol*. **2016**, 32,*191*.
19. Narayan,R.; Meena, R.P.; Patel, A.K.; Prajapati, A.K.; Srivastava, S.; Mondal, M.K. *Environ. Prog. Sustain. Energy,* **2016**, 35, 95-102.
20. Sugiyama, M. *Free. Radic. Biol. Med*., **1992**, 5, 397-407.
21. Scharf, B.; Clement, C.C.; Zolla, V.; Perino, G.; Yan, B.; Elci, S.G.; Purdue, E.;. Goldring, S.; Macaluso, F.; Cobelli, N.; Vachet, R.W.; Santambrogio, L. *Sci.rep.* **2014**, 4, 5729.
22. USEPA Analytical feasibility support document for the six year review of existing national primary drinking water regulation, office of ground water and drinking water EPA 815R 03; EPA: Washington DC, March 2003.
23. Banker, A. V.; Kumar, A.R.; Zinjarde, S.S. *J. Hazard. Mater.* **2009**, 170, 487-494.
24. Munoz, R.; Guieysse, B. *Water Res.* **2006**, 40, 2799- 2815.
25. Vijayaraghavan , K.; Yun, Y.S. *Biotechnol. Adv.* **2008**, 26, 266-291.
26. Pena-Castro, J.M.; Martinez jeronimo, F.; Esparza-Garca, F. Canizares-Villanueva, R.O. *Bioresour. Technol.* **2004**, 94, 219–222.
27. Terres, E.; Cid, A.; Herrero, C.; Abalde, J. *Bioresour. Technol.* **1998**, 63, 213-220.
28. Munoz, R.; Alvarez, M.T.; Munoz, A.; Terrazas, E.; Guieysse, B.; Mattisasson, B. *Chemosphere* **2006**, 63, 903–991.
29. Gopalan, R.; Veeramani, H. *Biotech. Bioeng.* **1994**, 43, 471–476.
30. Fomina, M.; Gadd, G. M. *Bioresour. Technol.*, **2014**, 160, 3-14.
31. Darnall, D.W.; Hosea, J.M. USEPA/540/5-90/005a, Cincinnati, **1990**, pp 4-5.
32. Volesky, B. *Hydrometallurgy*, **2001**, 59, 203–216.
33. Wang, J.; Chen, C. *Biotechnol. Adv.,* **2009**, 27, 195-226.
34. Tabak, H.H.; Lens, P.; Hullebusch, E.D.; Dejonghe, W. *Rev. Environ. Sci. Biotechnol.*, **2005**, 4, 115–156.
35. Choudhury, P.R.; Bhattacharya, P;, Ghosh,S.; Majumdar, S.; Saha, S.; Sahoo, G.C. *J. Environ. Chem. Eng.* **2017**, 5, 214-221.

36. Colica, G.; Mecarozzi, P.C.; De Philippis, R. *Ind. Eng. Chem. Res.* **2012**, 51**,** 4452−4457.

37. Kang, W.; Shukla, R.; Srikar, K.K. *Biotechnol. Bioeng*. **1990**, 36, 826-833.

38. Bardi, E.P.; Koutinas, A.A. *J. Agric. Food Chem*. **1994,** 42 , 221–226.

39. Krauter, P.; Martinelli, R.; Williams, K.; Martins, S.; *Biodegradation* **, 1996**, 7, 277–286.

40. Ksheminska, H.; Jaglarz, A.; Fedorovych, D.; Babyak, L.; Yanovych, D.; Kaszycki, P.; Koloczek, H. *Microbiol. Res.,* **2003**, 158, 59-67**.**

41. Lu,X.; Zhou, X.J.; Wang, T.S. *J. Hazard.Mater*. **2013**, 262, 297-303.

42. Machado, M.D.; Soares, E.V.; Helena; Soares, M .V.M . *J. Chem. Technol. Biotechnol*. **2010**, 85, 1353-1360.

43. Hasan, F.; Shah, A.A.; Hameed, A. *Enzyme Microb. Tech***. 2006**, 39, 235–251.

44. Contesini, F.J..; Lopes, D.B.; Macedo, D.A.; da Graca¸M.; Nascimento; Carvalho, P.O.; *J. Mol. Catal. B: Enzym.,* **2010**, 67, 163–171.

45. de A. Guimaraes, N.C.; Sorgatto, M.; de C. P.Nogueira, S.; Betini, J.H.A.; Zanoelo,F.F.; Marques, M.R.; Polizeli, M.; Giannesi, G.C. *Springer plus*, **2013**, 2, 380.

46. Gu, Y.; Xu, W.; Liu, Y.; Zeng, G.; Huang, J.; Tan, X.; Jian, H.; Hu, X.; Li, F.; Wang, D. *Environ. Sci. Pollut. Res.,* **2015**, 22, 6271- 6279**.**

47. Mungasavalli, D.P.; Viraraghavan, T.; Jin, Y.C. *Colloids Surf., A,* **2007**, 301, 214-223.

48. Park, D.; Yun, Y.S.; and Park, J.M. *Process Biochem.,* **2005**, 40, 2559-2565.

49. Das, S.K.; Mukherjee, M.; Guha, A.K. *Langmuir*, **2008**, 24, 8643-8650.

50. Kapoor, A.; Viraraghavan, T.; Cullimore, D.R.;*Bioresour. Technol*., **1999**, 70, 95-104.

51. Dias, M.A.; Lacerda, I.C.A. ; Pimentel, P.F.; de Castro, H.F.; Rosa, C.A. *Lett. Appl. Microbiol.*, **2002**, 34, 46–50.

52. Sullia, S.B. *Springer*, Netherlands, **1991,** pp. 49-53.

53. Liu, W.; Zhang, Y.; Jiang, S.; Deng, Y.; Christie, P.; Murray, P.J.; Li, X.; Zhang, J. *Sci. Rep.* **2016**, *6*, 24902.

54. Heggo, A.; Angle, A.S. *Soil Biol. Biochem.* **1990**, 22**,** 865-869.

55. Davies Jr , F.T.; Puryear, J.D.; Newton, R.J.; Egilla, J.N.; Saraiva Grossi, J.A. *J. Plant Nutr*. **2002**, 25, 2389–2407.

56. Gil-Cardeza, M.L.; Ferri, A.; Cornejo, P.; Gomez, E. *Sci. Total Environ*. **2014**, 493, 828–833.

57. Manuela, G.; Luciano, A.; Loredana, S. *Can. J Bot* **.1991**, 69, 161-167.

58. Sivakumaran, S., Lockhart, P.J. ; Jarvis, B.D., *Can. J.Microbiol.* **1997,** 43, 164-77 .

59. Ehteshamul-haque, S. & Ghaffar, A., *J. Phytopathology*. **1993**, 138**,** 157—163.

60. Rebah F.B.; Prévost D.; Yezza, A. ; Tyagi, R.D. *Bioresour Technol*. **2007,** 98, 3535-46.

61. Raaman, N.; Mahendran, B.; Jaganathan, C;, Sukumar, S. ; Chandrasekaran,V. *World. J.Microbiol.Biotechnol*. **2012**, 28, 627–636.

62. Karthik, C.; Oves, M.; Sathya, K;, Sri Ramkumar, V;. Arulselvi, P.I. *Arch. Agron. Soil. Sci.*, **2017**, 63, 1058-1069.

63. Chapman, B.D.; Schleicher, M.; Beuger, A.; Gostomski, P.;. Thiele, J.H. *J Microbiol Methods*. **2006**, 65 , 96–106.

64. Chain,P.; Lamerdin,J.; Larimer, F.; Regala,W.; Lao,V.; Miriam L.; Hauser, L.; Hooper, A.; Klotz, M.; Norton, J.; Soto, L.S.; Arciero, D.; Hommes,N.; Whittaker, M.; Arp, D. *J. Bacteriol,* **2003**, 185, 2759–2773.

65. Moon, R.J.; Martini, A.; Nairn, J.; Simonsen , J.; Youngblood, J. *Chem. Soc. Rev*., **2011**, 40, 3941–3994.

66. John,A.; Mahadeva,S.K.; Kim, *J.Smart.Mater.Struct*. **2010**, 19, 045011.

67. Pinkert, A.; Marsh, K.N.; Pang, S.; Staiger, M.P. *Chem Rev*. **2009**, 109, 6712.

68. Connell, D.W,O.; Birkinshaw, C.; O'Dwyer, T.F. *J. Appl. Polym. Sci.* **2006**, 99 2888.

69. Guclu, G.; Gurdag, G.; Ozgumus, S. *J. Appl. Polym. Sci*. **2003**, 90, 2034.

70. Gupta, K.M.; Jiang, J. *Chem. Eng. Sci*. **2015**, 121, 180.

71. Rabideau, B.D.; Agarwal, A. Ismail, A.E. *J. Phys. Chem*. B, **2013**, 117 , 3469.

72. Kalidhasan, S.; Kumar, A.S.K.; Rajesh, V.; Rajesh, N. *J. Colloid Interface Sci*. **2012**, 367, 398.

73. Kalidhasan, S.; Kumar, A.S.K.; Chollety, V.R.; Gupta , P.S.; Rajesh, V.; Rajesh, N *J. Colloid Interface Sci*. **2012**, 372, 88.

74. Wan Nagah, W.S.; Fatinathan, S. *Chem.Eng.J*. **2008**, 143, 62.

75. Chang, M.Y.; Juang, R.S.; *J.Colloid Interface Sc*i. **2004**, 278, 18-25.

76. Sun,S.; Wang, A. *Sep. Purif. Technol*. **2006**, 49, 197.

77. Kumar, A.S.K.; Kumar, C.U.; Rajesh, V.; Rajesh, N. *Int. J. Biol. Macromol*. **2014**, 66 135.

78. Huang,R.; Yang, B.; Liu, Q.; *J. Appl. Polym. Sci*. **2013**, DOI: 10.1002/APP.38685

79. Liu, Q., Yang, B., Zhang, L. *Korean J. Chem. Eng.* **2015** , 2, 1314-1322.

80. Sugashini, S.; Sheriffa Begum, K.M.M.; Ramalingam, A. *J. Mol. Liq.* **2015**, 208, 380–387.

81. Boddu, V.M.; Abburi, K.; Talbott, J.L.; Smith, E.D. *Environ. Sci. Technol*., **2003**, 37 4449-4456.

82. Kumar, A.S. K.; Kalidhasan, S.; Rajesh, V.; Rajesh, N. *Ind. Eng. Chem. Res*., **2012**, 51, 58–69.

83. Gunzun, A.S.; Stroescu, M.; Jinga, S.; Mihalache, N.; Botez, A.; Matei, C.; Berger, D.; Damian. C.N.; Valemtinolet, *Int J Biol Macromol*. **2016**, 91, 1062-1072.

84. Dima, J.M.; Sequeiros, C.; .Zaritzky, N.E.; *Chemosphere*, **2015**, 141, 100-111.

85. Guo, D.M.; An, Q.D.; Xiao, .Y.; Zhai, S.R.; Shi, Z. *RSC Adv*., **2017**, 7, 54039.

86. Beheshti, H.; Irani, M.; , Hosseini, L.; Rahimi, A.; Aliabadi, M. *Chem.Eng.J.* **2016**, **284**, 557-564.

87. Huang, X.; Liu,Y.; Liu, S.; Tan,X.; Ding, Y.; Zeng,G.; Zhou, Y.; Zhang, M.; Wang, S.; Zheng, B. *RSC Adv.*, **2016**,6, 94-104.

88. Anush, S.M.; Vishalakshi, B.; Chandan, H.R.; Geetha, B.R. *Sep. Sci. Technol*. **2018**, doi.org/10.1080/01496395.2018.1442859.

89. Bhattacharyya, K.G.; Gupta, S.S. *Adv. Colloid Interface Sci.* **2008**, 140, 114–131.

90. Zeng, Q.H.; Yu, A.B.; Lu, G.Q.; Paul, D.R. *J. Nanosci. Nanotechnol.*, **2005**, 5, 1574–1592.

91. Chen , D.; Li , W.; Wu , Y.; Zhu , Q.; Lu; Du, G. *Chem. Eng. J*., **2013**, 221, 8–15.

92. Lin, D.; Zhou, S.; Lu, L.; Shi-yang, C.; Ling-fang,Y.; Xiu-zhen, Y.; Li-shan, L. *J. Cent. South Univ.* **2014**, 21, 3918−3926

93. Tewari, N.; Guha, B.K.; Vasudevan, P. *Asian J. Chem.,* **2005,** 17, 2184-2190.

94. Padmavathy, K.S.; Murali, A.; Madhu, G.; Sahoo, D.K. *Indian. J. Chem. Techn.* **2017**, 24, 593-600.

95. Qurie, M.; Khamis, M.; Manassra, A.; Ayyad, I.; Nir, S.; Scrano, L.; Bufo, S.A.; Karaman, R. *Sci. World J.* **2013**, 2013, 942703.

96. Yuan, P.; Fana, M.; Yang, D.; He, H.; Liu, D.; Yuan, A.; Zhu, J.X.; Chen, T.H. *J. Hazard. Mater.* **2009**, 166, 821–829.

97. Brum, M.C.; Capitaneo, J.L.; Oliveira, J.F. *Miner. Eng.* **2010**, 23, 270–272.

98. Mohanty, K.; Jha, M.; Meikap, B.C.; Biswas, M.N. *Chem. Eng. Sci.* **2005**, 60, 3049 – 3059.

99. Rai, M.K.; Shahi, G.; Meena, V.; Meena, R.; Chakraborty, S.; Singh, R.S.; Rai, B.N. *Resource-Efficient Technologies,* **2016**, 2, S63–S70.

100. Labied, R.; Benturki, O.; Donnot, A. *Adsorpt.. Sci. Technol*. 2018, 36, 1066 – 1099.

101. Wepasnick, K.A.; Smith, B.A.; Schrote, K.E.; Wilson, H.K.; Diegelmann, S.R.; Fairbrother, D.H. *Carbon*, **201**1, 49, 24-36.

102. Parlayici, S., Eskizeybek, V., Avcı, A. & Pehlivan, E. *J Nanostruct Chem*. **2015**, 5, 255-263.

103. Lu, W.; Li, J.; Sheng, Y.; Zhang, X.; You, J.; Chen, L. *J Colloid Interface Sci*. **2017**, 505, 1134-1146.

104. Masheane, M.L.; Nthunya, L.N.; Malinga, S.P.; Nxumalo, E.N.; Mamba, B.B.; Mhlanga, S.D. *Sep. Purif. Technol*. **2017**, 184, 79-87.

105. Salam, M.A. *J. Mol. Liq*. **2017**, 233, 197-202.

106. Wu,C.; Fan,J.; Jiang, J.; Wang, J.; *RSC Adv*., **2015**, 5, 47165-47173.

107. Guo, F.Y.; Liu,Y.G.; Wang,H.; Zeng, G.; Hu, X.; Zheng, B.; Li, T.; Tan, X.; Wang, S.; Zhang, M. *RSC Adv*., **2015**, 5, 45384-45392.

108. He, C.; Yang, Z.; Ding, J.; Chen, Y.; Tong, X.; Li School, Y. *Colloids and Surfaces A: Physicochem. Eng. Aspects.* **2017**, 520, 448–458.

109. Jiang, X,; Luo, H.; Yin, Y.; Zhou, W. *RSC Adv*., **2017**, 7, 24149-24156.

110. Ma, H.L.; Zhang, Y.; Hu, Q.H.; Yan, D.; Yu, Z.Z.; Zhai, M. *J. Mater. Chem*., **2012**, 22, 5914.

111. Kumar, A.S.K.; Rajesh, N. *RSC Adv*. **2013**, 3, 2697-2709.

112. Taddei, M.; Dau, P.V.; Cohen, S.M.; Ranocchiari, M.; van Bokhoven,J.A.; Costantino, F.; Sabatini. S.; Vivani , R. *Dalton Trans*. **2015**, 44, 14019-14026.

113. Lausund, K.B.; Nilsen, O. *Nat Commun*., **2016**, 7, 13578-13586.

114. Katz, M.J.; Brown, Z.J.; Colo´n,Y.J.; Siu, P.W.; Scheidt, K.A.; Snurr,R.Q.; Hupp, J.T.; Farha, O.K. . *Chem. Commun*., **2013**, 49, 9449-9451.

115. Wei,C.; Feng, D.; Xi, Y. *RSC Adv.*, **2016**,6, 96339-96346.

116. Yin, N.; Wang, K.; Li, . *Chem. Lett.* **2016**, 45, 625–627.

117. Nandi, S.; De Luna, P.;. Daff, T.D.; Rother, J.; Liu, M.; Buchanan, W.; Hawari, A.I.; Woo, T.K.; Vaidhyanathan. R.; *Sci. Adv*. **2015**;1, 1500421.

118. Vellingiri, K.; Szulejko, J.E.; Kumar, P.;. Kwon, E.E.; Kim, K.H.; Deep, A.; Boukhvalov, D.W.; Brown, R.J.C. 6, *Sci. Rep*. **2016**, 6, 27813.

119. Peng, Y.; Huang, H.; Zhang, Y.; Kang, C.; Chen, S.; Song, L.; Liu, D.; Zhong, C. *Nat. Commun.* **2018**, 9, 187 .

120. El-Mehalmey, W.A.; Ibrahim, A.H.; Abugable, A.A; Hassan, M.H.; Haikal,R.R.; Karakalos, S.G.; Zakid, O.; Alkordi, M.H. *J. Mater. Chem. A*, **2018**, 6, 2742-2751.

121. Nasrollahpour, A.; Moradi, S.E. *Microporous Mesoporous Mater*. **2017**, 243, 47-55.

# Chapter – 2

# Materials and Methods

The current chapter deals with the chemicals and materials used in the experiments and the general methodology for the sequestration and recovery of chromium.

## 2.1. Chemicals and materials

All the chemicals and reagents used in the experiments were of analytical and guaranteed grade. The aqueous solutions were prepared in high purity water (Millipore, Merck, Elix 10, resistivity 18.2 MΩ $cm^{-1}$). Various chemicals and materials used were cellulose (Himedia), montmorillonite (Sigma Aldrich), multiwalled carbon nanotubes with an outer diameter of 30-50 nm and length 10-30 μm (Sisco Research Laboratories, India) , zirconium oxychloride (SD Fine Chemicals ), terephthalic acid (Sigma Aldrich ), potassium dichromate ($K_2Cr_2O_7$), diphenyl carbazide, nitric acid, sulfuric acid, sodium hydroxide, from Merck, India. Hydrochloric acid, hydrogen peroxide, BCR 715- waste water (trace elements) was procured from Fluka , BCR -032 (Moroccan Rock phosphate) was obtained from Sigma Aldrich. Methanol and acetone were procured from S.D. Fine Chemicals, Mumbai (India), (3-Dimethylaminopropyl)-N′-ethylcarbodiimide hydrochloride (EDC), Hydroxybenzotriazole (HOBT) were obtained from (Sisco Research Laboratories, India).

## 2.2. Isolation and identification of microbes

Various microbes used in the adsorption experiments are *Saccharomyces cerevisiae* (procured), *Aspergillus* species (isolated from bread mold), endomycorrhizal spores (isolated from soil), nitrogen fixing bacteria such as *Rhizobium* (isolated from soil) and *Nitrosomonas* (procured) species immobilized in various matrices. The microbes used were either isolated or procured from the culture centers. The detailed identification and characterization of microorganisms can broadly be classified into morphological, biochemical and molecular procedures.[1] Morphological methods are relatively easy to be performed and are rapidly done. They rely on growth and microscopic examination that give a general characteristic to the morphology of an organism. Biochemical methods involve varied set of recent technologies such as chromatography and spectroscopy experiments. Molecular biology based methods involve diverse range of techniques that involve microbial DNA.

## 2.3. Analytical characterization techniques used

A JASCO 4200 model spectrophotometer was used to record the FTIR of the samples in the range 4000-400cm$^{-1}$ by mixing the sample with potassium bromide (KBr). Thermogravimetric analysis (TGA) of the biosorbent was recorded using a Shimadzu DTG-60 thermal analyser under air/nitrogen atmosphere in the range of 30-800$^{o}$C. For the elemental analysis energy dispersive X-ray spectrum (EDAX) was recorded using Bruker – X Flash 6/30 and to study the surface morphology of the biosorbents, field emission scanning electron microscopic (FESEM) images were captured using Carl Zeiss Supra 55 and High resolution transmission electron microscopic (HRTEM) images taken by Tecnai 20 (FEI) 200 kV gives an insight into the microstructure and the defects at atomic resolution. The elemental speciation was ascertained by X-ray photo electron spectroscopy using PHI 5000 Versa Prob II, FEI Inc, and the source used is an aluminium monochromator at 25.4W and 187.85 eV. The BET surface area, BJH pore volume and average pore diameter of the biosorbent were measured using a BELSORP II mini (Microtrac BEL Corp). LeicaDMi8 laser scanning microscopy (S/N 418513) was used to capture confocal images. The quantitative Cr(VI) adsorption was monitored using a 883 Basic IC plus Ion chromatography with a 887 professional UV/Vis detector and also using Jasco V650 model UV visible spectrophotometer. The total chromium concentration was ascertained with a Shimadzu AA-7000 model Atomic Absorption Spectrophotometer using an air-acetylene flame at 357.8 nm The 16S rDNA sequencing was carried out using the Biosystems ABI 3730 xls Genetic analyzer at Bioserve Pvt. Ltd., Hyderabad, India. Matrix assisted laser desorption ionization time of flight (MALDI-TOF) was performed using VITEK MS (Biomerieux) spectrometer for the confirmation of the isolated bacteria. An Olympus CH20i model optical microscope was used to obtain the images of the adsorbent before and after the adsorption of chromium. The developed biosorbents were also characterized by Rigaku Ultima IV X-ray diffractometer using Cu $K_{\alpha}$ source at various scan rates. Ultra-sonication was done using a sonication bath (Biotechnics, India).

## 2.4. Characterization of biosorbents

The developed biosorbents were subjected to various characterization techniques to prove the formation of the desired material. Following are the instrumentation techniques that have been used in our work.

**2.4.1 Fourier transmission infrared spectroscopy (FT-IR):** FT-IR is one of the efficient tools to get the chemical functional groups of the material. The interaction of infrared radiation with molecular bonds leads to vibrational fluctuations such as bending, wagging and stretching in the molecule. Different vibrational frequencies correspond to different functional groups can indicate the structure. The technique can therefore be used to monitor the changes in functional group signature peaks as a function of reaction progress.

**2.4.2 Field emission scanning electron microscopy (FE-SEM):** The scanning electron microscopy is an important characterization technique that uses a focused electron beam. In FE-SEM secondary electrons are emitted from the solid sample, which are collected to create an area map of the secondary emission. The technique is used to determine the surface morphology and chemical composition (in energy dispersive spectroscopy mode) of the material samples.

**2.4.3 High resolution transmission electron microscopy (HR-TEM):** In this technique, high energy electron beams are utilized to transmit through the sample of interest. Using the contrast between transmitted and non-transmitted e-beams, the image is created. This technique provides very high resolution image to the extent of 0.2 Å. One would be able to measure the inter-planar distance for the crystalline materials using this technique.

**2.4.4 Brunauer–Emmett–Teller (BET) surface area measurements:** This measurement works on the basis of physical adsorption of the gaseous molecules on the solids (BET theory). According to the BET theory, the gaseous molecules adsorb on the surface of the adsorbent as monolayer. The monolayer adsorption and desorption of the gas will be carried out and surface area, pore volume and pore diameter can be calculated using BET formula.

**2.4.5 Thermo-gravimetric analysis:** TGA is a method of thermal analysis which executes the decomposition of material as a function of temperature. This technique shows the percentage mass loss, which is useful to optimize the reaction conditions like polymerization and calcination.

**2.4.6. X-ray photoelectron spectroscopy (XPS)**: XPS is a highly useful instrumentation tool to acquire detailed analysis of the surface at atomic level to understand the elemental composition. This technique was initially known as the Electron Spectroscopy for Chemical Analysis (ESCA), which works based on photoelectric effect (KE = hυ - BE). XPS is used to find the binding energy of the atoms except hydrogen and helium in the periodic table. From the binding energy values obtained from the surface of the material, one would be able to identify the elemental composition and their oxidation states.

## 2.5. Analysis of hexavalent chromium

The chromium concentration in the analyte was estimated using 883 Basic IC plus Ion chromatography using Metrosep A Supp 1 HS column, detected using 887 professional UV/Vis detector. The post column derivatization method used in UV-Vis detection for chromium was at $\lambda_{max}$ 540 nm. The mobile phase used was sodium carbonate and the post column reagent was prepared by dissolving diphenylcarbazide in methanol and sulphuric acid. The total chromium was estimated by (a) speciation method using ion chromatography and (b) using Atomic Absorption spectrophotometry (for total chromium) and UV-Vis (Cr VI) by oxidizing total chromium to Cr(VI) using NaOH, $H_2O_2$ mixture and estimating Cr(VI) as its diphenylcarbazide complex at 540 nm.

## 2.6. Adsorption studies

A 1000 mg $L^{-1}$ stock solution of Cr (VI) was prepared by dissolving 2.826 g of potassium dichromate in Milli Q water. The batch adsorption studies were performed by optimizing various parameters such as pH, adsorbent dosage, kinetics, and thermodynamics by using an orbital incubator shaker (Biotechnics, India). A known weight of the biosorbent was mixed with Cr(VI) of a known concentration and adjusted to the required pH using $H_2SO_4$, NaOH and agitated at various time intervals in an orbital incubator shaker. The reaction mixture was filtered after it

attained equilibrium and the supernatant was estimated for Cr(VI) concentration using ion chromatography coupled with a UV detector.[2] The amount of Cr(VI) biosorbed onto the developed biosorbents was calculated as

$$q_e = \frac{(C_o - C_e)V}{W} \qquad (2.1)$$

Where,

$q_e$= Amount of Cr(VI) adsorbed onto biosorbent at equilibrium (mg $g^{-1}$)

$C_o$ = initial Cr(VI) concentration (mg $L^{-1}$)

$C_e$ = Cr(VI) concentration left in the analyte at equilibrium (mg $L^{-1}$)

V = Volume of Cr(VI) solution used for biosorption (L)

W = weight of the biosorbent for Cr(VI) treatment (g)

**2.7. Adsorption isotherms**

The characteristic features of the interaction between biomass immobilized in various matrices and Cr(VI) could be accounted by correlating the experimental adsorption data with isotherm models.[3]

***2.7.1 Langmuir adsorption isotherm***

The Langmuir adsorption isotherm[4] is based on the assumptions such as that adsorption sites which are available on the biosorbent surface are fixed and are of equal size. It also assumes a monolayer adsorption. The Langmuir equation can be used for describing equilibrium conditions for the adsorption behavior in various adsorbate-adsorbent systems. The linear form of the Langmuir equation is given by

$$\frac{C_e}{q_e} = \frac{1}{q_o b} + \frac{C_e}{q_o} \qquad (2.2)$$

where, $C_e$ is the metal ion concentration at equilibrium, $q_e$ is the amount of adsorbate (Cr VI) adsorbed per gram of adsorbent at equilibrium (mg $g^{-1}$); $q_o$ and b are Langmuir constants related

to the sorption capacity and intensity, respectively. A plot of Ce/qe vs Ce gives the values for $q_o$ and b. The applicability of the Langmuir model was also confirmed from the dimensionless $R_L$ value[5] which relates $C_o$, a particular initial concentration of Cr(VI) to the energy of adsorption b as $R_L = 1/1 + bC_o$. A value below unity indicates a reversible isotherm whereas values greater than one and equal to zero indicate unfavorable and irreversible isotherms, respectively.

### *2.7.2 Freundlich isotherm*

The Freundlich adsorption isotherm[6] is considered as the special case of Langmuir which gives an empirical relation between the adsorbate which adsorbs onto the heterogeneous surface of an adsorbent. The linear form of Freundlich adsorption equation can be expressed as follows

$$\log q_e = \log K_F - \frac{1}{n}\log C_e \quad (2.3)$$

Where, $K_F$ and n are the Freundlich constants that represent the adsorption capacity and the adsorption intensity, respectively. If the value of n lies between 1 and 10, it is considered favorable adsorption wherein a higher n value implies[7] effective interaction between the adsorbent and adsorbate. The plot of $\log q_e$ against $\log C_e$ gives the constants $K_F$ and n.

### *2.7.3 Redlich–Peterson (R-P) isotherm*

The Redlich–Peterson model[8] is a unique three parameter adsorption isotherm model and is a combination of Langmuir and Freundlich isotherms which relates to the amount of chromium (VI) adsorbed at equilibrium $q_e$. The linear expression of the model is as follows

$$\ln\left[A\left(\frac{C_e}{q_e}\right) - 1\right] = g(\ln C_e) + \ln B \quad (2.4)$$

where A is the Redlich-Peterson adsorption capacity constant, B is the isotherm constant and for the efficient adsorption process exponent g lies between 0 and 1. As the R-P isotherm has three parameters it is perceived to be more accurate than the Langmuir and Freundlich isotherms. When g= 1, the R-P equation reduces to the Langmuir isotherm equation and when g=0, it is similar to the Freundlich equation though the accuracy of these interpretations strongly depends

on the fitting method.[9] The parameters g and B are obtained from the slope and intercept of the plot ln [A($C_e$ / $q_e$)- 1) against ln $C_e$.

### *2.7.4 Dubinin–Radushkevich (D-R) isotherm*

The adsorption mechanism with a Gaussian energy distribution onto the heterogeneous biosorbent surface is expressed by D-R isotherm.[10] The electrostatic interaction between the protonated functional groups in the biosorbent surface and Cr (VI) is reflected through the mean free energy of adsorption obtained from this model which is expressed as

$$\ln q_e = \ln q_m - \beta\varepsilon^2 \quad (2.5)$$

$$\varepsilon = RT\ln\left[1 + \frac{1}{C_e}\right] \quad (2.6)$$

$$E = \frac{1}{\sqrt{2B}} \quad (2.7)$$

Where ε is the polayani potential, $q_m$ is the maximum adsorption capacity, obtained from the plot of ln $q_e$ vs $\varepsilon^2$, β is the D-R constant , R is universal gas constant and E is the mean adsorption free energy. The D-R isotherm predicts that when the mean free energy of adsorption is less than 8 kJ $mol^{-1}$ the adsorption is more likely to be associated as physisorption.[11]

### *2.7.5 Elovich isotherm*

The isotherm is based on the assumption that there is an exponential increase in adsorption sites with adsorption leading to multilayer adsorption[12,13] which is governed by the following expression

$$\ln\frac{q_e}{c_e} = \ln K_E q_m - \frac{q_e}{q_m} \quad (2.8)$$

The Elovich isotherm parameters $K_E$ which is Elovich constant and $q_m$ which is adsorption capacity can be calculated from the plot of ln($q_e$/$C_e$) vs $q_e$.

### *2.7.6 Temkin isotherm*

Temkin isotherm is generally applied for the heterogeneous systems wherein as the surface area of the biosorbent increases (which has more sorption sites), the heat of adsorption tend to decrease linearly and attributed to the adsorbent-adsorbate interactions having uniformly distributed binding energies until it reaches a maximum value.[14,15] The isotherm model is given by the equation as

$$q_e = B_1 \ln A_T + B_1 \ln C_e \quad (2.9)$$

Where $B_1$= RT/b and $A_T$ is the equilibrium binding constant, B is heat of adsorption obtained by plotting $q_e$ against ln $C_e$ .

## 2.8. Adsorption kinetics

The efficiency of the method developed also depends on the kinetics of adsorption. A known amount of the developed biosorbent was taken and added to the known volume of Cr(VI) solution and adjusted at pH 2.0-3.0. The adsorption studies were performed at various time intervals from 5, 10, 15, 30, 60, 120, 180 min and checked for the Cr(VI) concentration simultaneously. The kinetics involved in the interactions between the metal and microbe immobilized matrix were evaluated using the pseudo first order [16]and pseudo second order[17] models which are expressed in the following equations

$$\log(q_e - q_t) = \log q_e - \frac{k_1 t}{2.303} \quad (2.10)$$

$$\frac{t}{q_t} = \frac{1}{k_2 q_e^2} + \frac{t}{q_t} \quad (2.11)$$

Where $q_e$ and $q_t$ are the amount of chromium adsorbed onto the biosorbent at equilibrium and time t, respectively and $k_1$ is the pseudo first order rate constant which is obtained from the plot log ($q_e$-$q_t$) vs time. $k_2$ is the pseudo second order rate constant which is calculated form the plot $t/q_t$ vs t. Additionally, the Weber-Morris intraparticle diffusion[18] (IPD) is also used to evaluate the adsorption kinetics and is expressed as

$$q_t = k_{int} t^{0.5} \quad (2.12)$$

If the plot of $q_t$ against $t^{0.5}$ gives a linear plot with zero intercept IPD is considered to be the only rate limiting step. The adsorption mechanism involved in the Cr(VI) uptake onto the biosorbent is governed by the following steps

(i) Cr(VI) ions are transported from the bulk of the solution to the exterior of the adsorbent surface which is termed as external film mass transfer.

(ii) Transport of Cr(VI) ions into the pores of the biosorbent which is termed as intraparticle or pore diffusion.

(iii) Adsorption of Cr(VI) ions onto the surface of the biosorbent.

## 2.9 Adsorption thermodynamics

An insight towards the spontaneity and energetics involved in the interaction between the host matrix (biosorbent) and the guest (Cr(VI)) can be best explained through the Gibb's free energy ($\Delta G^o$), enthalpy ($\Delta H^o$) and entropy ($\Delta S^o$) values. From the ratio of the concentrations of Cr(VI) present at equilibrium on the biosorbent surface and the solution phase, the equilibrium constant (K) was obtained at different temperatures. These equilibrium constant values were fitted into the Gibb's isotherm or the Vant Hoff's equation[19]

$$\Delta G^0 = -RT\ln K \quad (13)$$

Furthermore, through the slope and intercept of the plot of lnK against 1/T the entropy and enthalpy changes could be obtained for the interaction of Cr(VI) with the biosorbent. Essentially, all these parameters are categorized as extensive or additive properties and hence the first stage involving immobilization of the biomass as well as subsequent adsorption on to the surface would collectively influence the overall free energy, enthalpy and entropy changes associated with the adsorption.[20] The average activation energy, $E_a = \Delta H^o_{ads} + RT$ also reflects the favourable interaction between hexavalent chromium and the microbe immobilized matrix. The physisorption/chemisorption of the adsorption mechanism is determined by the magnitude of $\Delta H^o$. If $\Delta H^o > 80$ kJ mol$^{-1}$ is termed physisorption whereas if $\Delta H^o < 80$ kJ mol$^{-1}$ is considered as chemisorption.[21]

## 2.10 Column studies

Prior to applying the methodology in a simulated waste effluent, the suitability was examined in a laboratory scale fixed bed column study in the aqueous solution where the metal contamination is at higher volumes. Based on preliminary column experimental studies, a detailed investigation into various parameters such as effect of bed height, flowrate and initial Cr(VI) concentrations in the modeling studies such as Thomas model, Yoon Nelson model, BDST models were carried out.[22] The salient features of the column modeling adsorption studies are discussed in chapter 4.

## 2.11 Application studies

The influence of some common ionic constituents such as Fe(II), Cu(II), Ni(II), Cd(II), Pb (II), Mn (II), Zn(II) and chloride, nitrate, sulphate and phosphate present in the industrial wastewater samples were probed independently in a synthetic mixture . Following this, the methodology was tested in a certified industrial effluent wastewater sample BCR 715 and BCR 032 Moroccan rock phosphate. The composition of these certified materials are given in Table 2.1.

**Table 2.1.** Composition of certified reference material

| Certified reference material | Composition |
|---|---|
| BCR – 715<br>Industrial effluent | Cd (40±5 μg $L^{-1}$ ), As (29±4 μg $L^{-1}$), Fe ((3.00 ± 0.27) ·$10^3$ μg $L^{-1}$) , Cr ((1.0±0.09).$10^3$ μg $L^{-1}$), Mn (248 ± 25 μg $L^{-1}$), Ni ((1.20 ± 0.09) ·$10^3$ μg $L^{-1}$), Cu ((0.90 ± 0.14) ·$10^3$ μg $L^{-1}$), Pb ((0.49 ± 0.04) ·$10^3$ μg $L^{-1}$), Se (29 ± 4 μg $L^{-1}$) and Zn ((4.00 ± 0.4) ·$10^3$ μg $L^{-1}$). |
| BCR – 032<br>Moroccan Rock Phosphate | As (9.5±0.5), Cd (20.8±0.7), B (22.6±2.2), Cr (257±16), Co (0.59±0.06), Hg (0.055±0.011), Cu (33.7±1.4), Ni (34.6±1.9), Mn (18.8±1.3), Ti (171±10),Ni (34.6±1.9), Zn (253±6), V (153±7). |

**References**


1. Spiegelman, D.; Whissell, G.; Greer, C.W., *Can J Microbiol.* 2005, 51, 355-86.
2. Arar, E.J.; Pfaff, J.D. *J. Chromatogr. A,* **1991**, 546, 335-340.
3. Ayawei, N.; Ebelegi, A.N.; Wankasi, D.; *Journal of Chemistry*, **2017**, DOI 10.1155/2017/3039817.
4. Langmuir, I. *J. Am. Chem. Soc*. **1918**, 40, 1361.
5. Sun, C.J.; Sun, L.Z.; Sun, X.X. *Ind. Eng. Chem. Res*. **2013**, 52, 14251–14260.
6. Freundlich, H.M.F. *Z. Phy.Chem.* **1906**, 57, 385.
7. Ho, Y.S.; Chiu, W.T.; Wang, C.C. *Bioresour. technol*. **2005**, 96, 1285-1291.
8. Redlich, O.; Peterson, D.L. *J. Phys. Chem*. **1959,** 63, 1024.
9. Chung, H.K.; Kim, W,H.; Park, J.; Cho, J.; Jeong, T.Y.; Park, P.K. J. *Ind. Eng. Chem*., **2015**, 28, 241-246.
10. Dubinin, M.M.; Radushkevich, L.V. *Proc. Acad. Sci. USSR Phys. Chem. Sect*. **1947**, 55, 331.
11. Srivastava, V.; Weng, C.H.; Singh, V.K.; Sharma, Y.C. *J. Chem.Eng.Data*. **2011**, 56, 1414.
12. Elovich, S.Y.; Larinov, O.G. *Izv. Akad. Nauk. SSSR, Otd.Khim.Nauk*. **1962**, 2, 209.
13. Wu, F.C.; Tseng, R,L.; Juang, R.S. *Chem. Eng. J*. **2009**, 150, 366-373.
14. Temkin, M.I. *Zh. Fiz. Chim*. **1941**, 15, 296.
15. Erhayem, M.; Tohami, F.; Mohmad, R.; Ahmida, K. *Am J Analyt Chem*. **2015**, 6, 1-10.
16. Lagergren, S. *K. Sven.Vetenskapsakad. Handl*., **1898**, 24,1-39.
17. Ho, Y.S., Mckay, G. *Water Res*., **2000**, 34, 735-742.
18. Weber, W.J.; Morris, J.C. *J. Sanit. Eng. Div*. **1963**, 89, 31-60.
19. Kumar, A.S.K.; Kalidhasan, S.; Rajesh, V.; Rajesh, N. *Ind. Eng. Chem. Res*., **2012**, 51, 58–69.
20. Mallakpour, S.; Taghavi, M. *Polym. J*. **2008**, 40, 1049-1059.
21. Hamza, I.A.A.; Martincigh, B.S.; Ngila, J.C.; Nyamori, V.O. *Phys. Chem. Earth*, **2013**, 66, 157–166.
22. Hasan, S.H.; D. Ranjan, D.; Talat, M. J. *Hazard. Mater*. **2010**, 181, 1134–1142.

# Chapter -3

## Yeast immobilized in carbon based adsorbents for the effective removal of hexavalent chromium from aqueous solutions

This chapter deals with the adsorption of chromium using *Saccharomyces cerevisiae* immobilized in carbon based matrices. *Saccharomyces cerevisiae* commonly known as baker's yeast has good potential for heavy metal removal due to its advantages such as easy cultivation in large scale on inexpensive media with high yield. It is a non-pathogenic microbe widely used in food industry. As the complete genome sequence of *S.cerevisiae* is available which can be manipulated easily, it is considered as a model microbe to study the molecular level interactions taking place between the metal and microbe. Literature survey reveals that *S.cerevisiae* is explored in various forms such as living cells, dead cells, pretreated cells, immobilized cells in matrices for effective removal of heavy metals such as Pd, Cd, Ni, Cr, Cu, Zn.[1] In the current work, we demonstrate an environmentally benign approach for the efficient removal of chromium using *S.cerevisiae* immobilized in matrices such as glutaraldehyde cross-linked cellulose and MWCNTs.

**The first part of this chapter** deals with the immobilization of *S. cerevisiae* in glutaraldehyde cross-linked cellulose for the effective removal of hexavalent chromium.

**The second part of this chapter** deals with the immobilization of *S. cerevisiae* in functionalized multiwalled carbon nanotubes for the effective sequestration of Cr(VI).

## 3.1. Microwave assisted immobilization of yeast in cellulose biopolymer as a green adsorbent for the sequestration of chromium

### 3.1.1 Introduction

A greener option of microwave assisted methodology could be conceived as an energy efficient and expeditious process in the immobilization of the biomass. A systematic literature search reveals that this technique has not been explored to immobilize a microbe in a cellulose support. The efficient dielectric heating with decrease in the Gibb's activation energy ensures facile energy transfer [2-5] in accelerating the immobilization process. Cross linking cellulose with glutaraldehyde [6] strengthens the microbial cell surface and the interaction between the polar functional groups and microwave energy augments the immobilization of yeast in the biopolymer matrix. Cellulose offers the advantages of a biodegradable polysaccharide and is known to be an excellent support to immobilize microorganisms such as E.coli.[7] Various species of *Aspergillus, Pseudomonas* etc., are known to tackle chromium pollution quite well.[8,9] *Bacillus subtilus* is known to remove Cr(VI) from chromium polluted mining sites.[10] Alginate extracted from sea weeds[11] can remove Cr(VI) with an adsorption capacity of 0.819 mmol $g^{-1}$. The adsorption of trivalent chromium, cadmium and nickel has been reported using *Trichoderma* fungal species.[12] Under the category of fungi, yeast (*Saccharomyces cerevisiae)* also has the ability to remove heavy metals.[13-17]

However, to the best of our knowledge, immobilization of yeast in a biodegradable polymer matrix such as cellulose has not been reported for the detoxification of a carcinogenic metal ion such as chromium(VI). The hydroxyl groups available in the polysaccharide cellulose and diverse functional groups such as amine, hydroxyl, carboxylic etc. present on the yeast cell surface aids in the interaction with chromium(VI) oxyanion. With glutaraldehyde as the cross linking agent the covalent immobilization of the yeast cells on to the polymeric support[7] would improve the stability of the biosorbent. Hence, an uncomplicated and novel microwave assisted green procedure was adopted to immobilize yeast in glutaraldehyde cross linked cellulose and its subsequent application to remove Cr(VI) from aqueous solution.

### 3.1.2 Experimental section

**(i) Preparation of the biosorbent**

Granules of baker's yeast were procured commercially and maintained using a Yeast extract Peptone Dextrose (YEPD) medium.[15,18] The media was prepared by mixing 1 g yeast extract, 2 g peptone and 2 g dextrose with approximately 100 mL of distilled water and autoclaved. The culture was grown at 37$^{o}$C and after the complete growth was maintained at 4$^{o}$C. The biomass from the late exponential growth phase (72 h) were centrifuged (5000 rpm, 15 min) at room temperature and after decanting the supernatant, the biomass pellet was washed with sterile distilled water. The biomass was immobilized in cellulose matrix using the microwave assisted method.

A simple commercial microwave oven (Sharp (Japan), R-23 GT) with a maximum power range of 1600 W was used for immobilization. The internal chamber is made of stainless steel and the oven is equipped with ten adjustable power levels and a microprocessor controlled memory key pad. A 2.0 g weight of the pelletized biomass was mixed with 4.0 g of cellulose (Himedia, India) homogenously and 0.5 mL of dimethyl formamide (DMF). 4 mL of glutaraldehyde (S.d. Fine Chemicals, India) was added to crosslink cellulose in 10 mL of 0.1 mol L$^{-1}$ HCl solution and the mixture was subjected to microwave irradiation for 200 sec using only 10% of the total power (160 W) with intermittent time duration of 20 sec so as to ensure that cellulose does not undergo any degradation. The cross linking occurs upon exposure to microwave radiation resulting in acetal formation.[19] Immobilized yeast in the cross linked biopolymer was washed subsequently with Milli-Q water (Elix 3) and dried in a vacuum oven (Biotechnics, India) at 40$^{o}$C.

**(ii) Adsorption studies**

The removal of Cr(VI) was studied at room temperature (25$^{0}$C) by equilibrating 0.4 g of the yeast immobilized cellulose adsorbent with a 20 mL volume of 50 mg L$^{-1}$ Cr(VI) solution in a shaking incubator for a preset time duration (3 h) at pH 2.5. The concentration of chromium following equilibration was determined spectrophotometrically by adding diphenyl carbazide to develop the red violet color at 540 nm.[20,21]

The lowest concentration of chromium that prevented the microbial growth was taken as the Minimum Inhibitory Concentration (MIC) and this was acquired by adding varying concentrations of Cr(VI) ranging from 30 to 300 mg $L^{-1}$ to the freshly prepared growth medium. After 24 h incubation period at 26$^{o}$C, the optical density of biomass was measured at 600 nm.[22] The microbe found to be highly resistant to Cr(VI) with a minimal inhibitory concentration of 280 mg $L^{-1}$.

### 3.1.3 Results and Discussion

#### (i) Biosorbent characterization

The yeast cell surface is endowed with $NH_2$, COOH and OH functional groups and could play a vital role in interaction with the chromium (VI) oxy anion. The plausible interaction of yeast with cellulose and Cr(VI) was supported through the FT-IR spectral characterization. The FT-IR spectrum (Fig. 3.1.) shows typical changes in the functional group vibrational frequencies after the adsorption of chromium onto the microbe immobilized biopolymer surface. The absorption at 3326.4 $cm^{-1}$ is ascribed to the merged NH and OH stretching vibrations. The shift to 3314.8 $cm^{-1}$ after Cr (VI) adsorption shows the involvement of amine and hydroxyl groups in the interaction. The absorption at 2882.1 $cm^{-1}$ corresponds to C-H stretching of $CH_2$ groups in cellulose. The peak at 1634.3 $cm^{-1}$is attributed to the amide-I band of the protein-peptide bond of the fungal biomass.[23] The peak at 1421.3 $cm^{-1}$ in the unloaded biomass arises from symmetric C=O vibrations ($COO^{-}$) at terminal amino acid in the biomass.[24] The shift from 1030.6 $cm^{-1}$ to 1024.3 $cm^{-1}$ is an indication of the participation of C-O group of the polysaccharide in the biosorption process.[23] The presence of a small distinct peak at 888.05 $cm^{-1}$ in the Cr(VI) treated biomass, is a characteristic finger print region attributed to the Cr=O bond of the Cr(VI) anion.[25]

The surface characteristics in the yeast immobilized cellulose matrix show some distinct agglomerated clusters after the adsorption of chromium (Fig. 3.2). The presence of Cr is observable from the peak position between 5-6 keV in the energy dispersive X ray spectrum of the biosorbent. The optical images also gave good evidence to the presence of adsorbed chromium. Initially, the image of the biosorbent was captured and then the optical image after chromium adsorption was obtained by the addition of diphenyl carbazide [21] to the glass slide

containing the adsorbent. The manifestation of a red violet colour in the optical image shows that hexavalent chromium interacts with the biomass immobilized cellulose matrix. The addition of chelating agent (diphenyl carbazide) to the unloaded biomass does not give any distinct colour, while the metal loaded adsorbent clearly shows the difference in the image pattern (Fig. 3.3) thereby substantiating the presence of chromium. The thermal stability and composition (Fig. 3.4) of yeast-cellulose biosorbent revealed that the initial loss in weight around 30-100$^{o}$C is due to the evaporation of water. Heterolytic depolymerization[26] involving the cleavage of the glycosidic linkage in cellulose leading to the formation of levoglucosan (anhydrocellulose) occurs at temperatures less than 300$^{o}$C. The formation of char and other volatiles are more probable at higher temperatures. The surface area of the biosorbent was found to be 2.04 $m^2/g$ with a pore size of 53.92 nm and a pore volume of 0.0275 $cm^3/g$. The pore size which is almost close to the upper limit of mesoporous range signifies that the biosorbent surface could be perceived to possess a mesoporous nature. The mesoporous nature of the yeast immobilized cellulose sorbent aids in the effective permeation of hexavalent chromium oxy anion and enhances the interaction with the surface hydroxyl groups of cellulose and the functional groups present in the biomass.

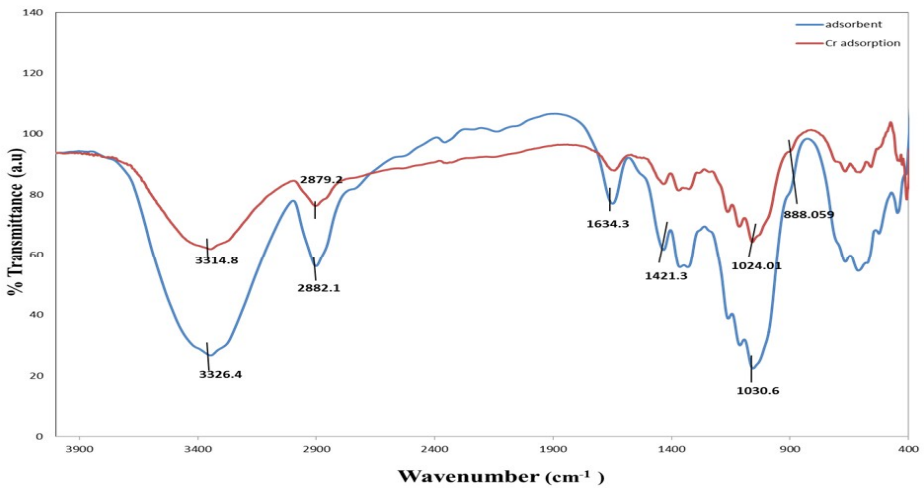


**Figure 3.1.** FT-IR spectrum of yeast impregnated cellulose adsorbent and after chromium adsorption

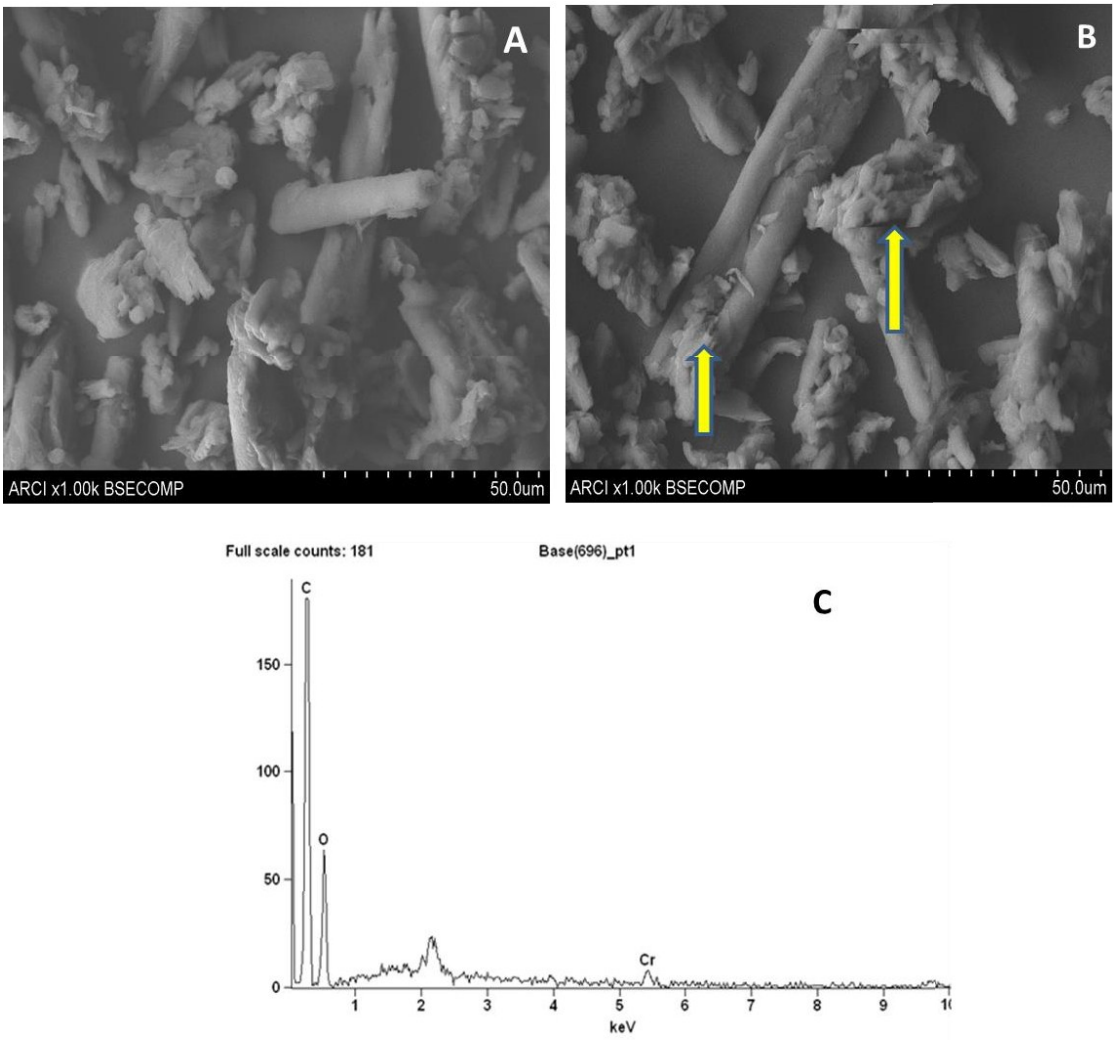


**Figure 3.2.** SEM images of yeast-cellulose biosorbent (A) and after chromium adsorption (B) and EDAX (C) after chromium adsorption

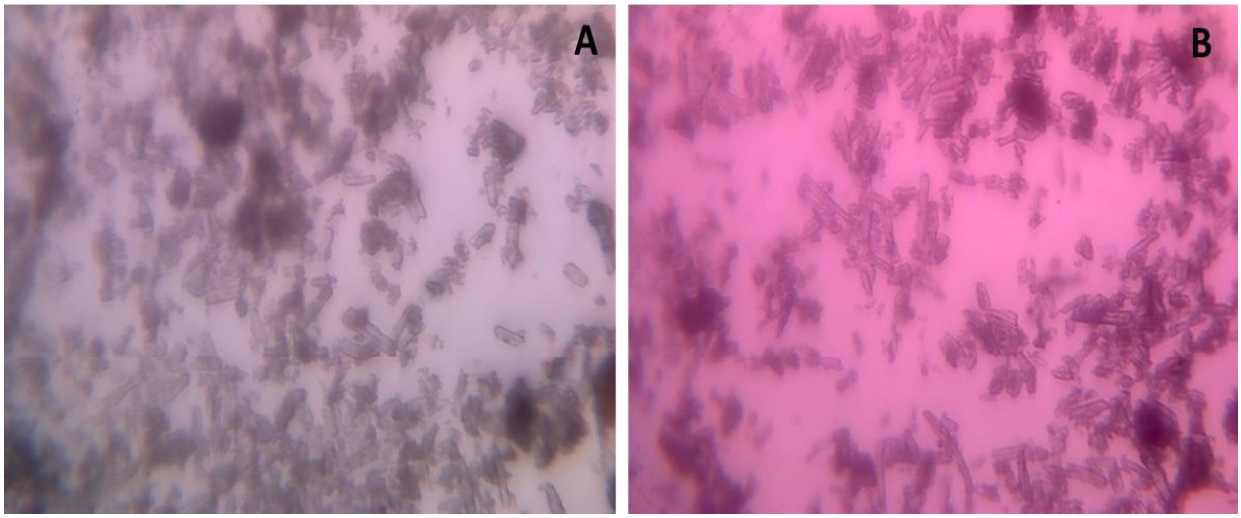


**Figure 3.3.** Optical images (A) before chromium adsorption (B) after chromium adsorption

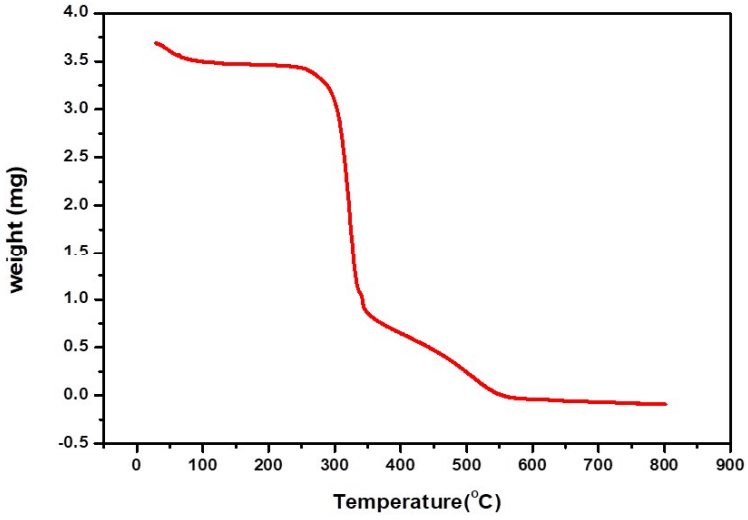


**Figure 3. 4.** Thermal analysis of the biosorbent

**(ii) Reproducibility of Cr(VI) adsorption under the microwave conditions**

Although, domestic microwave oven has certain limitations, it still finds good utility in some recently reported diverse applications such as preparation of nano sized metal oxides,[27] hydrolysis of proteins[28] and conversion of glycogen to glucose.[29] These applications are known to give good reproducibility and efficiency. Indeed, a Sharp R220A model multimode domestic microwave oven is also known for its utility [30] towards synthetic applications up to a reaction scale of 100 g. More recently, a Sharp 889R model house hold domestic microwave oven [31] has also proven to be very effective in the preparation of magnetic nanoparticles with good reproducibility. Literature reports suggest[30] that if the other experimental variables are kept constant, uniformity in the results are maintained in mono as well as multimode irradiation methods.

The pulse irradiation mode was adopted in the proposed methodology for the biosorbent preparation. The reproducibility of Cr(VI) adsorption was ascertained by adopting a procedure reported recently[28] in a study involving the protein hydrolysis using domestic microwave oven. Oakridge screw cap vials containing yeast and cellulose in the ratio 1:2 along with the other reagents were placed at four different positions inside the microwave oven to check the reproducibility. In order to foster uniform heating, the sample vials were placed inside a beaker filled with water. The placement of samples in a water bath ensures that any excess microwave energy to be absorbed by the water. Samples were irradiated for a total time interval of 200 sec in pulse mode at 160 W power levels with a 20 sec on and 30 sec off intermittent time duration. The temperature of the water bath after the microwave irradiation was measured as approximately 90$^{o}$C for the middle position and 60$^{o}$C at the other positions inside the oven. The vials containing the biosorbent were removed from the oven and cooled under tap water. The biosorbent was then given water wash (Millipore), filtered and dried in a vacuum oven at 40$^{o}$C. The reproducibility in the percentage adsorption was verified using a known concentration (30 mg $L^{-1}$) of Cr(VI) for the samples irradiated at various positions. Similar experiments were conducted in the absence of a water bath and the reproducibility in both instances was verified by performing the experiments in triplicate. The percentage adsorption of Cr(VI) was quite effective and almost consistent (Table 3.1 ) with an average deviation of ±1 %. The biosorbent was

prepared as and when required in small amounts and quantitative adsorption could be obtained for the optimized Cr(VI) concentrations. The pulse mode of microwave irradiation at fixed power ensures there is no overheating and also takes care of the possible degradation of the biosorbent. Yeast, cellulose and the other reagents used in biosorbent preparation are non-toxic and safe to handle and hence the low and intermittent exposure to microwave radiation is safe enough that it does not result in the build-up of toxic vapors inside the oven**.**

**Table 3.1.** Reproducibility check at different locations of the samples (in the presence and absence of water bath) inside the microwave oven

| **With water bath** | **Percentage (%) adsorption of Cr(VI)** |
|---|---|
| Position 1 (Middle ) | 97.0±1.02 |
| Position 2 | 94.0±0.80 |
| Position 3 | 93.4±0.90 |
| Position 4 | 93.0±0.85 |
| Without water bath | |
| Position 1 (Middle ) | 96.7±1.04 |
| Position 2 | 94.3±0.80 |
| Position 3 | 93.0±0.75 |
| Position 4 | 93.0±0.80 |

**(iii) Interaction mechanism**

The interaction between Cr(VI) and the microbe immobilized biopolymer is also influenced by the pH conditions prevailing in the aqueous phase and also the existence of Cr(VI) ions in various forms such as $HCrO_4^-$, $Cr_2O_7^{2-}$ , $CrO_4^{2-}$ and point of zero charge or isoelectric point of the biosorbent surface. The surface of biosorbent is neutral at a particular pH and this indicates the point of zero charge and was found out by performing the experiments using salt addition method. [32] About 0.15 g of yeast- cellulose adsorbent was added to 50 mL of 0.1 mol $L^{-1}$ NaCl solution at different initial pH (2.0-9.0) by addition of HCl or NaOH. The experiments were carried out in an orbital incubator shaker at 25 °C for 24 h at 120 rpm. After equilibration for 24 h, the final pH of the solutions was measured. The point of zero charge ($pH_{pzc}$) was determined from the plot of ΔpH [$pH_{initial} - pH_{final}$] against $pH_{initial}$. The resultant point of zero charge was found to be 4.0 (Fig 3.5a) which implies that the surface charge on the biosorbent is positive below $pH_{pzc}$ and negative above $pH_{pzc}$. The maximum equilibrium adsorption capacity of Cr(VI) was observed at pH 2.5-3.0. At varying pH conditions, the percentage adsorption was calculated and it was found that effective retention occurs at pH 2.5. More than 95% of Cr(VI) could be held onto the biosorbent surface in an acidic environment and indeed at this pH the existence of chromium is most probable as $HCrO_4^-$ oxy anion. [33] At pH values less than the $pK_a$ (5.8) of $HCrO_4^-$ anion, the hexavalent chromium is present as dichromate and hydrogen chromate oxy anion ($HCrO_4^-$). Although, the hydrogen chromate oxy anion can exist in equilibrium with dichromate, ($2HCrO_4^- \rightleftharpoons Cr_2O_7^{2-} + H_2O$) it is only at pH<2 and high Cr(VI) concentrations, the existence of dichromate anion would be more probable [34] and hence around pH 3.0, (Fig. 3.5b) it is the hydrogen chromate anion that interacts with the positively charged biosorbent surface. The protonation of the active surface functional groups in the biomass immobilized cellulose is also obvious at this pH and hence the electrostatic interaction would occur between the negatively charged oxy anion and the positively charged biosorbent surface. Furthermore, in accordance with the HSAB principle Cr(VI) as $HCrO_4^-$ (hydrochromate anion ) is harder in comparison to $CrO_4^{2-}$ anion.[35] The hardness of these anions follows the order $OH^- > HCrO_4^- > CrO_4^{2-}$ and hence at acidic pH the hydrochromate oxyanion interacts electrostatically with the protonated functional groups (hydroxyl and amine) of the biosorbent surface. Glutaraldehyde cross linking

stabilizes the biopolymer and the yeast could be immobilized in the voids present between the cellulose layers. The protonated amine and hydroxyl groups are involved in the ion-pair interaction (Fig. 3.6) and this columbic force of attraction reinforces the microbial cell surface and enhances the uptake of chromium. It is obvious that when the pH increases, the uptake of chromium by the yeast immobilized biopolymer decreases as a result of the competition between the oxy anion as well as hydroxide for the surface active sites present on the biosorbent. Electrostatic repulsion between the oxy anion and the surface negative biosorbent reduces the chromium uptake leading to considerably less adsorption at higher pH values. The time required for microwave radiation in the immobilization of yeast also had a profound influence on the percentage adsorption of chromium. Beyond 200 sec, there was a considerable decrease (Fig.3.7) in the retention of chromium. Higher time duration could probably lead to the slow degradation of the biopolymer thereby reducing the active adsorption sites required for the interaction with hexavalent chromium. With 0.4 g of the biosorbent (Fig.3.8) the uptake of hexavalent chromium was facile (98%) and this was observed up to 0.8 g. However, when the biosorbent dosage was increased to 1.0 g, there was a significant drop in the uptake of chromium.

Higher biosorbent concentrations leads to cell agglomeration and decreases the inter-cellular distance by screening the solid cell layers and this results in protecting the active binding sites from effective interaction with the $HCrO_4^-$ ion.[36] Simplistically, it can be stated that the metal ion uptake is higher at lower amounts of the biosorbent when the intercellular distance is higher and this ensures optimum electrostatic interaction between the protonated microbial cell surface and hexavalent chromium (VI).

In general, adsorption coupled reduction is probable when biomass is used for the sequestration of chromium. Under the optimum experimental conditions, the immediate reduction of Cr(VI) to Cr(III) was not observed on the biosorbent surface. The emergence of pale green coloration on the adsorbent surface, characteristic of trivalent chromium was discernible only after 72 hours. However, immediately after the adsorption of hexavalent chromium, the supernatant solution was also checked for the presence of any trace amounts of trivalent species. The total chromium concentration was measured using AAS. The reduction of Cr(VI) to Cr(III) was checked by taking a fixed concentration of hexavalent chromium ( 30 mg $L^{-1}$) and after treating with

biosorbent the final concentration of total chromium from AAS measurement was found to be 2.193 mg $L^{-1}$ in solution. Cr(VI) present in the supernatant was analyzed spectrophotometrically and was found to be 1.716 mg $L^{-1}$. The concentration of Cr(III) (Total Cr = Cr (VI) + Cr(III)) was found to be 0.4764 mg $L^{-1}$ in the solution phase. Hence, in alkaline medium, hexavalent chromium could be desorbed from the biosorbent surface as sodium chromate ($Na_2CrO_4$) with 2.0 mol $L^{-1}$sodium hydroxide solution.[27]

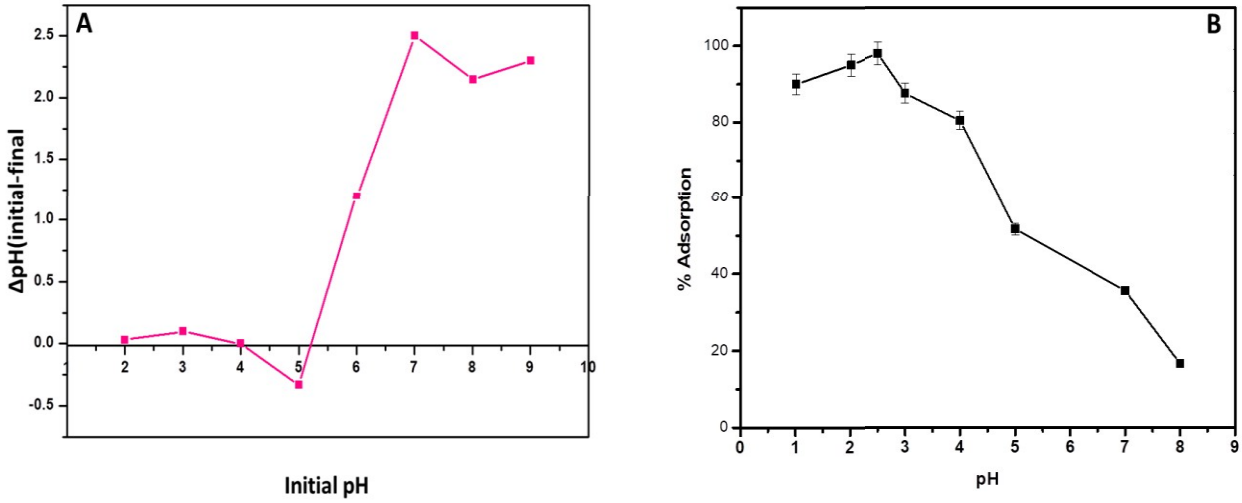


**Figure 3.5. (A)** Determination of $pH_{pzc}$ **(B)** Effect of pH **(**conditions: adsorbent dosage- 0.4 g/20 mL, Cr(VI) concentration- 50 mg $L^{-1}$, T=25$^{o}$C.)

,

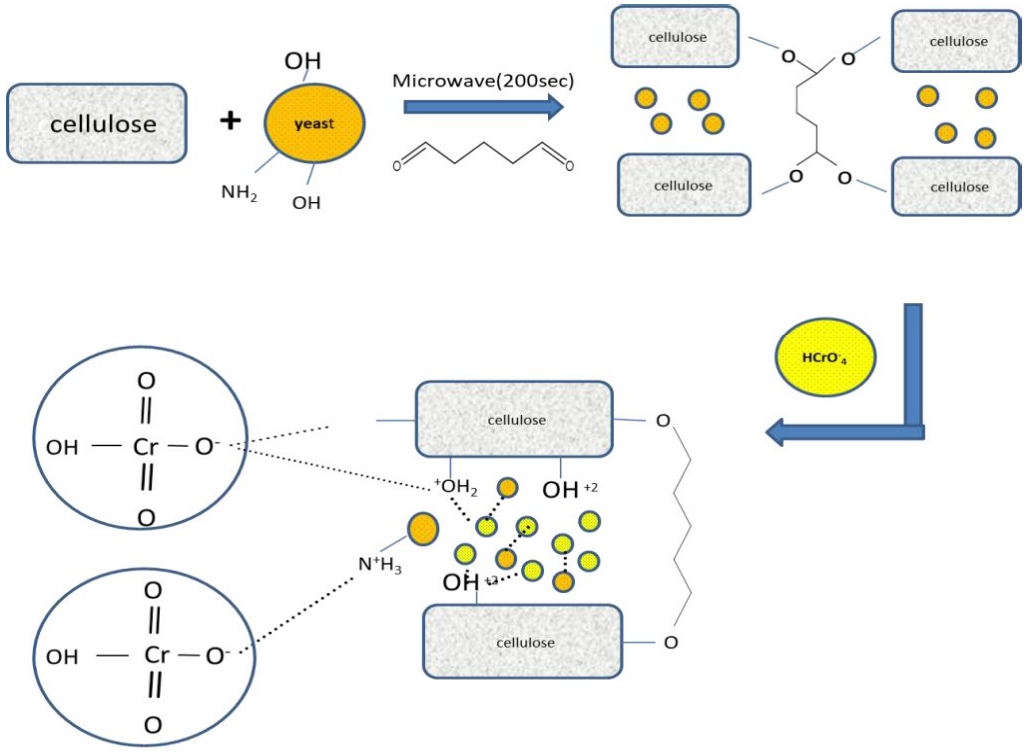


**Figure 3.6**. Schematic illustration showing the interaction of Cr(VI) and yeast–cellulose adsorbent

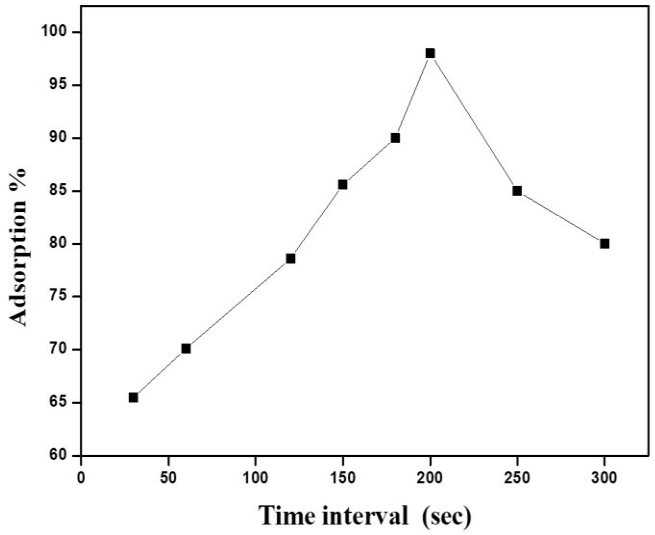


**Figure 3.7.** Variation of microwave irradiation time

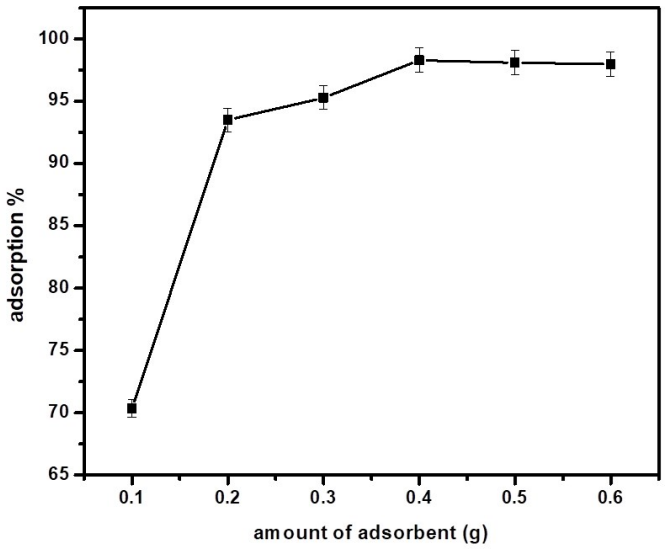


**Figure 3.8.** Effect of adsorbent dosage **(**conditions: pH-2.5

Cr(VI) concentration -50 mg $L^{-1}$, T=25$^{o}$C.)

**(iv) Equilibrium isotherms, kinetics and thermodynamics**

The characteristic features in the interaction between the biomass immobilized cellulose and Cr (VI) could be accounted by correlating the experimental adsorption data with isotherm models.[55-59] Equilibrium isotherms such as Langmuir and Freundlich are fairly popular in fitting the data. Several isotherm models (Fig.3.9 A-E) were tested and it was observed that the Langmuir isotherm plot offers a higher regression coefficient and a statistically low chi square value ($\chi 2$= 0.23). The applicability of the Langmuir model was also confirmed from the dimensionless $R_L$ value [42] which relates $C_o$, a particular initial concentration of Cr(VI) to the energy of adsorption b as $R_L$= 1/1+bCo, and a value below unity indicates a reversible isotherm. The parameters obtained for the other isotherm parameters are also shown (Table 3.2) for a comparative analysis of the adsorption data. The *'g''* value obtained through R-P isotherm could also serve as an indicator in understanding the utility of Langmuir model. Essentially, from this model a *'g*" value close to 1 was obtained and therefore the Redlich isotherm equation would now reduce to the simple Langmuir isotherm model. The mean free energy of adsorption (0.639 kJ $mol^{-1}$)

obtained through the Dubinin-Raduskevich (D-R) isotherm indicates the electrostatic interaction between the functional groups present in the biosorbent surface and the chromium (VI) oxy anion. The pH of the aqueous phase, temperature and adsorbent-adsorbate interactions govern the uptake of Cr(VI). Temkin isotherm is more suited to gas phase adsorption, since the biosorption from solution phase is governed by the above factors which are relatively more complex than the simple processes involved in gas phase adsorption. Hence, the Temkin isotherm model is not more appropriate to explain the adsorption data.

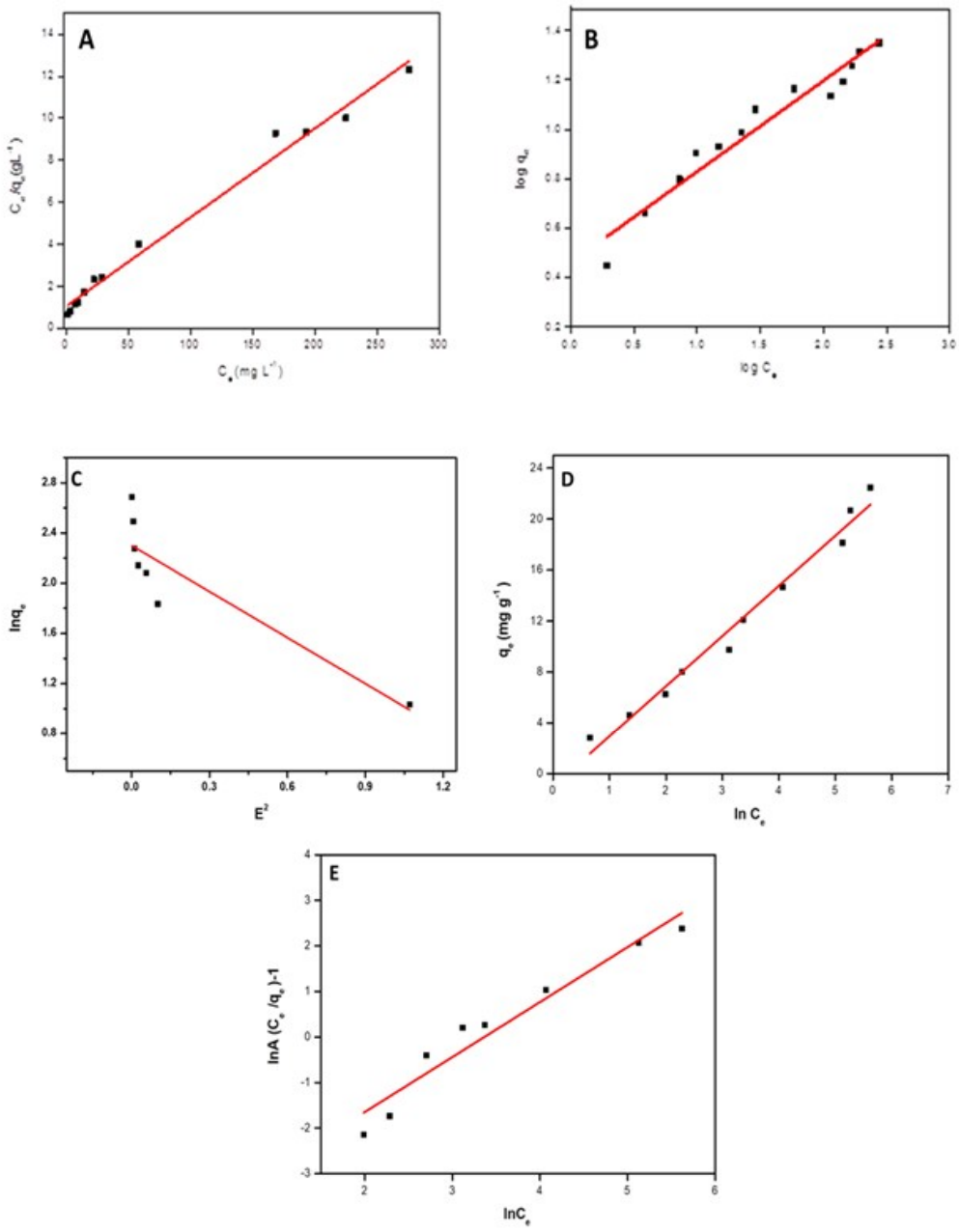


**Figure 3.9.** A) Langmuir isotherm B) Freundlich isotherm C) D-R isotherm D) Temkin isotherm E) Redlich isotherm (conditions: pH-2.5, adsorbent dosage- 0.4 g/20 mL, T=25$^{o}$C)

**Table 3.2.** Model adsorption isotherm parameters

| | | | | | |
|---|---|---|---|---|---|
| **Langmuir** | $q_o$(mg $g^{-1}$) | b(L $mg^{-1}$) | $R^2$ | $\chi^2$ | $R_L$ |
| | 23.61 | 0.0405 | 0.9865 | 0.229 | 0.4513 |
| **Freundlich** | $K_F$($mg^{11/n1}L^{1/n}$) | n | $R^2$ | $\chi^2$ | |
| | 2.893 | 2.7169 | 0.9494 | 0.409 | |
| **Dubinin Radushkevich** | $q_m$(mg $g^{-1}$) | β($mol^2kJ^{-2}$) | $R^2$ | E(kJ $mol^{-1}$) | $\chi^2$ |
| | 9.9755 | 1.2227 | 0.7597 | 0.6395 | 1.120 |
| **Temkin** | A (L $g^{-1}$) | B (J $mol^{-1}$) | $R^2$ | $\chi^2$ | |
| | 0.7784 | 3.9367 | 0.97809 | 0.9348 | |
| **Redlich-Peterson** | g | B(L $mg^{-1}$) | $R^2$ | $\chi^2$ | A(L $g^{-1}$) |
| | 1.2075 | 0.01721 | 0.9336 | 0.469 | 0.9576 |

In order to evaluate the kinetics involved in the interaction between the metal and the microbe immobilized biopolymer, the pseudo first order (Fig. 3.10 A) and second order kinetic models[43,44] were utilized to analyse the experimental adsorption data. Under magnetic stirring for 3 h, the uptake of Cr(VI) by the biomass immobilized cellulose was found to be maximum. The Cr(VI) uptake kinetics could be best depicted using the second order plot (Fig. 3.10 B) by virtue of a better regression coefficient value (Table 3.3). The experimental and calculated $q_e$ values were found to be 2.8 mg $g^{-1}$ and 3.12 mg $g^{-1}$ respectively. The influence of film, particle diffusion or surface adsorption is the usual phenomena associated with the transport of Cr(VI). At higher Cr(VI) concentration, intraparticle diffusion is favoured, while at lower metal ion concentration where there is effective interaction between the microbe immobilized cellulose and Cr(VI), film diffusion would influence the adsorption kinetics.[45] In fact, from the Weber-Morris

intraparticle diffusion model ($q_t = k_t\sqrt{t}$) and the graphical correlation between $q_t$ and $\sqrt{t}$ (Fig. 3.10 C) it could be inferred from the definite intercept value about the influence of boundary layer phenomenon in explaining the Cr(VI) uptake kinetics.

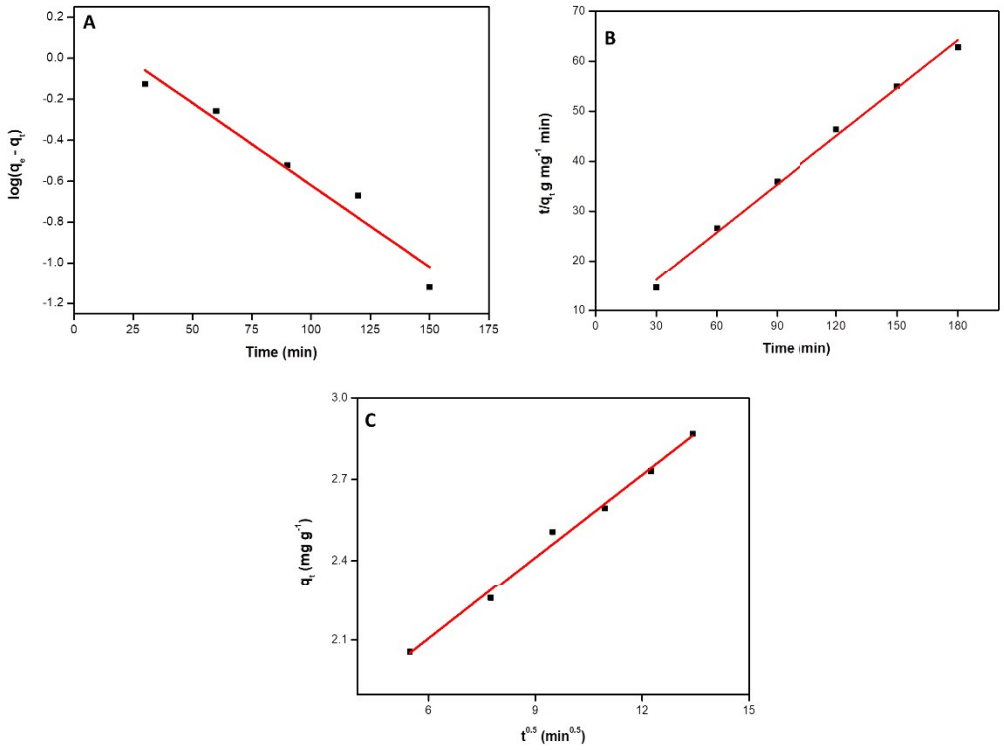


**Figure 3.10.** A) Pseudo first order kinetics B) Pseudo second order kinetics C) Intra particle diffusion (conditions: pH-2.5, adsorbent dosage- 0.4 g/20 mL, T=25$^{o}$C)

**Table 3.3** Kinetic data for chromium (VI) adsorption onto the biosorbent

| $C_o$ (mg $L^{-1}$) | $q_e$ (mg $g^{-1}$) | $k_2$ (g $mg^{-1}$ $min^{-1}$) | $R^2$ | $k_1$ ($min^{-1}$) | $R_1^2$ | $k_{int}$ (mg $g^{-1}$ $min^{-1/2}$) |
|---|---|---|---|---|---|---|
| 30 | 3.12 | 0.0156 | 0.9943 | 0.0184 | 0.9371 | 0.1019 |

An insight towards the spontaneity and energetics involved in the interaction between the host matrix (biosorbent) and the guest (Cr(VI)) can be best explained through the Gibb's free energy ($\Delta G^o$), enthalpy ($\Delta H^o$) and entropy ($\Delta S^o$) values. From the ratio of the concentrations of Cr(VI) present at equilibrium on the biosorbent surface and the solution phase, the equilibrium constant (K) was obtained at different temperatures. These equilibrium constant values were fitted into the Gibb's isotherm equation ($\Delta G^0 = -RTlnK$). Since, activity (a) is directly proportional to concentration (C) of the Cr (VI) in low concentrations. In solution phase, in the case of a reaction with several components, the free energy change of the reaction can be expressed as:

$$\Delta G^o = -RTlnK_c = -RTlnK_D \qquad (3.1)$$

Furthermore, through the plot of lnK against 1/T (Fig. 3.11) the entropy and enthalpy changes (Table 3.4) could be obtained for the interaction of Cr(VI) with the biosorbent. Essentially, all these parameters are categorized as extensive or additive properties and hence the first stage involving immobilization of the biomass as well as subsequent adsorption on to the surface would collectively influence the overall free energy, enthalpy and entropy changes associated with the adsorption.

$$(\Delta G^o) = \Delta G^o_{\text{cellulose-yeast}} + \Delta G^o_{\text{cellulose-yeast-chromium}} \qquad (3.2)$$

$$(\Delta S^o) = \Delta S^o_{\text{cellulose-yeast}} + \Delta S^o_{\text{cellulose-yeast-chromium}} \qquad (3.3)$$

$$(\Delta H^o) = \Delta H^o_{\text{cellulose-yeast}} + \Delta H^o_{\text{cellulose-yeast-chromium}} \qquad (3.4)$$

The transport of Cr(VI) oxy anion from the solution phase to the biosorbent surface is partially governed by the concentration gradient across the biosorbent-solution interphase. This is reflected in the free energy difference and since the concentration of Cr (VI) is greater in the solid surface than in solution, the spontaneity in the adsorption process is illustrated through the negative $\Delta G$ values obtained at different temperatures used for studying the uptake of chromium. Adsorption of Cr(VI) essentially occurs due to the transport of the ionic species from the bulk to the yeast immobilized biopolymer surface. The free energy associated with the solvation of the host (biosorbent) and guest ($HCrO_4^-$) also results in better ordering and the negatively charged $HCrO_4^-$ oxy anion could interact with the surrounding water molecules through hydrogen

bonding. Hence, the enthalpically favorable exothermic interaction (positive slope of lnK against 1/T) between Cr(VI) oxy anion and the biosorbent results in large negative entropy change indicating better ordering at the biosorbent-solution interphase. The average activation [33,46] energy, $E_a = \Delta H^o_{ads} + RT$ also reflects the exothermic interaction (Table 3.4) between hexavalent chromium and the microbe immobilized biopolymer surface.

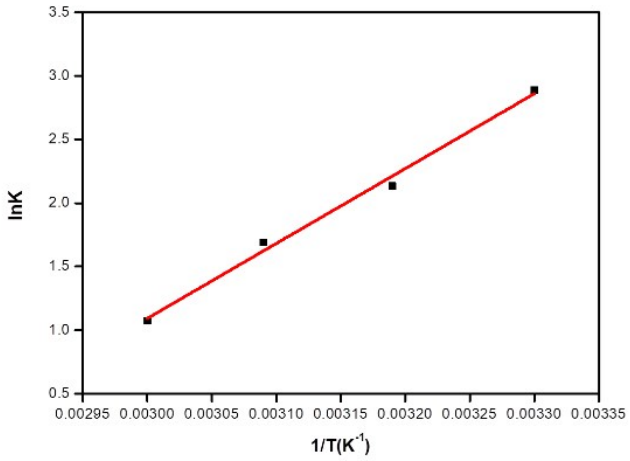


**Figure 3.11.** Van't Hoff plot

(conditions: pH-2.5, adsorbent dosage- 0.4 g, Cr(VI) concentration- 30 mg $L^{-1}$)

**Table 3.4.** Thermodynamic parameters for Cr(VI) adsorption

| **Temperature (Kelvin)** | **$\Delta G^0$ (kJ $mol^{-1}$)** | **$\Delta S^0$ (J $mol^{-1}K^{-1}$)** | **$\Delta H^0$ (kJ $mol^{-1}$)** | **$E_a$(kJ$mol^{-1}$)** |
|---|---|---|---|---|
| 303 | -7.275 | -137.757 | -48.949 | -43.8 |
| 313 | -5.551 | | | |
| 323 | -4.543 | | | |
| 333 | -2.973 | | | |

**(v) Laboratory scale fixed bed column studies**

Prior to applying the methodology in a simulated waste effluent, the suitability was examined in a laboratory scale fixed bed column study. With 2.0 g of the yeast immobilized biopolymer adsorbent packed onto a short glass column, 5 mg $L^{-1}$ of Cr(VI) could be retained well up to a sample volume of 300 mL. Retention of chromium onto the biosorbent surface was equally effective with a flow rate of 5 mL $min^{-1}$. Above this volume, there was a decrease in the retention efficiency (Fig. 3.12 A) and this could be attributed to bed expansion [33] thereby forcing the Cr(VI) out of the column. This eventually results in reducing the retention of chromium on to the biosorbent surface due to the weakening of the interaction between the oxy anion and the functional groups present in the biosorbent. Cr(VI) could also be easily desorbed using 2.0 mol $L^{-1}$ sodium hydroxide (Fig. 3.12 B) effectively as sodium chromate from the column.

Since, real effluent such as tannery waste water would contain Cr(III) appreciably than Cr(VI), it is also necessary to check the uptake of chromium in the +3 oxidation state. It was observed that at pH 7.5, 10 mg $L^{-1}$ of the trivalent chromium could be retained onto the biosorbent surface. This is quite expected at this pH, since the cationic [47] chromium (III) hydroxides ($Cr(OH)_2^+$,$Cr(OH)^{2+}$) can enter into an electrostatic interaction with the functional groups present on the biomass immobilized cellulose adsorbent surface. Trivalent chromium could be recovered from the biosorbent surface using dilute sulfuric acid (1.0 mol $L^{-1}$) as Cr(III) sulfate.[33] The difference in pH at which the trivalent and the hexavalent forms of chromium are retained onto the biosorbent surface would be very useful for the speciation of chromium.

A simulated waste water was prepared containing 100 mg $L^{-1}$ of commonly encountered ionic constituents such as chloride, nitrate, sulfate and phosphate and 50 mg $L^{-1}$of Fe(II), Co(II), Cu(II), Ni(II) and Zn(II). A 10 mg $L^{-1}$ solution of hexavalent chromium was mixed with the above ions and it was observed that 9.45 mg $L^{-1}$ could be retained onto the biosorbent surface. The reduction in the retention efficiency at acidic pH could arise due to the interference of Fe(II), due to its ability to reduce +6 chromium to +3 state.[33] The competition for the active adsorption sites from other anions could also be attributed to the decreased retention of Cr(VI).

After elution of the hexavalent chromium, the problem of Cr(VI) disposal is an important issue to be taken into consideration. Two strategies were adopted in order to avoid the direct disposal of higher concentration of chromium in the laboratory sink. The hexavalent chromium in the eluate was diluted and reduced to the less toxic Cr(III) and preserved separately. As a second strategy, the Cr(VI) from the eluate was diluted and utilized for the subsequent experiments.

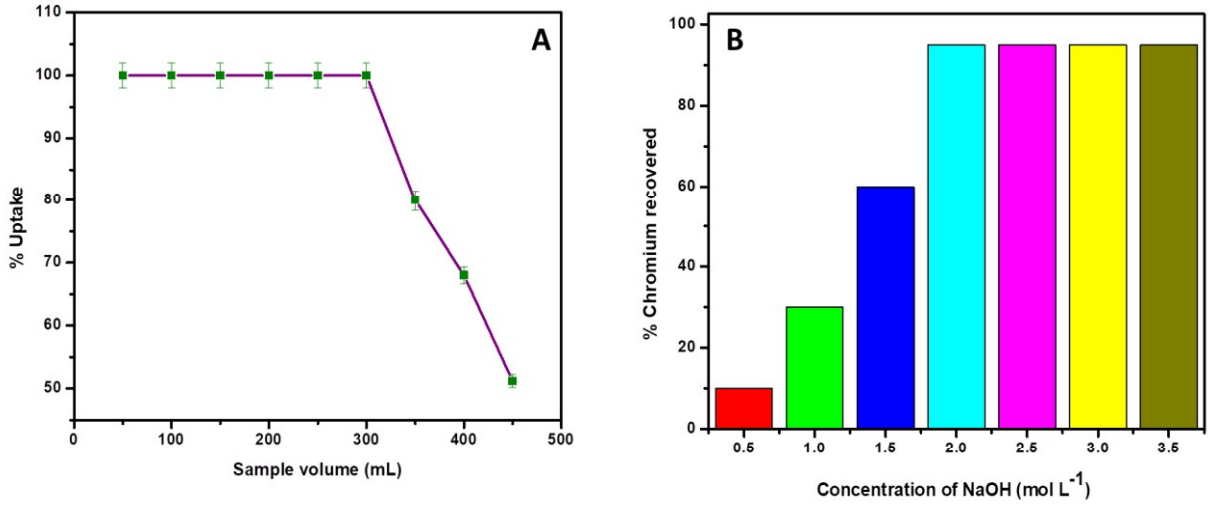


**Figure 3.12 (**A) Effect of Sample volume (conditions: weight of adsorbent- 2.0 g, Cr(VI) concentration- 5 mg $L^{-1}$, pH- 2.5, flow rate- 5 mL $min^{-1}$) (B) Effect of NaOH concentration

### 3.1.4. Conclusions

This work has shown that microwave irradiation provides an effective approach to immobilize yeast in a biodegradable cellulose polymeric support and bioremediation as a sustainable alternative to detoxify chromium. The conventional method for the preparation requires 3 hours for the immobilization of yeast. With a simple microwave oven, it requires just 200 sec for immobilizing yeast and shows a good adsorption capacity of 23.61 mg $g^{-1}$ for Cr(VI). In the range 10-30 mg $L^{-1}$ Cr(VI), yeast as such shows an average adsorption of 92.6 %, whereas glutaraldehyde cross linked cellulose immobilized with yeast gives an average adsorption value of 98.8 %. The adsorption of chromium with cellulose as such was found to be only 49.6 % and when yeast is immobilized within the biopolymer matrix the adsorption capacity of the cellulose

is enhanced two fold thereby improving its metal uptake to great extent. Cr(VI) as well as Cr(III) could be removed at acidic and alkaline pH respectively. The biosorbent could be regenerated using 2.0 mol $L^{-1}$ sodium hydroxide. The negative free energy ($\Delta G$) and the enthalpy changes ($\Delta H$) confirm the spontaneous and exothermic aspects of the biosorption process. The $\Delta S$ values were also found to be negative and this shows the decreased randomness at the fungi immobilized biopolymer-solution interface. Among the various isotherms, Langmuir model gave a good fit to the biosorption data with a high correlation coefficient and a statistically lower chi square value. Further, the uptake of Cr(VI) was also in accordance with the second order kinetic model. Furthermore, yeast and cellulose are non-toxic and hence this low cost blend adsorbent serves as a promising green option for chromium remediation.

## 3.2. *Saccharomyces cerevisiae* immobilized in MWCNTs for the effective removal of hexavalent chromium

### 3.2.1 Introduction

The possibility of utilizing microbes remains promising, making the microbe immobilized matrices open for exploration as suitable biosorbents. The current method deals with the immobilization of *Saccharomyces cerevisiae* (yeast) in MWCNTs. A eukaryotic unicellular microbe *Saccharomyces cerevisiae* (*S.cerevisiae*) commonly known as baker's yeast is easily available and is known to have broad applications in food industry[48] such as wine making, brewing, baking etc., As *S. cerevisiae* is classified under Generally Recognized as Safe (GRAS) product, it is widely used in industrial water treatment[49]. Sathvika et al.[50] developed microbe based biosorbents with yeast immobilized in glutaraldehyde crosslinked cellulose matrix for the effective removal of Cr(VI) with a monolayer adsorption capacity of 26.31 mg $g^{-1}$.Titania-yeast nanocomposite showed excellent potential of 99.2% removal for hexavalent chromium.[48]

The recently reported MWCNTs adsorbents for the treatment of Cr(VI) solutions are as follows:. magnetic $Fe_2O_3$ nanoparticle-MWCNTs composite developed by Lu et al.[51] was checked for the efficient removal of Cr(VI) at different temperatures with a $q_{max}$ of 42.02 mg $g^{-1}$ at 35$^{o}$C. Machine et al. developed Fe-Ag/f-MWCNT/PES Nanostructured-Hybrid Membranes which could remove 94.8% of Cr(VI) from aqueous solution.[52] Chitosan was immobilized in nanoparticles and carbon nanotubes by forming a nanocomposite which could efficiently remove Cr(VI) up to 84% within a short contact time.[53] Reports involving microbe-MWCNTs combination for the sequestration of heavy metals are scarce. Yan et al.[54] reported MWCNTs – calcium alginate complex immobilized in *Shewanella oneidensis* which showed higher reduction capacity of Cr(VI). *Pseudomonas aeruginosa* was immobilized in CNTs for effective adsorption of various heavy metals with $q_{max}$ 6.60 mg $g^{-1}$ for cobalt, 6.18 mg $g^{-1}$ for cadmium, 6.07 mg $g^{-1}$ for lead, 5.83 mg $g^{-1}$ for manganese, 6.23 mg $g^{-1}$ for chromium (III) and 5.25 mg $g^{-1}$ for Ni.[55] There are no reports on the combination of *yeast* -MWCNTs for sequestration of Cr(VI) . The pristine MWCNTs were functionalized and then were involved in coupling reaction with the

amines present on the cell wall of microbes to form amide which react with hydrochromate ion and thus sequesters Cr(VI) from aqueous solutions.

### 3.2.2 Experimental section

#### (i) Preparation of the *Yeast* – MWCNTs biosorbent

The yeast grown on YEPD medium was used.[50] $KMnO_4$ is used for the oxidation of pristine MWCNTs as reported previously. [56] For the initial step of oxidation, a 200 mL of 0.5 mol $L^{-1}$ $H_2SO_4$, was mixed with 0.25 g of $KMnO_4$. In another beaker, 0.1g of MWCNTs, 200 mL of 0.5 mol $L^{-1}$ $H_2SO_4$ was added and subjected to ultra-sonication for 30 min to ensure proper dispersion. The sonication is followed by heat treatment of MWCNTs to 150 $^oC$ prior to the addition of $KMnO_4$ solution dropwise. The solution was mixed properly and was refluxed for 5 hours at 150 $^oC$. After cooled down to room temperature, 10 mL of concentrated HCl was added to dissolve $MnO_2$. The oxidized MWCNTs were washed till the pH reached between 6.0-7.0 and then dried at 100 $^oC$.

For the preparation of the biosorbent, the dried MWCNTs were used along with microbes (free amine sources) by involving in EDC-HOBT coupling. To the DMF (dimethyl formamide) solvent 0.1g of oxidized MWCNTs, 0.1g each of EDC, HOBT and 3 mL of triethylamine were added stirred for 20 minutes. 3.0 g of yeast was added to the solution and the mixture was stirred overnight for the coupling reaction to take place.[57] The reaction mixture was filtered, washed with water and dried at 80$^oC$ and further used for metal adsorption studies.

#### (ii) Synthesis of probes for Cr(VI) and Cr(III)

The hexavalent and trivalent chromium have specific binding probes to differentiate them. Rhodamine based sensors such as Rhodamine B hydrazide (RBH)[58] and Rhodamine based chemo sensor (RF)[59] are selected due to its spiro lactam structure and spiro ring opening of sensing a molecule. The probes were synthesized as described in literature [58, 59] which are specific for Cr(VI) and Cr(III) respectively and the samples were prepared for capturing the laser confocal images.

**(iii) Batch adsorption studies**

The efficiency of the method was tested by performing batch adsorption parameters such as pH, adsorbent dosage, kinetics, and thermodynamics. To treat 20 mL of 5 mg $L^{-1}$ Cr(VI) solution at pH 2.0, a 0.1g of the biosorbent was used. The equilibration was attained in 180 min by using an orbital incubator shaker (Biotechnics, India) operating at 120 rpm maintained at 30$^{o}$C. The concentration of Cr(VI) was estimated using ion chromatography coupled with a UV detector.

### 3.2.3 Results and Discussion

**(i) Characterization of the biosorbent**

The FTIR spectra of pristine and oxidized CNTs, multiwalled carbon nanotubes-yeast (CNTY) before and after Cr(VI) adsorption were recorded (Fig. 3.14). The peak at 1732 $cm^{-1}$corresponds to C=O of carboxylic acid confirming the oxidation with the introduction of COOH groups on the surface of MWCNTs. The carboxyl groups fluctuations leads to comparatively broader O-H stretch at 3410 $cm^{-1}$ than in pristine CNTs. Symmetric and asymmetric $COO^{-}$ stretchings[60] gives rise to two peaks at 1387 $cm^{-1}$ and 1625 $cm^{-1}$. An amide bond at 1648 $cm^{-1}$ indicate the successful immobilization of microbe in MWCNTs assisted by EDC-HOBT coupling and also this peak is due to amide-1 of protein-peptide bond from the microbes.[23] The disappearance of carboxyl C=O peak after the amide formation indicates the involvement of carboxyl groups present on the surface of MWCNTs in amide formation. The band at 1546 $cm^{-1}$ corresponds to amide-II of in plane N-H bending.[61] The changes in the amide bond, O-H and C=O wavenumbers after Cr(VI) adsorption indicate they were involved in Cr(VI) uptake by protonating in acidic medium thereby forming electrostatic interactions with Cr(VI) . The field emission scanning electron microscope (FESEM) and high resolution scanning electron microscopy (HRTEM) images of pristine, oxidized MWCNT and the biosorbent before and after Cr(VI) adsorption were recorded. The tiny lumps in FESEM images (Fig. 3.14 c,d) and the particulates on MWCNTs in HRTEM images (Fig 3.15) indicate microbial immobilizations. The oxidation process caused minimal irregularities in the wall surfaces of MWCNTs[60] as indicated in Fig. 3.15 . The elemental analysis of the biosorbent before and after adsorption of Cr(VI) was

recorded using Energy Dispersive X-ray Spectroscopy indicating Cr(VI) adsorption onto the biosorbent with characteristic peak between 5-6 keV (Fig 3.14 e,f).

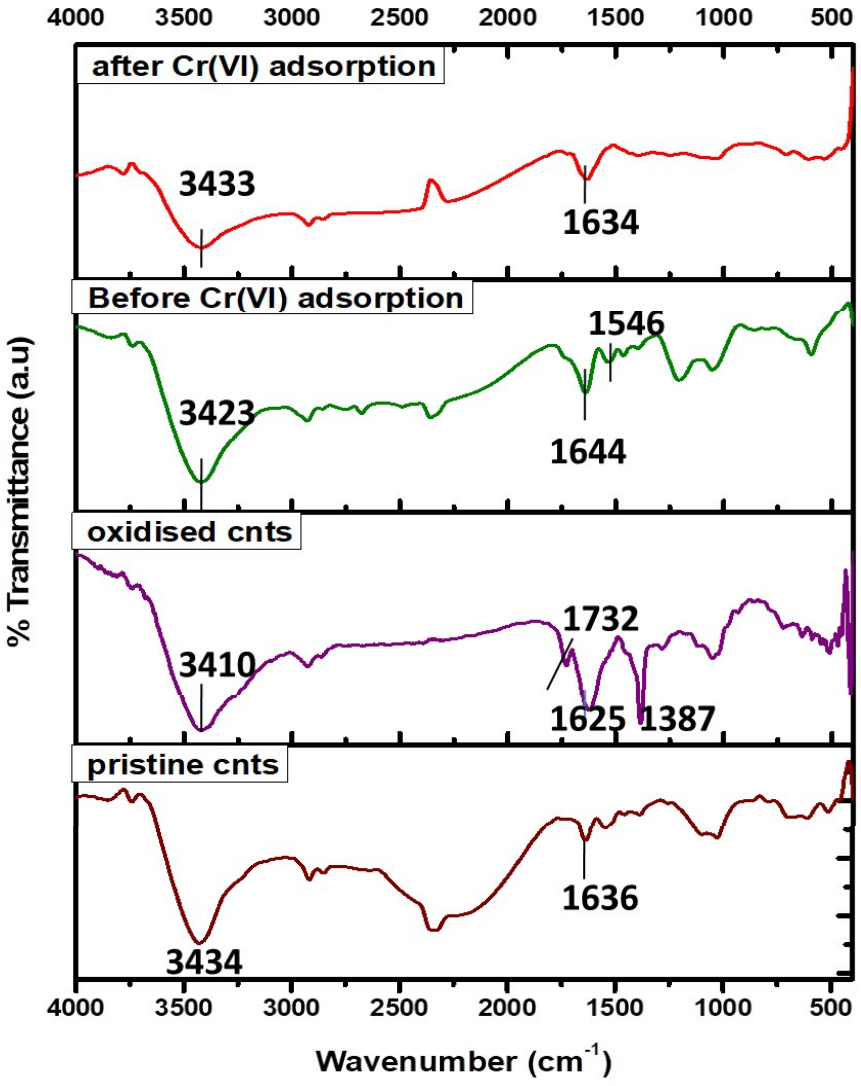


**Figure 3.13.** FTIR spectra of pristine, oxidized MWCNTs, biosorbent before and after Cr(VI) adsorption.

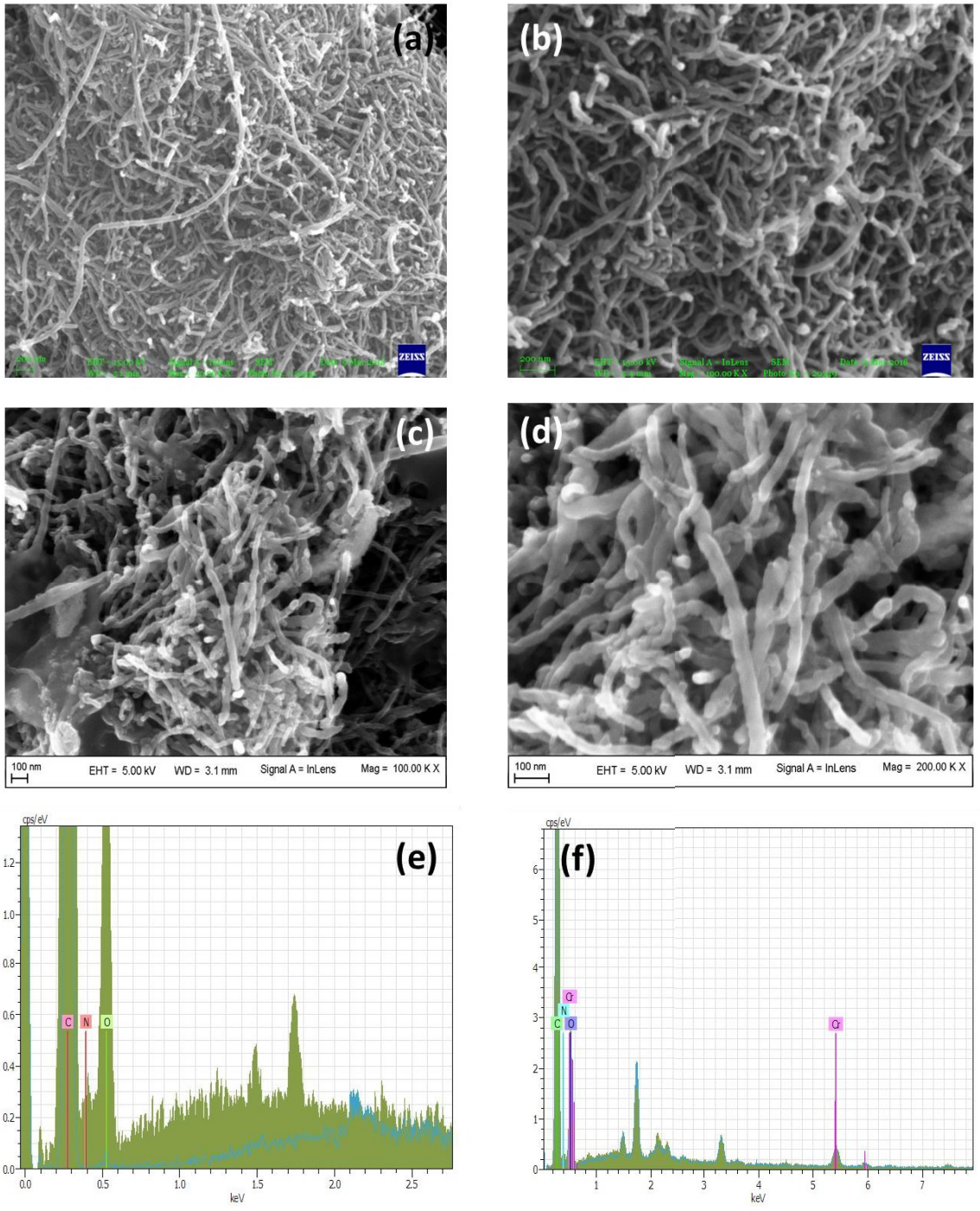


**Figure 3.14.** FESEM images of (a) pristine MWCNTs (b) oxidized MWCNTs (c,d) Biosorbent before and after Cr(VI) adsorption respectively. EDAX spectra of (e,f) CNTY before and after Cr(VI) adsorption.

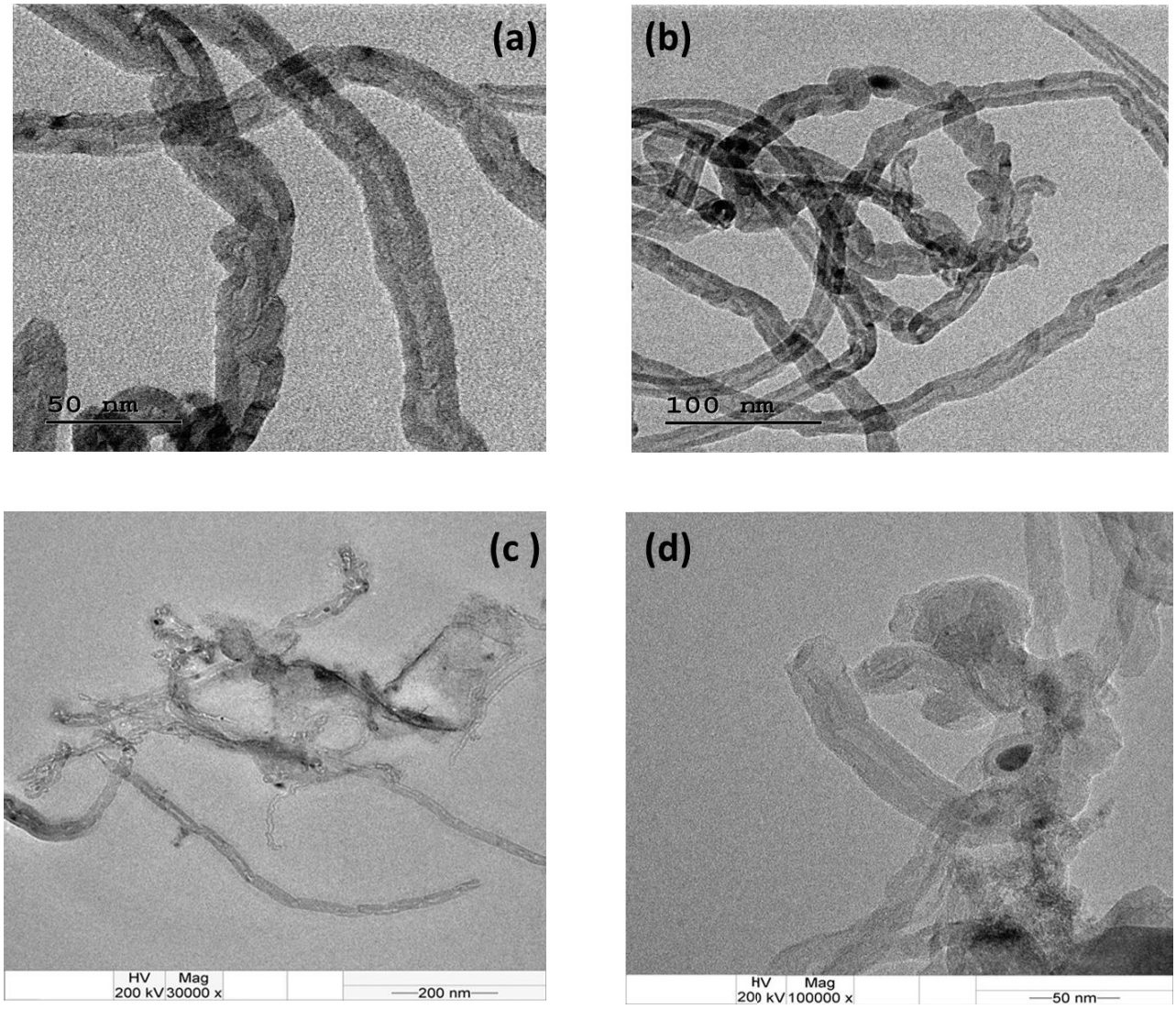


**Figure 3.15.** HRTEM images of (a,b) pristine and oxidized MWCNTs (c,d) biosorbent before and after Cr(VI) adsorption.

The strong evidence for the presence of Cr(VI) on the biosorbent surface was supported by the X-ray photo electron spectroscopy (XPS). The base peak was corrected to 284.8 eV in the high resolution carbon scan. The survey scan of the biosorbent confirmed the presence of C, N, O and Cr respectively. The high resolution spectra of Cr 2p gave two peaks $Cr2p_{3/2}$ and $Cr2p_{1/2}$. The deconvolution of $Cr2p_{3/2}$ resulted into two peaks at 577 eV, 578 eV which represent Cr(III) and Cr(VI) respectively[62] and $Cr2p_{1/2}$ at 587 eV corresponds to Cr(VI) as shown in Fig 3.16.

Immediate reduction of Cr(VI) was not observed after treatment with the biosorbent due to short agitation period and this was confirmed through chromium speciation by ion chromatography. The XPS analysis showed the presence of Cr(III) and as reported earlier[50] Cr(III) formation on the biosorbent surface was evident only after 4-5 days. This could be due to extended interactions of Cr(VI) with the carbon and specific iron regulated surface proteins in the microbes.[63,64] The Brunauer–Emmett–Teller (BET) adsorption isotherm was used to measure the specific surface area of the biosorbent.[65] The nitrogen adsorption/desorption curves provided by the BET isotherm gave the surface areas for oxidized MWCNTs as 115.72 $m^2$ $g^{-1}$and 37.029 $m^2$ $g^{-1}$ for CNTY. The average pore volume and pore diameter was found to be as follows: Oxidized CNTs (1.3857 $cm^3$ $g^{-1}$, 47.897 nm) and CNTY (0.6573 $cm^3$ $g^{-1}$, 71.0 nm) respectively. The thermal stability of the biosorbents were studied using thermogravimetric analysis (TGA). A sample mass of 5.569 mg of CNTR was analyzed in air atmosphere at a flow rate of 50 mL $min^{-1}$ in the temperature range 35-800$^oC$ ramped at 10$^oC$ per minute. The TGA curve (Fig. 3.17) signify that biosorbent was stable at higher temperatures i.e., till 600$^oC$ and the initial loss of mass is due to the moisture present in biosorbent.[66]

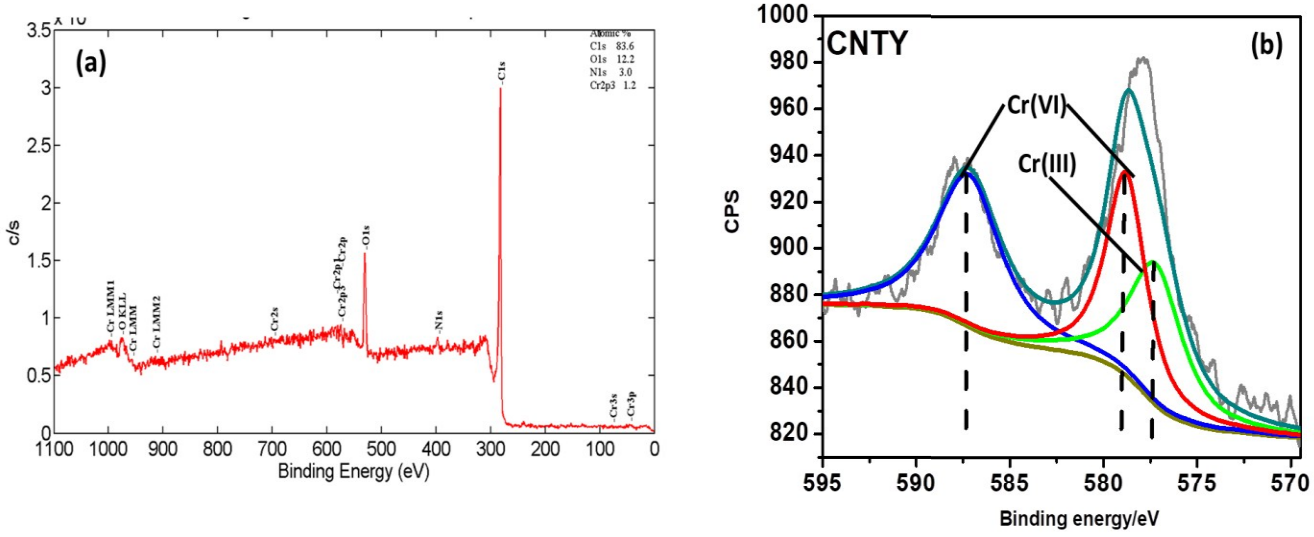


**Figure 3.16.** XPS spectra of (a) survey scan of CNTR (b) high resolution chromium scan spectra

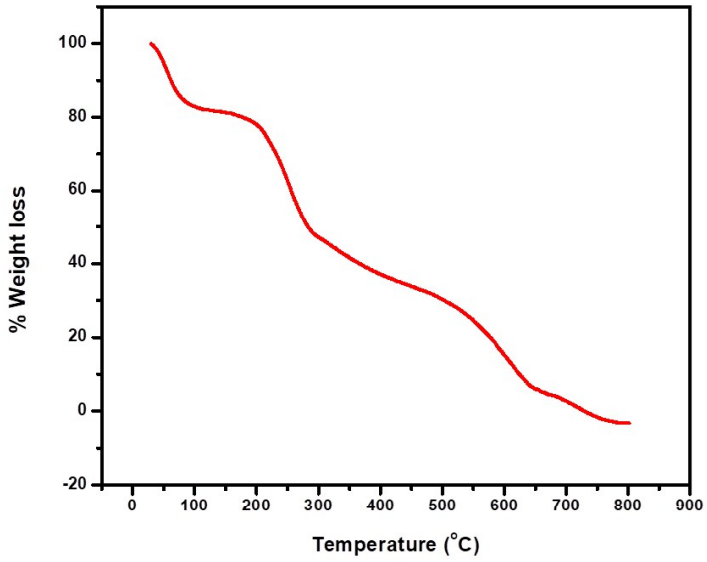


**Fig 3.17** TGA of the biosorbent

The confocal microscopy was used to differentiate the presence of chromium in its +3 and +6 form using specific rhodamine based chemosensors. The physical properties of RBH such as colorless, non-fluorescent nature owes to its spirolactam structure which is highly stable and detects Cr(VI) whereas RF is a pale pink solid which exhibits fluorescence and detects Cr(III). RBH was dissolved in 10 mmol $L^{-1}$ $H_2SO_4$ and added to the sample for further detection of Cr(VI). It was observed that after addition of RBH to the sample containing Cr(VI) it turned pink due to the conversion of RBH to RB in view of RBH oxidation caused by Cr(VI) in acid medium.[58] The excitation and emission was recorded at 560 nm and 585 nm respectively. RF when dissolved in 10 mmol $L^{-1}$ Tris-HCl is a colorless solution. The RF was added to the biosorbent with Cr(VI) which did not show any fluorescence indicating no immediate reduction of Cr(VI). After 4 days, the addition of biosorbent to RF turned pink due to chelation of RF with Cr(III) present on the surface of the biosorbent, generating a rhodamine type product in spirolactam by ring opening at C-N bond. [59] The excitation and emission for Cr(III) in RF was recorded at 525 nm and 590 nm respectively. The bright field and fluorescent images of CNTY are shown in Fig 3.18 i-viii. The images captured before and after addition of RBH confirmed

the presence of Cr(VI) in sample and also Cr(III) presence was confirmed by the addition of RF which exhibited fluorescence.

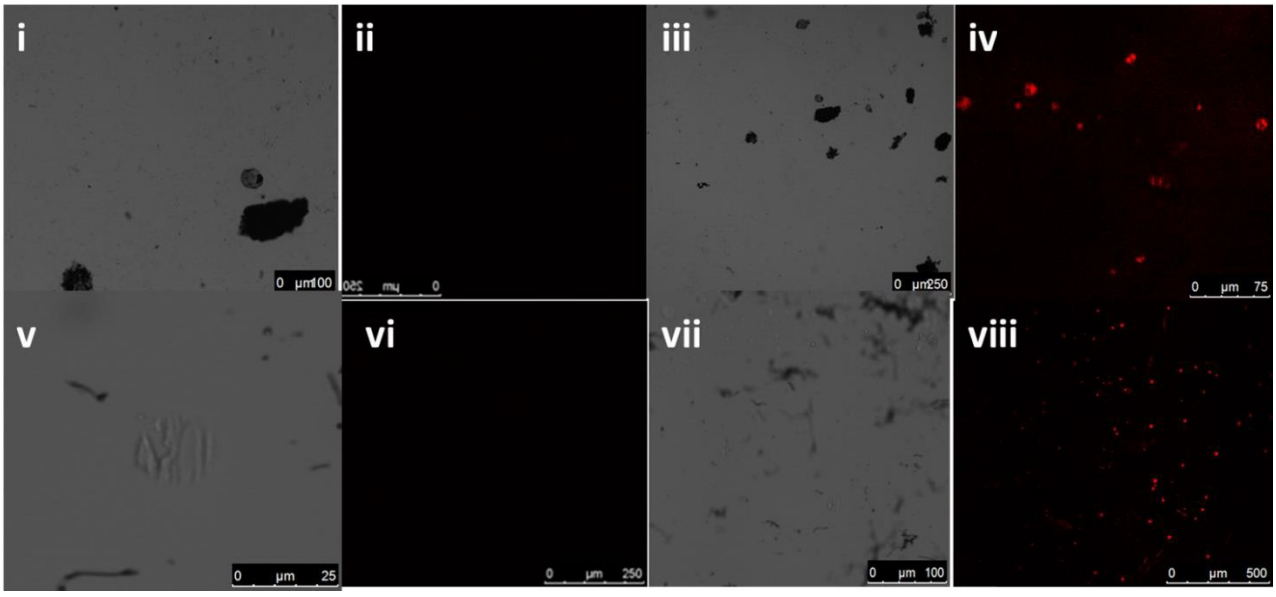


**Figure 3.18.** Confocal images of (i,ii) CNTY with RBH (iii,iv) CNTY after Cr(VI) adsorption with RBH (v,vi) CNTY with RF (vii,viii) Cr(VI) reduction to Cr(III) on CNTY with RF.

**(ii) Effect of pH , adsorbent dosage and interaction mechanisms**

Influence of pH plays a vital role in the uptake of Cr(VI) onto the biosorbent. A 0.1g weight of each of the biosorbent was weighed in a series of Erlenmeyer flasks and to that 20 mL of 5 mg $L^{-1}$ Cr(VI) solution was added and adjusted to pH 2.0-7.0 and agitated for 3 hours to attain equilibrium. After analysis, it was found that the biosorbents could equally adsorb hexavalent chromium completely at pH 2.0. At pH>2 it was observed that there was a decrease in the metal uptake (Fig 3.19a). This is due to the existence of Cr(VI) ions in various forms such as hydro chromate ($HCrO_4^-$) at pH 2-4, in strongly acidic medium (pH<2) it exists as dichromate ($Cr_2O_7^{2-}$) and at higher pH as chromate ($CrO_4^{2-}$). In acidic medium, the biosorbent surface which has functional groups such as hydroxyl, carboxylic and amide gets protonated and is involved in electrostatic interactions with $HCrO_4^-$ thus aiding the metal to participate in biosorption (Fig 3.20). Amides are usually poor leaving groups hence under highly acidic conditions (pH 2.0) the carbonyl oxygen of amide is protonated and further the protonation of amide nitrogen is also

probable[67] in influencing the metal uptake. According to HSAB (hard-soft acid base) principle $CrO_4^{2-} < HCrO_4^- < OH^-$ with regard to the hardness of the ions.[50] At higher pH, the hydroxide and chromate ions compete each other resulting in the electrostatic repulsion thereby decreasing the Cr(VI) uptake .The adsorbent dosages were varied from 0.01g to 0.5 g to observe the minimal dosage of the biosorbent which can remediate maximum amount of Cr(VI) at pH 2.0. A 20 mL volume of 5 mg $L^{-1}$Cr(VI) was taken with varying biosorbent dosage and agitated for 180 min and observed that 0.1g could adsorb Cr(VI) quantitatively indicating the saturation of adsorbent sites (Fig 3.19b ).

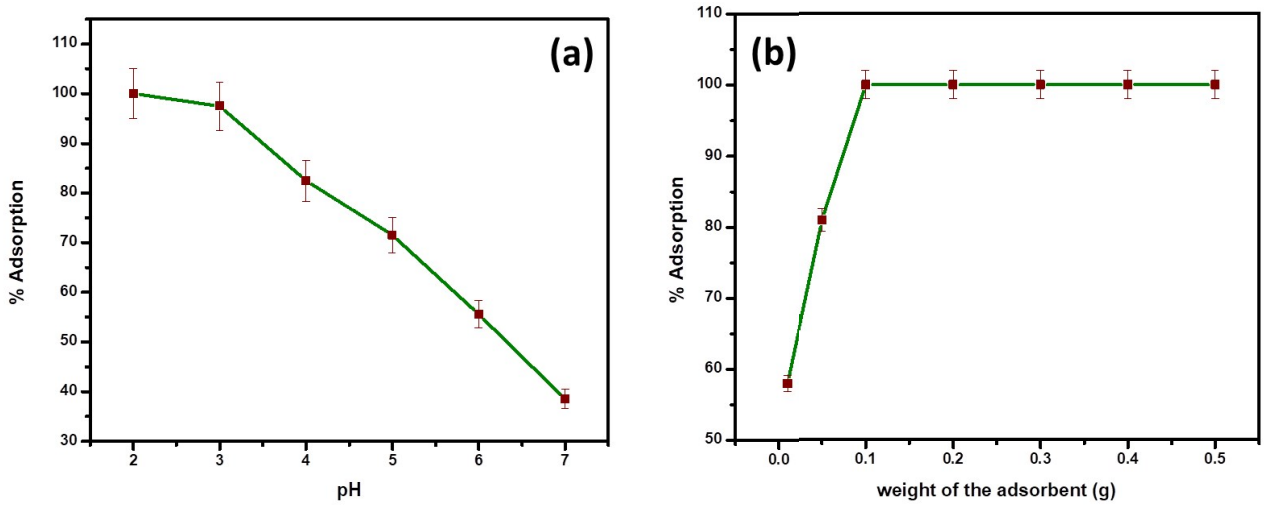


**Figure 3.19. (a)** pH effect on bio sorption (conditions: weight of adsorbent- 0.1 g/ 20 mL, Cr(VI) concentration- 5 mg $L^{-1}$) **(b)** Effect of adsorbent dosage on biosorption (conditions: pH- 2.0, Cr(VI) concentration- 5 mg $L^{-1}$)

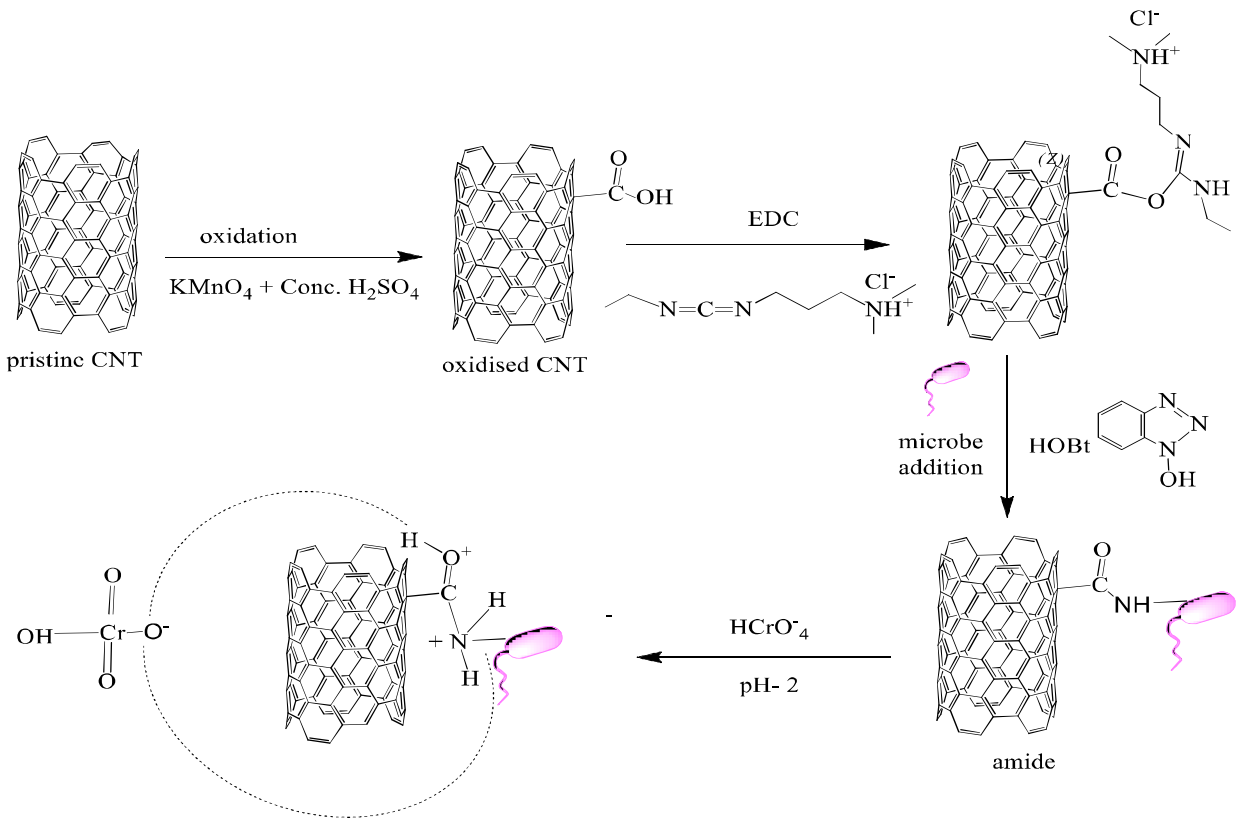


**Figure 3.20.** Interaction mechanism of the biosorbent with Cr(VI)

**(iii) Biosorption kinetics, Isotherms and Temperature effect studies**

The kinetic experiments were performed using 0.1 g of the biosorbent mixed with 20 mL of 5 mg $L^{-1}$ Cr(VI) at time intervals ranging from 5 – 180 min. The maximum uptake of the metal ion was observed at 180 min. The data obtained from the plots (Fig 3.21a-c) were fitted into the pseudo first order[43], second order[44] and intra particle diffusion to evaluate the adsorption kinetics. The kinetic parameters are presented in Table 3.5.

The rate at which Cr(VI) gets adsorbed is mostly influenced by the diffusion mechanisms such as (i) the Cr(VI) from the bulk aqueous medium is transferred onto the biosorbent surface via external mass transfer (ii) intraparticle diffusion wherein Cr(VI) diffuses through the pores of the biosorbent. The best suited kinetics depends on the experimental data which has the highest regression coefficient and the system follows pseudo second order kinetics with 1.844 mg $g^{-1}$ ($q_{eexp}$) , 1.8848 mg $g^{-1}$ ($q_{ecal}$). The plot $q_t$ vs $t^{1/2}$ relates to the intraparticle diffusion which is

evaluated using $q_t = k_i t^{1/2} + C$ where c corresponds to intercept and $k_i$ is the intra particle diffusion constant which is obtained from the slope of the plot. The rate at which Cr(VI) gets adsorbed is mostly influenced by the diffusion mechanisms such as (i) the Cr(VI) from the bulk of the solution gets transferred onto the biosorbent surface via external mass transfer (ii) intraparticle diffusion[68] wherein Cr(VI) diffuses through the pores of the biosorbent. From the plot (Fig 3.21c) it was observed that the straight line deviates from the origin having a significant intercept indicating the boundary layer phenomenon also plays role in the adsorption kinetics of hexavalent chromium.

Among several isotherms, commonly studied theoretical and empirical isotherms are Langmuir and Freundlich.[69] The data obtained from the plots (Fig 3.21 d, e) and the equations are presented in Table 3.6. The system assumed a monolayer Langmuir adsorption model as it has the low chi square value and high $R^2$ value. The biosorbent has an adsorption capacity of 31.6 mg $g^{-1}$ with an $R^2$ value of 0.96. The dimensionless constant $R_L$ value lies below unity indicating the reversibility of the isotherm which is represented as $R_L = 1/1+bC_o$.Where b is the Langmuir constant associated to adsorption energy, $C_o$ represents the equilibrium concentration of the heavy metal ion. The Freundlich constants n and $K_F$ are related to adsorption intensity and its capacity respectively. The values of n is greater than 1 indicating the favorability of metal adsorption onto the biosorbent. The pristine MWCNTs have an adsorption capacity of 11.93 mg $g^{-1}$, when oxidized the uptake capacity enhanced to 16.22 mg $g^{-1}$ and after the addition of yeast to the MWCNTs adsorption capacity increased to 31.6 mg $g^{-1}$. The comparison of adsorption capacities of various adsorbents with the current developed biosorbents is given in Table 3.7.

The thermodynamic parameters such as Gibbs free energy ($\Delta G^o$), enthalpy ($\Delta H^o$) and entropy ($\Delta S^o$) explain the spontaneity of adsorption process. The equilibrium constant K at different temperatures was derived from the ratio of Cr(VI) present on the surface of the biosorbent to that in the liquid phase and fitted into Gibbs free energy equation ($\Delta G = -RTlnK$). The changes in enthalpy and entropy of the biosorbents were obtained from the Van't Hoff plot of ln K against 1/T (Fig. 3.21f). The negative free energy values indicate the spontaneity in the biosorbent-sorbate interactions and the negative values of enthalpy and activation energy ($E_a = \Delta H^o_{ads} + RT$) indicates the system involves exothermic adsorption. The negative $\Delta S^o$ values indicate the

decrease in the disorderliness of the system with increase in temperature.[50] The ΔH value obtained (-72.2 kJ $mol^{-1}$) indicate the system observes exothermic physicochemical adsorption. The enthalpy-entropy compensation is well illustrated through the corresponding values (Table 3.8) obtained for the biosorbent.

**Table 3.5** The kinetic parameters for the adsorption of Cr(VI) onto CNTY

| **Kinetic parameters** | **CNTY** |
|---|---|
| $C_o$ (mg $L^{-1}$) | 10 |
| $q_e$ (mg $g^{-1}$) | 1.884 |
| $k_2$ (g $mg^{-1}$ $min^{-1}$) | 0.064 |
| $R^2$ | 0.996 |
| $k_1$ ($min^{-1}$) | 0.026 |
| $R_1^2$ | 0.868 |
| $k_{int}$ (mg $g^{-1}$ $min^{-0.5}$) | 0.065 |

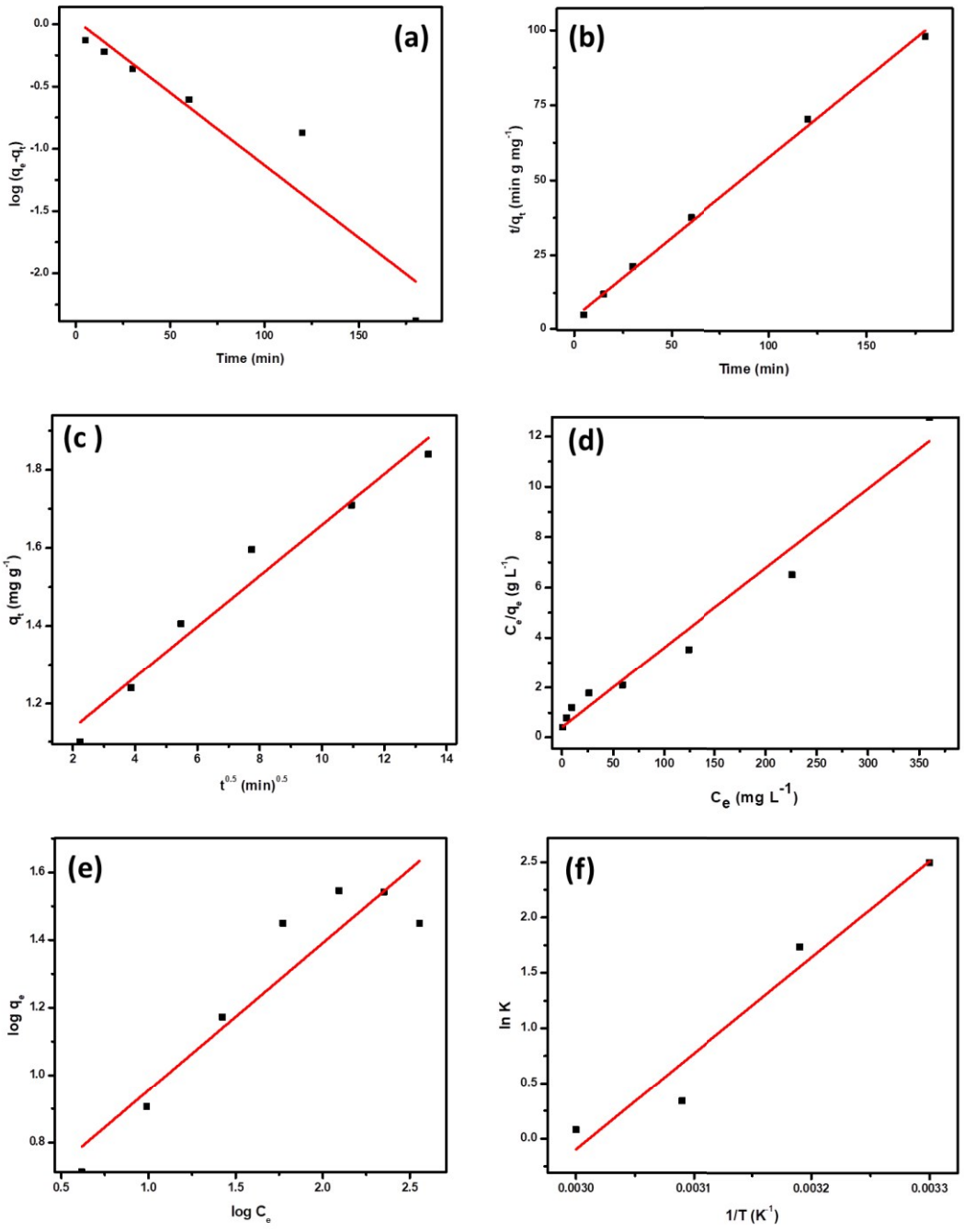


**Figure 3.21.** (a) Pseudo first order kinetics (b) pseudo second order kinetics (c) Intra particular diffusion (d) Langmuir (e) Freundlich (conditions: pH-2.0, adsorbent dosage- 0.1 g/20 mL, T=25$^{o}$C) (f) lnK against 1/T (conditions: pH-2.0, adsorbent dosage- 0.1 g/20 mL,)

**Table 3.6** Biosorption isotherm parameters for Cr(VI) adsorption

| **Langmuir $q_o$(mg $g^{-1}$)** | **b ($mg^{-1}$ L)** | **$R^2$** | **$\chi^2$** | **$R_L$** |
|---|---|---|---|---|
| 31.605 | 0.072 | 0.967 | 1.021 | 0.578 |
| **Freundlich $K_F$($mg^{1-1/n}g^{-1}L^{1/n}$)** | **n** | **$R^2$** | **$\chi^2$** | |
| 2.172 | 2.2925 | 0.854 | 1.667 | |

**Table 3.7** Comparison of adsorption capacities of various biosorbents

| **Adsorbents** | **pH** | **Adsorption capacity (mg $g^{-1}$)** |
|---|---|---|
| Cellulose-sodium montmorillonite[33] | 3.8-5.5 | 22.2 |
| MWCNTs –calcium alginate complex immobilized in *Shewanellaoneidensis*[54] | 6.0-7.0 | 6.07 |
| $Fe_2O_3$ nanoparticle-MWCNTs composite[51] | 2.0 | 42.02 |
| Activated carbon supported MWCNTs[56] | 2.0 | 113.29 |
| ***Present studies*** | 2.0 | |
| Saccharomyces cerevisiae | | 11.2 |
| Pristine MWCNTs | | 11.93 |
| Oxidised MWCNTs | | 16.22 |
| CNTY | | 31.6 |

**Table 3.8** Thermodynamic parameters associated with adsorption

| Temperature (Kelvin) | $\Delta G^0$ (kJ mol$^{-1}$) | $\Delta S^0$ (J mol$^{-1}$K$^{-1}$) | $\Delta H^0$ (kJ mol$^{-1}$) | $E_a$(kJmol$^{-1}$) |
|---|---|---|---|---|
| 303 | -6.29 | -217.3 | -72.2 | -69.55 |
| 313 | -4.513 | | | |
| 323 | -0.907 | | | |
| 333 | -0.2187 | | | |

**(iv) Effect of Sample volume, Regeneration and Interference studies**

Laboratory scale column studies were done to test the applicability of developed biosorbents for their sustainability to higher sample volume. A 1.5 g biosorbent was packed to 2 cm bed height in a glass column of 30 cm length with a diameter of 2 cm and was allowed to settle for a minimum of 2 hours to avoid air voids before the start of the experiment. A Cr(VI) concentration of 5 mg $L^{-1}$ was prepared and the column was loaded with 50 mL of 5 mg $L^{-1}$ at 5 mL $min^{-1}$flow rate and the eluate concentration was checked periodically for every 10 mL using ion chromatography. 50 mL of 5 mg $L^{-1}$ Cr(VI) was completely adsorbed effectively. Subsequently, 300 mL of the Cr(VI) solution was loaded continuously and the heavy metal was adsorbed completely beyond which there was saturation owing to the non-availability of active adsorption sites.[70] A sample volume of 350 mL was adsorbed effectively onto the biosorbent as shown in Fig.3.22 a. A significant property of the adsorbent is the ability to reuse thereby reducing the operational cost in treating pollutants. Varying sodium hydroxide concentrations (0.1-2.0 mol $L^{-1}$) were tried (Fig. 3.22 b) of which 1.0 mol $L^{-1}$ sodium hydroxide was effective in desorbing Cr(VI) as sodium chromate.[50] It was observed that in CNTY, second, third, fourth, fifth cycles completed 100% adsorption- desorption cycles beyond which there was a decrease in the

adsorption percentage. 70% adsorption was observed in 6$^{th}$ cycle, 45% in 7$^{th}$ cycle as shown in Fig. 3.21 c. A 100 mg L$^{-1}$concentration each of various cations such as $Mn^{+2}$, $Cu^{+2}$ $Fe^{+2}$ , $Co^{+2}$, $Ni^{+2}$, $Pb^{+2}$ and anions such as nitrate, chloride, sulfate were added to 5 mg L$^{-1}$ Cr(VI) solution and the adsorption studies were carried out to observe the influence of these ions in the uptake of chromium. It was observed that the adsorption percentage decreased by 2.0±0.5% attributed to the interference of anions which compete with hydrochromate ions to occupy the adsorption sites, whereas cations such as Fe(II) and Mn (II) have the ability to reduce Cr(VI) to Cr(III).[33]

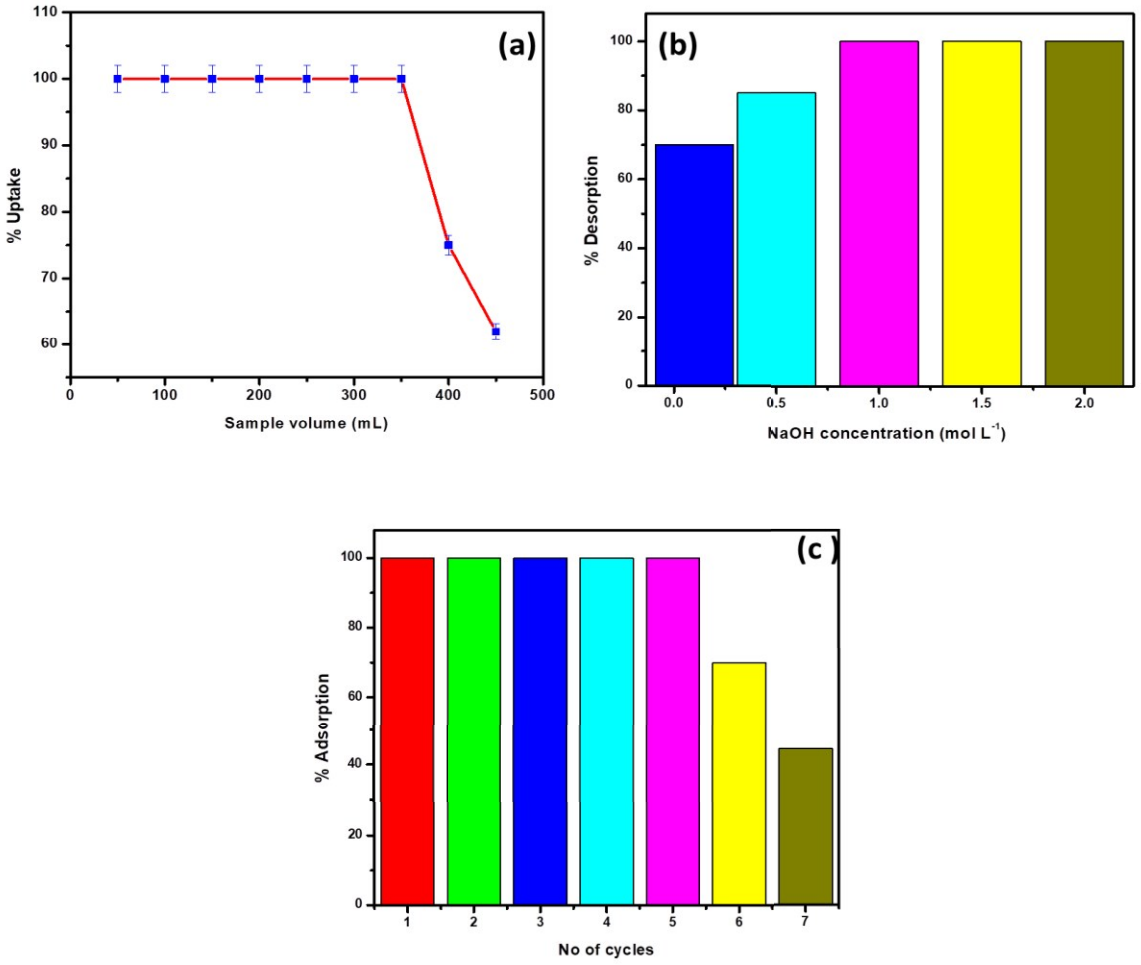


**Figure 3.22.** (a) Effect of sample volume of CNTY (conditions: weight of adsorbent- 1.5 g, Cr(VI) concentration- 5 mg L$^{-1}$, flowrate- 5 mL min$^{-1}$) (b) Effect of varied NaOH concentrations on CNTY (c) Regeneration efficiency of CNTY.

### 3.2.4 Conclusions

The proposed methodology has illustrated the ability of yeast immobilized in oxidized MWCNTs as effective adsorbent to sequester chromium in the +6 oxidation state. The biosorbent followed Langmuir isotherm with 31.6 mg $g^{-1}$ adsorption capacity respectively. The biosorption process was exothermic, spontaneous and pseudo second order model was effective in understanding the adsorption kinetics. The mechanism involves electrostatic interaction between the heavy metal ion and biosorbent surface. Characterization techniques confirmed the interaction of microbe and oxidized carbon nano tubes with Cr(VI). A good sample volume of 350 mL synthetic waste water sample was treated in lab scale column studies which could tolerate up to 5 cycles of adsorption and desorption by regenerating the biosorbents using 1.0 mol $L^{-1}$sodium hydroxide.

**References**


1. Farhan, S.N.; Khadom, A.A.; *Int J Ind Chem.* **2015**, 6, 119–130.
2. Wang, H.; Gurau, G.; Rogers. R.D.; *Chem. Soc. Rev*. **2012**, 41, 1519-1537.
3. Barathi, M.; Kumar, A.S.K.; Rajesh, N., J. *Environ. Chem. Eng*. **2013**, 1, 1325-1335.
4. Gupta, V.K.; Pathania, D.; Sharma,S.; Singh, P., *J. Colloid. Interface Sci.* **2013**, 401, 125-132.
5. Galema, S.A., *Chem. Soc. Rev*. **1997**, 26, 233-238.
6. Mahanta, N.; Leong, W.Y.; Valiyaveetil, S., *J. Mater. Chem*. **2012**, 22 , 1985-1993.
7. Wang, A.A.; Mulchandani, Chen, W., *Biotechnol. P*rog. **2001**, 17, 407-411.
8. Gopalan, R.; Veeramani, H., *Biotech. Bioeng*. **1994**, 43, 471–476.
9. Yan, G.; Viraraghavan, T., *Water Res*. **2003**, 37, 4486-4496.
10. Sameul, J.; Paul, M.L.; Pulimi, M.; Nirmala, M.J.; Chandrasekaran, N.; Mukherjee, A.; *Ind. Eng. Chem. Res.* **2012**, 51, 3740-3749.
11. Bertagnolli, C.; da Silva, M.G.C.; Guibal, E., *Chem. Eng. J*. **2014**, 237, 362-371.
12. Rahman, N.N.N.A.; Shahadat, M.; Won, C.A.; Omar, F.M., *RSC Adv*. **2014**, 4, 58156-58163.
13. Wang, J.; Chen, C., *Biotechnol Adv*. **2006**, 24, 427-451.
14. Lu, X.; Zhou, X.J.; Wang, T.S..; *J. Hazard.Mater*. **2013**, 262, 297-303.
15. Machado, M.D.; Soares, E.V.; Helena M.V.; Soares, M.; *J. Chem. Technol. Biotechnol*. **2010**, 85, 1353-1360.
16. Kang, W.; Shukla, R.; Srikar, K.K., *Biotechnol. Bioeng*. **1990**, 36, 826-833.
17. Bardi, .P.; Koutinas, A.A..; *J. Agric. Food Chem*. **1994**, 42, 221–226.
18. Liu, L.; Lv, J.P.; Uluko, H., *J. Agric. Food Chem*. **2013**, 61, 1279-1287.
19. Choi, H.M.; Kim, J.H.; Shin, S.; *J. Appl. Polym. Sci*. **1999**, 73, 2691–2699.
20. Zouboulis, A.I.; Loukidou, M.X.; Matis, K.A.; *Process Biochem*. **2004**, 39, 909-916.

21. Kumar, A.S.K.; Gupta, T.; Kakan, S.S..; Kalidhasan, S.; Manasi, Rajesh, V.; Rajesh, N., *J. Hazard. Mater.* **2012**, 239-240, 213-224.
22. Srinath, T.; Verma, T.; Ramteke, P.W.; Garg, S.K., *Chemosphere*, **2002**, 48, 427-435.
23. D. Naumann, Encylopedia of analytical chemistry, John Wiley and Sons, 2000, 102-131.
24. Yee, N.; Benning, L.G.; Phoenix, V.R.; Ferris, F.G., *Environ. Sci. Technol*. **2004**, 38, 775-782.
25. Kumar, A.S.K.; Rajesh,N., *RSC adv*. **2013**, 3, 2697-2709.
26. Mettler, M.S..; Mushrif, S.H.; Paulsen, A.D.; Javadekar, A.D.; Vlachosa, D.G.; Dauenhauer, P.J.; *Energy Environ. Sci*. **2012**, 5, 5414-5424.
27. Bhattacharjee, A.; Ahmaruzzaman, Md.; Sinha, T., *RSC Adv*. **2014**, 4, 51418–51429.
28. Wang, N.; Li, L., *J. Am. Soc .Mass. Spectrom*. **2010**, 21, 1573–1587.
29. Klein, M.; Pulidindi, I.N.; Perkas, N.; M-Mats, E.; Gruzman, A.; Gedanken, A., *RSC Adv*. **2012**, 2, 7262–7267.
30. Nüchter, M.; Ondruschka, B.; Bonrath, W.; Gum,A., *Green Chem*, **2004**, 6, 128 – 141.
31. Swaminathan, V.; Deheri, P.K.; Bhame, S.D.; Ramanujan, R.V.; *Nanoscale*, **2013**, 5, 2718-2725.
32. Ofomaja, A.E.; Ho, Y.S., *Bioresour. Technol*. **2008**, 99, 5411–5417.
33. Kumar, A.S.K.; Kalidhasan, S.; Rajesh, V.; Rajesh, N. *Ind.Eng. Chem. Res*. **2012**, 51, 58–69.
34. Ramsey, J.D.; McCreery, R.L., *J. Electrochem. Soc*. **1999**, 146, 4076-4081.
35. Suh, Y.J.; Chae , J.W.; Jang , H.D.; Cho , K., *Chem. Eng. J*. **2015**, 273, 401–405.
36. Pons, M.P.; Fuste, M.C.; *Appl. Microbiol and Biotechnol*. **1993**, 39, 661-665.
37. Ho, Y.S., *Carbon*, **2004**, 42, 2115-2116.
38. Ho, Y.S.; Chiu, W.T.; Wang, C.C., *Bioresour. technol*. **2005**, 96, 1285-1291.
39. Zheng , H.; Liu, D.; Zheng, Y.; Liang, S.; Liu, Z.; *J. Hazard. Mater*. **2009**, 167, 141–147.
40. Febrianto, J.; Kosasih, A.N.; Sunarso, J.; Ju, Y.H.; Indraswati. N.; Ismadji, S.; J. *Hazard. Mater*. **2009**, 162, 616–645.
41. Hamdaoui, O.; Naffrechoux, E., *J. Hazard. Mater*. **2007**, 147, 401-411.
42. Sun, C.; Sun, L.; Sun, X., *Ind. Eng. Chem. Res*. **2013**, 52 , 14251–1426.

43. Lagergren, S., *K. Sven. Vetenskapsakad. Handl*. **1898**, 24, 1-39.

44. Ho, Y.S.; Mckay, G. Water Res. **2000**, 34, 735-742.

45. Weber, W.J.; Morris, J.C., *J. San. Eng. Div*. 1963, 89 , 31-60.

46. Mallakpour, S.; Taghavi, M. *Polym. J.* **2008**, 40 , 1049-1059.

47. Tang, Y.; Webb, S.M.; Estes, E.R.; Hansel, C.M., *Environ. Sci.: Processes Impacts*, **2014**, 16 2127-2136.

48. Choudhury, P.R.; Bhattacharya, P.; Ghosh,S.; Majumdar, S.; Saha, S.; Sahoo, G.C.; ; *J. Environ. Chem. Eng.* **2017**, 5, 214-221.

49. Colica, G.; Mecarozzi, P.C.; De Philippis, R.; *Ind. Eng. Chem. Res*. **2012**, 51**,** 4452−4457

50. Sathvika, T.; Manasi; Rajesh,V.; Rajesh, N.; *Chem.Eng.J*. **2015**, 279, 38-46.

51. Lua, W.; Lia, J.; Sheng, Y.; Zhang, X.; You, J.; Chen, L. *J Colloid Interface Sci*. **2017**, 505, 1134-1146 .

52. Masheane, M.L.; Nthunya, L.N.; Malinga, S.P.; Nxumalo, E.N.; Mamba, B.B.; Mhlanga, S.D. *Sep. Purif. Technol.* **2017**, 184, 79-87.

53. Salam, M.A., *J. Mol. Liq* .**2017**, 233**,** 197-202.

54. Yan, F.F.; Wu, C.; Cheng, Y.Y.; He, Y.R.; Li , W.W.; Yu, H.Q..*Biochem. Eng. J.* **2013**, 77, 183– 189.

55. Tuzen, M.; Saygi, K,O.; Usta, B.; Soylak, M, *Bioresour Technol*. **2008**, 99, 1563–1570.

56. Parlayici, S.; Eskizeybek, V.; Avcı, A.; Pehlivan, E. *J Nanostruct Chem*. **2015,** 5, 255-263.

57. Sheehan, J.C.; Cruickshank, P.A.; Boshart, *J. Org. Chem*. **1961**, 26, 2525.

58. Xiang, Y.; Mei, L.; Li, N.; Tong, A. *Anal. Chim. Acta*. **2007**, 581, 132–136.

59. Zhou, Y.; Zhang, J.; Zhang, L.; Zhang, Q.; Ma, T.; Niu, J. *Dyes. Pigm*. **2013**, 97, 148-154.

60. Kumar, A.S.K.; Jiang, S.J.; Tseng, W.L. *J. Mater. Chem. A*. **2015**, 3, 7044-7057.

61. Zhao, J.; Wang, J., *J. Phys. Chem. B.* **2015**, 119, 14831–14839.

62. Kumar, A.S.K.; Jiang, S.J.; Warcho, J.K. *ACS Omega.* **2017**, 2, 6187−6200.

63. Zheng, W.; An, Q.; Lei, Z.; Xiao, Z.; Zhai, S.; Liu Q. *RSC Adv.* **2016,** 6**,** 104897-104910.

64. Reigh, G. & Connell, M. O. *J Bacteriol.* **1993,** 175, 94-102.

65. Bae, Y.S.; Yazaydın, A.O.; Snurr, R.Q. *Langmuir*, **2010**, 26, 5475–5483.

66. Yadav, S.K.; Mahapatra, S.S.; Yadav, M.K.; Dutta, P.K. *RSC Adv.* **2013,** 3**,** 23631-23637.

67. Anslyn. E.V.; Dougherty, D.A. Modern Physical Organic Chemistry, University Science Books, 603-604, (2005).

68. Fierro, V.; Torne-Fernandez, T.; Montane, D.; Celzard, A.; *Mesoporous Mater.* **2008**, 111, 276–284.

69. Sun, L.; Zhang, Y.; Ye, X.; Liu, H.; Zhang, H.; Wu, A.; Wu, Z., *ACS Sustainable Chem. Eng.*, **2017**, 5, 7700–7708.

70. Hasan, S.H.; Ranjan, D.; Talat, M.; *J. Hazard. Mater*. **2010**, 181,1134–1142.

# Chapter – 4

## Filamentous fungi immobilized in clays and biopolymers for the effective sequestration of hexavalent chromium

Convergence of biotechnology and chemistry offers greener alternatives in environmental remediation. Hexavalent chromium is genotoxic and carcinogenic. Methods such as biosorption involving the use of microbes, biopolymers and clays are environmentally benign. Fungal species can be obtained in considerable amount as by product from industrial fermentation processes. These are known to have good potential in removing toxic metals such as cadmium, lead, copper etc. from aqueous medium. *Aspergillus* species finds applications in biotechnological processes such as citric acid production, transformations of progesterone, citral etc. *Aspergillus* is also used to synthesize extracellular enzymes such as amylase, lipase and pectinase and the FDA has recognised these enzymes to be safe and non-toxic.[1] Filamentous fungi such as *Aspergillus sp* are known for their excellent potential to remediate hexavalent chromium.[2] The functional groups (carboxyl, amino, hydroxyl) present in the cell surface shows good binding affinity towards heavy metals through complexation, ion exchange and surface precipitation interactions.[3] The aim of the present study is to investigate the removal of hexavalent chromium from aqueous solution in batch and fixed bed column experiments using dead biomass of isolated *Aspergillus* fungal species immobilized in sodium montmorillonite and epichlorohydrin crosslinked cellulose.

**The first part of this chapter** deals with the immobilization of the isolated fungus (*Aspergillus BRVR*) in sodium montmorillonite using ultrasonication for the effective removal of hexavalent chromium from aqueous medium. The method developed was supported by analytical characterization techniques such as FTIR, SEM-EDAX, optical images studies followed by batch and column adsorption studies.

**The second part of this chapter** deals with the immobilization of *Aspergillus BRVR* in epichlorohydrin crosslinked cellulose for the sequestration of Cr(VI) from aqueous solution. The adsorption of Cr(VI) onto the biosorbent was confirmed using characterization techniques such as FTIR, SEM-EDAX, XPS. Batch studies were performed and column studies are discussed in detail.

## 4.1. Prospective application of *Aspergillus* species immobilized in sodium montmorillonite to remove toxic hexavalent chromium from wastewater

### 4.1.1 Introduction

Biosorption is regarded as an environmentally benign option to remove metal ions from wastewater at varying concentrations.[4] Microorganisms such as bacteria, fungi and algae are known for their excellent ability to adsorb heavy metals from diverse wastewaters.[5,6] The well-studied bacterial and fungal species for metal adsorption includes *Bacillus, Pseudomonas, Aspergillus and Rhizopus* respectively.[7-9] *Aspergillus sp* are known for their excellent potential to sequester hexavalent chromium.[2] Pre-treatment of *Aspergillus niger* with CTAB followed by immobilization in a polysulfone matrix[10] gives a biosorption capacity of 3.1 mg $g^{-1}$. A removal efficiency of 29% has been reported using dead mass of the same fungal species.[11]

Biocomposites such as cellulose-clay[12] and starch-montmorillonite[13] effectively adsorb chromium in the presence of diverse ionic constituents. Clay-polymer nanocomposites and type of clays such as kaolinite, bentonite etc are equally efficient in the treatment of wastewater.[14,15] Acid activated kaolinite gives a Langmuir adsorption capacity of 13.9 mg $g^{-1}$ for Cr (VI) adsorption in acidic pH medium.[16] Surfactant modified montmorillonite[17] has the ability to remove anionic chromium (VI) from water with an adsorption capacity of 18 mg $g^{-1}$. The ability of dithionite reduced clays in the transformation of Cr(VI) to Cr(III) has been correlated with the ferrous content present in montmorillonite.[18]

Clay minerals are recognized to be good supports and offer a defensive environment for microbes by forming a biofilm.[19] Hence, the microbe-clay combination can even degrade pollutants such as volatile organic compounds. Literature reports on the immobilization of living fungi in a clay matrix for Cr(VI) adsorption are scarce. Considering the advantages of non-living microorganisms towards enhancing the adsorption capacity as well as efficiency, we felt it worthwhile to investigate the combination of inorganic materials such as clay and a non-living fungal species to adsorb hexavalent chromium. This concept provides a good illustration of the convergence of chemistry and biotechnology towards the application to remove heavy metals. In this work, we demonstrate the potential of a filamentous fungal strain (isolated as *Aspergillus BRVR*) in sodium montmorillonite for the effective adsorption of Cr(VI) from wastewater.

Systematic characterization of the biosorbent, batch studies and preliminary column tests has been undertaken towards the development of this novel methodology.

### 4.1.2. Experimental section

#### (i) Production and identification of *Aspergillus* species

The fungal species was isolated from bread, characterized and maintained on Sabaroud Dextrose Agar and broth[20] having dextrose as carbon source and peptone as the respective carbon and nitrogen sources. After autoclaving and inoculation, the flasks were incubated at 27°C for 4-5 days. The morphological identification of *Aspergillus* culture was done by staining the fungi with lactophenol cotton blue[21] (Fig. 4.1). Harvesting of the fungi was done through filtration and subsequently dried overnight at 70°C and the powdered form was used for the adsorption of chromium.

#### (ii) Isolation of fungal genomic DNA and cultivation

Fungal DNA was isolated using the Moller's et al.[22] method as reported previously. The cultivated fungal culture was freeze dried overnight at -80°C. 50 mg of dried material was taken and 500 µl of Tris- EDTA-sodium dodecyl sulphate (TES) buffer was added and mixed thoroughly. 60 µg of Proteinase K was added from the stock solution and incubated for at 60°C for 60 min with intermittent mixing. The salt concentration was adjusted using NaCl followed by the addition of 1 mL of 10% CTAB and incubated for 15min. Extraction was accomplished using chloroform: isoamyl alcohol and precipitated with isopropanol and the DNA pellet was washed with ethanol and suspended in Tris-EDTA (TE) for further studies.

#### (iii) PCR amplification of 18S rDNA

The PCR amplification was performed in a 25 µl reaction mixture using 100 ng/ µl genomic DNA as a template having 200 ng of forward [nu-ssu- 0817-59 5'(TTAGCATGGAAT AATGCAATAGG)] and reverse primers [nu-ssu-1196 5'(TCTGGACCTGGTGAGTTTCC)], 200 µM dNTP, 1µl of *Taq polymerase*, 2.5 µl of 10X PCR buffer, containing 1.5 mM of $MgCl_2$.[23,24] The PCR programme incorporates an initial denaturation at 95°C for 3 min and 32 cycles of denaturation at 95°C for 1min, annealing at 60°C for 1 min, extension at 72°C for 3

min with a final extension at 72°C for 5min. DNA of 400 bp was observed as a single band when resolved on 1% agarose gel (Fig. 4.2). Commercial sequencing of the gel purified samples was done at Bioserve Pvt. Ltd, Hyderabad, India using ABI 3730 xls Genetic analyser (Applied Biosystems). The sequences were identified through the BLAST search in the Gene Bank database (Nucleotide Blast) after the chromatogram verification.

**(iv) Preparation of biosorbent**

The $Na^+$ form of montmorillonite was prepared from montmorillonite as described in the literature.[25] The powdered fungi was mixed with sodium montmorillonite in 1:1 ratio in aqueous medium and sonicated for about 5 min to facilitate the immobilization of *Aspergillus* in clay matrix. The obtained biosorbent was filtered, washed with water and dried at 40°C in a vacuum oven and utilized for the adsorption of chromium (VI).

**(v) Batch adsorption procedure**

The preliminary biosorption studies were conducted at 30°C by equilibrating 0.2 g of the fungal-clay biosorbent with 30 mL of 30 mg $L^{-1}$ chromium(VI) solution taken in an Erlenmeyer flask at pH 2.0-2.5 using an orbital incubator shaker at 120 rpm for varying time intervals. The concentration of chromium remaining in the solution phase was estimated using the post column derivative ion chromatography technique.[26]

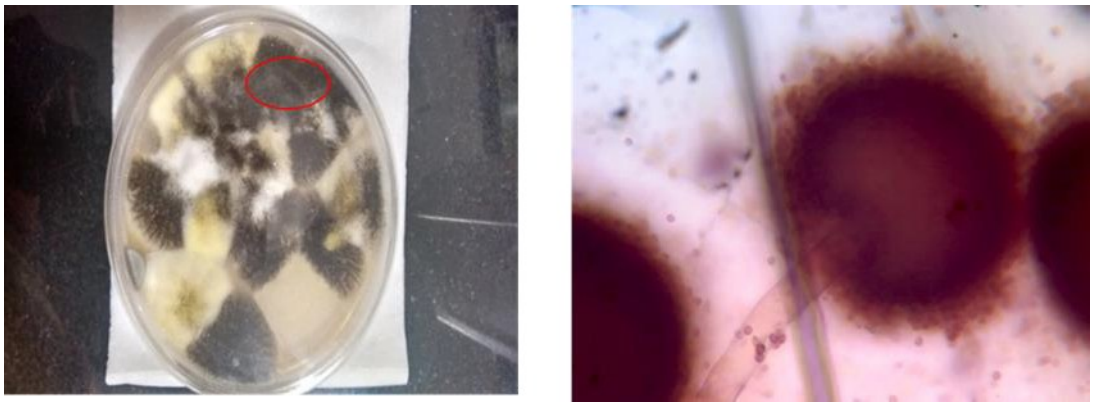

**Figure 4.1.** Photographic image of a three day old culture of *Aspergillus BRVR* on SDA and optical image of *Aspergillus BRVR* under 40X objective.

### 4.1.3. Results and discussion

#### (i) Molecular identification of the isolated fungal strain

The microscopic examination of *Aspergillus* stained with lactophenol cotton blue showed the presence of transparent hyphae and conidiophores with a bulging end known as '*vesicule*' that produces significant amounts of conidia or spores (Fig. 4.1). The confirmation of the isolated fungal strain was acquired through 18S rDNA sequencing. Comparison of 18S rDNA gene sequence of the isolated strain with the database (Gen Bank) showed 98% similarity with the *Aspergillus* genera. The phylogenetic tree was constructed by neighbour joining method using MEGA version 6.0 software to analyse the evolutionary relationships among the various sequences of isolated fungal strain and its nearest neighbours (Fig. 4.3). The data obtained confirms that the fungal strain isolated (*Aspergillus BRVR)* belongs to the *Aspergillus* genera. The fungal strain sequence is assigned the accession number KT699195 upon submission to NCBI Gen Bank database.

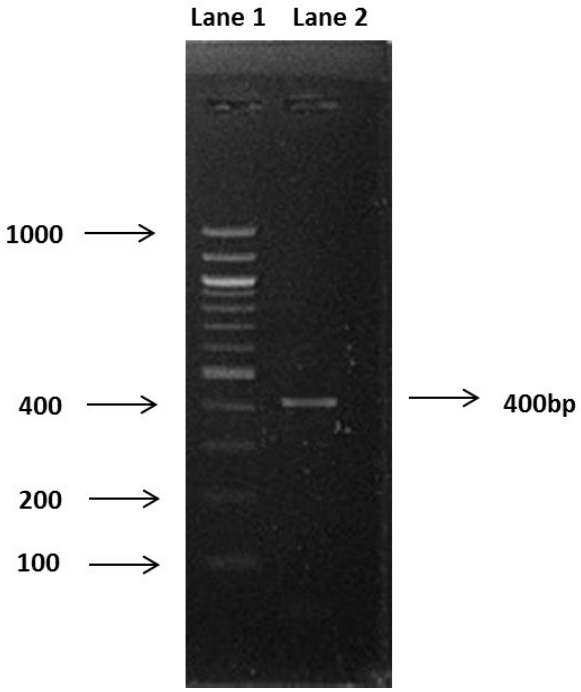


**Figure 4.2** Lane 1 Invitrogen 100 bp DNA ladder (catalogue no. 15628-019), lane 2 *Aspergillus BRVR* 18S rDNA PCR amplified product

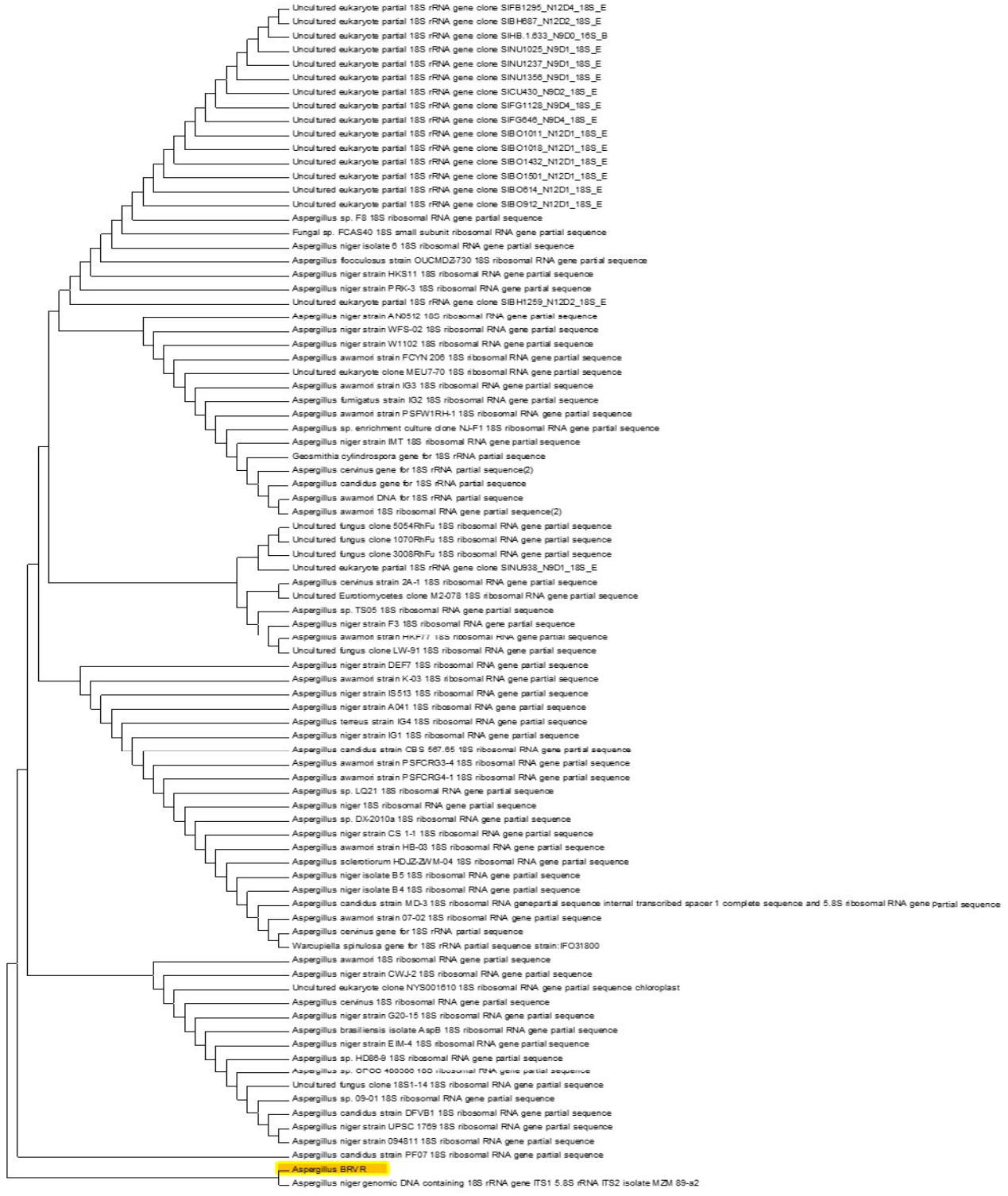


**Figure 4.3** Phylogenetic tree based on the 18S r DNA sequences of fungi using MEGA version 6.0

**(ii) Characterisation of biosorbent**

The fungi cell wall has diverse functional groups such as amine, hydroxyl , carboxyl and the FT-IR spectrum (Fig. 4.4) indicates the characteristic bands corresponding to the functional groups in *Aspergillus* as well as montmorillonite.[27-29] The band near 3603 $cm^{-1}$ is attributed to the silanol groups (Si–OH), while the broader band near 3402 $cm^{-1}$is ascribed to the merging of N-H and O-H stretching vibrations in the fungus as well as the Al–O–H stretching vibration bands of montmorillonite clay. An intense peak at 1016 $cm^{-1}$can be correlated to the C-O group of polysaccharide present in the cell walls of *Aspergillus* and Si- O-Si stretching vibration band of montmorillonite. The other peaks that are typical for montmorillonite were observed at 774 $cm^{-1}$ (Si-O stretching of quartz and silica), 663$cm^{-1}$ (Si-O deformation), respectively.[30] The peak at 1627 $cm^{-1}$is linked to the amide-I band of the protein-peptide bond of the fungi and also the H-OH bonding in water. The participation of the hydroxyl groups of the fungi and the clay surface as well as the amine groups in *Aspergillus* are reflected in the spectral shift to 3418 $cm^{-1}$ after the adsorption of hexavalent chromium along with the appearance of a sharp characteristic Cr=O bond vibration at 912 $cm^{-1}$.[31] The thermogravimetric analysis (TGA) (Fig. 4.5) gives an insight into the thermal stability of the clay-*Aspergillus* biosorbent and the first step corresponding to the temperature range 70$^{o}$C -100°C relates to water desorption from clay, the second one at 300°C corresponds to dehydration of hydrated cation in the interlayer and last step at 450°C is attributed to the dehydroxylation of aluminosilicate of montmorillonite.[32]

The interaction between the *Aspergillus* cell surface and the clay matrix depends on physicochemical (electrostatic, hydrophobic, hydrogen bonding, Van der Waals) and biological phenomena involving production of enzymes, polysaccharides etc.[33] The surface area of sodium montmorillonite clay (NaMMT) used to immobilize the *Aspergillus sp*. was found to be 195.17 $m^2g^{-1}$ with a pore volume of 0.0841 $cm^3$ and a pore size of 1.72 nm indicating the microporous nature[34] of the clay.

After the addition of fungi, the surface area of the biosorbent was found to be 69.1 $m^2$ $g^{-1}$ with a pore size of 6.575 nm indicating the mesoporous nature of biosorbent with a pore volume of 0.1136 $cm^3$ $g^{-1}$. The enzymes produced by *Aspergillus* sp contain functional groups that can

interact with the surface silanol hydroxyl groups of NaMMT through hydrogen bonding. Hence, they can act as effective sites for linkage with the enzymes produced by the fungal species. After intercalation of *Aspergillus* sp, the immobilized enzymes block the pores in the clay matrix thereby altering the surface area after immobilization.[35]

The morphological features in the fungi immobilized clay matrix show assorted clusters and the hyphae (Fig. 4.6). The accompanying energy dispersive X ray spectrum of the *Aspergillus* immobilized clay surface indicated the adsorption of chromium in the range 5-6 keV (Fig. 4.7) and also supported well through the optical images. The *Aspergillus* immobilized clay was spread on a glass slide and the images were taken at 10X objective (Fig. 4.8). The addition of diphenyl carbazide[36] as a complexing agent to the biosorbent containing chromium oxo anion showed a characteristic red violet colour indicating the presence of adsorbent Cr (VI) onto the fungi immobilized clay surface.

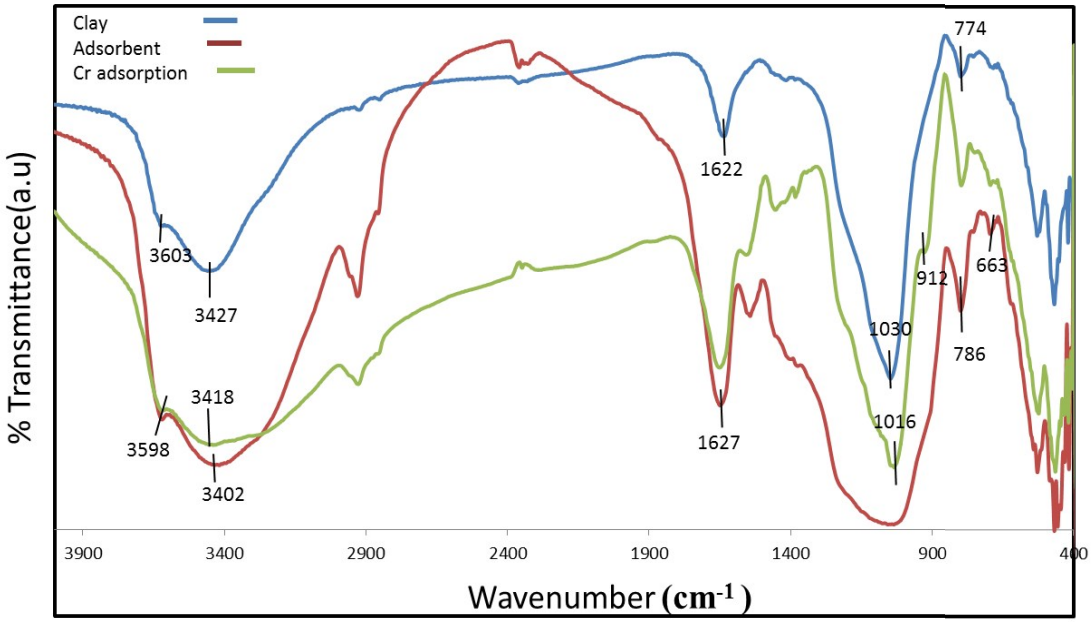


**Figure. 4.4** FTIR spectrum of sodium montmorillonite and the immobilized fungi before and after Cr(VI) adsorption

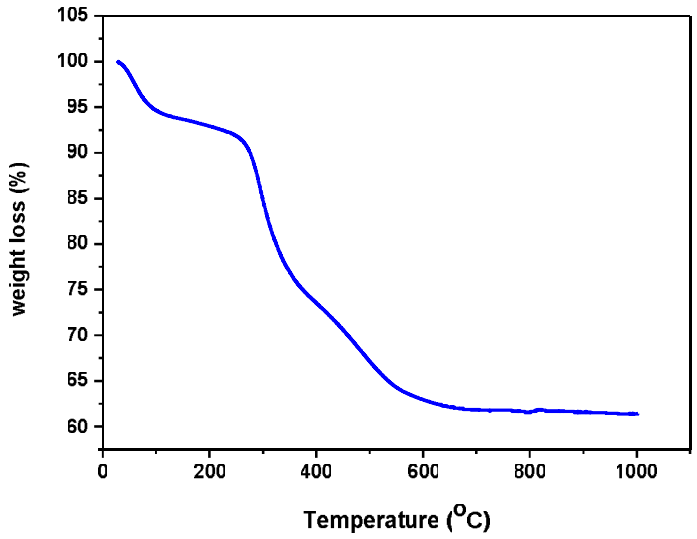


**Figure 4.5** Thermogravimetric analysis of the biosorbent

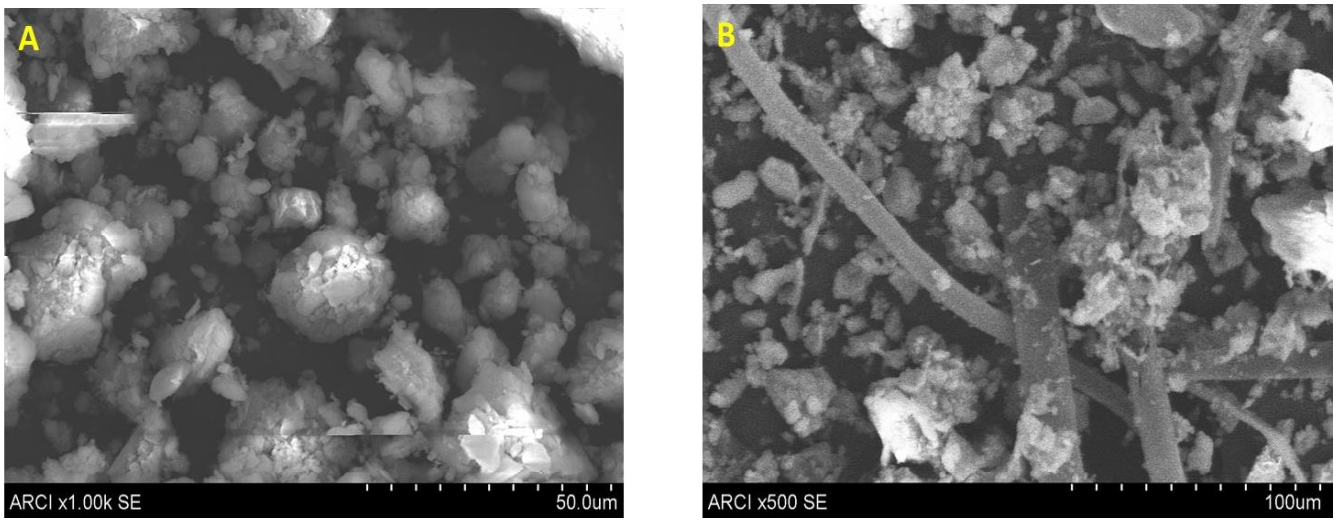


**Figure 4.6** SEM analysis of (A) sodium montmorillonite (B) and biosorbent after adsorption

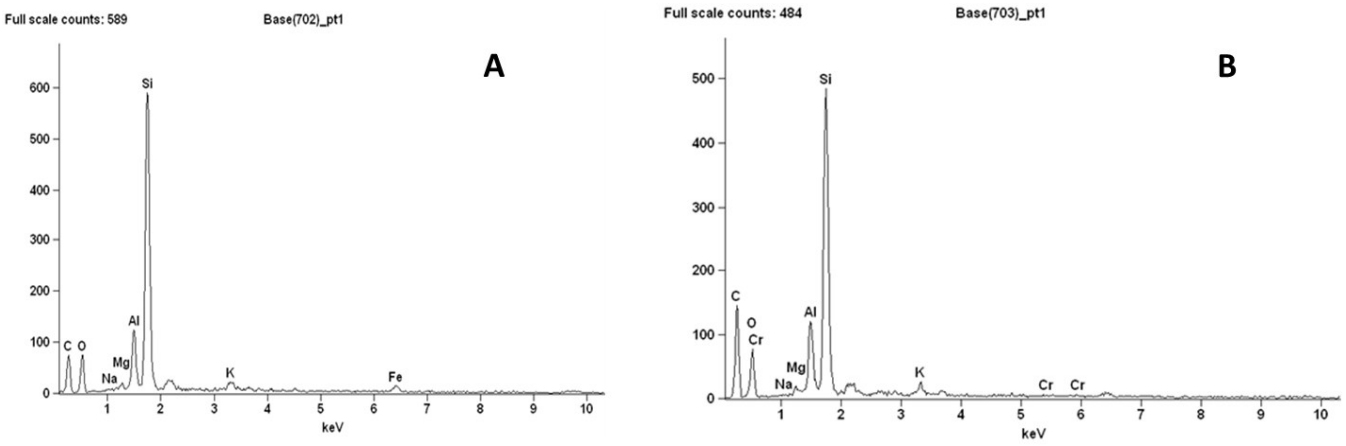


**Figure 4.7** EDAX of (A) sodium montmorillonite (B) and biosorbent after adsorption

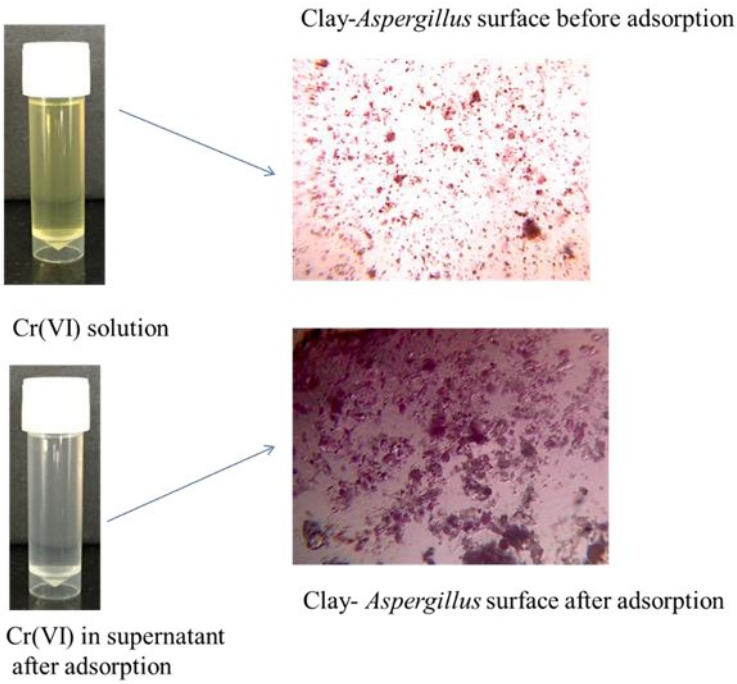


**Figure 4.8** Images of Cr(VI) in solution phase and the biosorbent surface

**(iii) pH effect and interaction of biosorbent with Cr(VI)**

The pH of aqueous phase is quite important in knowing about the existence of chromium as $HCrO_4^-$, $Cr_2O_7^{2-}$ and $CrO_4^{2-}$ oxy anions. [36] At a concentration of 10 mg $L^{-1}$ and in the acidic pH range 2.0-2.5, more than 94% of Cr(VI) was adsorbed onto the fungi immobilized clay surface (Fig . 4.9 A). As a matter of fact, between pH 2.0-2.5 hexavalent chromium is present as it's $HCrO_4^-$ (hydrochromate) oxy anion since this pH range is also lower than the $pK_a$ (~6) of the oxy anion. Representing the equilibrium as $2HCrO_4^- \rightleftharpoons Cr_2O_7^{2-} + H_2O$ and when the pH is in the range 1.0-2.0, the existence of dichromate anion would be more probable. The hydrochromate anion is involved in the electrostatic interaction with the protonated functional groups (amine, carboxyl and hydroxyl) of *Aspergillus* as well as the silanol and aluminol groups ($SiOH_2^+ \ldots HCrO_4^-$ and $AlOH_2^+ \ldots HCrO_4^-$) on the clay surface.[12] The conceptual illustration depicting the immobilization of *Aspergillus* in the clay matrix and subsequent interaction with hexavalent chromium is shown in Fig. 4.10. Hence, these interactions involving the clay matrix as well as the fungal cell surface collectively helps in influencing the adsorption performance of Cr(VI). At higher pH, the surface of the microbe begins to attain a negative charge coupled with the deprotonation of the silanol and aluminol groups of clay leading to the repulsion with the chromium oxy anion. This results in the lowering of adsorption with increase in pH.

The amount of biosorbent was also varied in the range 0.1-0.6 g (Fig. 4.9 B) using 30 mg $L^{-1}$ chromium (VI) solution. Hexavalent chromium was adsorbed very effectively with as low as 0.2 g of the biosorbent in 30 mL aqueous phase. The presence of active surface adsorption sites augments the biosorption process with 0.2 g of the biosorbent and beyond this amount saturation is attained.

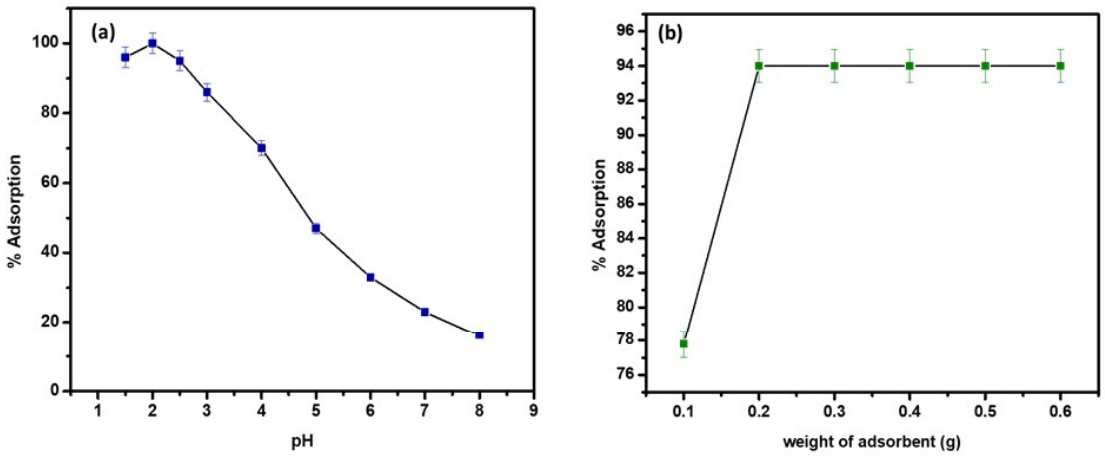


**Figure 4.9** (a) Effect of pH on adsorption (Conditions: weight of the adsorbent- 0.2 g/ 30 mL, Cr(VI) concentration- 30 mg $L^{-1}$) (b) Effect of adsorbent dosage (Conditions: pH-2.0-2.5, Cr(VI) concentration- 30 mg $L^{-1}$)

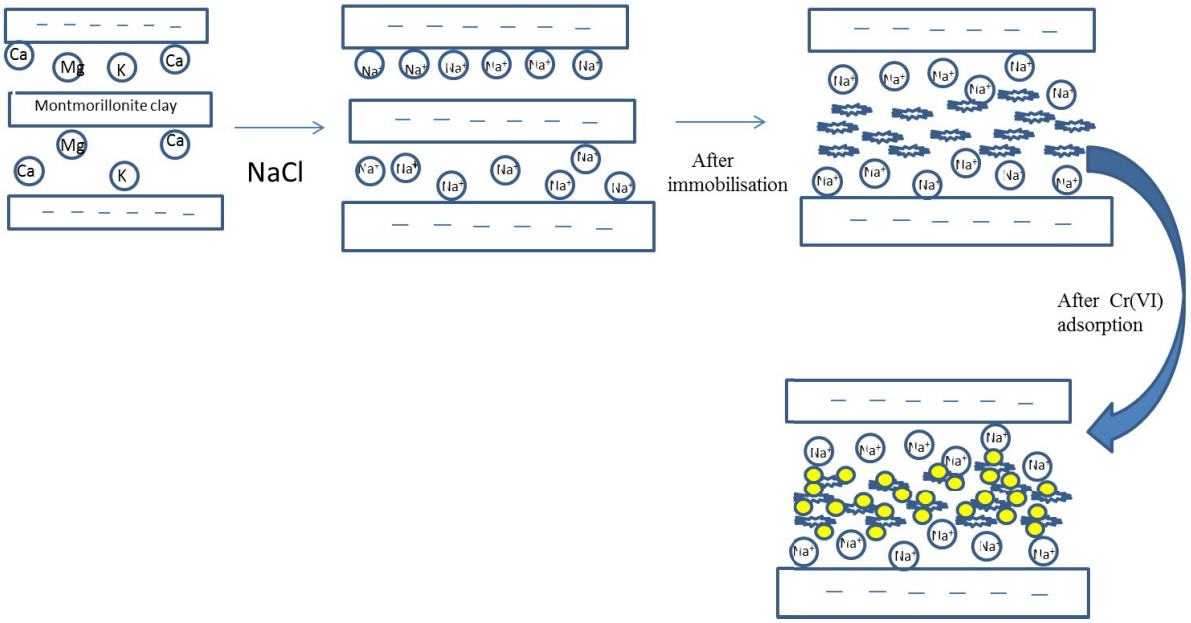


**Figure 4.10** Conceptual graphic showing the interaction of Cr(VI) and clay-fungal biosorbent

**(iv) Equilibrium adsorption isotherms and kinetics**

Biosorption is generally classified under a sub category of adsorption wherein the adsorbent is a microorganism. Biosorption is primarily a metabolically independent physicochemical process. The solution pH, temperature, effect of initial Cr(VI) concentration, speed of agitation can significantly affect the biosorption. In addition to adsorption, complexation, ion exchange and precipitation mechanisms are also equally important. The biosorption process involves a rapid, reversible equilibrium adsorption process involving the binding of $HCrO_4^-$ oxy anion from aqueous solution onto the protonated functional groups present in the fungal cell surface. The biological part thus plays a vital role in the adsorption. Hence, adsorption equilibrium, kinetics and thermodynamics are of equal importance in biosorption processes as well. By choosing an appropriate concentration range of the metal ion, it is therefore possible to extend the commonly used isotherms (Langmuir, Freundlich, etc) to biosorption in a manner similar to other conventional adsorption processes.[5,37] The experimental biosorption data were fitted using four well established isotherm models namely, Langmuir, Freundlich, Redlich-Peterson (R-P) and Dubinin Radukskevich (D-R)[38,39] respectively (Table 4.1).The respective isotherm plots are shown in Fig. 4.11. Each of these gives adequate information regarding the mode of adsorption. The Langmuir isotherm which principally accounts for monolayer adsorption is one of the time tested models that is used to relate the equilibrium adsorption capacity ($q_e$) with the equilibrium concentration $C_e$ and the Langmuir adsorption capacity ($q_o$) respectively. Freundlich isotherm is yet another empirical model that gives a logarithmic relationship between the adsorption capacity, adsorption intensity (n) and the constant $K_F$.

The Langmuir adsorption capacity was found to be 45.72 mg $g^{-1}$ with a correlation coefficient of 0.978. Also, the applicability to this model was established through a dimensionless parameter $R_L$ [40] given as $R_L = 1/1+bC_o$, wherein *b* indicates the energy of adsorption. The $R_L$ value was higher than unity for the biosorption process and shows the validity of this particular isotherm in correlating the biosorption data quite well. The Freundlich constant $K_F$ and n were obtained as 3.37 $mg^{1-1/n}g^{-1}L^{1/n}$ and 2.14 respectively with a correlation coefficient of 0.99. The value of n in the range 1-10 also indicates favourable biosorption and the implication of Freundlich model as well. The statistical chi square values for both these isotherm models were also quite low

indicating their good fit towards describing the biosorption data. The R-P isotherm model has striking similarity with Langmuir equation. The *g* value (0.89) which is near unity as obtained from the three parameter R-P isotherm model also indicates that the biosorption data can be explained reasonably well using the Langmuir model. The electrostatic interaction between the protonated functional groups in the biosorbent surface and Cr (VI) is reflected through the mean free energy of adsorption (-0.524 kJ $mol^{-1}$) obtained from D-R isotherm model. The D-R isotherm predicts that when the mean free energy of adsorption is less than 8 kJ $mol^{-1}$ the adsorption is more likely to be associated as physisorption.

The kinetics associated with the interaction between Cr(VI) and *Aspergillus* immobilized montmorillonite was studied using the pseudo first and second order kinetic models.[41,42] The removal of chromium Cr(VI) by the fungi immobilized clay attained its maximum within 60 min. The data obtained from the kinetic plots (Fig. 4.12) at 30 mg $L^{-1}$ Cr (VI) concentration shows effective correlation to the second order model as shown in Table 4.2 with the experimental and calculated $q_e$ values as 4.19 and 4.30 mg $g^{-1}$. Generally, particle, film diffusion and surface adsorption are the processes that affect the transport of Cr(VI) during agitation from solution phase to the *Aspergillus* immobilized clay surface. Intraparticle diffusion influences the kinetics at higher concentrations of the metal ion and at lower levels film diffusion governs the adsorption kinetics of Cr(VI).[36] The Weber-Morris intraparticle diffusion model[43] that connects $q_t$ and $\sqrt{t}$ as a straight line fit (Fig. 4.12) results in a finite intercept indicating the influence of boundary layer phenomenon in accounting for the adsorption of Cr(VI) by the fungi-clay biosorbent surface.

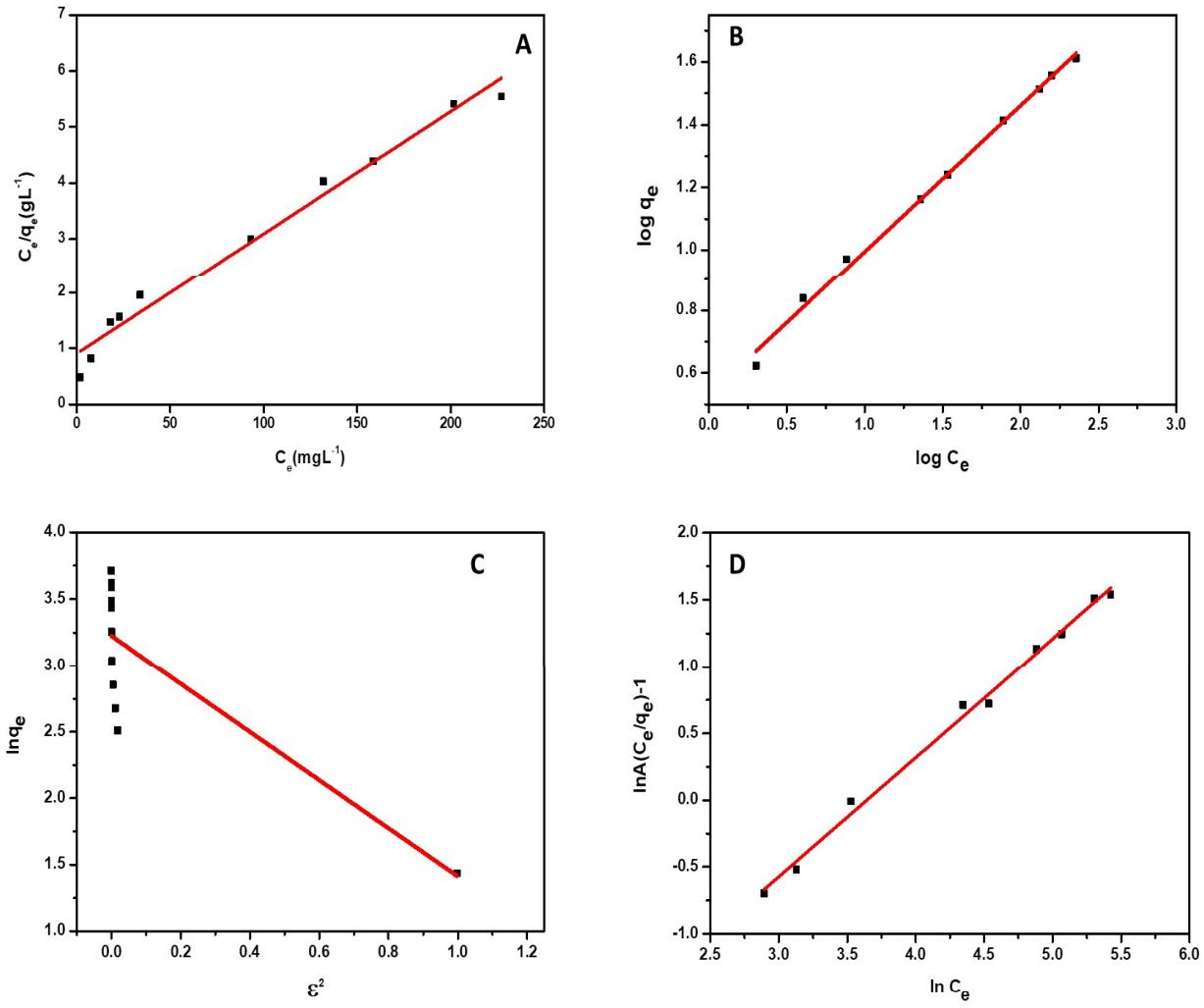


**Figure 4.11** (A) Langmuir isotherm (B) Freundlich isotherm (C) D-R isotherm (D) R-P isotherm (conditions: pH-2.0, adsorbent dosage- 0.2 g/30 mL, T=25$^{o}$C)

**Table 4.1** Biosorption isotherm parameters

| Langmuir<br>$\frac{C_e}{q_e} = \frac{1}{q_o b} + \frac{C_e}{q_o}$ | $q_o$(mg $g^{-1}$) | b(L $mg^{-1}$) | $R^2$ | $\chi^2$ | $R_L$ |
|---|---|---|---|---|---|
| | 45.72 | 0.022 | 0.978 | 0.424 | 0.599 |
| Freundlich<br>$\log q_e = logK_F - \frac{1}{n} logC_e$ | $K_F$($mg^{1-1/n} g^{-1} L^{1/n}$) | n | $R^2$ | $\chi^2$ | |
| | 3.371 | 2.142 | 0.995 | 0.019 | |
| Dubinin Radushkevich<br>$lnq_e = lnq_m - \beta\varepsilon^2$ | $q_m$(mg $g^{-1}$) | β($mol^2 kJ^{-2}$) | $R^2$ | $\chi^2$ | E(kJ $mol^{-1}$) |
| | 25.196 | 1.816 | 0.62 | 3.378 | -0.524 |
| Redlich-Peterson<br>$lnA\left\{\left[\frac{C_e}{q_e}\right] - 1\right\} = glnC_e + lnB$ | g | B(L $mg^{-1}$) | $R^2$ | $\chi^2$ | A(L $g^{-1}$) |
| | 0.890 | 0.039 | 0.99 | 0.107 | 1.019 |

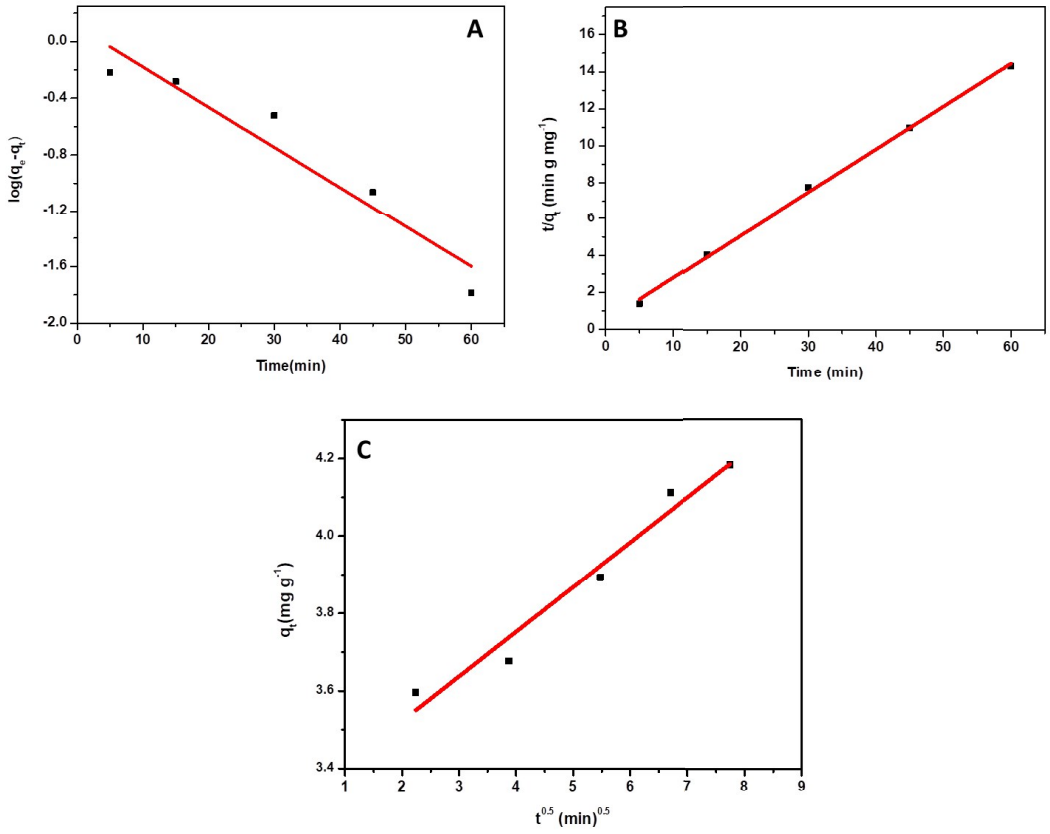


**Figure 4.12** (A) Pseudo first order kinetic plot (B) Pseudo second order kinetic plot (C) Intra particle diffusion (conditions: pH-2.0, adsorbent dosage- 0.2 g/30 mL, T=25$^{o}$C)

**Table 4.2** Kinetic parameters for chromium (VI) adsorption onto the clay-fungi biosorbent

| $C_o$(mg $L^{-1}$) | $q_e$ (mg $g^{-1}$) | $k_2$ (g $mg^{-1}$ $min^{-1}$) | $R^2$ | $k_1$ ($min^{-1}$) | $R_1^2$ | $k_{int}$ (mg $g^{-1}min^{-0.5}$) |
|---|---|---|---|---|---|---|
| 30 | 4.301 | 0.115 | 0.998 | 0.065 | 0.897 | 0.115 |

**(v) Biosorption thermodynamics**

The assessment of the spontaneity and the energetics of interaction between the host clay-biosorbent matrix and the guest (hexavalent chromium) were obtained from the Gibb's free energy ($\Delta G^o$), enthalpy ($\Delta H^o$) and entropy ($\Delta S^o$) values. The ratio of the concentrations of Cr (VI) present as $HCrO_4^-$ at equilibrium on the clay-*Aspergillus* surface and the aqueous phase gives the equilibrium constant (K) at different temperatures.[36] The equilibrium constant is correlated with the Gibb's isotherm equation ($\Delta G^0 = -RTlnK$) and from the straight line Van't Hoff plot of lnK against 1/T (Fig. 4.13) we obtain the $\Delta H$ and $\Delta S$ changes for the biosorption process. The above extensive thermodynamic properties arise due to primary and secondary host-guest interactions. Montmorillonite acts as a primary host in immobilizing the fungi (guest) and together they act as secondary host in inviting hexavalent chromium as guest. The respective thermodynamic properties could be expressed as

$$(\Delta G) = \Delta G_{\text{clay-}Aspergillus} + \Delta G_{\text{clay-}Aspergillus\text{-chromium}} \quad (4.1)$$

$$(\Delta S) = \Delta S_{\text{clay-}Aspergillus} + \Delta S_{\text{clay-}Aspergillus\text{-chromium}} \quad (4.2)$$

$$(\Delta H) = \Delta H_{\text{clay-}Aspergillus} + \Delta H_{\text{clay-}Aspergillus\text{-chromium}} \quad (4.3)$$

The concentration gradient across the clay-fungi biosorbent surface and the viscosity of the medium influences the transport of chromium from the aqueous phase. Accordingly, the free energy change in the biosorbent surface is greater than in the solution phase as evident from the negative values of free energy obtained at various temperatures. The free energy is also associated with the solvation of the host (biosorbent) and guest ($HCrO_4^-$) resulting in the lowering of chemical potential. Therefore, the enthalpically favourable exothermic biosorption that gives a relatively more negative entropy change signifies decreased randomness at the biosorbent-solution interface. The negative values of the average activation energy, $E_a = \Delta H^o_{ads} + RT$[36] also reflects this exothermic interaction (Table 4.3) between hexavalent chromium and the fungi immobilized clay matrix. The enthalpy values obtained are quite high to account for a total physisorption process and are also relatively low for pure chemisorption.[44] Hence, the

interaction between the functional groups on the clay-fungal adsorbent is conceptualized as a physicochemical adsorption phenomenon.

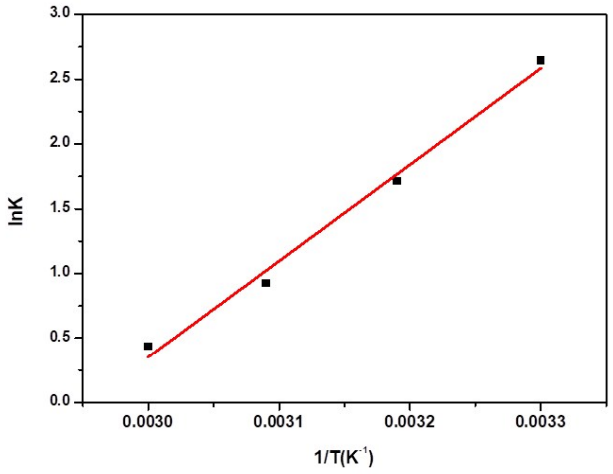


**Figure 4.13** Plot of lnK against 1/T (conditions: pH-2.0, adsorbent dosage- 0.2 g/ 30 mL)

**Table 4.3** Thermodynamics of biosorption

| **Temperature (Kelvin)** | **$\Delta G^0$ (kJ mol$^{-1}$)** | **$\Delta S^o$(J mol$^{-1}$K $^{-1}$)** | **$\Delta H^o$(kJ mol$^{-1}$)** | **$E_a$ (kJ mol$^{-1}$)** |
|---|---|---|---|---|
| 303 | -6.663 | -182.675 | -61.867 | -61.602 |
| 313 | -4.460 | | | |
| 323 | -2.483 | | | |
| 333 | -1.211 | | | |

**(vi) Column studies**

The applicability of the biosorbent material for Cr(VI) removal was examined in a higher sample volume through preliminary laboratory scale column studies. For this purpose, a 1.5 g clay-fungal biosorbent was packed onto a short glass column of 2 cm diameter upto a bed height of 3 cm. A 50 mL volume of 5 mg $L^{-1}$ Cr(VI) solution at pH 2.0 was loaded onto the column at a flow rate of 6 mL $min^{-1}$. The concentration of chromium (VI) that emerged out of the column was checked periodically (for every 10 mL collected in the eluate) with diphenyl carbazide as the derivatizing agent using ion chromatography. There was no trace of chromium detectable in the solution phase and this shows that the adsorption onto the biosorbent was quantitative for an initial concentration (5 mg $L^{-1}$) of chromium and a sample volume of 50 mL.

**Effect of sample volume**

In order to check the efficacy of the biosorbent for higher sample volumes, the initial sample volume was varied from 50 mL- 350 mL using 5 mg $L^{-1}$ chromium (VI). The pH was maintained at 2.0 and loaded onto the biosorbent (1.5 g) column at a flow rate of 6 mL $min^{-1}$. The concentration of chromium in the aqueous phase was determined after post column derivatisation with diphenyl carbazide as the chelating agent using ion chromatography. We observed the adsorption to be quantitative up to 200 mL sample volume (Fig. 4.14 A). Beyond, 200 mL there was a progressive decrease in the percentage adsorption of chromium. Since, clay materials are liable to undergo expansion it is probable that beyond 200 mL, the clay-*Aspergillus* biosorbent surface would expand leading to smaller voids in the packed column bed thereby resulting in the lowering of adsorption. .

The number of bed volumes, empty bed residence time (EBRT) and adsorbent exhaustion rate (AER) was also obtained for this fixed-bed adsorption process.

$$\text{Number of bed volumes} = \frac{\text{volume of solution treated}}{\text{volume of biosorbent bed}} \qquad (4.4)$$

$$\text{EBRT} = \frac{\text{packed bed volume}}{\text{flow rate}} \qquad (4.5)$$

$$AER = \frac{\text{weight of biosorbent in column}}{\text{volume of Cr(VI) solution treated at breakthrough}} \qquad (4.6)$$

The AER was found to be 7.5 g $L^{-1}$ and EBRT indicated that the Cr (VI) solution was in contact with the biosorbent for approximately 1.6 min corresponding to 21.23 bed volumes. With larger amount of the biosorbent in the packed bed, there is more potential to treat still higher sample volumes with lower AER and higher EBRT values. [45]

**Regeneration of biosorbent**

The reusability of biosorbent is quite important in order to understand the economics of the entire adsorption process. Sodium hydroxide was explored as a potential reagent for desorption since in alkaline medium, hexavalent chromium forms the yellow tetraoxochromate ($CrO_4^{2-}$) oxy anion. The concentration of NaOH was varied between 0.5-3.0 mol $L^{-1}$ and we observed the elution of chromium as sodium chromate[36] from the biosorbent surface with 2.0-3.0 mol $L^{-1}$ NaOH to be quite high as shown in Fig. 4.14 B. The biosorbent surface was washed with water and after mild acid conditioning was subjected to further use. The *Aspergillus* immobilized clay adsorbent could be reused without any apparent decrease in the efficiency for 4 adsorption-desorption cycles. A regeneration efficiency of 86% and 78% were observed in the fifth and sixth cycles respectively Fig. 4.14 C. The repetitive alkaline and acid treatment of the biosorbent surface resulted in the reduction in the regeneration efficiency beyond four cycles. The eluted chromium (VI) containing solution was utilized for the other ongoing biosorption methods that are in progress and a part of the eluate was also diluted considerably. This solution was converted to the less toxic Cr(III) and collected separately. The process was undertaken so as to minimize the disposal of higher concentrations of the hexavalent form.

The reduction of hexavalent chromium to the trivalent state was also not apparent after biosorption on the clay-fungi surface. Although, microbes have the ability to reduce Cr(VI), we observed the partial reduction to occur quite gradually after 4-5 days and this was seen in the form of a light green coloration (due to Cr(III)) appearing on the clay-*Aspergillus* biosorbent surface. This phenomenon was quite similar as observed earlier with yeast immobilized cellulose[36] as the adsorbent for chromium (VI). Hence, the *Aspergillus* immobilized clay

biosorbent is more likely to adsorb chromium quantitatively in its hexavalent form than the instant coupled reduction to the +3 state.

**(vii) Application to a certified wastewater sample**

The effect of some familiar ionic constituents known to be present in the industrial wastewater samples were probed independently in a synthetic wastewater containing 20 mg $L^{-1}$ concentrations of Fe(II), Cu(II), Ni(II), Cd(II), Pb (II), Mn (II), Zn(II) and chloride, nitrate, sulphate and phosphate ions and 10 mg $L^{-1}$ Cr(VI). A 9.53 ± 0.02 mg $L^{-1}$ of Cr(VI) could be retained onto the biosorbent surface in the presence of these diverse ions.

Following this, the methodology was tested in an industrial effluent wastewater sample BCR 715 which is a certified mixture having low concentration of various ions as mentioned in chapter 2. A 5 mL volume of the waste water sample (corresponding to an amount of 5 µg Cr) was converted to Cr (VI) by gentle oxidation using sodium hydroxide and hydrogen peroxide[46]. The solution was then diluted to 100 mL volume and passed through the biosorbent column (1.5 g) at pH 2.0. Cr (VI) was completely adsorbed onto the column and this was confirmed by finding the concentration of chromium left in the solution phase through ion chromatography. The adsorbed Cr (VI) was also eluted effectively using 10 mL of 2.0 mol $L^{-1}$ sodium hydroxide.

With 5 µg of chromium in 1.5 g of the biosorbent, the adsorption of chromium was found to be quantitative. Chromium was not detectable in the solution phase and this was verified by measuring the chromium concentration using ion chromatography in the solution phase after loading 100 mL of the sample. Chromium (VI) adsorbed on the biosorbent was eluted using 10 mL of 2.0 mol $L^{-1}$ NaOH solution. The corresponding chromatogram and the concentration of chromium eluted are shown in Fig. 4.15. The effective concentration of chromium in the eluate was found to be 0.5 mg $L^{-1}$ corresponding to a retention time of 2.46 min thereby resulting in a pre-concentration factor of 10 in the certified waste water sample. The results obtained indicate that the biosorbent has good potential to remove chromium from industrial waste water samples.

Electroplating effluents that discharge hexavalent chromium are quite acidic and the industrial effluents are usually in the pH range 2.0-3.0.[47,48] In this pH range Cr(VI) exists as hydrochromate

($HCrO_4^-$) anion and interacts very well with the protonated biosorbent surface. Hence, the clay-*Aspergillus* biosorbent could be well suited to treat such highly acidic actual industrial waste waters.

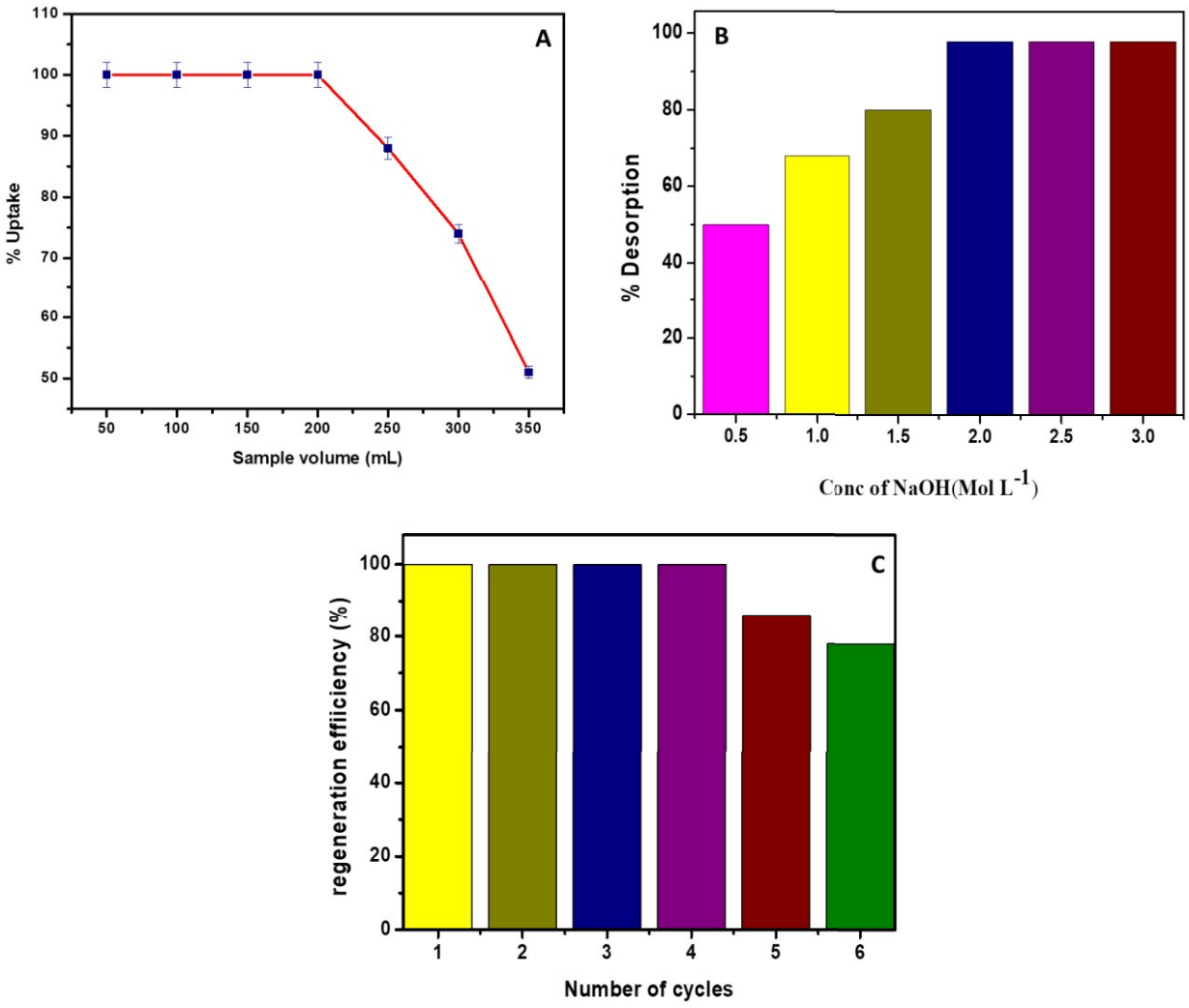


**Figure 4.14** (A) Effect of sample volume (conditions: weight of adsorbent- 1.5 g, Cr(VI) concentration- 5 mg $L^{-1}$, pH- 2.0, flowrate- 5 mL $min^{-1}$) (B) Effect of NaOH concentration (C) Regeneration efficiency of the biosorbent

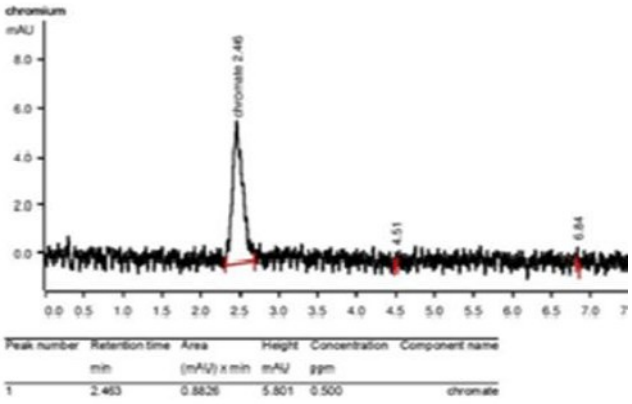


**Figure 4.15** Ion chromatogram of the certified waste water sample (BCR 715) containing chromium.

**(viii) Application to real sample (Chrome plating effluent)**

The chrome plating effluent was collected from a small scale electroplating industry unit whose composition is presented in Table 4.4.

**Table 4.4** Composition of the chrome plating effluent

| Analyte | Concentration | Unit |
|---|---|---|
| Fe | 66.95955 | μg $L^{-1}$ |
| Cu | 100.3 | μg $L^{-1}$ |
| Co | 25.345 | μg $L^{-1}$ |
| Ni | 2.71 | μg $L^{-1}$ |
| Ba | 185.95 | μg $L^{-1}$ |
| Pb | 0.0 | μg $L^{-1}$ |
| Cd | 3.275 | μg $L^{-1}$ |
| Na | 237.25 | mg $L^{-1}$ |
| K | 0.655 | mg $L^{-1}$ |
| Ca | 84.5 | mg $L^{-1}$ |
| Mg | 44.225 | mg $L^{-1}$ |
| Mn | 0.515 | mg $L^{-1}$ |
| Zn | 171.6 | mg $L^{-1}$ |
| **Cr** | **278.6** | **mg $L^{-1}$** |
| Al | 0.775 | mg $L^{-1}$ |
| B | 1.56 | mg $L^{-1}$ |

The concentration of chromium originally present in the sample (analysed by ICP- AES) was found to be 278.6 mg $L^{-1}$. A known volume of the effluent sample was digested using 10 mL of aqua-regia and diluted to bring the concentration level of chromium to 5 mg $L^{-1}$. The diluted chromium concentration was found to be in the +6 oxidation state as analysed through ion chromatography. A 4.0 g weight of the biosorbent was packed in the column and a sample volume of 500 mL effluent containing 5 mg $L^{-1}$ Cr(VI) could be adsorbed quantitatively.

**(ix) Comparison of adsorption capacity against allied fungal strains and clays**

The isolated *Aspergillus BRVR* fungal strain as such showed an adsorption capacity of 13.5 mg $g^{-1}$ and the *Aspergillus* immobilized sodium montmorillonite (NaMMT) showed a relatively higher adsorption capacity of 45.75 mg $g^{-1}$. The original clay material (montmorillonite) and sodium modified montmorillonite showed adsorption capacities of only 8.14 mg $g^{-1}$ and 9.16 mg $g^{-1}$ respectively. Hence, the synergistic or co-operative effect is manifested through the effective microbe-NaMMT interaction with the hexavalent chromium.

Furthermore, the biosorbent also shows relatively higher adsorption capacity in comparison with other allied fungal strains and some clay composites[12, 49-53] as well (Table 4). The above results quantify the improvement in chromium removal performance. The good adsorption capacity shows that this biosorbent has the potential to remove chromium from wastewaters quite efficiently**.**

**Table 4.5** Comparison of maximum adsorption capacity against few fungi and biopolymer- clay composites

| **Adsorbents** | **Adsorption capacity (mg $g^{-1}$)** | **pH** | **Temperature** |
|---|---|---|---|
| *Agaricus bisporus*[49] | 8.0 | 1.0 | 20°C |
| *Rhizopus arrhizus*[50] | 23.92 | 1.3 | 30°C |
| *Aspergillus sydoni*[51] | 9.07 | 2.0 | 25°C |
| *Lentinus sajor*- caju[52] | 22.10 | 2.0 | 40°C |
| Chitosan – sodium montmorillonite –$Fe_3O_4$ microspheres[53] | 58.82 | 5.0 | 30 °C |
| Cellulose-sodium[12] montmorillonite | 22.20 | 3.8-5.5 | 45°C |
| (Present studies)<br>*Aspergillus BRVR*<br>Montmorillonite<br>$Na^+$ Montmorillonite<br>*Aspergillus BRVR* immobilized in sodium montmorillonite | <br>13.50<br>8.14<br>9.16<br>45.72 | <br>2.0<br>2.0<br>2.0<br>2.0 | <br>30 °C<br>30°C<br>30 °C<br>30 °C |

### 4.1.4 Conclusions

This study has illustrated the combined influence of fungi and sodium montmorillonite for the prospective removal of hexavalent chromium. The inorganic support imparts good stability thereby giving a high adsorption capacity of 45.72 mg $g^{-1}$. Second order model is more appropriate in describing the adsorption kinetics of chromium (VI). The thermodynamics of biosorption process indicates the spontaneous and exothermic interaction. The preliminary laboratory scale column tests have indicated the prospects of this biosorbent in the scale up operations to a higher sample volume. The detailed fixed bed column modeling aspects which we plan to undertake as a further study would certainly enhance the worth of this biosorbent. The ability of the biosorbent to treat industrial wastewater and the regeneration using sodium hydroxide highlights the convergence of chemistry and biotechnology in formulating sustainable solutions to address heavy metal contamination.

## 4.2. Adsorption of chromium supported with various column modelling studies through the synergistic influence of *Aspergillus* and cellulose

### 4.2.1 Introduction

The present study explores the utility of the *Aspergillus* immobilized in epichlorohydrin crosslinked cellulose biosorbent for chromium removal and a detailed investigation into the column modelling studies. Biopolymers such as cellulose and chitosan function as good supports for chromium removal as they are easily available at low cost and are also degradable. [12,54] *Aspergillus* species is also a potential microbe to remediate heavy metals.[2] There are several reports on the Cr(VI) removal by various fungi such as biomass of *Penicillium chrysogenum* by grafting polyethylenimine on its surface.[55] The adsorbent shows good efficacy in the adsorption of chromium(VI) which involves adsorption as well as partial reduction of +6 to +3 state and were confirmed through XPS studies. Sujoy et al [56] reported the interaction of chromium with *Aspergillus versicolor* using Atomic force microscopy (AFM) and Transmission electron microscopies (TEM) and the XPS, FTIR studies revealed that bound Cr was in the form Cr(III) involving adsorption coupled reduction. Mungasavalli et al [10] reported that the pre-treated *Aspergillus niger* could adsorb chromium effectively with 15.2 mg $g^{-1}$ Langmuir adsorption capacity. *Aspergillus sp* immobilized in sodium montmorillonite[57] is reported to have good potential for Cr(VI) removal with an adsorption capacity of 45.67 mg $g^{-1}$ . Microwave assisted preparation of biosorbent[36] such as yeast immobilized in cellulose can efficiently remove Cr(VI) with an adsorption capacity of 23.61 mg $g^{-1}$ .

The numerous methods available for removal of chromium using batch studies have some limitations during scale up operations. There are few reports on the successful pilot scale up studies for the removal of Cr(VI) using a biofilm of *Arthrobacter viscosus* supported on granular activated carbon [58] and also by reduction with ferrous sulfate.[59] Fixed bed column studies are operative in the treatment of larger volumes of the heavy metals contaminated waste water.[60] The column modelling studies aid in understanding the various characteristics as well as limitations in the design of larger columns in industrial treatment operations. The batch experimental studies carried out in the present system help in understanding several features about the adsorbent-adsorbate interaction and the maximum adsorption capacity that would be useful in column

design along with optimizing the other vital column parameters such as bed height, flow rate etc. Subsequently, column modelling studies were investigated at room temperature correlating the above factors.

### 4.2.2. Experimental Procedure

#### (i) Preparation of the biosorbent

4 g of cellulose was taken in a 100 mL beaker and 25 mL of 2.0 mol $L^{-1}$ sodium hydroxide, 4 mL of epichlorohydrin[61] (as cross linker) were added and stirred for 120 min at 55$^{o}$C. An equal amount of the powdered fungal strain (4g) was added and stirred further for 60 min. The obtained biosorbent was washed with Millipore water and dried overnight at 40$^{o}$C in a vacuum oven.

#### (ii) Batch adsorption studies

A 0.4 g amount of the *Aspergillus*-cellulose biosorbent was mixed with 30 mL of Cr(VI) of various working solution concentrations derived from simple stock solution at pH 2.0. The mixture was incubated in an orbital shaker incubator at a constant stirring rate of 120 rpm at 30$^{o}$C to reach equilibration. The biosorption kinetics was evaluated between 5 min to 180 min at a working Cr(VI) concentration of 10 mg $L^{-1}$ whereas the isotherm experiments were done in the range from 5 mg $L^{-1}$ to 450 mg $L^{-1}$. The thermodynamic studies were carried in the range 303K - 333K at a working solution concentration of 30 mg $L^{-1}$ Cr(VI). The residual chromium concentration was estimated using the post column derivatization with diphenyl carbazide using ion chromatography. The concentrations of chromium were also compared using UV visible spectrophotometry [62,63] by complexation with diphenyl carbazide.

#### (iii) Column studies

Fixed bed column experiments were performed in a glass column with a diameter of 3.0 cm, and a length of 45 cm packed with the fungi-cellulose biosorbent at room temperature. A known amount of the biosorbent was packed to a bed height of 10 cm and 15cm and care was taken to avoid air voids by soaking the adsorbent in water for 2 hours prior to the start of the experiment. The known chromium working solution concentrations were prepared i.e., 50 mg $L^{-1}$, 100 mg $L^{-1}$

and adjusted to pH 2.0 were allowed to pass through the column at flow rates 5 mL $min^{-1}$ and 10 mL $min^{-1}$ respectively. Samples from the column effluent were collected at regular intervals of 15 min and analysed for the chromium concentration.

### 4.2.3. Results and discussion

#### (i) Biosorbent Characterisation

The fungal microbial cell wall has amine, carboxyl and hydroxyl functional groups that are useful in Cr(VI) uptake and the FTIR spectrum obtained (Fig.4.16) showed prominent changes before and after adsorption of Cr(VI).[27] The broad band observed at 3299 $cm^{-1}$ and 3314 $cm^{-1}$ before and after adsorption of chromium corresponds to the merged peak of OH and NH stretching vibrations and the shift in the peak confirms the involvement of the functional groups in the Cr(VI) uptake. The C-H stretching in $CH_2$ of cellulose gives a peak at 2885 $cm^{-1}$ and the peak shift from 1610- 1627 $cm^{-1}$ before and after adsorption corresponds to the participation of amide-I band of protein-peptide linkage of the fungal cell wall. Further, the shift from 1022-1080 $cm^{-1}$ indicates the participation of C-O group of polysaccharide in biosorption. [27] The Cr =O bond in the finger print region appears as a small distinct peak at 881 $cm^{-1}$ supporting the Cr(VI) biosorption as $HCrO_4^-$ onto the biosorbent surface.[64] The SEM micrographs depict the morphological features of the biosorbent (Fig.4.17) which shows the interspersed rods of cellulose and fungal hyphae and further the compositions were evaluated using elemental analysis from the energy dispersive X-ray spectrum which gives the chromium peak between 5-6 keV.

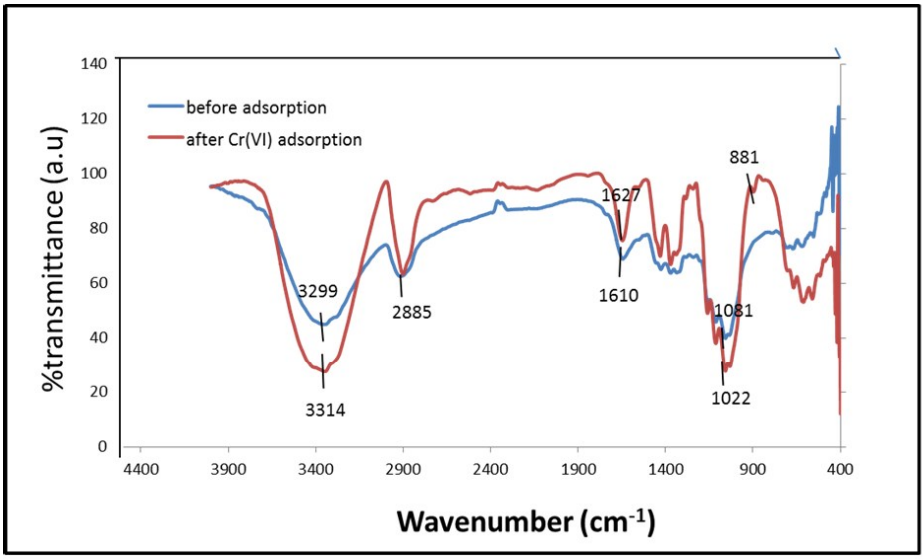


**Figure 4.16.** FTIR spectra of the biosorbent before and after Cr(VI) adsorption

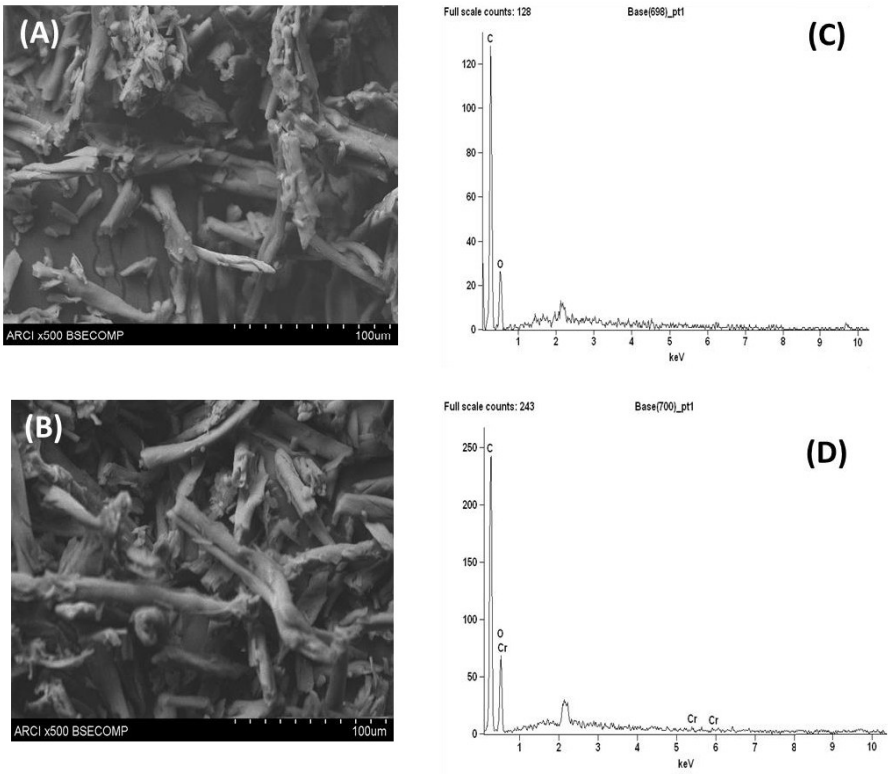


**Figure 4.17.** (A,B) SEM of biosorbent before and after adsorption.

(C,D) EDAX analysis of biosorbent before and after adsorption

X-ray photo electron spectroscopy (XPS) was used to probe the surface and compositions of the biosorbent. The survey scan spectra showed the existence of Cr(VI), oxygen along with carbon peak at 284.87 eV (Fig 4.18A). The amplified narrow scan spectra of Cr 2p3/2 has a binding energy of 576.8 eV (Fig. 4.18B) characteristic of Cr(III) [65] and 587.6 eV which is the peak due to Cr (VI). In the present study, during the adsorption of hexavalent chromium there was no abrupt reduction of Cr(VI) to Cr(III) and it was only after 3 days a pale green coloration was observed on the surface of the biosorbent indicating the probable reduction to Cr(III) and it was also supported through the XPS characterization. A similar feature was also noticed in our earlier studies [36] when adsorption studies for chromium were carried out using yeast immobilized in cellulose matrix. The biosorbent has a BET surface area of 1.95 $m^2$ $g^{-1}$ with a pore volume of 0.003 $cm^3/g$ and pore size of 6.153 nm indicating the mesoporous nature of the *Aspergillus*-cellulose biosorbent. The initial weight loss observed in thermal analysis of the biosorbent is attributed to the evaporation of water and the formation of levoglucosan below 200°C (Fig. 4.19) due to the cellulose glycosidic bond cleavage leading to heterolytic depolymerisation.[66]

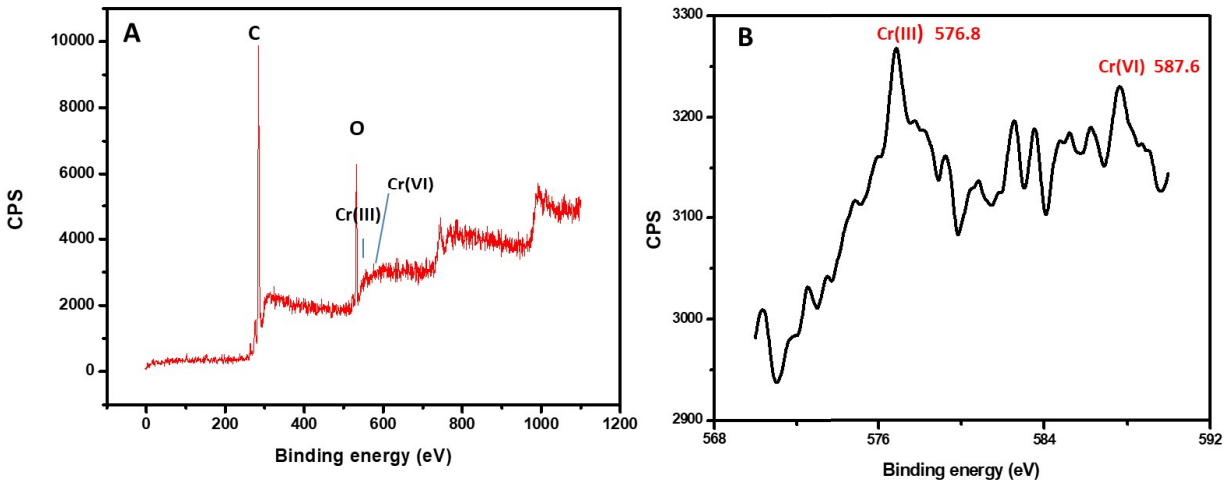


**Figure 4.18.** (A) The XPS survey scan spectra of the biosorbent after Cr(VI) adsorption (B) Amplified narrow scan spectra between 568-592 eV

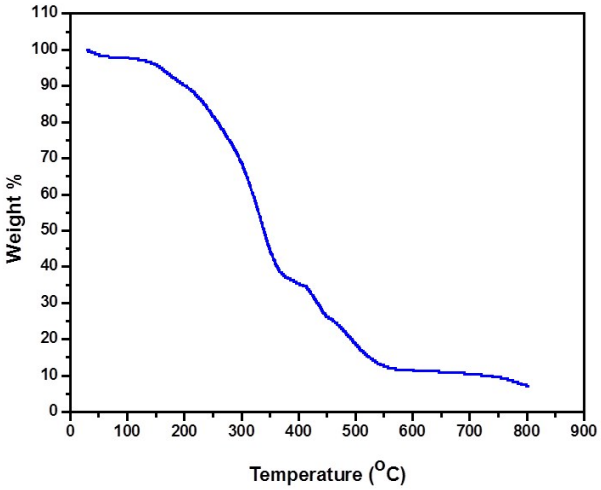


**Figure 4.19** TGA curve of the biosorbent.

**(ii) Effect of pH and mechanism of the biosorption**

The percentage removal of chromium increased with the decreasing pH, owing to the effective interaction of the functional groups in the biosorbent with the Cr(VI) species[57] existing in the form of $HCrO_4^-$ and $Cr_2O_7^{2-}$. Cr(VI) at varying pH, exists as tetraoxohydrochromate ($HCrO_4^-$), chromate ($CrO_4^{2-}$) and dichromate ($Cr_2O_7^{2-}$) ions. In the acidic pH around 2.0 – 3.0 the surface of the biosorbent which contains various functional groups such as amines, carboxyl and hydroxyl groups gets protonated and interacts electrostatically with $HCrO_4^-$ ions and hence adsorption takes place. This is also evident from the Cr=O peak obtained at 881 $cm^{-1}$ in FT-IR spectrum. At pH 2.0 and at a working Cr(VI) concentration of 5 mg $L^{-1}$ there was 100% Cr(VI) removal efficiency and the percentage adsorption decreased with increasing pH. As shown in Fig.4.20 A, $HCrO_4^-$ exists at the acidic pH (2.0) and at this acidic pH the functional groups present in the fungal cell wall ($NH_2$, OH and COOH) as well as cellulose gets protonated resulting in electrostatic interactions [57] (Fig.4.21) . The epichlorohydrin used for the crosslinking of cellulose strengthens the biopolymer and the fungus when immobilized in the crosslinked cellulose has increased the probability of entering the voids of cellulose layer. At higher pH, electrostatic repulsion occurs between the *Aspergillus*-cellulose biosorbent and $HCrO_4^-$ ions leading to decrease in Cr(VI) adsorption. Cr(III) was not immediately detectable in the adsorbent. This could be due to slow reduction of Cr(VI) to Cr(III) as also evident in the XPS

spectra. Hence, the adsorption process is also accompanied by reduction after a considerable time period. Cr(III) exists as cationic hydroxides $Cr(OH)_2^+$, $Cr(OH)^{2+}$ in the pH range 6.5-7.5 and interacts with the negatively charged biosorbent surface and adsorption of Cr(III) occurs accordingly.[46] The effect of the biosorbent amount was studied by varying the dosage of biosorbent from 0.1 to 0.7g. The maximum adsorption of Cr(VI) was observed at 0.4 g and after that the saturation observed is due to reduction of active adsorption sites. (Fig.4.20 B)

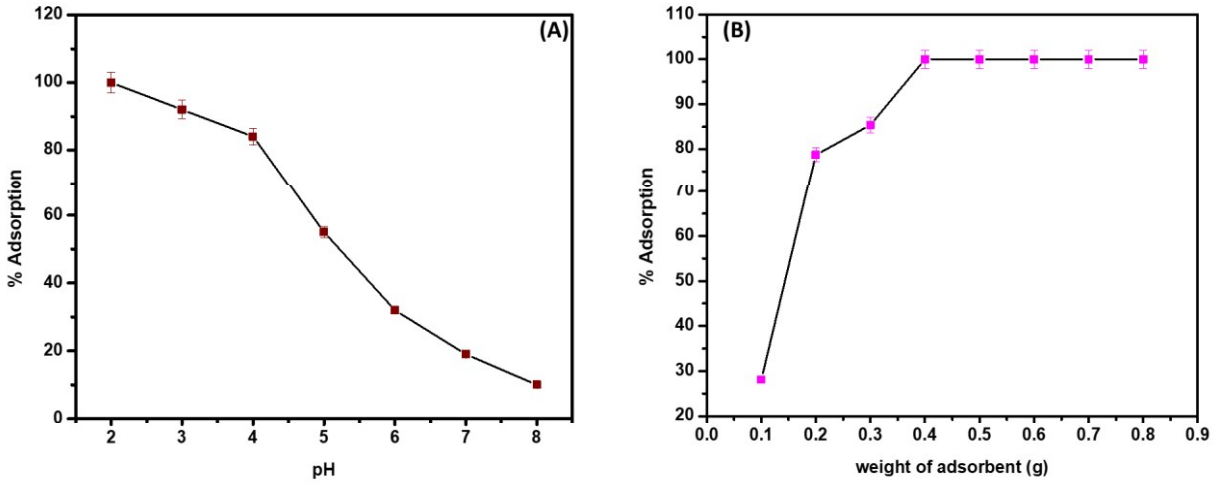


**Figure 4.20**.(a) Effect of pH on biosorption **(**conditions: adsorbent dosage- 0.4 g/30 mL, Cr(VI) concentration- 5 mg $L^{-1}$, T=25$^oC$) (b) Effect of Adsorbent dosage **(**conditions: adsorbent dosage- 0.4 g/20 mL, Cr(VI) concentration- 5 mg $L^{-1}$, T=25$^oC$)

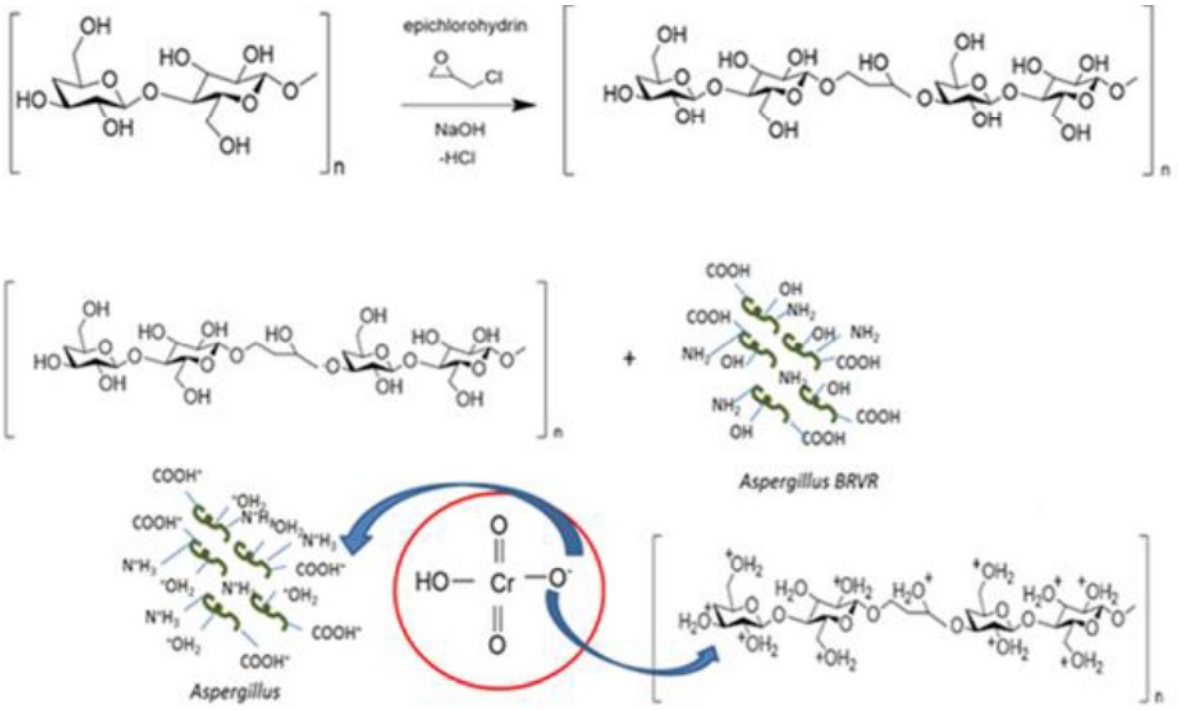


**Figure. 4.21** Schematic representation showing the interaction mechanism of biosorbent with hexavalent chromium (Source: Chembio draw Ultra11.0)

**(iii) Equilibrium kinetics, isotherms and thermodynamic studies**

Several kinetic models are proposed to conceptualize the mechanism by which metal ions are adsorbed onto the surface of the biosorbents. The pseudo first order and second order kinetics [41,42] were used for the evaluation of the adsorption kinetics. Where $q_e$ and $q_t$ are amounts of Cr(VI) adsorbed at time t and at equilibrium in mg $g^{-1}$ and $k_1$ and $k_2$ are the rate constants of the pseudo first order and second order reactions. For the study, 30 mL of 10 mg $L^{-1}$ was taken with 0.4 g of the biosorbent and the kinetic data were acquired by varying the equilibration time from 5 min to 180 min. The maximum adsorption occurred within 180 min. From the data obtained (Fig.4.22A-B) the pseudo second order provides a better fitting model (Table 4.5) than the first order with $R^2$ coefficient of 0.9824 and with the experimental and calculated $q_e$ values as 0.69 mg $g^{-1}$ and 0.7170 mg $g^{-1}$ respectively. The transport of Cr(VI) from aqueous phase onto the surface of *Aspergillus*-cellulose biosorbent involves particle, film and surface adsorption.

Intraparticle diffusion is favourable for Cr(VI) at higher concentration and at a lower concentration effective interaction between chromium and biosorbent would drive the adsorption kinetics.[57] The Weber-Morris intra particle diffusion model [43] correlates the $q_t$ and $\sqrt{t}$ (Fig.4.22C) and the plot shows the role of boundary layer mechanism in accounting for the effective Cr(VI) uptake.

The isotherms give further insights into the adsorption process and the commonly applied isotherms are Langmuir and Freundlich [68] to which the experimental data were fitted (Table 4.6). Out of the two isotherms, Freundlich fitted better with a regression coefficient of 0.9782 (Fig.4.22D-E) which indicates the system followed multilayer adsorption and a low $\chi^2$ value (0.0955). Also the value of n in the range 1-10 indicates favourable biosorption. Langmuir isotherm that assumes a monolayer adsorption process is useful in getting the adsorption capacity of the biosorbent which is 23.838 mg $g^{-1}$ with a $R^2$ value of 0.8368. A dimensionless constant $R_L = 1/1+bC_o$ is used to verify the suitability of Langmuir isotherm.[69] The $R_L$ value obtained was below unity which indicates the biosorption is reversible.

The Gibbs free energy, entropy and enthalpy changes are useful towards understanding the spontaneity and energetics of the biosorption process. The equilibrium constant K was calculated from the ratio of the concentrations of Cr(VI) present in the *Aspergillus*-cellulose biosorbent surface to liquid phase [57] which was then fitted into Gibb's isotherm equation ($\Delta G^0 = -RTlnK$) . From the plot between lnK and 1/T (Fig.4.22F), the changes in the enthalpy and entropy are obtained and the properties are attributed due to the host- guest interactions wherein *Aspergillus* immobilized cellulose acts as primary host to the hexavalent chromium.

The transport of $HCrO_4^-$ from the solution phase to the *Aspergillus*-cellulose biosorbent surface depends on the concentration gradient across the $HCrO_4^-$ and the biosorbent interphase. The $[Cr(VI)]_{biosorbent}$ is greater than the $[Cr(VI)]_{solution}$ at equilibrium and this is evident from the negative $\Delta G$ values obtained for the biosorbent – Cr(VI) interaction. The chemical potential $\mu_{HCrO4}^-$ can also be related to the standard chemical potential and activity of $HCrO_4^-$ is represented as

$$\mu_{HCrO4}^- = \mu^o_{HCrO4}^- + RTlna_{HCrO4}^- \qquad (4.7)$$

In dilute solutions activity (a) is directly proportional to the concentration (c), hence

$$\mu_{HCrO4^-} = \mu^o_{HCrO4^-} + RT\ln [HCrO_4^-] \quad (4.8)$$

$$[HCrO_4^-]_{solution} \rightleftharpoons [HCrO_4^-]_{asp\text{-}cellulose\ surface} \quad (4.9)$$

Hence, the free energy of adsorption and the standard free energy can be related as

$$\Delta G_{ads} = \Delta G^o_{ads} + RT\ln[\ Cr(VI)_{surface} - Cr(VI)_{solution}] \quad (4.10)$$

At equilibrium $\Delta G_{ads}=0$

$$\Delta G^o_{ads} = - RT\ln [Cr(VI)_{surface} / Cr(VI)_{solution}] \quad (4.11)$$

The enthalpy-entropy compensation is quite significant in understanding the adsorption process that occurs between $HCrO_4^-$ and the biosorbent surface. [70] The negative value of $\Delta G$ and $\Delta H$ indicates that the biosorption process is spontaneous and exothermic respectively. The negative values of activation energy [12] $E_a = \Delta H^o_{ads} + RT$ (Table 4.7) confirms the exothermic nature and the negative entropy shows decreased randomness at biosorbent – solution interphase. The enthalpy values obtained indicate the system follows physico-chemical adsorption.[71] The free energy change also depends upon the electrostatic, hydrogen bonding and van der Waals interactions between the biopolymer and the functional groups in the fungi cell surface. Negative $\Delta H$ or $\Delta S$ indicates the good binding of Cr(VI) with *Aspergillus*-cellulose functional groups. Since, the adsorption experiments were carried out at various temperatures it was observed that the system follows exothermic adsorption indicating effective adsorbent-adsorbate interaction at room temperature. In addition, the Gibbs free energy and entropy changes help in understanding the spontaneity of the biosorption process.

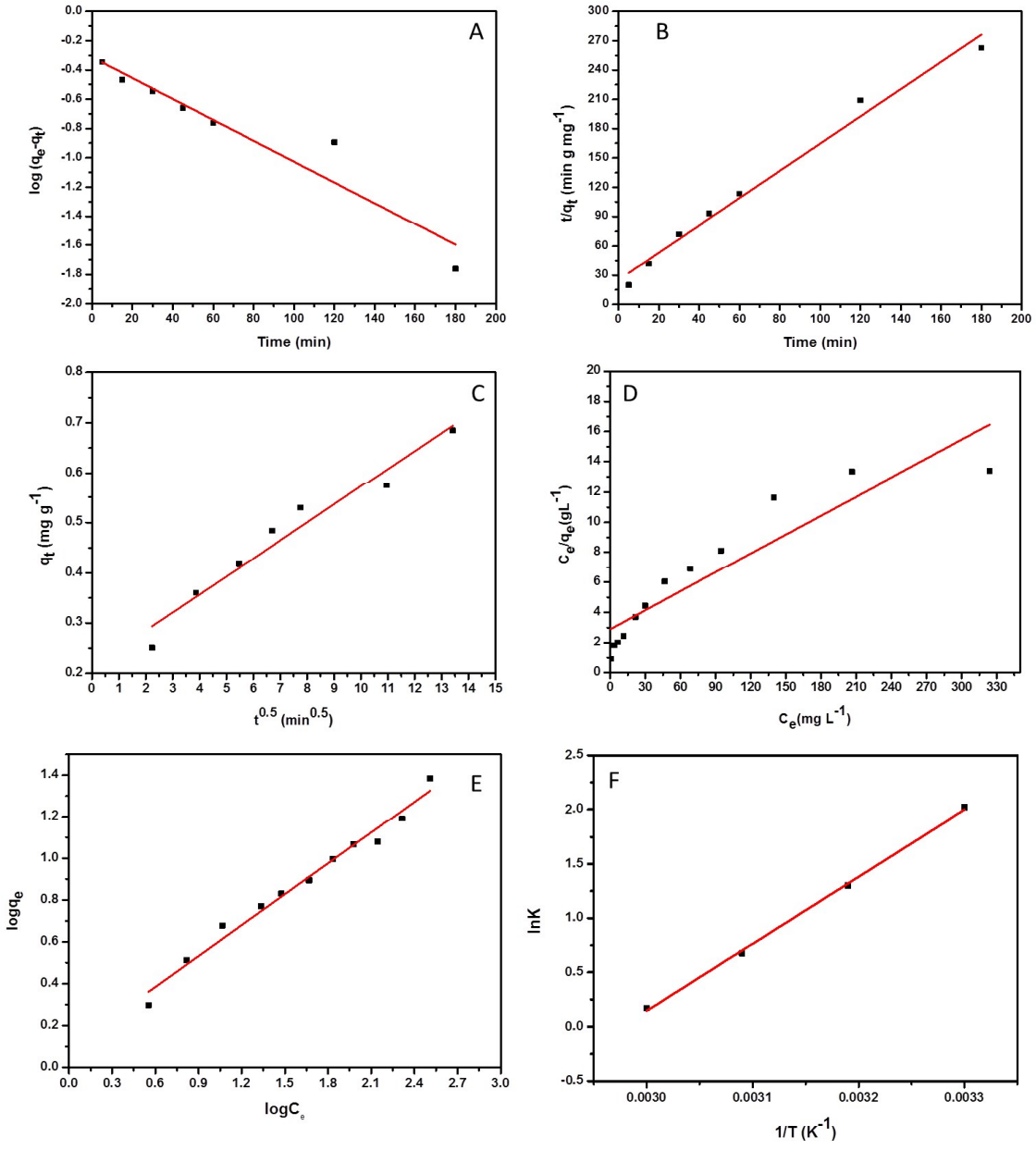


**Figure. 4.22** (A) Pseudo first order kinetic plot (B) Pseudo second order kinetic plot (C) Intra particle diffusion (D) Langmuir isotherm (E) Freundlich isotherm (F) Plot of lnK Vs 1/T (conditions: pH-2.0, adsorbent dosage- 0.4 g/30 mL)

**Table 4.6.** Kinetic parameters for chromium (VI) adsorption onto the fungi-cellulose biosorbent

| $C_o$(mg $L^{-1}$) | $q_e$ (mg $g^{-1}$) | $k_2$ (g $mg^{-1}$ $min^{-1}$) | $R^2$ | $k_1$ ($min^{-1}$) | $R_1^2$ | $k_{int}$ ($mgg^{-1}min^{-0.5}$) |
|---|---|---|---|---|---|---|
| 10 | 0.7170 | 0.0771 | 0.982 | 0.0165 | 0.903 | 0.03584 |

**Table 4.7.** Biosorption isotherm parameters

| Langmuir $\frac{C_e}{q_e} = \frac{1}{q_o b} + \frac{C_e}{q_o}$ | $q_o$(mg $g^{-1}$) | b(L $mg^{-1}$) | $r^2$ | $\chi^2$ | $R_L$ |
|---|---|---|---|---|---|
| | 23.838 | 0.0145 | 0.8368 | 2.078 | 0.0334 |
| Freundlich $\log q_e = logK_F - \frac{1}{n} logC_e$ | $K_F$($mg^{1-1/n}g^{-1}L^{1/n}$) | n | $r^2$ | $\chi^2$ | |
| | 1.226 | 2.0296 | 0.9782 | 0.0955 | |

**Table 4.8.** Effect of temperature on biosorption

| Temperature (Kelvin) | $\Delta G^0$ (kJ mol$^{-1}$) | $\Delta S^o$(J mol$^{-1}$K $^{-1}$) | $\Delta H^o$(kJ mol$^{-1}$) | $E_a$ (kJ mol$^{-1}$) |
|---|---|---|---|---|
| 303 | -4.920 | -153.0092 | -51.404 | - 51.139 |
| 313 | -3.383 | | | |
| 323 | -1.809 | | | |
| 333 | -0.4737 | | | |

**(iv) Preliminary Column studies**

The application of biosorbent material for Cr(VI) removal was also studied through laboratory scale column studies. A 2 g amount of the biosorbent was packed to 4 cm bed height in a glass column. A 100 mL volume of 5 mg L$^{-1}$ working solution of Cr(VI) solution at pH 2.0 was loaded onto the column at a flow rate of 4 mL min$^{-1}$. The concentration of chromium (VI) collected was checked periodically (for every 25 mL collected in the eluate) with diphenyl carbazide as the complexing agent using UV visible spectrophotometry. Cr(VI) was adsorbed effectively in the glass column.

Varying concentrations of NaOH (Fig. 4.23 A) were studied to desorb the Cr(VI) from the column and the biosorbent could effectively adsorb and desorb up to two full cycles. Beyond there is a gradual decrease in the regeneration efficiency of the biosorbent (Fig.4.23 B). A 10 mL of 1.5 mol L$^{-1}$ sodium hydroxide could effectively desorb the Cr(VI) as sodium chromate.

$$(Aspergillus - \text{cellulose}) - -HCrO_4^- + NaOH_{aq} \rightleftharpoons Na_2CrO_{4\,(aq)} + (Aspergillus - \text{Cellulose})_{surface} \quad (4.12)$$

Since the pH of the column increased, it was washed with water and reused for further adsorption studies.

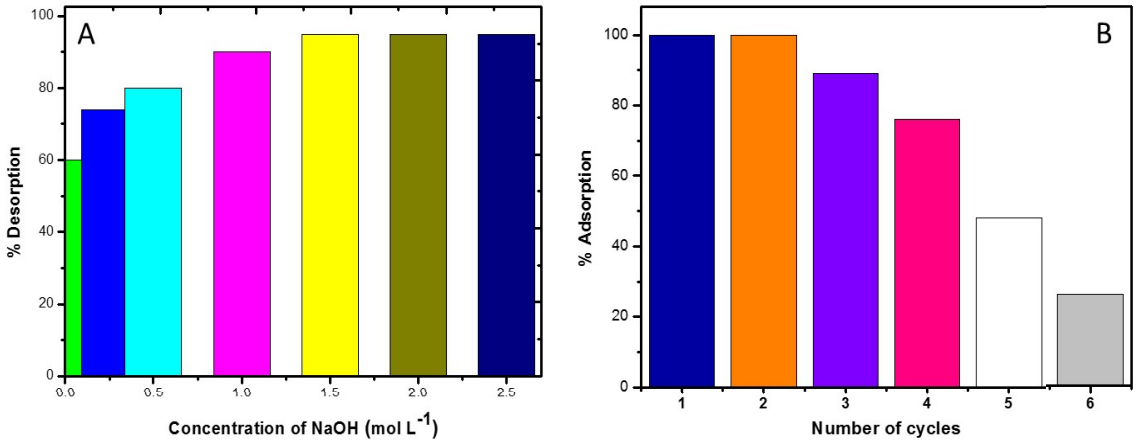


**Figure. 4.23** (A) Effect of NaOH concentration (B) Regeneration efficiency of the biosorbent.

**(v) Application studies**

A synthetic wastewater containing diverse ions ($Cu^{+2}$, $Pb^{+2}$, $Hg^{+2}$, $Fe^{+2}$, $Co^{+2}$, $Ni^{+2}$, chloride nitrate) of varying concentrations were mixed with 5 mg $L^{-1}$ Cr(VI) and their results are shown in (Table 4.9).The adsorption studies were carried out as before and it was observed that the removal of Cr(VI) efficiency was greater than 90% with four different compositions and synthetic mixtures. In presence of high $Fe^{2+}$ (300 mg $L^{-1}$) and $Cl^-$ (100 mg $L^{-1}$) the reduction of Cr(VI) to Cr(III) by $Fe^{2+}$ and the competition of stable chloro complexes [12] of the metal ions ( $HgCl_4^{2-}$, $CoCl_4^{2-}$, $NiCl_4^{2-}$) for active adsorption sites reduces the removal efficiency of Cr(VI). Further the methodology was tested in a certified industrial effluent wastewater sample (BCR 715) comprising of various elements as mentioned in chapter 2. 5 mL of this sample was pre-treated with sodium hydroxide and hydrogen peroxide [26] to oxidise all the Cr to Cr(VI) and final volume was diluted to 100 mL bringing the concentration to 0.05 mg $L^{-1}$. The mixture was passed through the column containing the biosorbent and Cr(VI) was not detectable in the eluate. This shows that chromium as Cr(VI) is retained on the column effectively.

**Table 4.9.** Recovery of Cr(VI) from simulated synthetic mixtures

| Mixture of various ions | Adsorption (%) |
|---|---|
| $Cu^{+2}$( 100 mg $L^{-1}$), $Pb^{+2}$( 100 mg $L^{-1}$), $Hg^{+2}$( 100 mg $L^{-1}$), $Fe^{+2}$(100 mg $L^{-1}$), $Co^{+2}$(100 mg $L^{-1}$), $Ni^{+2}$ (100 mg $L^{-1}$), $Cr^{+6}$(5 mg $L^{-1}$) | 96.8 ± 0.5 |
| $Cl^-$ (100 mg $L^{-1}$) $NO_3^-$ (100 mg $L^{-1}$), $Cr^{6+}$ (5 mg $L^{-1}$) | 99.8 ±0.1 |
| $Cu^{+2}$(50 mg $L^{-1}$), $Pb^{+2}$ (150 mg $L^{-1}$) , $Hg^{+2}$(200 mg $L^{-1}$) $Co^{+2}$ (50 mg $L^{-1}$) $Ni^{+2}$(150 mg $L^{-1}$), $Cr^{+6}$ (5 mg $L^{-1}$), $Cl^-$ (100 mg $L^{-1}$), $NO_3^-$ (150 mg $L^{-1}$) | 99 ± 0.6 |
| $Cu^{+2}$(50 mg $L^{-1}$), $Fe^{+2}$ (300 mg $L^{-1}$) , $Hg^{+2}$(200 mg $L^{-1}$) $Co^{+2}$ (50 mg $L^{-1}$) $Ni^{+2}$(150 mg $L^{-1}$), $Cr^{+6}$ (5 mg $L^{-1}$), $Cl^-$ (100 mg $L^{-1}$), $NO_3^-$ (150 mg $L^{-1}$) | 94.6 ±1.0 |

**(vi) Column modelling studies**

Based on preliminary column experimental studies, various parameters such as effect of bed height, flowrate and initial Cr(VI) concentrations in the modeling studies were carried out.

**Effect of bed height, flowrate and initial Cr (VI) concentration**

The effect of bed height was determined through breakthrough curves using 50 mg $L^{-1}$ Cr (VI) concentration and a flow rate of 5 mL $min^{-1}$. The bed heights chosen were respectively 10 cm and 15 cm. From the plot of $C_t/C_o$ against time (Fig. 4.24A), it was observed that break through time increased from 195 min to 240 min with increase in bed height from 10 cm to 15 cm. This is attributed to the increase in number of active adsorption sites with increase in bed height.[72] Axial dispersion phenomenon is more important at lower bed heights thereby reducing the diffusion of Cr(VI). Packing the biosorbent at this bed height provides more depth in effective

mass transfer for Cr (VI) to exit the column.[73] In evaluating the performance of the biosorption, flow rate plays an important role. The effect was studied using different flow rates such as 5 mL $min^{-1}$ and 10 mL $min^{-1}$ at 10 cm bed height with an input concentration of 50 mg $L^{-1}$ (Fig.4.24B). The break through time decreased from 195 min to 60 min with increase in flow rate. This is due to the lesser time of contact available for interaction between Cr(VI) solution and the biosorbent thereby decreasing the dynamic uptake of chromium. Low flow rates promote diffusion and increases the residence time thereby augmenting the adsorption efficiency.[74] The effect of two different initial Cr(VI) concentrations ($C_o$) at constant bed height of 10 cm and flow rate of 5 mL $min^{-1}$ are shown in (Fig. 4.24C). There is a decrease in the break through time at higher Cr(VI) concentration from 195 min to 75 min due to the fast saturation of the active adsorption sites at higher Cr(VI) concentration. [75]

**Application of Thomas Model**

Thomas model for column adsorption was applied to the data obtained at different bed heights 10 cm and 15 cm, at varying flow rates 5 mL $min^{-1}$ and 10 mL $min^{-1}$, and Cr(VI) concentrations of 50 mg $L^{-1}$ and 100 mg $L^{-1}$. The linear expression for the Thomas model for adsorption is expressed as [76]

$$\ln\left[\left(\frac{C_0}{C_t}\right)-1\right]=\frac{k_{Th}q_o m}{Q}-k_{Th}\,C_o t \quad (4.13)$$

Where the $k_{Th}$ (mL $min^{-1}$.mg) is the Thomas model constant, $q_o$ (mg $g^{-1}$) is the maximum adsorption capacity, m is mass of adsorbent (g), Q is influent flow rate (mL $min^{-1}$), $C_0$ is initial Cr(VI) concentration (mg $L^{-1}$), and $C_t$ is effluent Cr(VI) solution concentration (mg $L^{-1}$). The constant $k_{th}$ and $q_o$ were calculated from slope and intercept of the plot obtained from the plot of ln $[(C_o/C_t)-1]$ vs t (min) along with the regression coefficients presented in (Table 4.10) From the plots (Fig. 4.24D-F) it is observed that at a constant bed height, increase in flow rate decreased the sorption capacity due to faster exhaustion and lower contact time between Cr(VI) and the biosorbent surface. Also it was observed that as the flow rate increases the adsorption capacity decreases and the rate constant increases but with the increase in Cr(VI) concentration, both the adsorption capacity and the $k_{Th}$ value decreases. The obtained $R^2$ values were low which explains this model could not be quite suited to fit the data.

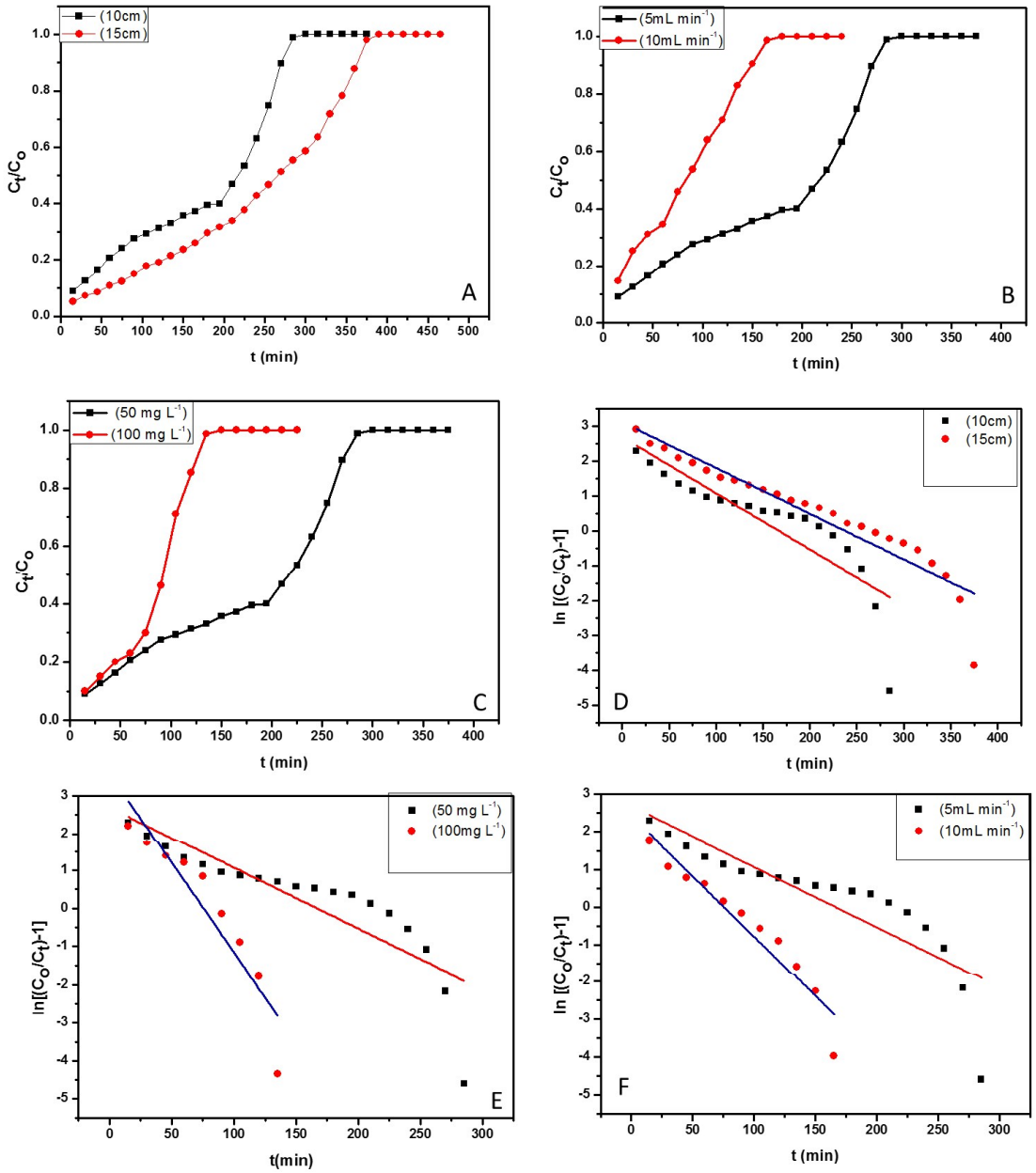


**Figure 4.24** Break through curves obtained at (A) different bed heights (B) different flow rates (C) different Cr(VI) concentrations. Plots of Thomas model at (D) different bed heights (E) different Cr(VI) concentrations (F) different flow rates .

**Table 4.10** Parameters obtained from Thomas model

| Z(cm) | Q(mL $min^{-1}$) | $C_o$ (mg $L^{-1}$) | $q_o$ (mg $g^{-1}$) | $k_{Th}$ x $10^{-4}$(mL $min^{-1}$ $mg^{-1}$) | $R^2$ |
|---|---|---|---|---|---|
| 10 | 5 | 50 | 6984.11 | 3.2 | 0.7306 |
| 10 | 5 | 100 | 6596.69 | 2.62 | 0.8512 |
| 10 | 10 | 50 | 6345.59 | 6.4 | 0.9146 |
| 15 | 5 | 50 | 6293.34 | 3.57 | 0.8895 |

**Application to Yoon Nelson model**

Yoon and Nelson proposed a model based on the postulate that the decrease in the rate of the probability of adsorption for the analyte (chromium) is proportional to the probability of its sorption and also the breakthrough concentration on the biosorbent. [77] The linearized Yoon and Nelson equation can be expressed as

$$\ln\left(\frac{C_o}{C_{o-}C_t}\right) = k_{YN}t - \tau k_{YN} \qquad (4.14)$$

where t is the sampling time, $k_{YN}$ is the Yoon-Nelson rate constant, $\tau$ the time required for 50% adsorbate breakthrough (min), where $k_{YN}$ and $\tau$ are determined from the slope and intercept of the plot $\ln\left(\frac{C_o}{C_{o-}C_t}\right)$ vs t (Fig. 4.25A-C).

The Yoon–Nelson model was also applied to the column data obtained and various parameters were calculated as shown in Table 4.11. The $k_{YN}$ values were found to decrease significantly with the increase in bed height and increase with increase in flow rate and influent Cr(VI) concentration (Table 4.11). The 50% breakthrough time $\tau$ values decreased significantly at higher flow rate and Cr(VI) concentration due to the early saturation of the column. Also the $R^2$ values increased with increase in flow rate and initial Cr(VI) concentration but are low indicating that this model might also not be very ideal to model the column data.

**Application to Bed Depth Service Time (BDST) model**

The linear relationship between depths, Z and service time t is given by BDST model. The model is based on hypothesis that the Cr(VI) is directly adsorbed onto the *Aspergillus*-cellulose biosorbent where the intra particle diffusion and external mass transfer are negligible and assumes that equilibrium is not attained rapidly.[78] This model is applied more in the depiction of the initial part of the breakthrough curve. The BDST model equation is given as

$$\ln\left(\frac{C_t}{C_o} - 1\right) = k_{AB}C_o t - k_{AB}N_o\left(\frac{Z}{U_o}\right) \qquad (4.15)$$

where $C_o$ is the initial concentration of Cr(VI) (mg $L^{-1}$), $C_t$ is the concentration of Cr(VI) at breakthrough (mg $L^{-1}$), $k_{AB}$ is the adsorption rate constant ($L^{-1}$ $mg^{-1}$ min), $N_o$ is the adsorption capacity (mg $L^{-1}$), Z is the bed depth of column (cm), $U_o$ is the linear flow velocity of feed to bed (cm $min^{-1}$), t the service time of column under above conditions (min). The equation can be written in simpler form as below

$$t = aZ - b \qquad (4.16)$$

Where a represents the slope of the plot $\left(a = \frac{N_o}{vC_o}\right)$ and b is the intercept given as

$$b = \frac{1}{kC_o}\ln\left(\frac{C_o}{C_t} - 1\right) \qquad (4.17)$$

The values $k_{AB}$ and $N_o$ were calculated (Table 4.12) from the plot obtained between bed height (Z) and service time (t) (Fig. 4.25D). At $C_t/C_o$ = 0.3, as the flowrate increases there is a decrease in $N_o$ values and increase in rate constant ( $k_{AB}$) values indicating the external mass transfer dominated the system kinetics in the initial part of biosorption in the column.[79] The correlation coefficients $R^2$ are higher compared to the Thomas and Yoon Nelson models.

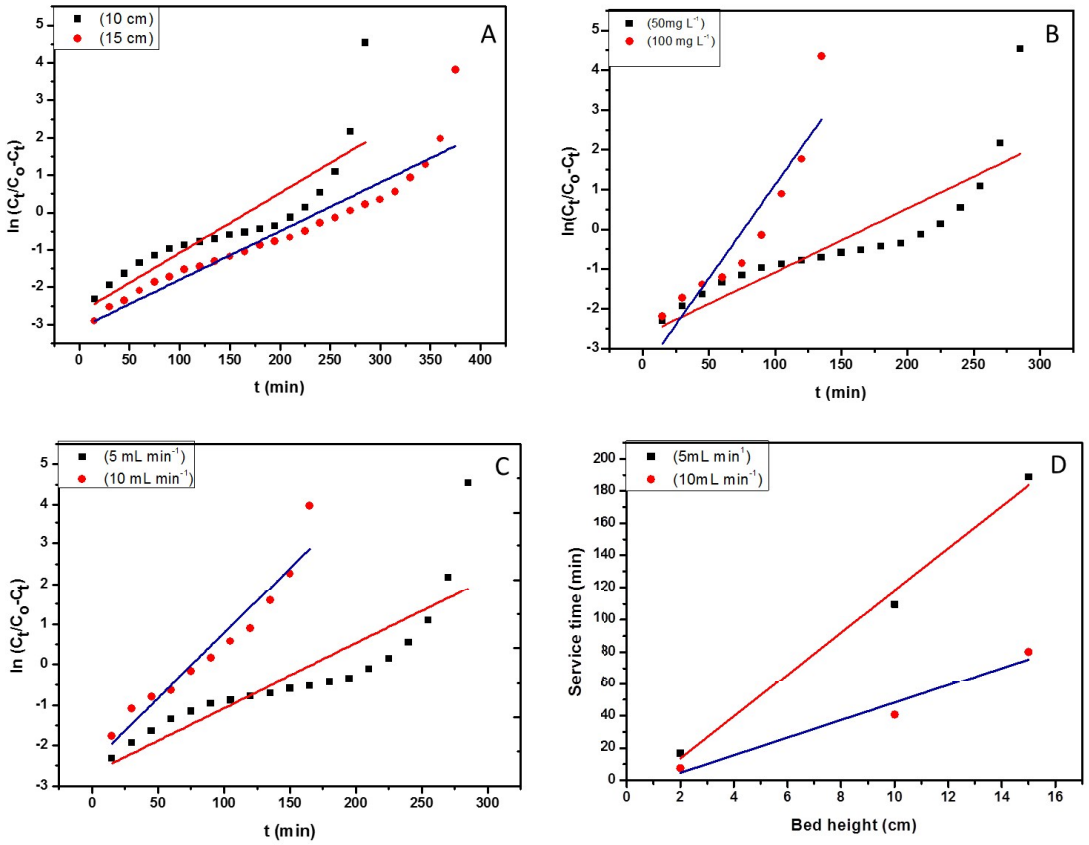


**Figure 4.25.** Plots of Yoon Nelson model at (A) different bed heights (B) different Cr(VI) concentrations (C) different flow rates (D) Plot of BDST model at $C_t/C_o$= 0.3

**Table 4.11.** Parameters obtained from Yoon-Nelson model

| Z(cm) | Q (mL $min^{-1}$) | $C_o$ (mg $L^{-1}$) | $k_{YN}x10^{-2}$ ($min^{-1}$) | τ(min) | $R^2$ |
|---|---|---|---|---|---|
| 10 | 5 | 50 | 1.604 | 167.201 | 0.7353 |
| 10 | 5 | 100 | 4.7 | 76.212 | 0.8383 |
| 10 | 10 | 50 | 3.211 | 75.86 | 0.9147 |
| 15 | 5 | 50 | 1.304 | 237.99 | 0.8911 |

**Table 4. 12.** Parameters obtained from BDST model

| $C_t/C_o$ | Q(mL $min^{-1}$) | $k_{AB}$ x $10^{-3}$ (L $mg^{-1}$ $min^{-1}$) | $N_o$ (mg $L^{-1}$) | $R^2$ |
|---|---|---|---|---|
| 0.3 | 5 | 1.9 | 462.55 | 0.98483 |
| 0.3 | 10 | 3.86 | 385.72 | 0.93321 |

### 4.2.4 Conclusions

The fungus immobilized in epichlorohydrin crosslinked cellulose yields a Langmuir adsorption capacity of 23.83 mg $g^{-1}$. An increase in bed height increased the adsorption capacity while an increase in flow rate and Cr(VI) concentration reduces the adsorption efficiency. The system follows pseudo second order kinetics and thermodynamically spontaneous and exothermic. Various column parameters were studied through the breakthrough curves and mathematical models such as Thomas, Yoon-Nelson, and BDST were applied to the system, of which BDST model was the best fit with a good adsorption capacity. The biosorbent efficiently removes Cr(VI) from synthetic waste water sample and certified industrial effluent sample. The regeneration of Cr (VI) was done using 1.5 mol $L^{-1}$ sodium hydroxide and the *Aspergillus*-cellulose combination has good ability to treat Cr(VI) contaminated waste water.

**References**


1. Wang, J.; Chen, C. *Biotechnol. Adv*., **2009**, 27, 195-226.
2. Gu, Y.; Xu, W.; Liu, Y.; Zeng, G.; Huang, J.; Tan, X.; Jian, H.; Hu, X.; Li, F.; Wang, D. *Environ. Sci. Pollut. Res*. **2015**, 22, 6271- 6279.
3. Li, W.W.; Yu, H.Q. *Bioresour. Technol.,* **2014**, 160, 15-23.
4. Xafenias, N.; Zhang,Y; Banks, C.J. *Environ. Sci. Technol*. **2013**, 47, 4512–4520.
5. Wang, J.; Chen, C.; *Biotechnol. Adv*. **2009**, 27, 195-226.
6. Fomina, M.; Gadd, G.M.; *Bioresour. Technol*. **2014**, 160, 3-14.
7. Li, L.; Hu, N.; Ding,D.; Xin, X.; Wang, Y.; Xue, J.; Zhang, H.; Tan, Y. *RSC Adv*. **2015**, 5, 65827-65839.
8. Vijayaraghavan, K.; Yun,Y.S. *Biotechnol. Adv*. **2008**, 26, 266-291.
9. Samuel, J.; Paul, M.L.; Pulimi, M.; Nirmala, M.J.; Chandrasekaran, N.; Mukherjee, A. *Ind. Eng. Chem. Res*. **2012**, 51 ,3740–3749.
10. Mungasavalli, D.P.; Viraraghavan, T.; Jin, Y.C. *Colloids Surf., A*. **2007**, 301, 214-223.
11. Park, D.; Yun, Y.S.; Park, J.M. *Process Biochem*. **2005**, 40, 2559-2565.
12. Kumar, A.S.K.; Kalidhasan, S.; Rajesh, V.; Rajesh, N. *Ind. Eng. Chem. Res*., **2012**, 51, 58–69.
13. Koriche, Y.; Darder, M.; Aranda, P.; Semsari, S.; Hitzky, E.R. *Dalton Trans*. **2014**, 43, 10512-10520.
14. Unuabonah, E.I.; Taubert, A. *Appl. Clay Sci*. **2014**, 99, 83-92.
15. Matlok, M.; Petrus, R.; Warchol, J.K. *Ind. Eng. Chem. Res*., **2015**, 54, 6975–6984.
16. Bhattacharyya, K.G.; Gupta, S. S.; *Ind. Eng. Chem. Res*., **2006**, 45 , 7232–7240.
17. Brum, M.C.; Capitaneo, J.L.; Oliveira, J.F. *Miner. Eng*. **2010**, 23, 270-272.
18. Taylor, R.W.; Shen, S.; Bleam, W.F.; Tu, S.I. *Clays Clay. Miner*., **2000**, 48, 648-654.
19. Biswas, B.; Sarkar, B.; Rusmin, R.; Naidu, R. *Environ. Int.,* **2015**, **85**, 168–181.
20. Sugita, C.; Makimura, K.; Uchida, K.; Yamaguchi, H.; Nagai, A. *Med. Mycol*., **2004**, 42, 433-437.
21. Leck, A. *Community Eye Health*, **1999**, 12, 24.

22. Moller, E.M.; Bahnweg, G.; Sandermann, G.; Geiger, H.H.; *Nuc. Acids Res*, **1992**, 20, 6115-6116.
23. Pancher, M.; Ceol, M.; Corneo, P.E.; Longa, C.M.O.; Yousaf, S.; Pertot,I.; Campisano, A. *Appl. Environ. Micr*obiol., **2012**, 78, 4308 – 4317.
24. Manasi, Rajesh, V.; Kumar , A.S.K.; Rajesh, N. *Chem. Eng. J*. **2014**, 235, 176-185.
25. Boufait, M.; Amar, H.A. *Desalination*, **2007**, 206, 300-310.
26. Arar, E.J.; Pfaff, J.D. *J. Chromatogr. A*, **1991**, 546, 335-340.
27. Naumann, D. ed. R.A. Meyers, Infra-red spectroscopy in microbiology, Encyclopaedia of Analytical Chemistry, John Wiley and Sons Ltd., Chichester, **2000**, pp. 102-131.
28. Flessner, U.; Jones, D.J.; Rozière , J.; Zajac , J.; Storaro , L.; Lenarda , M.; Pavanc, M.; J.López , A.; Castellón , E.R.; Trombetta , M.; Busca , G. *J. Mol. Catal. A- Chem*. **2001**, 168, 247–256.
29. Zhongying , L.; Tang, R.; Liu, G. *Catal Lett*., **2013**, 143, 592–599.
30. Liang, Z.M.; Yin. J.; Xu, H.J. *Polymer*, **2003**, 44, 1391–1399.
31. Singh, V.; Sharma, A.K.; Kumari, P.; Tiwari, S. *Ind. Eng. Chem. Res*. **2008**, 47, 5267–5276.
32. Xie, W.; Gao, Z.; Pan, W.P.; Hunter, D.; Singh, A.; Vaia, R. *Chem. Mater*. **2001**, 13, 2979-2990.
33. Fomina, M.A.; Kadoshnikov, V.M.; Zlobenko, B.P. *Process Metallurgy*,**1999**, 9, 245-254.
34. Malla, P.B.; Komarneni, S. *Clays Clay. Miner*., **1990**, 38, 363-372.
35. Gopinath. S.; Sugunan, S. *Appl. Clay Sci*. **2007**, 35, 67–75.
36. Sathvika, T.; Manasi, Rajesh, V.; Rajesh, N. *Chem. Eng. J*., **2015**, 279, 38-46.
37. Wang , B.E.; Hu, Y.Y.; Xie, L.; Peng, K. *Bioresour. Technol*., **2008**, 99, 794−800.
38. Chung, H.K.; Kim, W,H.; Park, J.; Cho, J.; Jeong, T.Y.; Park, P.K. *J. Ind. Eng. Chem*., **2015**, 28, 241-246.
39. Barathi, M.; Kumar, A.S.K.; Kumar , C.U.; Rajesh, N. *RSC Adv*., **2014**, 4, 53711-53721.
40. Hall, K.R.; Eagleton, L.C.; Acrivos, A.; Vermeulen, T. *Ind. Eng. Chem. Fundamen.,* **1966**, 5 , 212–223.
41. Lagergren, S. *K. Sven.Vetenskapsakad. Handl*., **1898**, 24,1-39.

42. Ho, Y.S., Mckay, G. *Water Res*., **2000**, 34, 735-742.

43. Weber, W.J.; Morris, J.C. *J. Sanit. Eng. Div*. **1963**, 89, 31-60.

44. Hamza, I.A.A.; Martincigh, B.S.; Ngila, J.C.; Nyamori, V.O. *Phys. Chem. Earth*, **2013**, 66, 157–166.

45. Malkoc, E.; Nuhoglu, Y.; Abali,Y. *Chem. Eng. J*. **2006**, 119, 61-68.

46. Rajesh, N.; Kumar, A.S.K.; Kalidhasan, S.; Rajesh, V. *J. Chem. Eng. Data*. **2011**, 56 , 2295–2304.

47. Park, D.; Yun, Y.S.; Jo, J.H.; Park, J.M. *Water Res*. **2005**, 39, 533-540.

48. Baral, A.; Engelken, R.D.; *Environ. Sci. Policy*, **2002**, 5, 121–133.

49. Ertugay, N.; Bayhan, Y.K.; *J. Hazard. Mater*., **2008**, 154, 432–439.

50. Preetha, B.; Viruthagiri, T. *Sep. Purif. Technol*. **2007**, 578, 126–133.

51. Kumar, R.; Bishnoi , N.R.; Bishnoi, G,K. *Chem. Eng.* J. **2008**, 135, 202-208.

52. Bayramoglu, G.; Celik, G.; Yalcin¸ E.; Yilmaz, M.; Arica, M.Y. *J. Hazard. Mater*, **2005**, 119, 219–229.

53. Chen , D.; Li , W.; Wu , Y.; Zhu, Q.; Lu, Z.; Du, G. *Chem. Eng.* J. **2013**, 221, 8–15.

54. Boddu, V.M..; Abburi, K.; Talbott, J.L.; Smith, E.D. *Environ. Sci. Technol*. **2003**, 37 4449-4456.

55. Deng, S.; Ting, Y.P. *Environ.Sci. Technol*., **2005**, 39, 8490-8496.

56. Das, S.K.; Mukherjee, M.; Guha, A.K. *Langmuir*, **2008**, 24, 8643-8650.

57. Sathvika,T.; Manasi, Rajesh, V.; Rajesh, N. *RSC Adv*., **2015**, 5 ,107031-107044.

58. Sathvika,T.; Manasi , Rajesh,V.; Rajesh, N. *Chem. Eng. J*. **2015**, 279, 38–46.

59. Quintelas, C.; Fonseca, B.; Silva, B.; Figueiredo, H.; Tavares, T. *Bioresour. Technol*. **2009**, 100 , 220-226.

60. Qin , G.; McGuire , M.J.; Blute , N.K.; Seidel, C.; Fong , L. *Environ. Sci. Technol*., **2005**, 39, 6321–6327.

61. Sankararamakrishnan, N.; Kumar, P.; Chauhan, V.S. *Sep. Purif. Technol*., **2008**, 63, 213–219.

62. Ishimura, D.; Morimoto, Y.; Saito, H. *Cellulose*, **1998**, 5, 135-51.

63. Pobozy, E.; Wojasinska, E.; Trojanowicz, M. *J. Chromatogr*. A, **1996**, 736, 141-150.

64. Eaton, A.D.; Clescri, L.S.; Greenberg, A.E. Standard methods for the examination of water and wastewaster; American Public Health Association (APHA), AWWA, V PCF: Washington, DC, **1995**, 4-23.
65. Kumar, A.S.K.; Rajesh, N. *RSC Adv*., **2013**, 3, 2697–2709.
66. Mu, Y.; Ai, Z.; Zhang, L.; Song, F. *ACS Appl. Mater. Interfaces*, **2015**, 7, 1997–2005.
67. Mettler, M.S.; Mushrif, S.H.; Paulsen, A.D.; Javadekar, A.D.; Vlachosa, D.G.; Dauenhauer, P.J. *Energy Environ. Sci*. **2012,** 5, 5414–5424.
68. Foo, K.Y.; Hameed, B.H. *Chem. Eng. J*. **2010**, 156, 2–10.
69. Sun, C.J.; Sun, L.Z.; Sun, X.X. *Ind. Eng. Chem. Res*. **2013**, 52, 14251–14260.
70. Houk, K.N.; Leach, A.G.; Kim, S.P.; Zhang, X. *Angew. Chem. Int. Ed*. 2003, 42, 4872-4897.
71. Hamza, I.A.A.; Martincigh, B.S.; Ngila, J.C.; Nyamori, V.O. *Phys. Chem. Earth*., **2013**, 66, 157–166.
72. Hamdaoui,. O. *J Hazard Mater*. **2006**, 138, 293–303.
73. Foo, K.Y.; Hameed, B.H. *Chem. Eng. J*., **2012**, 203, 81–87.
74. Soetaredjo, F.E.; Kurniawan, A.; Ong, L.K.; Widagdyo, D.R.; Ismadji, S. *RSC Adv*., **2014**, 4, 52856-52870.
75. Hasan, S.H.; D. Ranjan, D.; Talat, M. *J. Hazard. Mater*. **2010**, 181, 1134–1142.
76. Chen, S.; Yue, Q.; Gao, B.; Li, Q.; Xu, X.; Fu,K. *Bioresour. Technol*. **2012**, 113, 114-120.
77. Bharathi, K.S.; Ramesh, S.K.P.T. *Appl. Water. Sci*., 2013, **3**, 673–687.
78. Lakshmipathy, R.; Sarada, N.C. *Environ. Sci.: Water Res. Technol*., **2015**, 1, 244 –250.
79. Ahmed, A.A..; Hameed, B.H. *J.Hazard.Mater*. **2010**, 175, 298-303.

# Chapter – 5

## Leveraging the Potential of Endomycorrhizal Spores and Montmorillonite for Hexavalent Chromium Adsorption from Aqueous Phase

# Leveraging the Potential of Endomycorrhizal Spores and Montmorillonite for Hexavalent Chromium Adsorption from Aqueous Phase

## 5.1. Introduction

In this chapter, we have explored the potential of endomycorrizhal fungal spores in conjunction with a clay mineral as a novel approach for chromium (VI) adsorption. Microbes provide nutrients to the plants which are not easily available from the soil. The synergistic association between phycomycetes fungi and plant roots results in the formation of arbuscular mycorrhiza and the spores produced by these fungi are mainly located in the rhizosphere soil. [1,2] Arbuscular mycorrhizal fungus (AMF) absorbs minerals, phosphates, nitrogen from the soil and supply to the plants. AMF is also known to regulate the heavy metal uptake by soya bean (*Glycine max*) depending on the concentration of the heavy metals in the soil. [3] Arbuscular mycorrhizae present in sunflower plants increases the tolerance towards higher chromium concentrations.[4] Gil-Cardesa et al. reported[5] that *Ricinus communis* and *Conium maculatum* used Cr- mycorrhizal stabilization mechanism for the removal of Cr from soil near industrial site. Studies on the clay-microbial combination for heavy metal sequestration are scarce. The current study demonstrates the adsorption of heavy metal chromium using the AMF spores isolated from agricultural soil. Cr(VI) removal was augmented using the AMF-clay biosorbent wherein the isolated AMF spores were immobilized in clay using ultra-sonication. The microbe-clay combination could also adsorb several organic pollutants as they persist in similar ecological conditions. [6] The developed biosorbent was tested for Cr (VI) removal in batch studies by varying pH, adsorbent dosage, kinetics and thermodynamics.

## 5.2 Experimental section

### (i) Preparation of the AMF-clay biosorbent

The AMF spores were isolated according to the procedure reported previously [7] from the soil (taken from a local groundnut *(Arachis hypogea*) cultivation field) and also from the commercial formulation (soil) provided by K.N. Biosciences, Hyderabad, India. The soil collected was suspended in water and stirred for few minutes to break the lumps. The soil solution was then passed through the sieves of 250 μm and 37 μm stacked over one another with 250 μm on the

top. The finer particles are collected in the 37 μm sieve and water washing was done till the aqueous phase emerged colourless through the sieves. The particles from the 37 μm were collected in a beaker and centrifuged at 4000 rpm for 20 min and the supernatant was discarded. The particulate matter remaining at the bottom was treated with 50% sucrose solution and centrifuged once again and the procedure was repeated twice. After centrifugation, the supernatant was passed through the sieve and washed with water to remove traces of sucrose. Finally the spores collected in the sieve were transferred to a beaker containing water and stored at 4$^{o}$C for short term use. The spores were then identified under the optical microscope.

The treatment of montmorillonite with sodium chloride enables its conversion to the $Na^{+}$ form as described earlier. [8] Ultra-sonication has been reported to be very effective for bacterial cell growth through convection mechanism. [9] Sonication also serves as a quick and energy efficient method in the preparation of adsorbents. Essentially, it results in acoustic cavitation by increasing the convection thereby accelerating the adsorbent preparation time. Ultra-sonication using a simple sonication bath was utilized in our earlier studies to immobilize *Aspergillus* in sodium montmorillonite. [10] Likewise, a table top ultrasonic bath (1.5 L) sonicator of 50W operating at an alternating current 230 V power supply was used also for the amalgamation of clay and AMF spores. Different combinations (ratios) of the AMF spores and clay were explored (0.25:1, 0.5:1, 1:1 ratio of spores-clay) and tested for Cr(VI) adsorption efficiency and a ratio of 1:1 of spores to clay was found to give an average adsorption efficacy of 78%. Accordingly, a 1.0 g of sodium montmorillonite was weighed and mixed in 20 mL of distilled water in a 100 mL beaker to which 1.0 g of AMF spores were added and subjected to ultra-sonication for 10 min. The AMF-clay biosorbent was separated by filtration and the dry biomass was used for further experimental studies.

**(ii) Batch adsorption procedure**

The preliminary biosorption experiments were undertaken with 0.2 g amount of the AMF-clay biosorbent (spores isolated from soil collected from a local groundnut (*Arachis hypogea*) cultivation field) in 20 mL of 5 mg $L^{-1}$working Cr(VI) concentration at pH 2.0. Equilibration was performed at 120 rpm and 30$^{o}$C in an incubator shaker for a 3 h duration. The Cr(VI)

concentration remaining in the solution phase after equilibration was quantitatively analysed through ion chromatography with post column derivatization using diphenyl carbazide as the chelating reagent. [11]

### 5. 3 Results and discussion

The AMF infected roots were stained with acid fuschin-lactic acid solution according to the procedure given in literature.[7] The AMF hyphae (Fig.5.1b) and isolated spores were observed under optical microscope at 10x and 100x magnification (Fig.5.1c). The microscopic observation shows the plant roots colonized by AMF where hyphae and vesicles can be identified. As most of the Indian agricultural soils contain *Glomus* species [12] and also from the basic microscopic observation of the AMF spores isolated in the method spores were similar to those species. The confocal microscopy images of the spores were captured by treating AMF spores with rhodamine B dye and the average size of the spores was found to be 62 μm (Fig.5.1d).

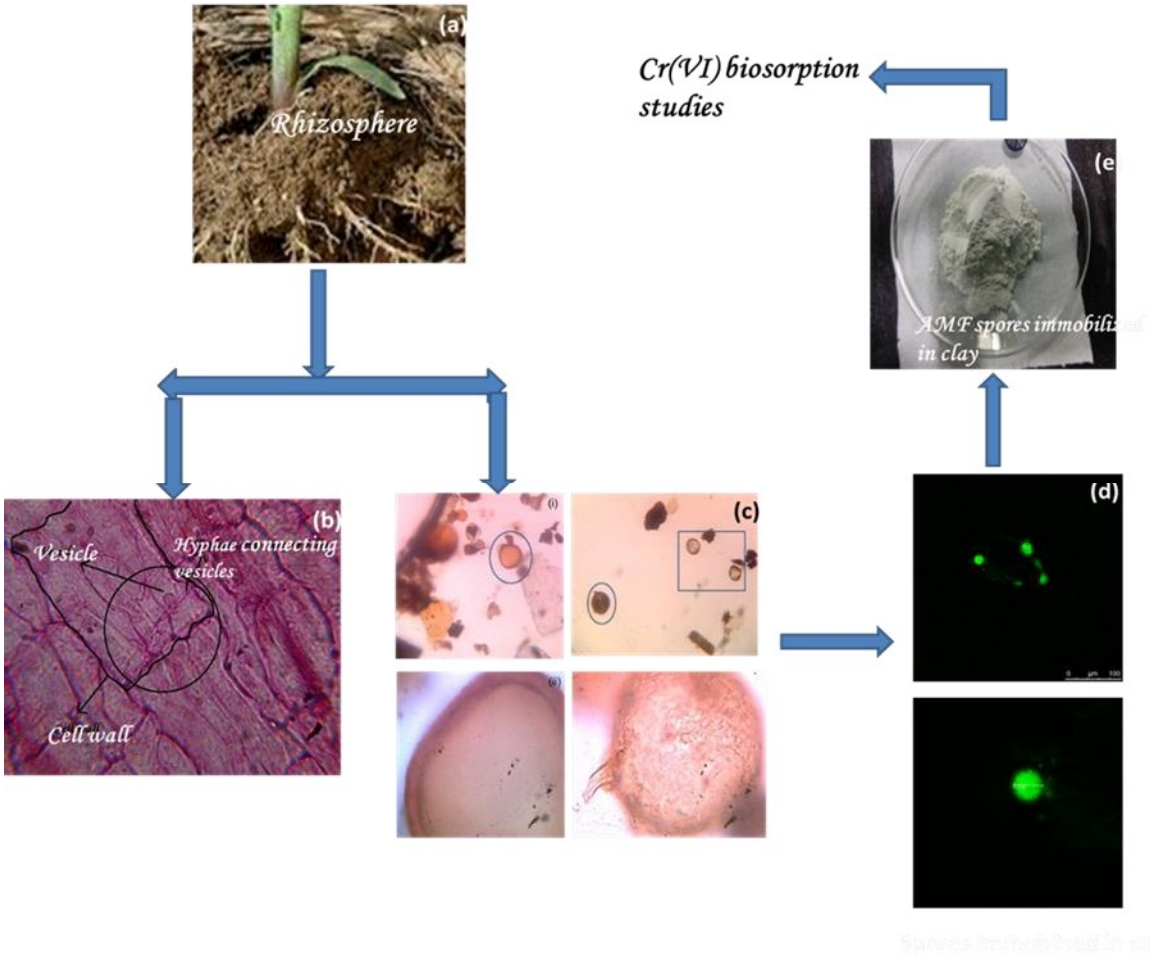


**Figure 5.1** (**a**) Rhizosphere (**b**) Hyphae and vesicles of endomycorrhiza in the plant root cells (**c**) Optical Microscopic images of AMF spores observed under (**i**) 10x and (**ii**) 100x objectives (**d**) Confocal images of AMF spores after treating with Rhodamine B. (**e**) AMF spores immobilized in clay.

**(i) Characterisation of the AMF-clay biosorbent**

The AMF spore cell walls have hydroxyl, amino, carboxyl functional groups which co-ordinate with the metal ion and various FTIR characteristic shifts in the wavelengths are observed during Cr(VI) adsorption. [13] The individual spectra (AMF spores, sodium montmorillonite, AMF-clay biosorbent before and after Cr(VI) adsorption) were recorded. The peak at 3438 $cm^{-1}$ in AMF spores is due to N-H and O-H stretching and absorption at 1639 $cm^{-1}$ is due to amide I band of protein–peptide bond and 1061 $cm^{-1}$ indicates the involvement of C=O of polysaccharide.

The smaller band at 3625 $cm^{-1}$ is the characteristic band for clays which is ascribed to the Si–OH functional groups. The broader band at 3439 $cm^{-1}$ is due to the amalgamation of amine and hydroxyl vibrational frequencies of the AMF spores and also due to Al–O–H stretching in montmorillonite clay. A strong broad peak of C-O at 1045 $cm^{-1}$ can be related to the cellulose in spore cell wall and also attributed to Si- O-Si stretching band of clay. The peak at 1639 $cm^{-1}$ indicates amide-I band [13] of the fungal spores. A small shouldering peak at 912 $cm^{-1}$attributed to the merging of Cr=O [14] vibration in $HCrO_4^-$ and Al-Al-OH deformation in clay minerals [15,16] was observed after adsorption as shown in Fig 5.2a. The optical (bright field images) and electron micrograph images (scanning electron microscopy images) of the VAM spores on clay particles were captured (Fig 5.2 b,c). In order to prove that spores are not leached into the solution evaporation of the aqueous phase after Cr(VI) adsorption was performed. In this experiment, the filtrate containing residual Cr (VI) solution was taken in a petri plate and dried at 70$^oC$, washed into a 37 μ sieve and the washings were collected in a beaker. The washings were observed under bright field imaging in confocal microscope to check the presence of spores. There were no indication of spores in the confocal images (Fig 5.2d,e) which shows that there is no apparent leaching of spores into the aqueous phase after adsorption. The elemental analysis was investigated through X-ray fluorescence studies (XRF) of AMF-clay biosorbent after Cr(VI) adsorption. Si, Al, K, Na, Mg were detected as the elements present in sodium montmorillonite along with Cr thereby confirming the metal adsorption between 5-6 keV (Fig 5.2f).

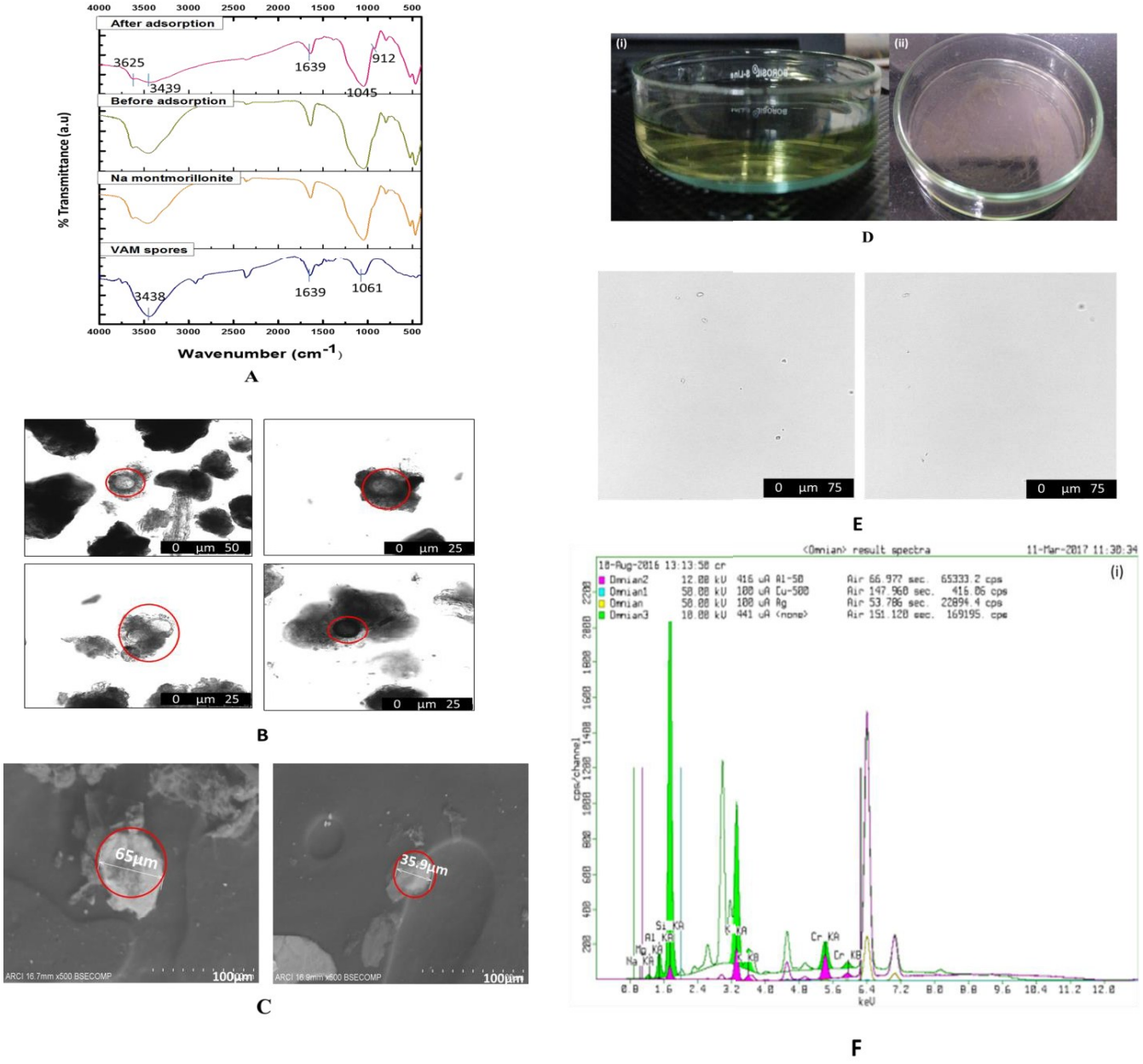


**Figure 5.2** (**A**) FTIR of AMF clay biosorbent before and after Cr(VI) adsorption. **(B)** Bright field images of the AMF-clay biosorbent (**C**) SEM images of the AMF-clay biosorbent (**D**) Cr(VI) filtrate before and after evaporation (**E**) Bright field images after the evaporation of the aqueous phase (**F**) XRF of the biosorbent after Cr(VI) adsorption

The biosorption mechanisms are often associated with adsorption coupled reduction and hence the possibility of Cr(VI) reduction was investigated using XPS (X-ray photo electron spectroscopy) which provides the surface characterization. Elements such as C, O, N, Cr were evident in the survey scan spectra obtained (Fig 5.3a**)** and the short scan of the C1s showed a peak at 283.6eV (Fig 5.3b). The Cr 2p3/2 binding energy of 582.0 eV corresponds to Cr in the +6 oxidation state, indicating there is no perceptible reduction of Cr(III) on the AMF-clay biosorbent surface. [17] Hence, after biosorption there was no immediate reduction of Cr(VI) on the biosorbent surface.

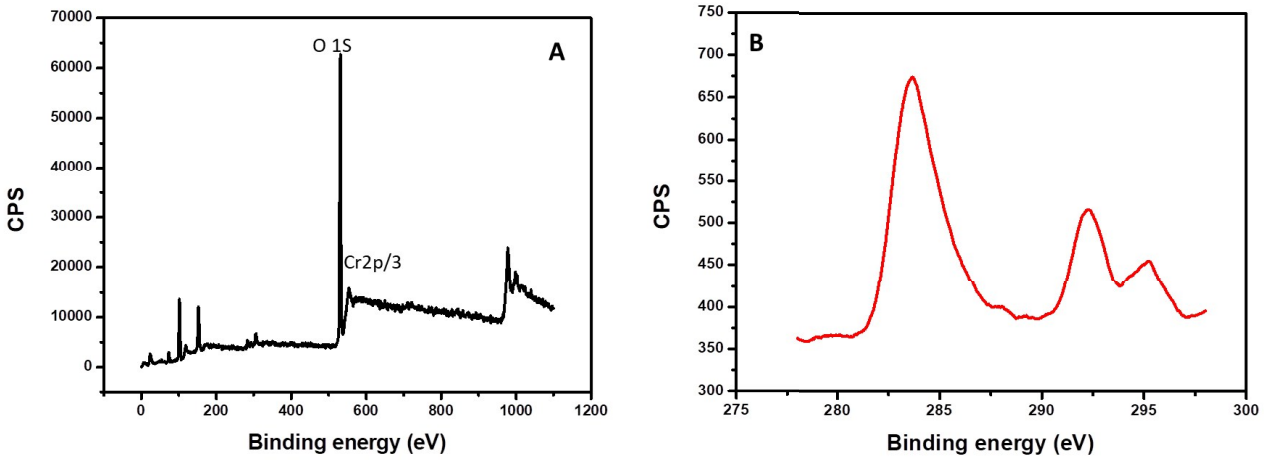


**Figure 5.3.** XPS spectra of the biosorbent after Cr(VI) adsorption (**a**) Survey scan spectra (**b**) High resolution spectra of C1s.

### (ii) Plausible mechanism for biosorption

The hydrochromate ion ($HCrO_4^-$) exists in the pH range 2-4 in equilibrium with dichromate anion ($2HCrO_4^- \rightleftharpoons Cr_2O_7^{2-} + H_2O$) but $Cr_2O_7^{2-}$ ion is more prominent at pH less than 2 at higher Cr(VI) concentrations [18] while $CrO_4^{2-}$ is more prominent at higher alkaline pH. [19] At 5 mg $L^{-1}$ of hexavalent chromium concentration at pH 2.0, 78% Cr(VI) was biosorbed on to the surface of AMF-clay biosorbent (Fig 5.4a).

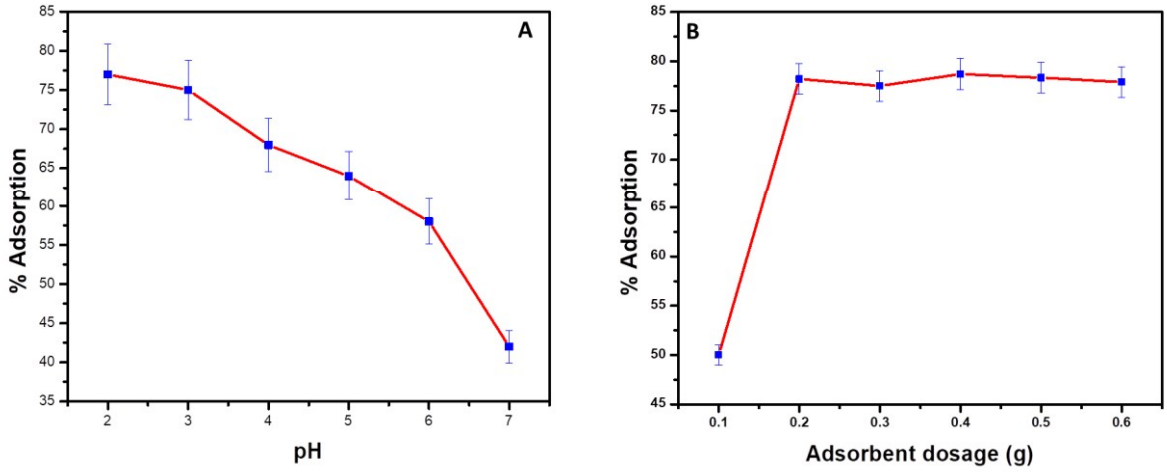


**Figure 5.4.** (**a**) pH effect on biosorption (Conditions: weight of the adsorbent- 0.2 g, Cr(VI) concentration- 5 mg $L^{-1}$) (**b**) Variation of biosorbent dosage (Conditions: pH-2.0, Cr(VI) concentration- 5 mg $L^{-1}$)

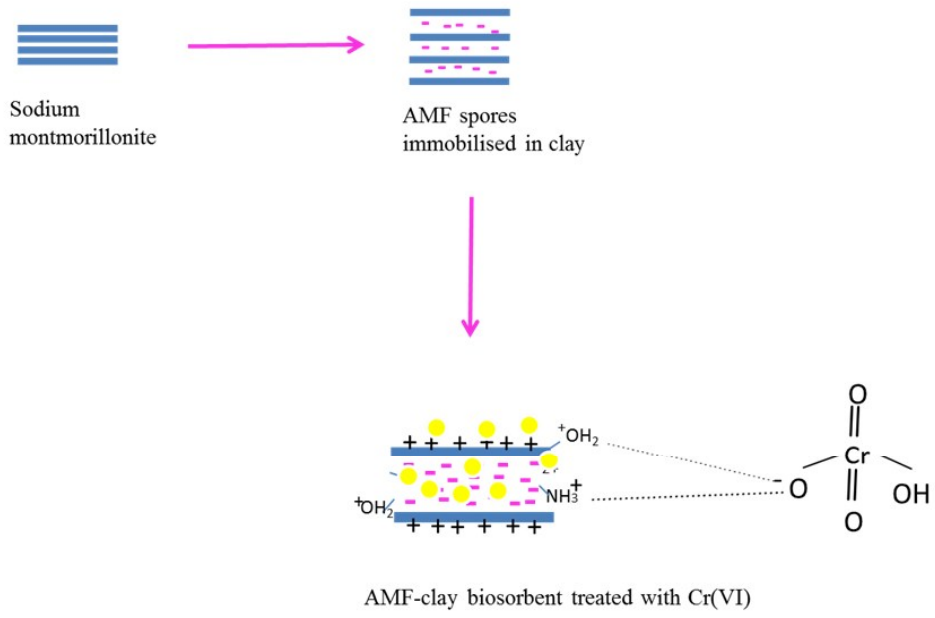


**Figure 5.5.** Schematic representation of AMF immobilized in clay and the interactions between the AMF-clay biosorbent and Cr(VI).

The biosorbent surface containing hydroxyl, amine, carboxyl groups and the SiOH (silanol) and AlOH (aluminol) groups in clay are protonated (Fig 5.5) resulting in an electrostatic interaction with hydrogen chromate anions. [14,20]With increase in pH, there is deprotonation of the functional groups present on AMF-clay biosorbent surface and hence decrease in adsorption was observed. With 5 mg $L^{-1}$Cr(VI) solution containing 0.2 g of the biosorbent, an adsorption efficiency of 78% was attained. Beyond 0.2 g, there was no enhancement in the adsorption of Cr(VI), indicating the saturation of the binding sites (Fig 5.4b). Cornejo et al [21] studied the compartmentalization mechanism of copper in AMF spores which involved accumulation of metal in the spores. Spores were treated with copper sulfate over a wide time period ranging from 24 hours to 14 days after which the blue green spores were observed indicating the accumulation of copper. In the present study, the spores were immobilized in clay matrix and treated with Cr(VI) for a relatively short time period (180 min) wherein there is effective adsorption. Beyond 180 min, there was a saturation in the percentage of metal uptake. Therefore, biosorption is more probable in this host-guest interaction rather than compartmentalization of the metal inside the spores.

**(iii) Equilibrium adsorption isotherms, kinetics and thermodynamic studies**

The biosorbent-adsorbate equilibrium was analysed using established isotherms.[22,23] The linearized Langmuir and Freundlich isotherm plots (Fig 5.6a,b) and the corresponding isotherm parameters are shown in Table 5.1. Among the two models, Langmuir isotherm with a 0.987 ($R^2$ value) and a low $\chi^2$ value (0.00982) was quite appropriate in describing the adsorption process. A dimensionless parameter $R_L$ given as $R_L = 1/1+bC_o$, [24] where the value is below unity verifies the suitability and reversibility of adsorption. Further, the value of n in the Freundlich isotherm lies in the range 1-10 which indicates the favourability of the adsorption. The system gave Langmuir adsorption capacity of 11.185 mg $g^{-1}$ with a high correlation coefficient. The Langmuir adsorption capacity of AMF spores as such was found to be 4.5 mg $g^{-1}$. The comparison of maximum Langmuir adsorption capacities studied independently with various adsorbents [25-29] is shown in Table 5.2.

**Table 5.1** Isotherm parameters involved in the biosorption of Cr (VI) on AMF-clay biosorbent surface

| | | | | | |
|---|---|---|---|---|---|
| Langmuir $\frac{C_e}{q_e} = \frac{1}{q_o b} + \frac{C_e}{q_o}$ | $q_{max}$ (mg $g^{-1}$) | b(L $mg^{-1}$) | $R^2$ | $\chi^2$ | $R_L$ |
| | 11.185 | 0.0265 | 0.9879 | 0.0098 | 0.8833 |
| Freundlich $\log q_e = \log K_F - \frac{1}{n} \log C_e$ | $K_F$($mg^{1-1/n} g^{-1} L^{1/n}$) | n | $R^2$ | $\chi^2$ | |
| | 0.6279 | 1.7636 | 0.9803 | 0.0269 | |

**Table 5.2** Comparison of Langmuir adsorption capacities against few related adsorbent materials for Cr(VI) removal

| **Adsorbents** | **Optimum pH** | **Adsorption capacity (mg $g^{-1}$)** |
|---|---|---|
| Cellulose-sodium montmorillonite[14] | 3.8-5.5 | 22.2 |
| *Aspergillus BRVR*-sodium montmorillonite [10] | 2.0 | 45.72 |
| *Lentinus sajorcaju* [25] | 2.0 | 22.10 |
| *Agaricus bisporus* [26] | 1.0 | 8.0 |
| Montmorillonite supported nanoparticles[27] | 2.0-2.5 | 15.3 |
| Bacterial cellulose [28] | 1.5 | 5.13 |
| *Bacillus marisflavi* [29] | 4.0 | 5.78 |
| (Present studies)<br>AMF spores<br>AMF spores immobilized in sodium montmorillonite | <br>2.0<br>2.0 | <br>4.5<br>11.185 |

The kinetic studies were performed at a Cr (VI) concentration of 10 mg $L^{-1}$. Cr(VI) was adsorbed to the extent of 45% within five minutes and the percentage adsorption continued to increase steadily and attained a maximum of 73% at 180 min. The pseudo first order [30] and second order equations [31] were utilized to evaluate the adsorption kinetics.

The obtained data from the kinetic plots (Fig 5.6c,d) at 10 mg $L^{-1}$ concentration of Cr(VI) is tabulated in Table 5.3 and the adsorption follows second order kinetics with experimental and calculated $q_e$ values as 0.77 mg $g^{-1}$and 0.74 mg $g^{-1}$. The processes such as particle, film diffusion and surface adsorption play major part in the Cr(VI) uptake from the solution onto the AMF immobilized clay surface. The biosorption kinetics is determined by the intraparticle diffusion at higher Cr(VI) concentrations and the effective interactions through pore diffusion play major role at a lower concentrations. [20] The relation between $q_t$ and $\sqrt{t}$ (Fig 5.6e) is given by the Weber-Morris intra particle diffusion model [22] and the obtained plot with a non-zero intercept elucidates the impact of the boundary layer mechanism towards Cr(VI) uptake.

**Table 5.3** Kinetic parameters influencing the biosorption process

| $C_o$(mg $L^{-1}$) | $q_e$ (mg $g^{-1}$) | $k_2$ (g $mg^{-1}$ $min^{-1}$) | $R^2$ | $k_1$ ($min^{-1}$) | $R_1^2$ | $k_{int}$ (mg $g^{-1}min^{-0.5}$) |
|---|---|---|---|---|---|---|
| 10 | 0.7735 | 0.0763 | 0.984 | 0.0212 | 0.8918 | 0.0379 |

The thermodynamic parameters associated with biosorption such as change in enthalpy (ΔH), Gibbs free energy (ΔG), and entropy (ΔS) at various temperatures were estimated to evaluate the feasibility and nature of the adsorption process. The free energy change involving the concentration gradient across the biosorbent-solution interphase is given as

$$\Delta G_r = \Delta G_r^o + RTln\frac{[Cr(VI)]_{\text{AMF}-clay\ biosorbent\ surface}}{[Cr(VI)]_{solution}} \quad (5.1)$$

$$\Delta G_r = \Delta G_r^o + RTlnK \quad (5.2)$$

At equilibrium,

$$\Delta G_r^0 = -RTlnK \quad (5.3)$$

The transfer of hexavalent chromium from the aqueous medium onto the AMF immobilized clay surface could be visualized as a host-guest interaction. The biosorbent acts as a host to the incoming metal ion involving negative entropy and enthalpy changes. The Van't Hoff plot that connects lnK and 1/T is shown in Fig 5.6f and the significant thermodynamic parameters are tabulated in Table 5.4. The negative ΔG showed the adsorption mechanism was spontaneous and negative values of enthalpy and also the activation energy [10] ($E_a = \Delta H^o_{ads}+RT$) indicates a physico-chemical exothermic adsorption. [32] The enthalpically favourable process is driven by the exergonic free energy change ($\Delta G^0$) while the negative entropy indicates the decrease in randomness at the AMF-clay adsorbent surface.

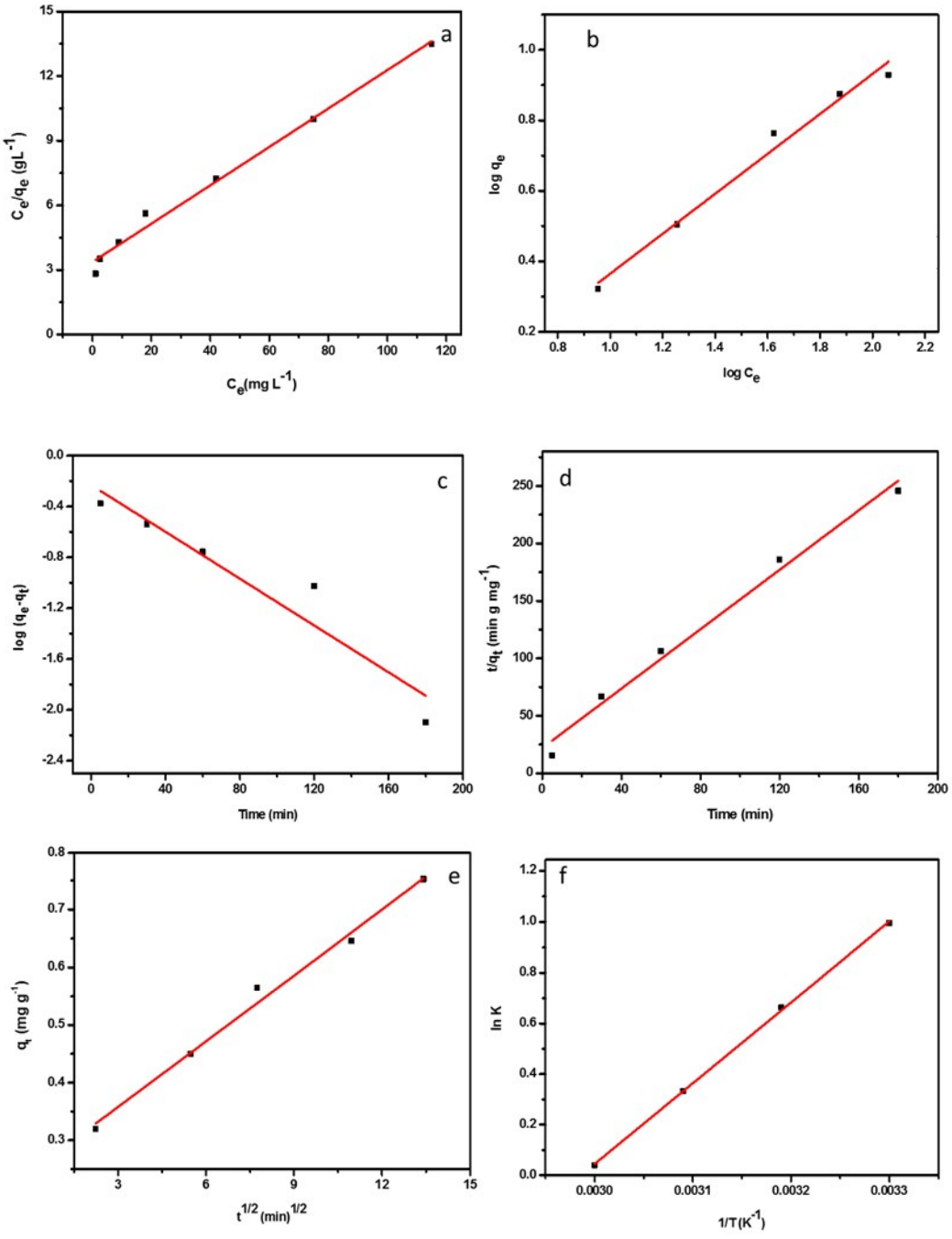


**Figure 5.6.** (**a**) Langmuir isotherm (**b**) Freundlich isotherm (**c**) plot depicting pseudo first order kinetics (**d**) Plot depicting pseudo second order kinetics (**e**) Weber-Morris plot showing the variation of $q_t$ against $t^{1/2}$ (**f**) Van't Hoff plot correlating lnK against 1/T (conditions: pH-2.0, adsorbent dosage- 0.1 g/20 mL)

**Table 5.4** Thermodynamic parameters associated with the biosorption of Cr (VI)

| **Temperature (Kelvin)** | **$\Delta G^0$ (kJ mol$^{-1}$)** | **$\Delta S^o$ (J mol$^{-1}$K$^{-1}$)** | **$\Delta H^o$ (kJ mol$^{-1}$)** | **$E_a$ (kJ mol$^{-1}$)** |
|---|---|---|---|---|
| 303 | -2.504 | -79.215 | -26.530 | - 23.88 |
| 313 | -1.725 | | | |
| 323 | -0.893 | | | |
| 333 | -0.110 | | | |

**(iv) Regeneration of the AMF-clay biosorbent and application studies**

Biosorbents should possess the ability to be used for repeated adsorption-desorption cycles which is reflected in the regeneration of the biosorbent surface. Also the desorbing agents should be mild enough so as to protect the biosorbent surface from deterioration during regeneration. In this regard, NaOH (1.5 mol $L^{-1}$, 3 mL) was used to desorb 5 mg $L^{-1}$ Cr(VI) thereby eluting Cr as sodium chromate from the AMF-clay biosorbent surface.

A simulated waste water mixture prepared with various ionic components such as $Ni^{+2}$, $Cu^{+2}$ $Hg^{+2}$, $Pb^{+2}$, $Fe^{+2}$, $Co^{+2}$, chloride , nitrate, sulphate each at a concentration 100 mg $L^{-1}$ was added to 5mg $L^{-1}$ Cr(VI) solution. There was a reduction in Cr(VI) adsorption from 78% to 70% in the presence of these ionic constituents. This could be attributed to the fact that Fe (II) has the ability to reduce Cr (VI) to Cr (III). Sulfate, chloride and nitrate would also compete with the tetraoxohydrochromate anion for the active AMF-clay biosorbent sites and furthermore the adsorption is also affected by the formation of stable tetrachloro complexes of other metal ions that lessens the active biosorption sites for Cr(VI) adsorption. [14,20]

## 5.4. Conclusions

The developed AMF-clay biosorbent has the potential to adsorb Cr(VI) at pH 2.0-3.0 up to an extent of 78% at 5 mg $L^{-1}$ concentration. Langmuir adsorption capacity obtained was 11.185 mg $g^{-1}$ and the system kinetics followed pseudo second order by attaining equilibrium in 180 min. The immobilization of AMF spores in sodium montmorillonite enhanced the Langmuir adsorption capacity from 4.5 mg $g^{-1}$ to 11.185 mg $g^{-1}$. The exergonic system thermodynamics yields a negative entropy (-79.215 J $mol^{-1}$ $K^{-1}$) and enthalpy (-26.530 kJ $mol^{-1}$). The regeneration of the biosorbent using NaOH was facile and this AMF-clay combination would prove to be quite beneficial to adsorb hexavalent chromium from diverse matrices. However, compared to the vegetative cells of yeast or *Aspergillus* wherein there is more surface area, the AMF spores possess comparatively lesser adsorption capacity. The AMF-clay combination would certainly open the doors towards exploring other supports involving cellulose, silica or alumina as a practical approach for heavy metal remediation.

**References**


1. Sullia, S.B.; Use of Vesicular - ArbuscularMycorrhiza (AMF) as Biofertilizer for Horticultural Plants in Developing Countries, Springer, Netherlands, **1991**, pp. 49-53.
2. Liu, W.; Zhang, Y.; Jiang, S.; Deng, Y.; Christie, P.; Murray, P.J.; Li, X.; Zhang, J. *Sci. Rep.* **2016**, 6, 24902.
3. Heggo, A.; Angle, A.S.; *Soil Biol. Biochem.* **1990**, 22, 865-869.
4. Davies Jr, F.T.; Puryear, J.D.; Newton, R.J.; Egilla, J.N.; Saraiva Grossi, J.A. *J. Plant Nutr.* **2002**, 25, 2389–2407.
5. Gil-Cardeza, M.L.; Ferri, A.; Cornejo, P.; Gomez, E. *Sci. Total Environ*. **2014**, 493, 828–833.
6. Dong, H.; *Elements*. **2012**, 8, 113–118.
7. Charvat, I. Methods to process and identify Symbiotic fungi in the roots of vascular plants ,Proceedings of the Ninth Workshop/Conference of the Association for Biology Laboratory Education (ABLE) 2008, pp.131-137.
8. Boufait, M.; Amar, H.A. *Desalination*, **2007**, 206, 300–310.
9. William, G.P.; Aaron, R.S. *Biotechnol Prog*. **2003**, 19, 1038–1044.
10. Sathvika, T.; Manasi, Rajesh, V.; Rajesh, N. *RSC Adv*. **2015**, 5, 107031-107044.
11. Arar, E.J.; Pfaff, J.D. *J. Chromatogr. A*, **1991**, *546*, 335–340.
12. Swarnalatha , K.; Trimurtulu, N.; Ammani, K.; Ashok, S. *Int. J. Curr. Microbiol. App .Sci.* **2017**, 6, 1496-1505.
13. Naumann, D. Infra-red spectroscopy in microbiology, Encyclopaedia of Analytical Chemistry, ed. R. A. Meyers, John Wiley and Sons Ltd., Chichester 2000 pp.102–131.
14. Kumar, A.S.K.; Kalidhasan, S.; Rajesh, V.; Rajesh. N. *Ind. Eng. Chem. Res*. **2012**, 51, 58–69.
15. Shameli, K.; Ahmad, M.B.; Zargar, M.; Yunus, W.M.; Ibrahim, N.A.; Shabanzadeh, P.; Moghaddam, M.G. *Int J Nanomedicine*. **2011**, 6, 271-284.
16. Beena, T.; Chudasama, C.D.; Jasra, R.V. *Spectrochim. Acta* A. **2006**, 64, 273-278.
17. Mu, Y.; Ai, Z.; Zhang, L.; Song , F. *ACS Appl. Mater. Interfaces*. **2015**, *7*, 1997–2005.
18. Ramsey, J.D.; McCreery, R.L. *J. Electrochem. Soc.* **1999**, 146, 4076–4081.
19. Scancar, J.; Berlinger, B.; Thomassen,Y.; Milacic, R. *Talanta*. **2015**, 142, 164-169.
20. Sathvika, T.; Manasi, Rajesh, V.; Rajesh, N. *Chem.Eng.J.* **2015**, 279, 38-46.
21. Cornejo, P.; Tienda, J.P.; Meier, S.; Valderas, A.; Borie, F.; Aguilar, C.A.; Ferrol, N. *Soil Biol Biochem.* **2013**, 57, 925-928.
22. Yu, B. Xu, J.; Liu , J.H.; Yang, S.T.; Luo, J.; Zhou, Q.; Wan, J.; Liao, R.; Wang, H.; Liu , Y.; *J. Environ. Chem. Eng*. **2013**, 1, 1044−1050.

23. Ho, Y.S. *Carbon*. **2004**, 42, 2115–2116.

24. Sun, C.; Sun, L.; Sun, X.; *Ind. Eng. Chem. Res*. **201**3, 52, 14251–14260.

25. Bayramoglu, G.; Celik, G.; Yalcin, E.; Yilmaz, M.; Arica, M.Y. *J. Hazard. Mater*. **200**5, 119, 219–229.

26. Ertugay, N.; Bayhan, T.K. *J. Hazard. Mater*. **2008**, 154, 432–439.

27. Yuan, P.; Fana, M.; Yang, D.; He, H.; Liu,D.; Yuan,A.; Zhu, J.; Chen, T. J. *Hazard. Mater.* **200**9, 166, 821–829.

28. Lu, M.; Xu, Y.; Guan, X.; Wei, D. *J Wuhan Univ Technol Mat Sci Edit.*. **2012**, 27, 572-575.

29. Mishra, S.; Doble, M. *Ecotoxicol. Environmental. Saf*. **2008**, 71, 874–879.

30. Foo, K.Y.; Hameed, B.H. *Chem. Eng. J*. **2010**, 156, 2–10.

31. Ho, Y.S.; Mckay, G. *Water Res*. **2000**, 34, 735–742.

32. Sathvika, T.; Manasi, Rajesh, V.; Rajesh. N. *J. Environ. Chem. Eng*. **2016**, 4, 3193–3204.

# Chapter – 6

## Rhizobium sp immobilized in carbon and clay based adsorbents for the remediation of hexavalent chromium

## 6.1. Potential Application of *Rhizobium* species Immobilized in Multi Walled Carbon nanotubes to Adsorb Hexavalent Chromium

The convergence of biotechnology and nanoscience offers a sustainable alternative in treating contaminated waters. Hexavalent chromium, being carcinogenic deserves effective and sustainable methods for sequestration. In the current study, a nitrogen fixing bacteria (*Rhizobium*) immobilized in multiwalled carbon nanotubes and sodium montmorillonite for the effective sequestration of hexavalent chromium is demonstrated. A prokaryotic nitrogen fixing bacteria *Rhizobium* is a symbiotic, rod shaped, gram negative bacteria which is a potential biofertilizer for plants. It also helps in biological nitrogen fixation thereby influencing the agricultural productivity and is used in controlling root rot infections caused by fungi.[1,2] The legumes inoculated with *Rhizobium* inoculants is a common agriculture practice, which is a cost effective process to provide nutrients to the bacteria. Sludge generated from the agro based industries is rich in carbon and nitrogen sources which help in the growth of *Rhizobium* thereby offering a green alternative to treat waste water as well as reducing the cost of inoculant preparation.[3]

**The first part of this chapter** deals with the immobilization of *Rhizobium sp* in multiwalled carbon nanotubes for the effective removal of hexavalent chromium.

**The second part of this chapter** deals with the immobilization of *Rhizobium sp* in sodium montmorillonite for the effective sequestration of Cr(VI).

### 6.1.1 Introduction

Greener alternatives such as biosorbents which involve the use of microbes and biopolymers are more environmentally benign in nature. The direct use of microbes in its native form for metal removal has several disadvantages such as poor mechanical strength, difficulty in microbe separation from the solution and there is always a possibility of loss of microbial mass after regeneration studies. To combat the disadvantages, microbes are immobilized in suitable matrices which help to improve of cell strength, rigidity, porosity and metal removal ability.[4] The current developed method deals with the immobilization of nitrogen fixing bacteria in MWCNTs for the effective Cr(VI) removal.

Several MWCNTs adsorbents were developed for the treatment of aqueous solutions contaminated with Cr(VI). Lu et al.[5] developed magnetic $Fe_2O_3$ nanoparticle-MWCNTs composite and was checked for the efficient removal of Cr(VI) at different temperatures with a $q_{max}$ of 42.02 mg $g^{-1}$ at 35$^{o}$C. Fe-Ag/f-MWCNT/PES Nanostructured-Hybrid Membranes developed by Machine et al. could remove 94.8% of Cr(VI) from aqueous solution.[6] Chitosan was immobilized in nanoparticles and carbon nanotubes by forming a nanocomposite which could efficiently remove Cr(VI) up to 84% within a short contact time.[7] Reports involving microbe-MWCNTs combination for the sequestration of heavy metals are scarce. Yan et al.[8] reported MWCNTs –calcium alginate complex immobilized in *Shewanella oneidensis* which showed higher reduction capacity of Cr(VI). *Pseudomonas aeruginosa* was immobilized in CNTs for effective adsorption of various heavy metals with $q_{max}$ 6.60 mg $g^{-1}$ for cobalt, 6.18 mg $g^{-1}$ for cadmium, 6.07 mg $g^{-1}$ for lead, 5.83 mg $g^{-1}$ for manganese, 6.23 mg $g^{-1}$ for chromium (III) and 5.25 mg $g^{-1}$ for Ni.[9] Following a thorough literature review, there are no reports on the combination of *Rhizobium* -MWCNTs for sequestration of Cr(VI) . The pristine MWCNTs were oxidized and then were involved in coupling reaction with the amines present on the cell wall of microbes to form amide which react with hydrochromate ion and thus sequesters Cr(VI) from aqueous solutions.

### 6.1.2 Experimental section

#### (i) Isolation and identification of microbial species

*Rhizobium* species was isolated from soil that was collected from nearby legume crop fields and followed a simple isolation procedure using standard pour plate technique on a YMA medium containing yeast extract, mannitol, NaCl, $MgSO_4$, $K_2HPO_4$, Congo red and agar. The inoculated plates were incubated at 37$^oC$ for 48 hours. Based on the morphological characteristics of the colonies, four isolates of the bacteria were selected (BI 1, BI 3, BI 4, BI 6). Further the isolates were subjected to morphological tests such as gram staining and motility tests, biochemical tests popularly known as IMVIC tests and molecular characterizations for the bacterial confirmation.[10]

#### (ii) Genomic DNA isolation and 16S rDNA PCR amplification

The bacterial genomic DNA was isolated according to a standard DNA isolation protocol.[11,12] The strains isolated were grown in 5 mL YMA medium at 37$^oC$ overnight and mid log phase of the culture obtained was harvested as a pellet by centrifugation. The pellet obtained was re-suspended in 500 µL of TEG buffer (Tris-50mM EDTA-50mM Glucose -20%) for the cell lysis. Further it was treated with lysozyme and RNAase at 37$^oC$ for 40 min followed by action of 10 % SDS solution at 37 $^oC$ for 60 min. Isolation was accomplished by adding equivalent quantities of Phenol, Chloroform and Isoamyl alcohol followed by precipitating with 90% isopropanol (ice cold). The white DNA precipitate which was obtained was washed with 70% ethyl alcohol and suspended in 30 µL TE (Tris-EDTA) buffer for further analysis.

The amplification of 16S rDNA was performed using Polymerase chain reaction (PCR). The PCR reaction was setup using 25 µL reaction mixture containing 200 µM dNTP, 1µL of *Taq polymerase*, 10X PCR buffer (2.5µL) with $MgCl_2$ (1.5 mM), 100 ng/ µl genomic DNA, with 200 ng of forward [27 F 5'-AGAGTTTGATCMTGGCTCG-3'] and reverse primers [1492R 5'-GGTTACCTTGTTACACTT-3'].[13] The PCR program was operated starting with initial denaturation at 94$^oC$ for 4 min, followed by denaturation for 1min at 94$^oC$ for 32 cycles, annealing at 58.5$^oC$ for 50 min, extended for 2 min at 72$^oC$ followed by a final extension at 72$^oC$ for 10 min[14] and the obtained product was resolved using electrophoresis. The purified amplicons

were commercially sequenced. The sequences obtained were used to carry out a NCBI blast search analysis to confirm the identity of bacteria as *Rhizobium BVR*.

**(iii) Preparation of the *Rhizobium* – MWCNTs biosorbent**

The isolated *Rhizobium* species was grown in yeast- mannitol broth medium and spun down to make a pellet. Pristine MWCNTs were oxidized using $KMnO_4$ as reported previously.[15] A 200 mL of 0.5 mol $L^{-1}$ $H_2SO_4$, was mixed with 0.25 g of $KMnO_4$ as an initial step for oxidation. In another beaker, 0.1g of MWCNTs, 200 mL of 0.5 mol $L^{-1}$ $H_2SO_4$ was added and subjected to ultra-sonication for 30 min to ensure proper dispersion. After sonication the solution containing MWCNTs was heated up to 150 $^oC$ prior to the addition of $KMnO_4$ solution dropwise. The mixed solution was refluxed for 5 hours at 150 $^oC$ and cooled down to room temperature proceeded by the addition of 10 mL of concentrated HCl to dissolve $MnO_2$. The oxidized MWCNTs were washed till the pH reached between 6.0-7.0 and then dried at 100 $^oC$.

The dried MWCNTs were further used in the preparation of biosorbent along with microbes (free amine sources) by involving in EDC-HOBT coupling. To 0.1g of oxidized MWCNTs, 0.1g each of EDC, HOBT were added. The solvent used was DMF (dimethyl formamide) and 3 mL of triethylamine was added to the above mixture and stirred for 20 minutes. 3.0 g of *Rhizobium BVR* was added to the solution and the mixture was stirred overnight for the coupling reaction to take place.[16] The coupling mixture was filtered, washed with water and dried at 80$^oC$ for 4 hours before proceeding for metal adsorption studies.

**(iv) Synthesis of probes for Cr(VI) and Cr(III)**

Cr(VI) and Cr(III) have specific binding probes to differentiate them. Rhodamine based sensors are selected due to its spiro lactam structure and spiro ring opening of sensing a molecule. Rhodamine B hydrazide (RBH)[17] and Rhodamine based chemo sensor (RF)[18] were synthesized as described in literature which are specific for Cr(VI) and Cr(III) respectively and the samples were prepared for capturing the laser confocal images.

**(v) Batch adsorption studies**

The batch adsorption studies were performed by optimizing various parameters such as pH, adsorbent dosage, kinetics, thermodynamics. A 0.1g of the biosorbent was used to treat 20 mL of 5 mg $L^{-1}$ Cr(VI) solution at pH 2.0. The equilibration was attained in 180 min by using an orbital incubator shaker operating at 120 rpm maintained at 30$^{o}$C. The concentration of Cr(VI) was estimated using ion chromatography coupled with a UV detector.

### 6.1.3 Results and Discussion

**(i) Molecular identification of the isolated microbial strains**

The morphological study of the gram stained bacteria (BI 1,3,4,6) showed the presence of rod shaped (BI 4,6) and cocco bacilli (BI 1,3) gram negative bacteria (Fig. 6.1a.). The isolated bacteria formed circular, translucent, white mucoid colonies on YMA Congo red medium which is a positive test for *Rhizobium*. Further biochemical tests were performed and the results of four isolates were tabulated in Table 6.1. 16S rDNA sequencing was performed to confirm the genus of the bacterial isolates with 1500 bp amplicon obtained after PCR (Fig. 6.1b,c). Among the sequences obtained, the database available in NCBI gene bank BI 6 strain showed 99% similarity to *Rhizobium* species (Fig. 6.2a) and thus bacterial isolate was named as *Rhizobium BVR* which was used for further study. The sequence was assigned an accession number MF136764 when submitted to NCBI Genbank. The MALDI TOF spectrum also confirmed the isolated strain to be *Rhizobium* (Fig. 6.2b). The evolutionary relationships as seen in the phylogenetic tree (Fig. 6.3) generated using MEGA 6.0 version showed the *Rhizobium BVR* is distantly related to other *Rhizobium* species.

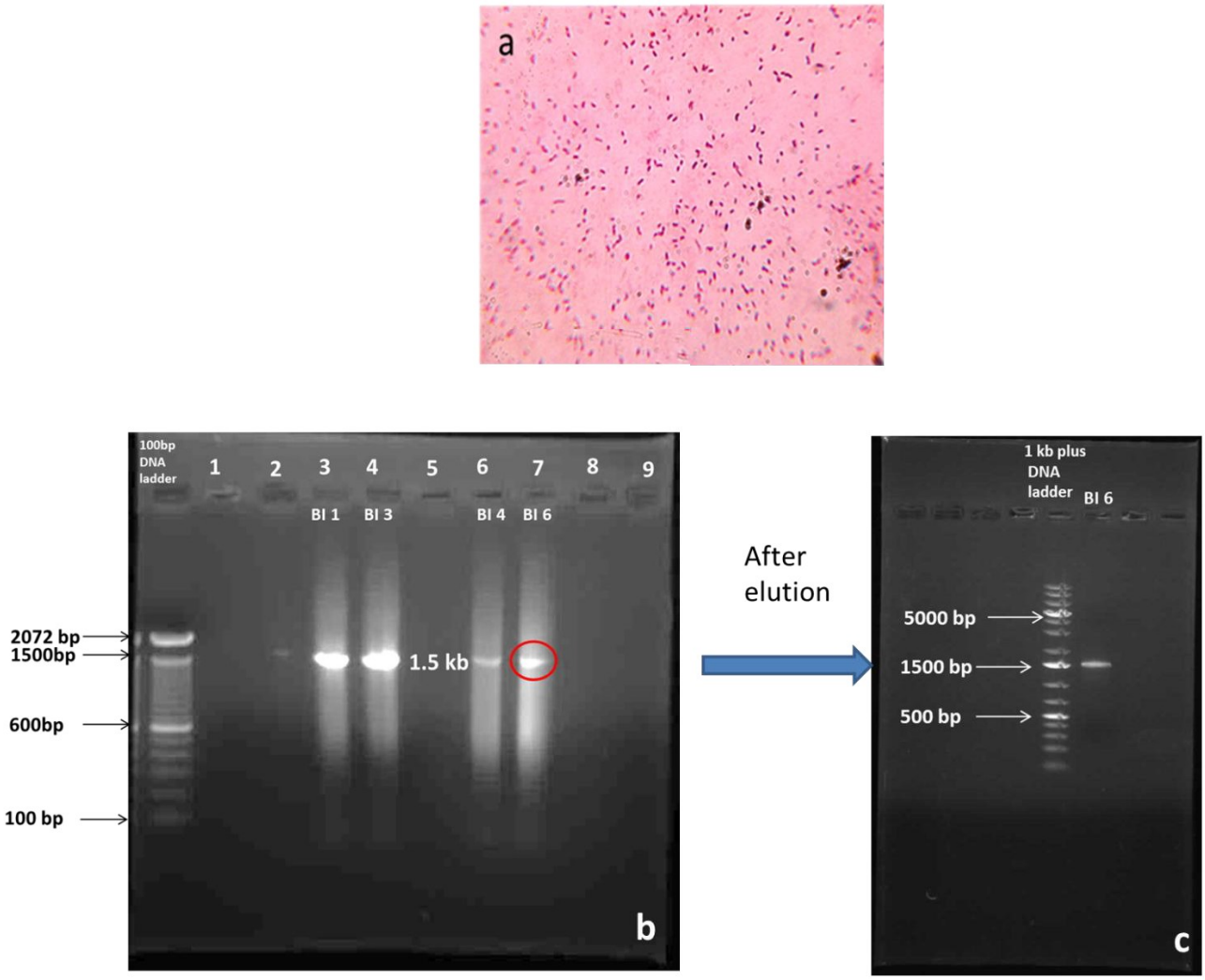


**Figure 6.1.**(a) Gram stain image of *Rhizobium BVR* (b) Gel picture of amplified products of 16S rDNA (1.5kb) of the bacterial isolates; lane 1- 100bp DNA ladder Invitrogen (cat no: 15628050)]; 3 - bacterial isolate BI 1, ; 4- bacterial isolate BI 3; 6 - bacterial isolate BI 4; 7- bacterial isolate BI 6. (c) Gel elution image of BI 6 [1 kb DNA ladder , Thermo scientific (cat no: SM1331)]

a

| Description | Max score | Total score | Query cover | E value | Ident | Accession |
|---|---|---|---|---|---|---|
| Rhizobium aegyptiacum strain 1010 16S ribosomal RNA, partial sequence | 2425 | 2425 | 98% | 0.0 | 99% | NR_137399.1 |
| Rhizobium binae strain BLR195 16S ribosomal RNA, partial sequence | 2425 | 2425 | 98% | 0.0 | 99% | NR_137242.1 |
| Rhizobium bangladeshense strain BLR175 16S ribosomal RNA, partial sequence | 2425 | 2425 | 98% | 0.0 | 99% | NR_137241.1 |
| Rhizobium bangladeshense strain 1017T 16S ribosomal RNA gene, partial sequence | 2425 | 2425 | 98% | 0.0 | 99% | JQ670241.3 |
| Rhizobium bangladeshense strain BLR175 16S ribosomal RNA gene, partial sequence | 2425 | 2425 | 98% | 0.0 | 99% | JN648931.2 |
| Rhizobium etli strain CCBAU 65830 16S ribosomal RNA gene, partial sequence | 2425 | 2425 | 98% | 0.0 | 99% | EU618034.1 |
| Rhizobium etli strain CCBAU 65708 16S ribosomal RNA gene, partial sequence | 2425 | 2425 | 98% | 0.0 | 99% | EU618033.1 |
| Rhizobium sp. Dz12 16S ribosomal RNA gene, partial sequence | 2425 | 2425 | 98% | 0.0 | 99% | AY210710.1 |

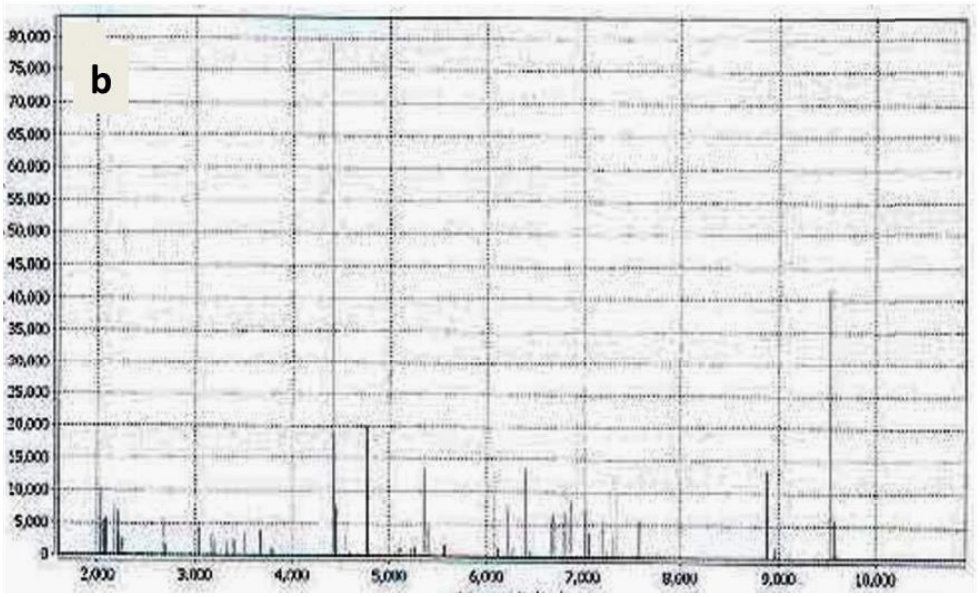


**Figure 6.2** (a) Blast search for BI 6 sequence confirming *Rhizobium* species (b) MALDI TOF of *Rhizobium BVR.*

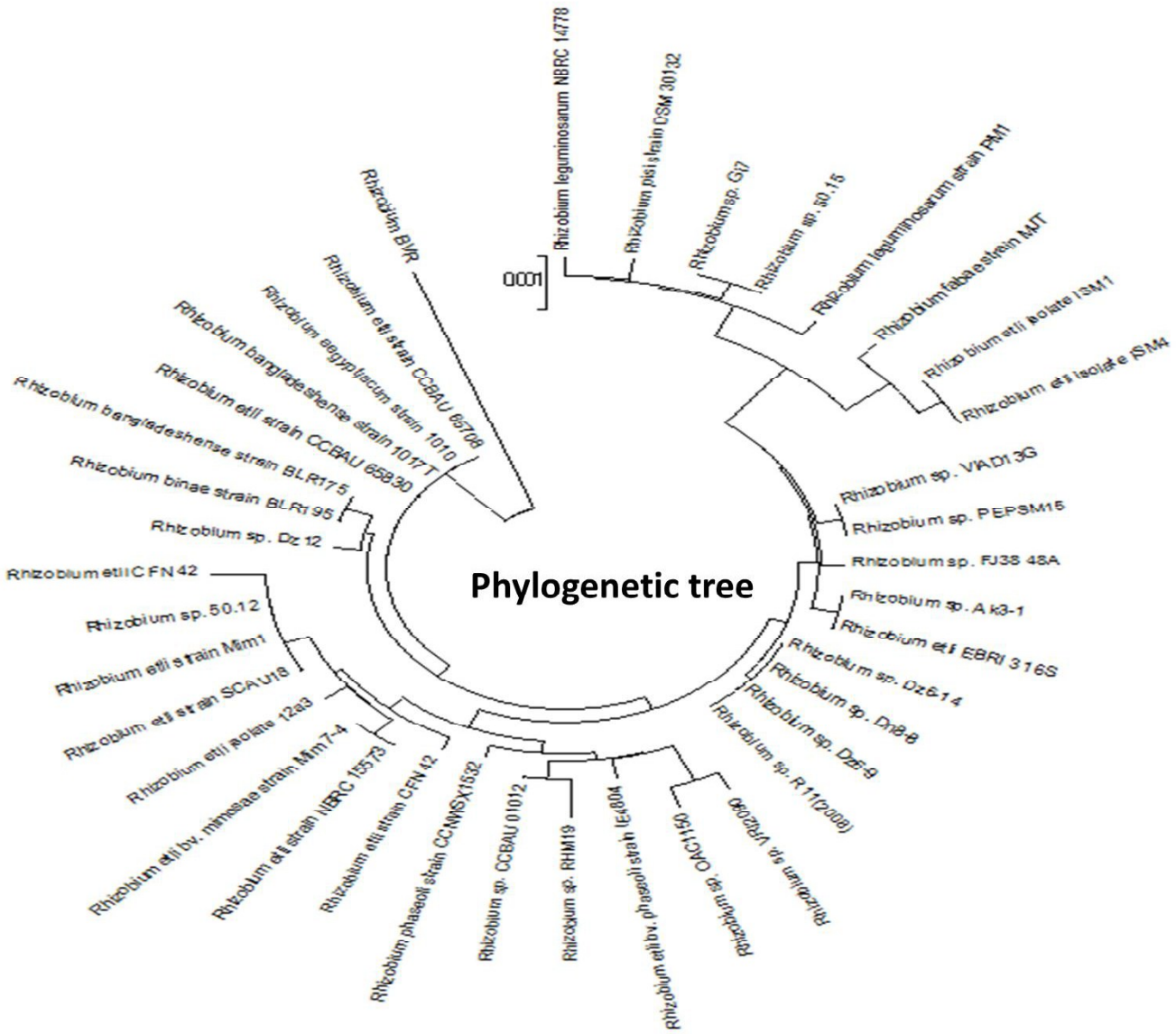


**Figure 6.3** Phylogenetic tree of the *Rhizobium BVR* created using MEGA (version 6.0)

**Table 6.1** Morphological and biochemical characteristics of the bacterial isolates

| Strain | Shape | Motility | Gram test | Indole | Methyl red | Voges-Prokasver | Citrate | Starch |
|---|---|---|---|---|---|---|---|---|
| BI1 | Cocco bacillus | Motile | Gram negative | + | - | - | - | + |
| BI3 | Cocco bacillus | Motile | Gram negative | + | - | - | - | + |
| BI4 | Rods | Motile | Gram negative | - | - | - | + | - |
| BI6 | Rods | Motile | Gram negative | - | - | - | + | - |

**(ii) Characterization of the biosorbent**

The FTIR spectra of pristine and oxidized CNTs, multiwalled carbon nanotubes-*Rhizobium* (CNTR) before and after Cr(VI) adsorption were recorded (Fig. 6.4). The pristine MWCNTs was oxidized using $KMnO_4$ and $H_2SO_4$. The peak at 1732 $cm^{-1}$corresponds to C=O of carboxylic acid confirming the introduction of COOH groups on the surface of MWCNTs. The carboxyl groups fluctuations leads to comparatively broader O-H stretch at 3410 $cm^{-1}$ than in pristine CNTs. Symmetric and asymmetric $COO^-$ stretchings[19] gives rise to two peaks at 1387 $cm^{-1}$ and 1625 $cm^{-1}$. The successful immobilization of microbe in MWCNTs is assisted by EDC-HOBT coupling by forming amide bond at 1648 $cm^{-1}$ and also this peak is due to amide-1 of protein-peptide bond from the microbes.[20] The disappearance of carboxyl C=O peak after the amide formation indicates the involvement of carboxyl groups present on the surface of MWCNTs in amide formation. The band at 1541$cm^{-1}$ corresponds to amide-II of in plane N-H bending.[21] After Cr(VI) adsorption the changes in the amide bond, O-H and C=O wavenumbers indicate they

were involved in Cr(VI) uptake by protonating in acidic medium thereby forming electrostatic interactions with Cr(VI) . The field emission scanning electron microscope (FESEM) and high resolution scanning electron microscopy (HRTEM) images of pristine, oxidized MWCNT and the biosorbent before and after Cr(VI) adsorption were recorded. The tiny lumps in FESEM images (Fig. 6.5c,d) and the particulates on MWCNTs in HRTEM images (Fig 6.6c) indicate microbial immobilizations. The oxidation process caused minimal irregularities in the wall surfaces of MWCNTs[19] as indicated in Fig. 6.6 . The elemental analysis of the biosorbent before and after adsorption of Cr(VI) was recorded using Energy Dispersive X-ray Spectroscopy indicating Cr(VI) adsorption onto the biosorbent with characteristic peak between 5-6 keV (Fig 6.5 e,f).

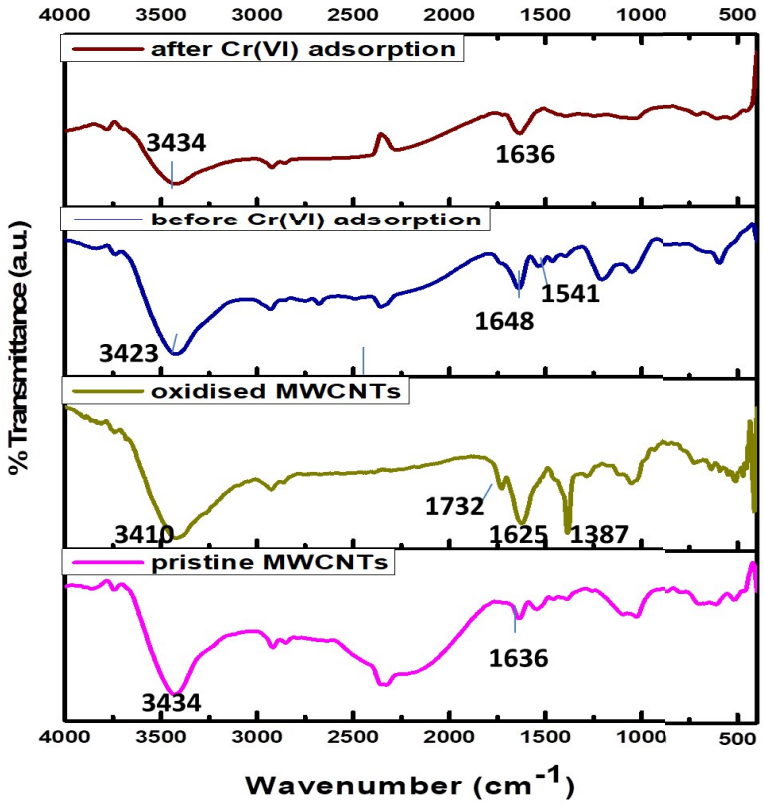


**Figure 6.4.** FTIR spectra of pristine, oxidized MWCNTs, biosorbent before and after Cr(VI) adsorption.

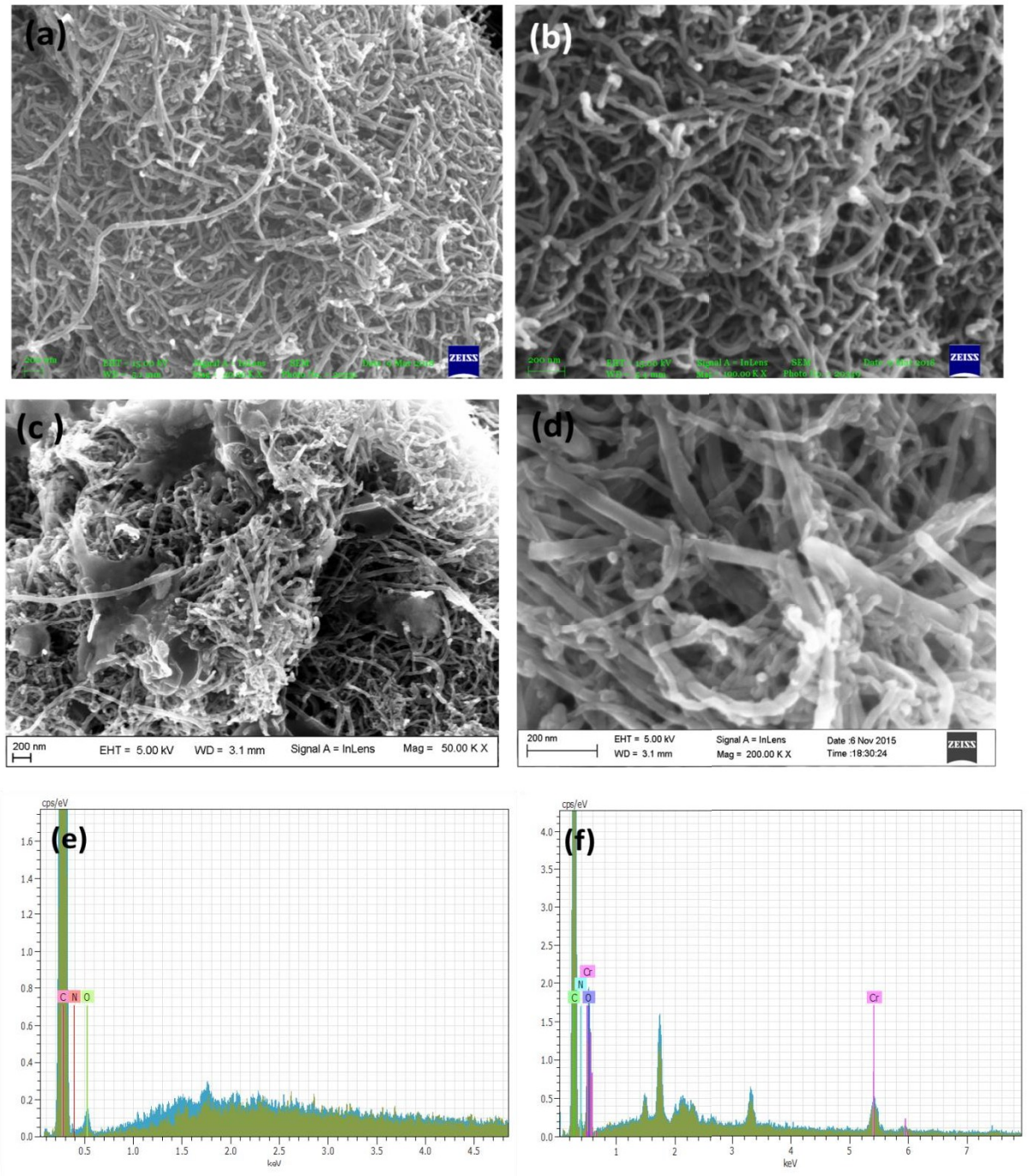


**Figure 6.5.** FESEM images of (a) pristine MWCNTs (b) oxidized MWCNTs (c,d) Biosorbent before and after Cr(VI) adsorption respectively. EDAX spectra of (e,f) CNTR before and after Cr(VI) adsorption.

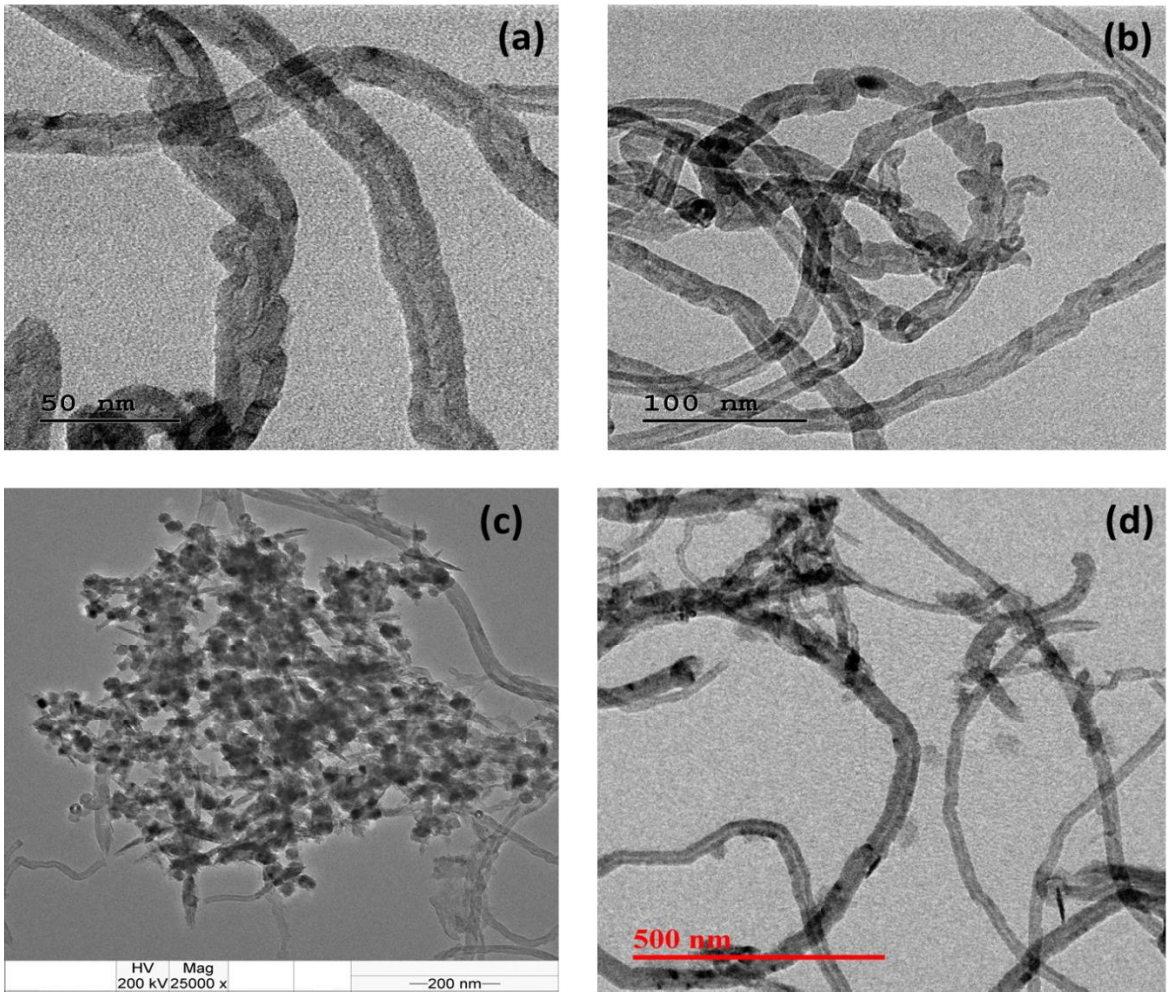


**Figure 6.6.** HRTEM images of (a,b) pristine and oxidized MWCNTs (c,d) biosorbent before and after Cr(VI) adsorption.

The presence of Cr(VI) on the biosorbent surface was also strongly supported by the X-ray photo electron spectroscopy (XPS). The base peak was corrected to 284.8 eV in the high resolution carbon scan. The survey scan of the biosorbent confirmed the presence of C, N, O and Cr respectively. The high resolution spectra of Cr 2p gave two peaks $Cr2p_{3/2}$ and $Cr2p_{1/2}$. $Cr2p_{3/2}$ is deconvoluted into two peaks at 577 eV, 578 eV which represent Cr(III) and Cr(VI) respectively[22] and $Cr2p_{1/2}$ at 587 eV corresponds to Cr(VI) as shown in Fig 6.7. Instant reduction of Cr(VI)

was not observed after treatment with the biosorbent due to short agitation period and this was confirmed through chromium speciation by ion chromatography. The XPS analysis showed the presence of Cr(III) and as reported earlier[23] Cr(III) formation on the biosorbent surface was evident only after 4-5 days. This could be due to extended interactions of Cr(VI) with the carbon and specific iron regulated surface proteins in the microbes.[24,25] The Brunauer–Emmett–Teller (BET) adsorption isotherm was used to measure the specific surface area of the biosorbent.[26] The nitrogen adsorption/desorption curves provided by the BET isotherm gave the surface areas for oxidized MWCNTs as 115.72 $m^2$ $g^{-1}$and 69.81 $m^2$ $g^{-1}$ for CNTR. The average pore volume and pore diameter was found to be as follows: Oxidized CNTs (1.3857 $cm^3$ $g^{-1}$, 47.897 nm) and CNTR (0.9183 $cm^3$ $g^{-1}$ , 52.613 nm) respectively. The thermal stability of the biosorbents were studied using thermogravimetric analysis (TGA). A sample mass of 2.43 mg of CNTR was analyzed in air atmosphere at a flow rate of 50 mL $min^{-1}$ in the temperature range 35-800$^oC$ ramped at 10$^oC$ per minute. The TGA curves (Fig. 6.8) signify that biosorbent was stable at higher temperatures i.e., till 677$^oC$ and the initial loss of mass is due to the moisture present in biosorbent.[27]

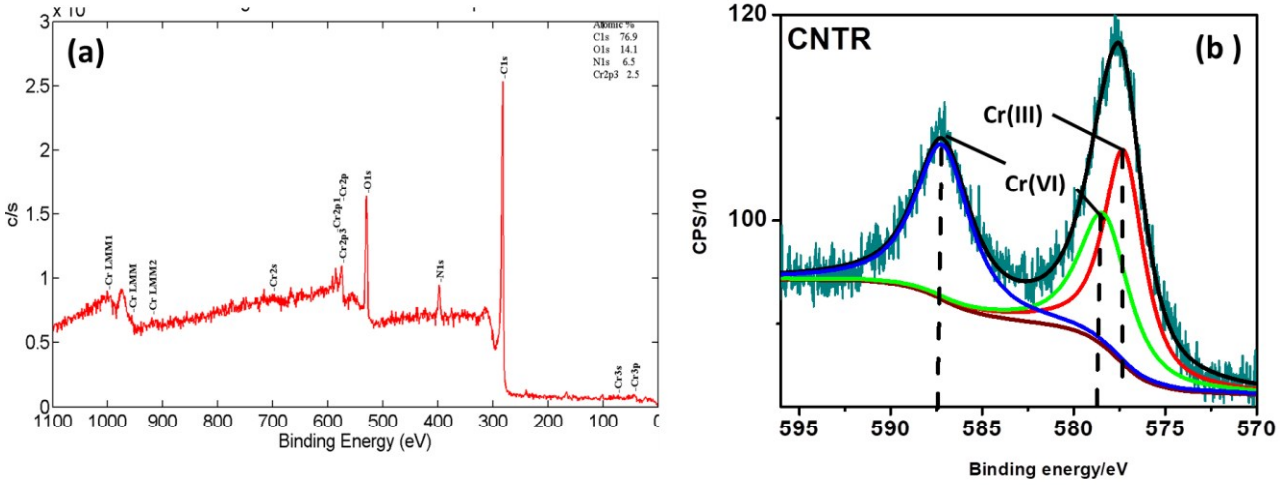


**Figure 6.7** XPS spectra of (a) survey scan of CNTR (b) high resolution chromium scan spectra

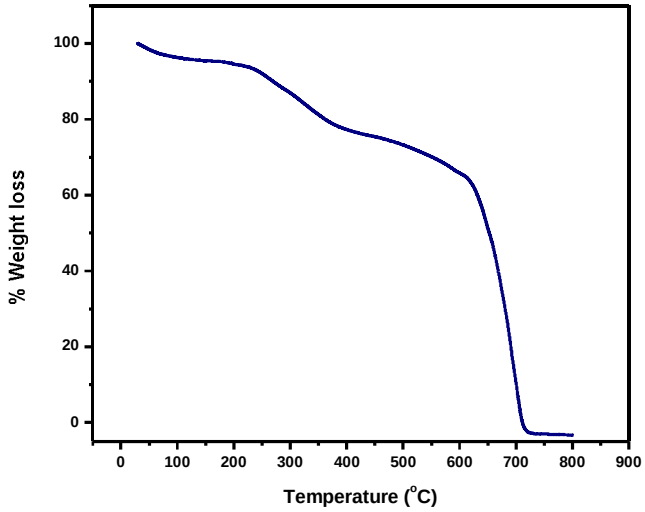


**Figure 6.8** TGA of the biosorbent

The presence of chromium in its +3 and +6 form were also differentiated using laser confocal microscopy using specific rhodamine based chemosensors. The physical properties of Rhodamine b hydrazide (RBH) such as colorless, non-fluorescent nature owes to its spirolactam structure which is highly stable and detects Cr(VI) whereas rhodamine-furfural complex (RF) is a pale pink solid which exhibits fluorescence and detects Cr(III). RBH was dissolved in 10 mmol $L^{-1}$ $H_2SO_4$ and added to the sample for further detection of Cr(VI). It was observed that after addition of RBH to the sample containing Cr(VI) it turned pink due to the conversion of RBH to RB in view of RBH oxidation caused by Cr(VI) in acid medium.[17] The excitation and emission was recorded at 560 nm and 585 nm respectively. RF when dissolved in 10 mmol $L^{-1}$ Tris-HCl is a colorless solution. The RF was added to the biosorbent with Cr(VI) which did not show any fluorescence indicating no immediate reduction of Cr(VI). After 4 days, the addition of biosorbent to RF turned pink due to chelation of RF with Cr(III) present on the surface of the biosorbent, generating a rhodamine type product in spirolactam by ring opening at C-N bond. [18] The excitation and emission for Cr(III) in RF was recorded at 525 nm and 590 nm respectively. The bright field and fluorescent images of CNTR are shown in Fig 6.9a-h. The images captured

before and after addition of RBH confirmed the presence of Cr(VI) in sample and also Cr(III) presence was confirmed by the addition of RF which exhibited fluorescence.

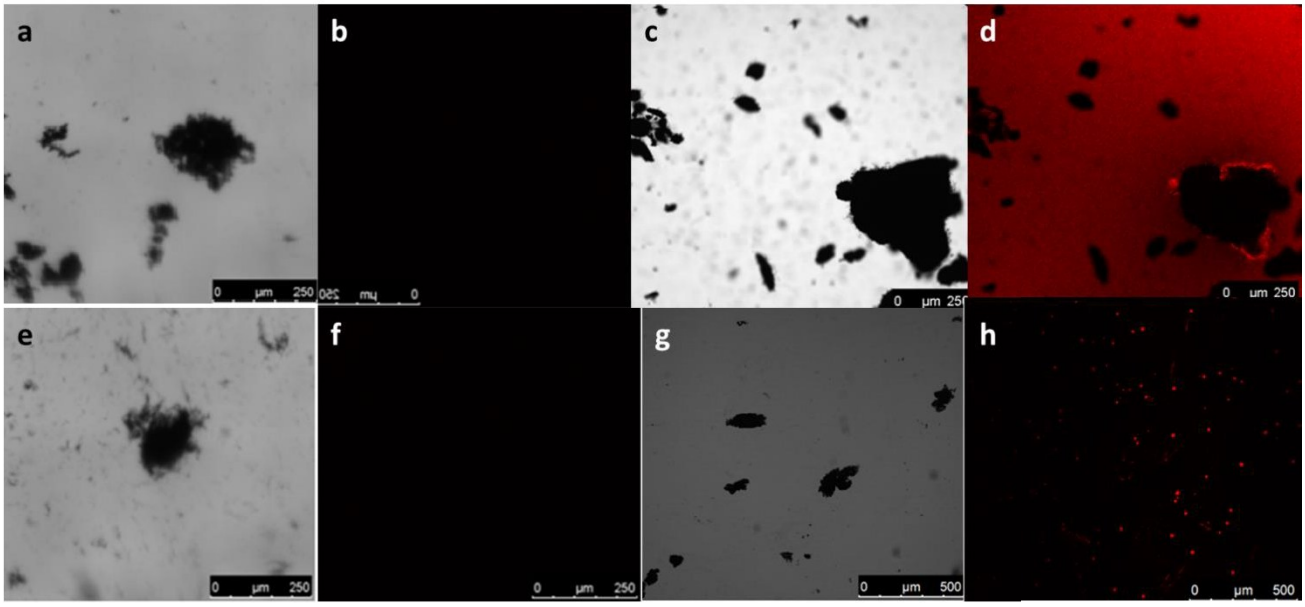


**Figure 6.9.** Confocal and bright field images of the bio sorbent after Cr(VI) adsorption: (a,b) CNTR with RBH (c,d) CNTR after Cr(VI) adsorption with RBH (e,f) CNTR with RF (g,h) Cr(VI) reduction to Cr(III) on CNTR with RF.

**(iii) Effect of pH , adsorbent dosage and interaction mechanisms**

Influence of pH plays a vital role in the uptake of Cr(VI) onto the biosorbent. A 0.1g weight of each of the biosorbent was weighed in a series of Erlenmeyer flasks and to that 20 mL of 5 mg $L^{-1}$Cr(VI) solution was added and adjusted to pH 2.0-7.0 and agitated for 3 hours to attain equilibrium. After analysis, it was found that the biosorbents could equally adsorb hexavalent chromium completely at pH 2.0. At pH>2 it was observed that there was a decrease in the metal uptake (Fig 6.10a). This is due to the existence of Cr(VI) ions in various forms such as hydro chromate ($HCrO_4^-$) at pH 2-4, in strongly acidic medium (pH<2) it exists as dichromate ($Cr_2O_7^{2-}$) and at higher pH as chromate ($CrO_4^{2-}$). In acidic medium, the biosorbent surface which has functional groups such as hydroxyl, carboxylic and amide gets protonated and is involved in electrostatic interactions with $HCrO_4^-$ thus aiding the metal to participate in biosorption as

depicted in chapter 3 Fig 3.20. Amides are usually poor leaving groups hence under highly acidic conditions (pH 2.0) the carbonyl oxygen of amide is protonated and further the protonation of amide nitrogen is also probable[28] in influencing the metal uptake. According to HSAB (hard-soft acid base) principle $CrO_4^{2-} < HCrO_4^- < OH^-$ with regard to the hardness of the ions.[23] At higher pH, the hydroxide and chromate ions compete each other resulting in the electrostatic repulsion thereby decreasing the Cr(VI) uptake .The adsorbent dosages were varied from 0.01g to 0.5 g to observe the minimal dosage of the biosorbent which can remediate maximum amount of Cr(VI) at pH 2.0. A 20 mL volume of 5 mg $L^{-1}$Cr(VI) was taken with varying biosorbent dosage and agitated for 180 min and observed that 0.1g could adsorb Cr(VI) quantitatively indicating the saturation of adsorbent sites (Fig 6.10b ).

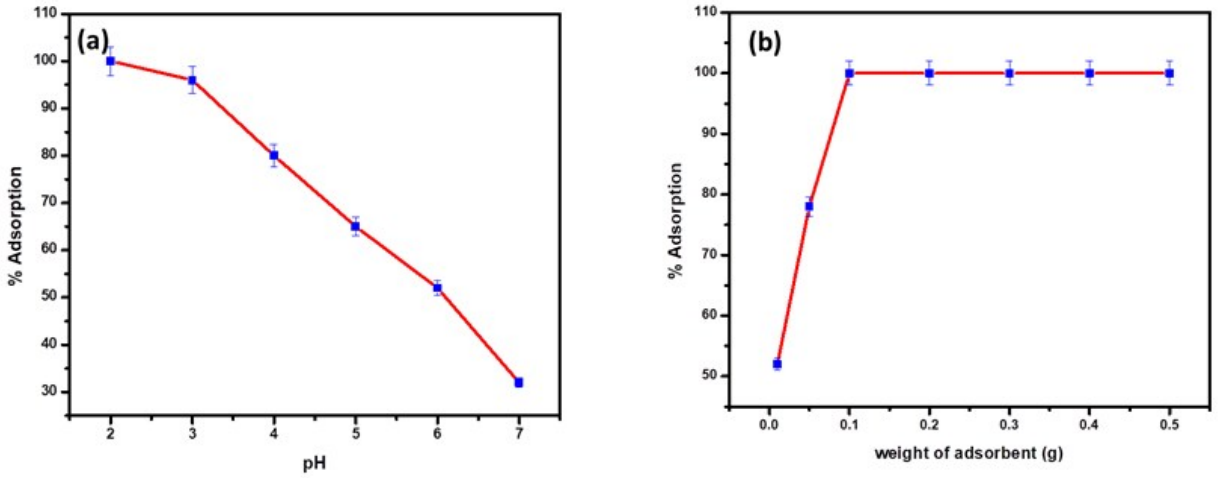


**Figure 6.10. (a)** pH effect on bio sorption (Conditions: weight of the adsorbent- 0.1 g, Cr(VI) concentration- 5 mg $L^{-1}$/20 mL) **(b)** Effect of adsorbent dosage on biosorption (Conditions: pH-2.0, Cr(VI) concentration- 5 mg $L^{-1}$/20 mL)

**(iv) Biosorption kinetics, isotherms and temperature effect studies**

The kinetic experiments were performed using 0.1 g of the biosorbent mixed with 20 mL of 5 mg $L^{-1}$ Cr(VI) at time intervals ranging from 5 – 180 min. The maximum uptake of the metal ion was observed at 180 min. The data obtained from the plots (Fig 6.11a-c) were fitted into the

pseudo first order[29], second order[30] and intra particle diffusion equations to evaluate the adsorption kinetics. The kinetic parameters are presented in Table 6.2.

The rate at which Cr(VI) gets adsorbed is mostly influenced by the diffusion mechanisms such as (i) the Cr(VI) from the bulk aqueous medium is transferred onto the biosorbent surface via external mass transfer (ii) intraparticle diffusion wherein Cr(VI) diffuses through the pores of the biosorbent. The best suited kinetics depends on the experimental data which has the highest regression coefficient and the system follows pseudo second order kinetics with 1.8026 mg $g^{-1}$ ($q_{e\ exp}$), 1.826 mg $g^{-1}$ ($q_{e\ cal}$). The plot $q_t$ vs $t^{1/2}$ relates to the intraparticle diffusion which is evaluated using $q_t = k_i\ t^{1/2} + C$ where c corresponds to intercept and $k_i$ is the intra particle diffusion constant which is obtained from the slope of the plot. The rate at which Cr(VI) gets adsorbed is mostly influenced by the diffusion mechanisms such as (i) the Cr(VI) from the bulk of the solution gets transferred onto the biosorbent surface via external mass transfer (ii) intraparticle diffusion[31] wherein Cr(VI) diffuses through the pores of the biosorbent. From the plot it was observed that the straight line deviates from the origin having a significant intercept indicating the boundary layer phenomenon also plays role in the adsorption kinetics of hexavalent chromium.

Among several isotherms, commonly studied theoretical and empirical isotherms are Langmuir and Freundlich.[32] The data obtained from the plots (Fig 6.11d, e) and the equations are presented in Table 6.3. The system assumed a monolayer Langmuir adsorption model as it has the low chi square value and high $R^2$ value. The biosorbent has an adsorption capacity of 24.8 mg $g^{-1}$ with an $R^2$ value of 0.96. The dimensionless constant $R_L$ value lies below unity indicating the reversibility of the isotherm ($R_L = 1/1+bC_o$ ) where b is the Langmuir constant associated to adsorption energy, $C_o$ represents the equilibrium concentration of the heavy metal ion. The Freundlich constants n and $K_F$ are related to adsorption intensity and its capacity, respectively. The value of n is greater than 1 indicating the favorability of metal adsorption onto the biosorbent. The pristine MWCNTs have an adsorption capacity of 11.93 mg $g^{-1}$, when oxidized the uptake capacity enhanced to 16.22 mg $g^{-1}$ and after the addition of *Rhizobium* to the

MWCNTs adsorption capacity increased to 24.82 mg $g^{-1}$. The comparison of adsorption capacities of various adsorbents with the current developed biosorbents is given in Table 6.4.

The thermodynamic parameters such as Gibbs free energy ($\Delta G^o$), enthalpy ($\Delta H^o$) and entropy ($\Delta S^o$) explain the spontaneity of adsorption process. The equilibrium constant K at different temperatures was derived from the ratio of Cr(VI) present on the surface of the biosorbent to that in the liquid phase and fitted into Gibbs free energy equation ($\Delta G = -RT\ln K$). The changes in enthalpy and entropy of the biosorbents were obtained from the Van't Hoff plot of ln K against 1/T (Fig. 6.11f). The negative free energy values indicate the spontaneity in the biosorbent-sorbate interactions and the negative values of enthalpy and activation energy ($E_a = \Delta H^o_{ads} + RT$) indicates the system involves exothermic adsorption. The negative $\Delta S^o$ values indicate the decrease in the disorderliness of the system with increase in temperature.[23] The $\Delta H$ value obtained (-31.6 kJ $mol^{-1}$) indicate the system observes exothermic physicochemical adsorption. The enthalpy-entropy compensation is well illustrated through the corresponding values (Table 6.5) obtained for the biosorbent.

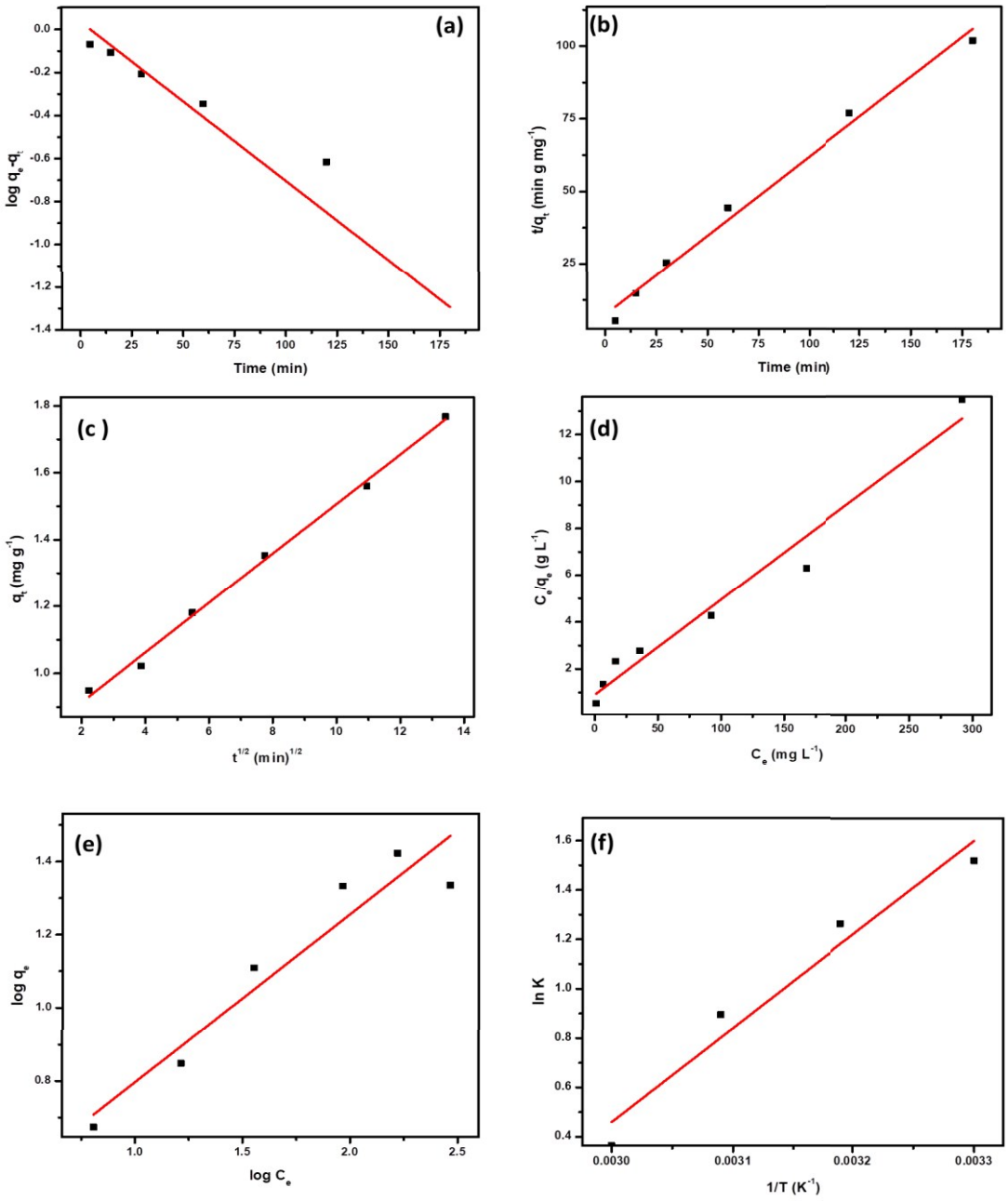


**Figure 6.11.** (a) Pseudo first order kinetics (b) pseudo second order kinetics (c) Intra particular diffusion (d) Langmuir (e) Freundlich (f) lnK against 1/T (conditions: pH-2.0, adsorbent dosage-0.1 g/20 mL)

**Table 6.2** The kinetic parameters for the adsorption of Cr(VI) onto CNTR

| **Kinetic parameters** | **CNTR** |
|---|---|
| $C_o$ (mg $L^{-1}$) | 10 |
| $q_e$ (mg $g^{-1}$) | 1.826 |
| $k_2$ (g $mg^{-1}$ $min^{-1}$) | 0.041 |
| $R^2$ | 0.986 |
| $k_1$ ($min^{-1}$) | 0.017 |
| $R_1^2$ | 0.915 |
| $k_{int}$ (mg $g^{-1}$ $min^{-0.5}$) | 0.074 |

**Table 6.3** Biosorption isotherm parameters for Cr(VI) adsorption

| **Langmuir $q_o$(mg $g^{-1}$)** | **b ($mg^{-1}$ L)** | **$R^2$** | **$\chi^2$** | **$R_L$** |
|---|---|---|---|---|
| 24.82 | 0.043 | 0.962 | 0.46 | 0.695 |
| **Freundlich $K_F$($mg^{1-1/n}g^{-1}L^{1/n}$)** | **n** | **$R^2$** | **$\chi^2$** | |
| 2.172 | 2.178 | 0.895 | 0.61 | |

**Table 6.4** Comparison of adsorption capacities of various biosorbents based on both microbe and CNTs

| **Adsorbents** | **pH** | **Adsorption capacity (mg $g^{-1}$)** |
|---|---|---|
| Cellulose-sodium montmorillonite[34] | 3.8-5.5 | 22.2 |
| MWCNTs –calcium alginate complex immobilized in *Shewanellaoneidensis*[8] | 6.0-7.0 | 6.07 |
| $Fe_2O_3$ nanoparticle-MWCNTs composite[5] | 2.0 | 42.02 |
| Activated carbon supported MWCNTs[15] | 2.0 | 113.29 |
| (Present studies) | | |
| *Rhizobium BVR* | 2.0 | 9.50 |
| Pristine MWCNTs | | 11.93 |
| Oxidized MWCNTs | | 16.22 |
| CNTR | | 24.82 |

**Table 6.5** Thermodynamic parameters associated with adsorption

| **Temperature (Kelvin)** | **$\Delta G^0$ (kJ mol$^{-1}$)** | **$\Delta S^0$ (J mol$^{-1}$K$^{-1}$)** | **$\Delta H^0$ (kJ mol$^{-1}$)** | **$E_a$(kJmol$^{-1}$)** |
|---|---|---|---|---|
| 303 | -3.705 | -91.1 | -31.6 | -29.0 |
| 313 | -3.186 | | | |
| 323 | -2.329 | | | |
| 333 | -0.997 | | | |

**(v) Effect of sample volume, regeneration and interference studies**

Laboratory scale column studies were done to test the applicability of developed biosorbents for their sustainability to higher sample volume. A 1.5 g biosorbent was packed to 2 cm bed height in a glass column of 30cm length with a diameter of 2 cm and was allowed to settle for a minimum of 2 hours to avoid air voids before the start of the experiment. A Cr(VI) concentration of 5 mg L$^{-1}$ was prepared and the column was loaded with 50 mL of 5 mg L$^{-1}$ at 5 mL min$^{-1}$flow rate and the eluate concentration was checked periodically for every 10 mL using ion chromatography. 50 mL of 5 mg L$^{-1}$Cr(VI) was completely adsorbed effectively. Subsequently, 300 mL of the Cr(VI) solution was loaded continuously and the heavy metal was adsorbed completely beyond which there was saturation owing to the non-availability of active adsorption sites.[33] A sample volume of 250 mL was adsorbed effectively onto the biosorbent as shown in Fig.6.12 a. A significant property of the adsorbent is the ability to reuse thereby reducing the operational cost in treating pollutants. Varying sodium hydroxide concentrations (0.1-2.0 mol L$^{-1}$) were tried (Fig. 6.12 b,c) of which 1.0 mol L$^{-1}$sodium hydroxide was effective in desorbing Cr(VI) as sodium chromate.[23] It was observed that there were four complete adsorption-desorption cycles (100%) and the decrease in adsorption was observed from 5$^{th}$ cycle.

A 100 mg $L^{-1}$concentration each of various cations such as $Mn^{+2}$, $Cu^{+2}$ $Fe^{+2}$ , $Co^{+2}$, $Ni^{+2}$, $Pb^{+2}$ and anions such as nitrate, chloride, sulfate were added to 5 mg $L^{-1}$ Cr(VI) solution and the adsorption studies were carried out to observe the influence of these ions in the uptake of chromium. It was observed that the adsorption percentage decreased by 2.0±0.5% attributed to the interference of anions which compete with hydrochromate ions to occupy the adsorption sites, whereas cations such as Fe(II) and Mn (II) have the ability to reduce Cr(VI) to Cr(III).[34]

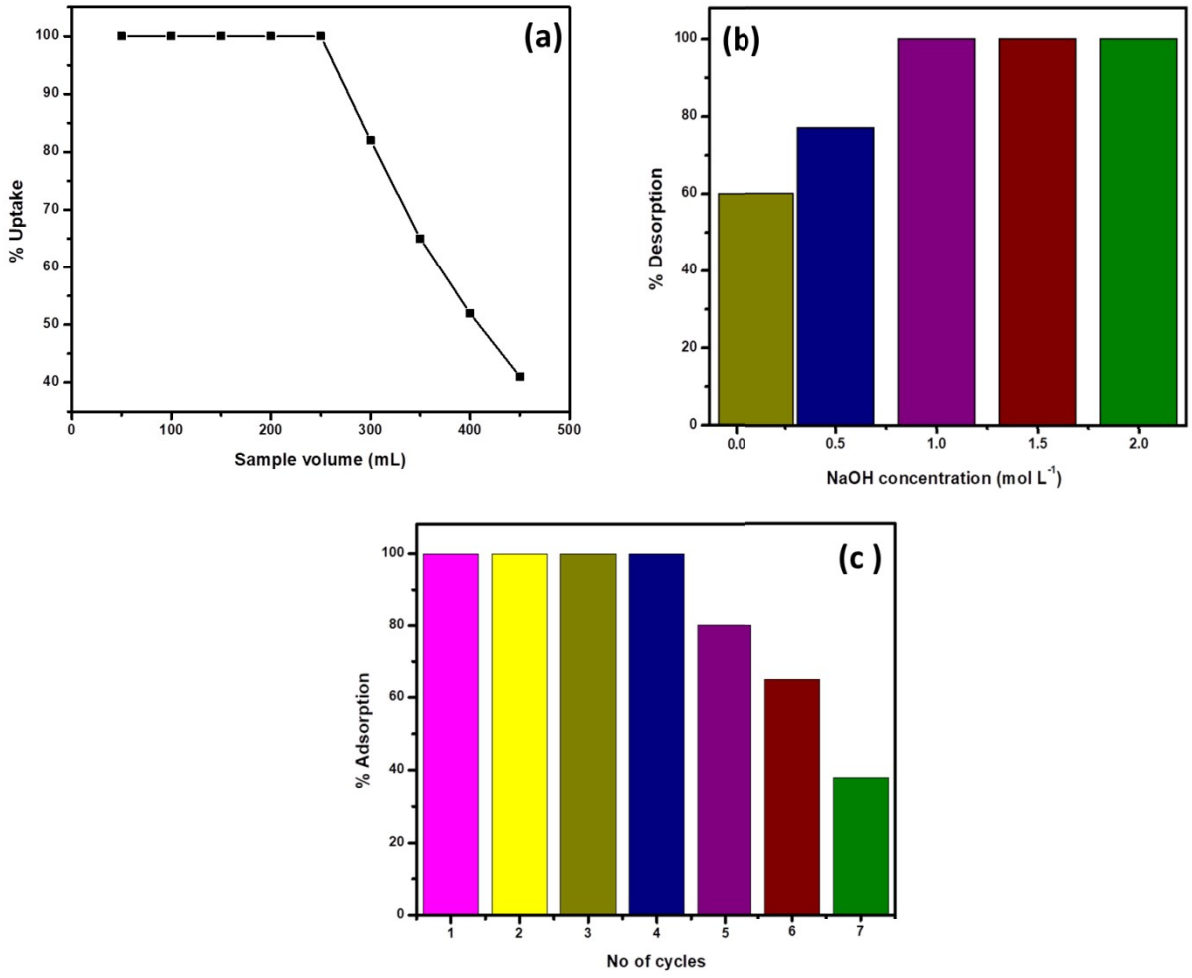


**Figure 6.12.** (a) Effect of sample volume of CNTR (conditions: weight of adsorbent- 1.5 g, Cr(VI) concentration- 5 mg $L^{-1}$, pH- 2.0, flowrate- 5 mL $min^{-1}$) (b) Effect of varied NaOH concentrations on CNTR (c) Regeneration efficiency of CNTR.

### 6.1.4 Conclusions

In conclusion, this work has highlighted the confluence of biotechnology and nano materials as an emerging area towards heavy metal remediation. The proposed methodology has illustrated the ability of nitrogen fixing bacteria immobilized in oxidized multiwalled carbon nano tubes as effective adsorbent to sequester chromium in the +6 oxidation state. The biosorbent followed Langmuir isotherm with 24.86 mg $g^{-1}$ adsorption capacity respectively. The biosorption process was exothermic, spontaneous and pseudo second order model was effective in understanding the adsorption kinetics. The mechanism involves electrostatic interaction between the heavy metal ion and biosorbent surface. Characterization techniques confirmed the interaction of microbe and oxidized carbon nano tubes with Cr(VI). A 200 mL sample volume of synthetic waste water sample was treated in lab scale column studies which could tolerate up to 4 cycles of adsorption and desorption by regenerating the biosorbents using 1.0 mol $L^{-1}$sodium hydroxide.

## 6.2. Efficacy of Sodium Montmorillonite-*Rhizobium* combination as a prospective biosorbent to sequester hexavalent chromium

### 6.2.1 Introduction

Combination of interdisciplinary techniques is quite efficient in developing biosorbents for heavy metal sequestration. The current study demonstrates Cr(VI) removal using the clay-*Rhizobium* biosorbent. Immobilisation of *Rhizobium* (isolated from soil) in sodium montmorillonite provides a conducive environment to capture hexavalent chromium. A simple and an economically reliable process like adsorption would be feasible for sequestration of heavy metals. [35] Adsorbents such as carbon nanotubes,[36] graphene oxide,[37] modified resins,[38] modified activated carbon[39]etc have been reported to sequester Cr(VI). To meet several disadvantages of chemical adsorbents, greener alternatives have emerged. Several reports are there on biosorption as a sustainable removal technique to apprehend toxic and detrimental substances.

Recently reported biosorbents for the sequestration of Cr(VI) include *Saccharomyces cerevisiae* immobilised in crosslinked cellulose[23] using microwave immobilisation could remove upto 23.61mg $g^{-1}$, whereas the activated biomass of *Rhizobium leguminosarum*[40] could remove upto84.4±3.6% Cr(III) at 35$^{o}$C at pH 7.0. *Aspergillus BRVR* immobilised in sodium montmorillonite[41] and cellulose[42]also showed good efficacy in adsorbing Cr(VI). An interesting feature, adsorption coupled reduction of Cr(VI) using dead biomass of *Aspergillus niger* was reported by Park et al .[43] Also there are several reports on adsorption of Cr(VI) using clays such as montmorillonite supported magnetite nanoparticles could adsorb upto 15.3 mg $g^{-1}$ Cr(VI), clay-biopolymer composites such as cellulose-clay[34] also show good potential for Cr(VI) removal, clays also help in Cr(VI) reduction wherein Cr(VI) reduction is correlated to the $Fe^{+2}$containing dithionite reduced smectite.[44,45] There are less reported studies on the clay-microbial combination for heavy metal sequestration. The developed clay-*Rhizobium* biosorbent was tested for Cr(VI) removal in batch studies by varying pH, adsorbent dosage, kinetics and thermodynamics.

### 6.2.2 Experimental section

#### (i) Preparation of the Clay-*Rhizobium* biosorbent

The sodium form of montmorillonite (NaMMT) was prepared by treating montmorillonite with sodium chloride as described in literature.[46] The isolated *Rhizobium BVR* was grown in YMA broth medium and complete characterization of the microbe has been reported in our earlier studies (Chapter 6.1) and assigned an accession number MF136764 by NCBI genbank. The grown culture was centrifuged to obtain a pellet. A 2.0g weight of *Rhizobium* was mixed with 1.0g of NaMMT in aqueous medium and subjected to sonication for about 8 min (50W, 230V) to ensure the bacterial surface immobilization in sodium montmorillonite. The NaMMT- *Rhizobium* biosorbent was filtered, rinsed with water and dried for further experimental studies.

#### (ii) Biosorption studies

The biosorption experiments were optimized by conducting batch studies using 0.2 g of the prepared NaMMT-*Rhizobium* biosorbent in 30 mL of 5 mg $L^{-1}$working Cr(VI) solution. The temperature variations at different time intervals with a agitation speed of 120 rpm was performed in an incubator shaker. The Cr(VI) concentration left in solution was quantitatively analyzed using ion chromatography technique through post column derivatization using diphenyl carbazide.

### 6.2.3 Results and Discussion

#### (i) Characterization of the Clay-*Rhizobium* biosorbent

The frequency shifts in the IR spectrum reveals the participation of hydroxyl, amino, carboxyl functional groups present in the microbial cell walls.[20] The characteristic band for clays was observed at 3643 $cm^{-1}$ corresponding to the Si–OH functional groups. The hydroxyl and amine functional groups and also the Al-O-H stretching vibrations together contribute to the broad band at 3454 $cm^{-1}$. The Si- O-Si stretching of clay was observed at 1114 $cm^{-1}$ and the amide-I band at 1640 $cm^{-1}$ [20] could be attributed to the bacteria and hydrogen bonding in water. The other characteristic peaks for montmorillonite at 792 $cm^{-1}$ and 688 $cm^{-1}$ indicates the broadening of

quartz and silica and Si-O bond deformation respectively.[34] A shouldering peak at 918 $cm^{-1}$ corresponding to Cr=O after adsorption of hexavalent chromium[34] is an evidence for metal adsorption as shown in Fig 6.13.

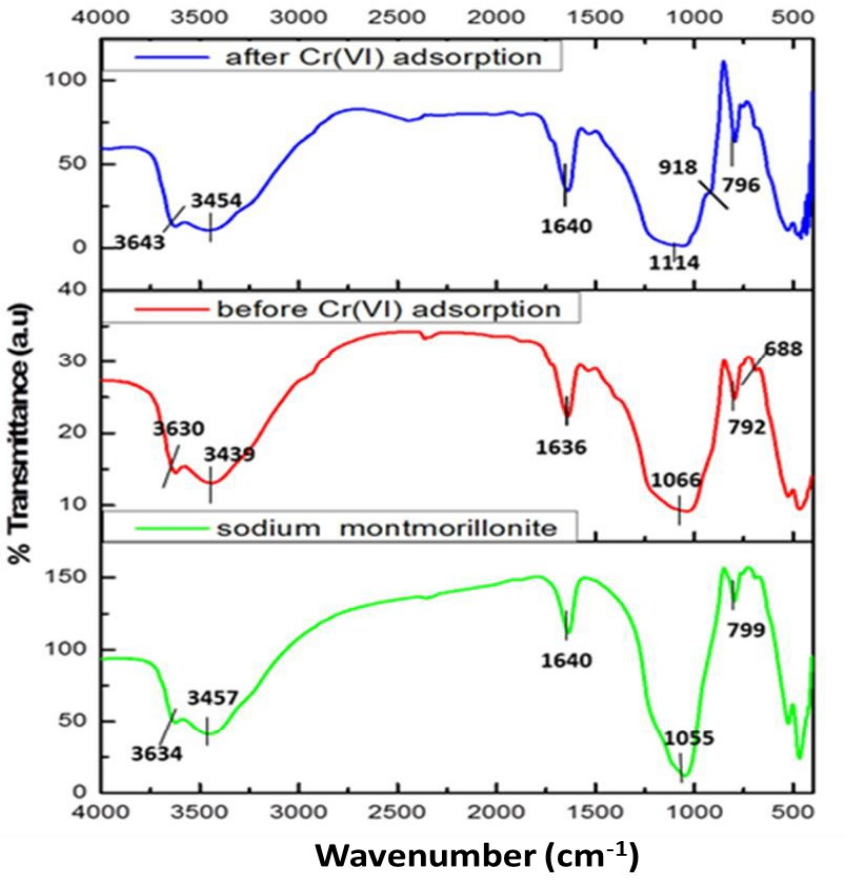


**Figure 6.13** FTIR of sodium montmorillonite, biosorbent

before and after Cr(VI) adsorption

The morphological features of the *Rhizobium* immobilized in clay captured using SEM showed assorted clusters (Fig. 6.14) and also the elemental analysis through EDAX showed the presence of elements such as Na, K, Al, Si respectively. The presence of Cr peak between 5-6 keV after adsorption confirmed Cr(VI) adsorption. (Fig. 6.14). The possible reduction of Cr(VI) was explored using X-ray photo electron spectroscopy since microbial adsorption mechanism is often

coupled with reduction. The survey scan revealed the presence of elements such as C,O,N,Cr.(Fig 6.15**)** and the short scan of the C1s peak was corrected to 284.8eV(Fig 3b).The binding energies in the survey scan showed a peak at 576.9 eV that corresponds to Cr(III) and 585.7eV which is characteristic of Cr(VI).[47] It was observed that there was no immediate reduction after biosorption of Cr(VI) and the clay-rhizobium surface turned pale green only after few days signifying the formation of Cr(III).

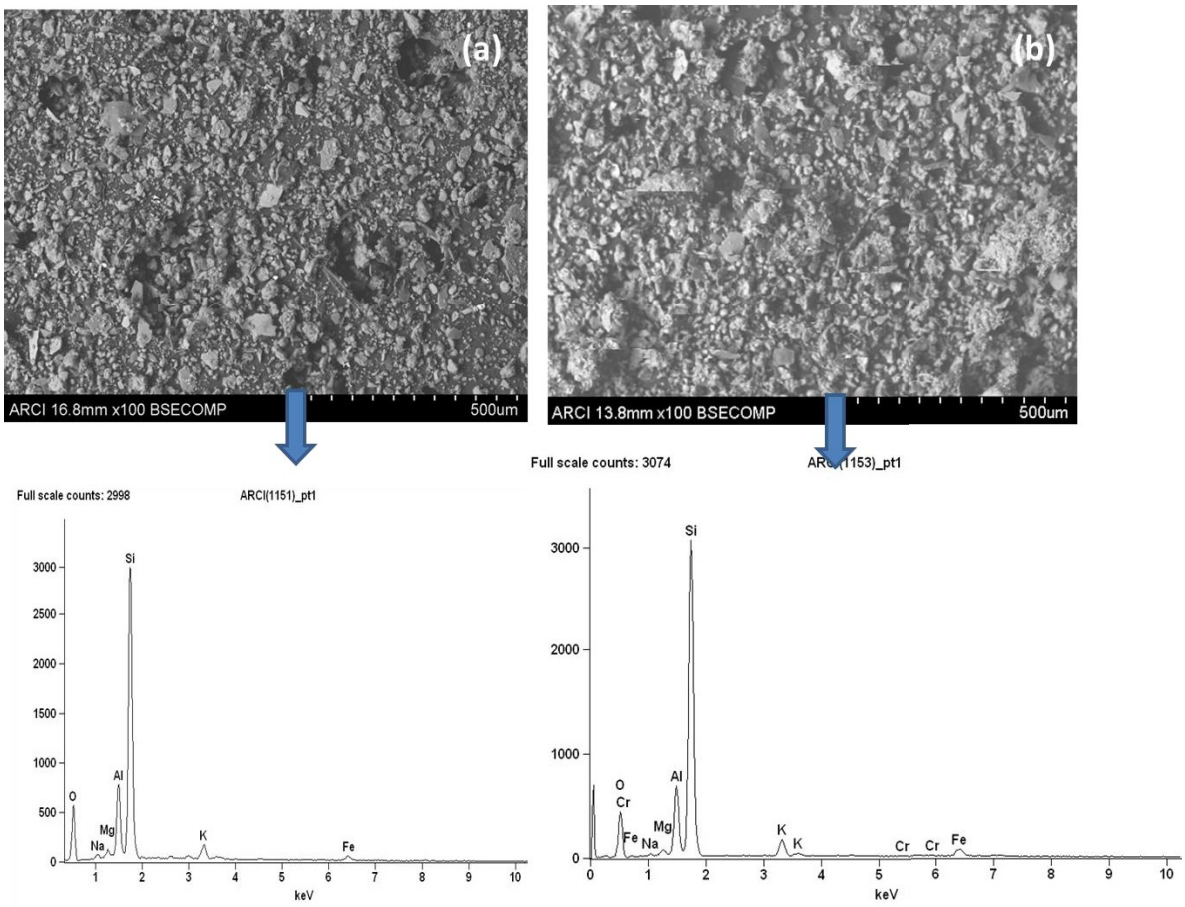


**Figure 6.14** SEM and EDAX images of the biosorbent (a) before Cr(VI) adsorption (b) after Cr(VI) adsorption

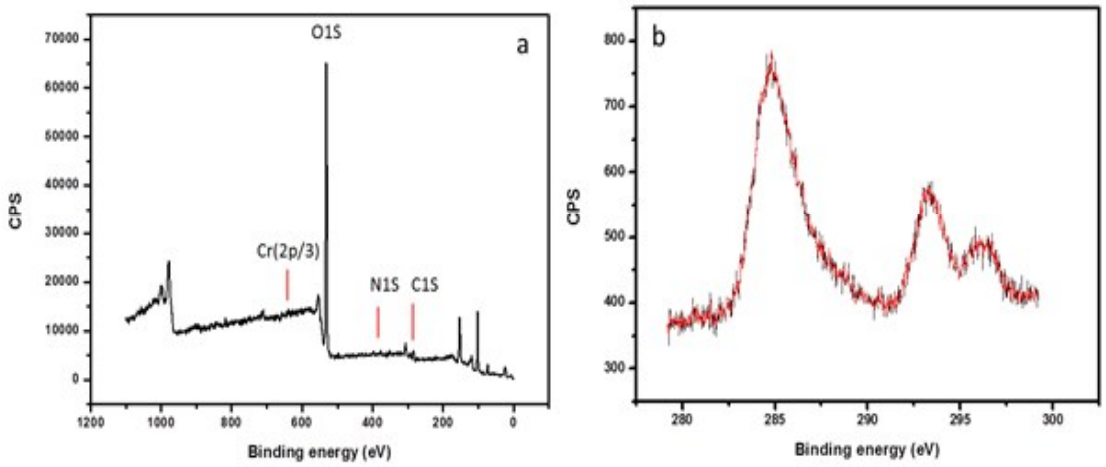


**Figure 6.15** XPS spectra of the biosorbent after Cr(VI) adsorption (a) Survey scan spectra (b) High resolution spectra of C1S.

Specific rhodamine based sensors were utilized in the characterization to differentiate Cr(III) and Cr(VI) with laser confocal microscopy by using probes such as RBH and RF as discussed in Chapter 6.1. The bright field and fluorescent images are shown in Fig 6.16. The images captured before and after addition of probes which confirmed the presence of Cr(VI) and Cr(III) respectively. The pink color formation indicates the presence of chromium in their respective oxidation states using the above probes.[17,18]

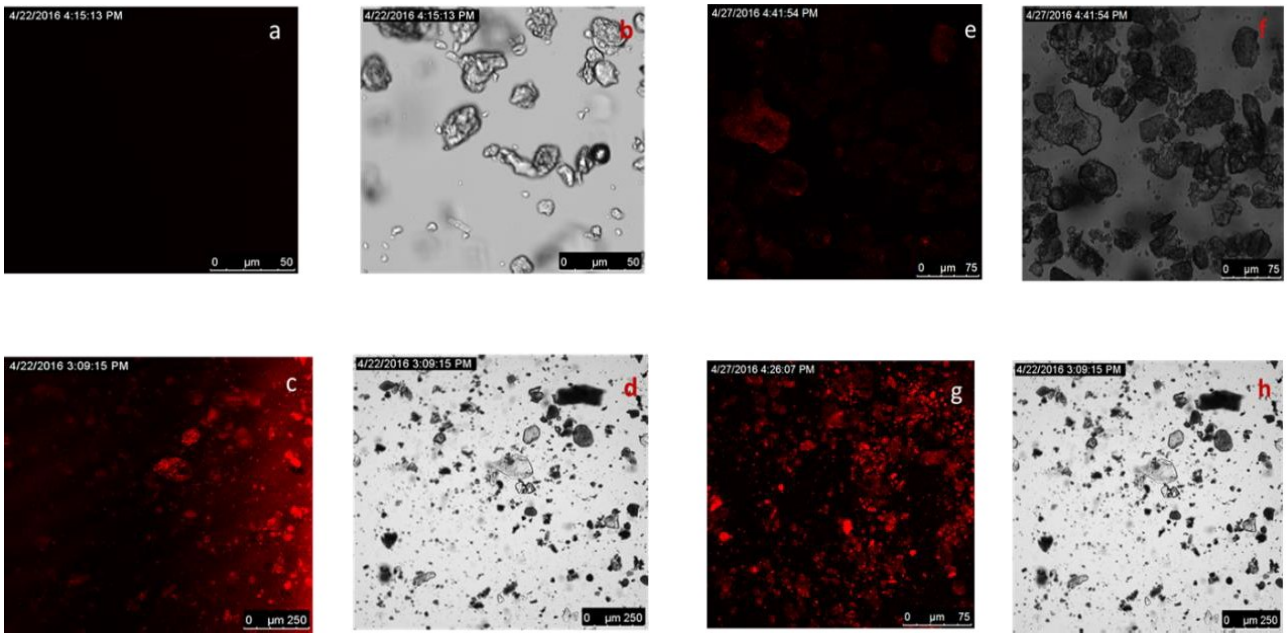


**Figure 6.16**. Confocal using laser source and bright field images of the biosorbent after Cr(VI) adsorption (a,b) without RBH (c,d) with RBH (e,f) without RF (g,h) with RF

**(ii) Effect of pH, adsorbent dosage and interaction mechanism for biosorption**

In accordance with the pH of the aqueous phase, hexavalent chromium is present as hydrogen chromate ($HCrO_4^-$), dichromate ($Cr_2O_7^{2-}$) and chromate ($CrO_4^{2-}$) oxy anions respectively. The dichromate and hydrogen chromate anions exist in equilibrium and the plausible mechanism indicates the existence of $HCrO_4^-$ at pH greater than or equal to 2.0.[47] Quantitative adsorption was observed on the surface of the biosorbent at pH 2.0 for a 30 mL volume of 5 mg $L^{-1}$ hexavalent chromium concentration. (Fig 6.17a). The functional groups such as amine, carboxyl, hydroxyl (from microbial surface), silanol and aluminol groups (from clay) are protonated at pH 2.0 resulting in electrostatic interactions with hydro chromate ions .[34] According to Hard-Soft acid base concept, Cr(VI) in the form of hydrochromate anion reacts with protonated nitrogen and oxygenated functional groups of the biosorbent resulting in electrostatic interactions.[25] At pH 2.0 and at a adsorbent dosage of 0.2 g, 30 mL of 5 mg $L^{-1}$ Cr(VI) was adsorbed completely beyond which saturation of active binding sites was observed. (Fig 6.17b). With increase in pH,

decline in adsorption was observed due to the deprotonation of functional groups present on the surface of clay-*Rhizobium* biosorbent.

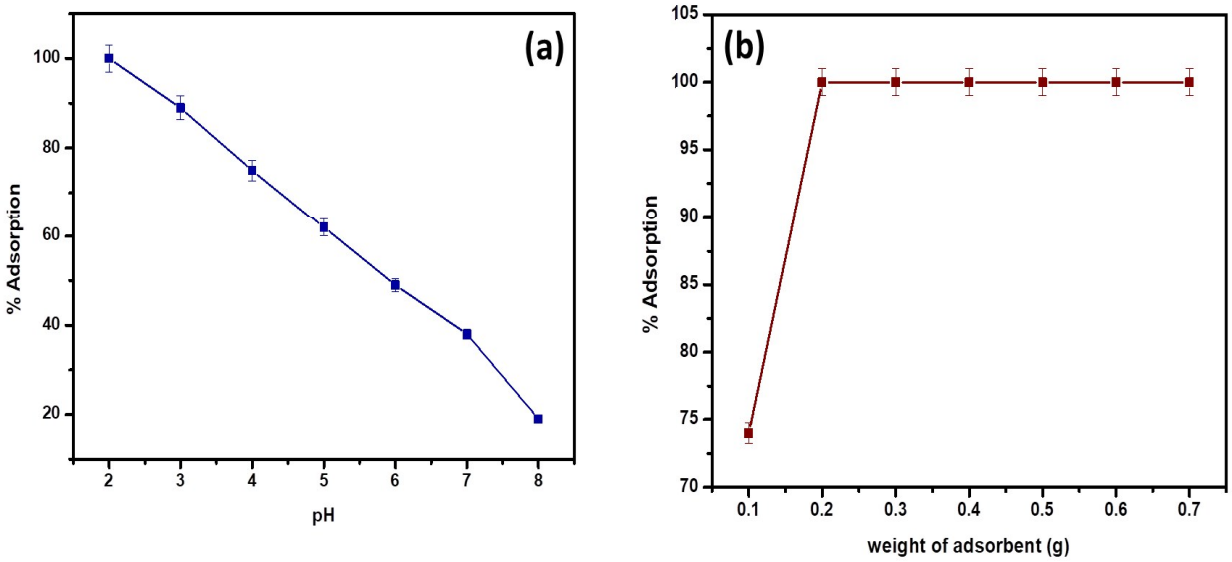


**Figure 6.17** (a) pH effect on biosorption (Conditions: weight of the adsorbent- 0.2 g/ 30 mL, Cr(VI) concentration- 5.0 mg $L^{-1}$) (b) variation of adsorbent dosage (Conditions: pH-2.0, Cr(VI) concentration- 5.0 mg $L^{-1}$)

**(iii) Equilibrium adsorption isotherms, kinetics and thermodynamic studies**

The association between the adsorbent and the adsorbates at equilibrium was studied using isotherms.[48] The data obtained (Table 6.6) from isotherm studies is very useful in understanding the mechanism and was fitted with two classical isotherms (Langmuir and Freundlich).[49] The data obtained (Fig 6.18 a,b) depicts the increase in adsorption at higher Cr(VI) concentrations gradually leading to saturation. The Langmuir model assumes monolayer sorption in which metal ion adsorption occurs on a homogenized surface and there is no contact between the adsorbed ions. The multilayer adsorption which occurs on a heterogeneous surface is described by Freundlich model. Among of the two models, Freundlich isotherm, with a $R^2$ value of 0.99 and a low $\chi^2$ value of 0.03 was quite appropriate in describing the adsorption process. The

favorability of adsorption is also indicated by the value of the exponent n which lies between 1-10. The Langmuir adsorption capacity of the system was found to be 22.22 mg $g^{-1}$ with 0.93 as correlation coefficient and $R_L$ (a dimensionless parameter) given as $R_L = 1/1+bC_o$, [50] was below unity and this confirmed the suitability and reversibility of adsorption. *Rhizobium BVR* strain as such could adsorb Cr(VI) with an adsorption capacity of 11.5 mg $g^{-1}$.

The kinetics of the Cr(VI) adsorption data is shown in Fig 6.18c,d for various contact times ranging from 5 min to 180 min. An adsorption efficacy of 60% was achieved during initial five minutes and later the adsorption rate continued to rise steadily and attained equilibrium at 180 min. The adsorption kinetics were evaluated using the pseudo first order[29] and second order kinetics.[50] A working solution of 10 mg $L^{-1}$ Cr(VI) was used for the kinetic studies. The data obtained from the kinetic plots (Fig. 6.18c,d) are tabulated in Table 6.7. The system followed pseudo second order kinetics with observed and calculated $q_e$ values as 1.0446 and 1.020 mg $g^{-1}$. The Cr(VI) uptake is majorly driven by the mechanisms such as film, particle diffusion and surface adsorption. At high Cr(VI) concentrations, intraparticle diffusion plays a major role whereas at low metal concentrations pore diffusion takes place.[10] The boundary layer mechanism for efficient metal uptake is well explained by Weber-Morris intra particle diffusion model and was obtained by plotting $q_t$ and $\sqrt{t}$ (Fig.6.18e) and ascertained through the non-zero intercept.

The changes in the thermodynamic parameters such as enthalpy ($\Delta H$), Gibbs free energy ($\Delta G$), and entropy ($\Delta S$) at various temperatures signifies the feasibility and nature of the adsorption reaction. The transfer of chromium from solution phase occurs onto the immobilized bacterial cell surface wherein montmorillonite acts as the primary host and the clay-bacteria biosorbent acts as a secondary host for Cr(VI). The overall reaction Gibb's free energy change ($\Delta G_r$) can be explained as a summation from clay-rhizobium surface and clay-rhizobium-chromium surface.

$$\Delta G_r = \Delta G_{\text{clay-rhizobium surface}} + \Delta G_{\text{clay-rhizobium-Cr}} \qquad (6.1)$$

The reaction Gibbs free energy is related to the enthalpy and entropy changes as

$$\Delta G_r = \Delta H_{\text{clay-rhizobium –Cr}} - T\Delta S_{\text{clay-rhizobium-Cr}} \qquad (6.2)$$

At equilibrium,

$$\text{Clay-rhizobium-Cr}_{(\text{solution})} \rightleftharpoons \text{Clay-rhizobium-Cr}_{(\text{surface})} \quad (6.3)$$

$$\Delta G_r = \Delta G_r^{\,0} + RT\ln \frac{a_{clay-rhizobium-Cr|surface}}{a_{clay-rhizobium-Cr|solution}} \quad (6.4)$$

Since, activity (a) is directly proportional to concentration (C) of the Cr (VI) in low concentrations,

$$\text{Therefore, } \Delta G_r = \Delta G_r^{\,0} + RT\ln \frac{[clay-rhizobium-Cr]_{surface}}{[clay-rhizobium-Cr]_{solution}} \quad (6.5)$$

Hence

$$\Delta G_r = \Delta G_r^{\,0} + RT\ln K \quad (6.6)$$

At equilibrium $\Delta G_r = 0$

$$\Delta G^o_r = - RT\ln K_{eq} \quad (6.7)$$

From the plot of lnK against 1/T (Fig 6.18f) the thermodynamic parameters namely, enthalpy and entropy changes were obtained from slope and intercept (Table 6.8). The biosorption process was spontaneous as observed from negative free energy values. Further, from the negative values of enthalpy, it is obvious that adsorption reaction is exothermic. The range of $\Delta H$ (20-40 kJ $mol^{-1}$) also indicates physico-chemical adsorption phenomenon.[42] The negative $\Delta S$ value is attributed to the decreased randomness at the clay-rhizobium-aqueous interface.

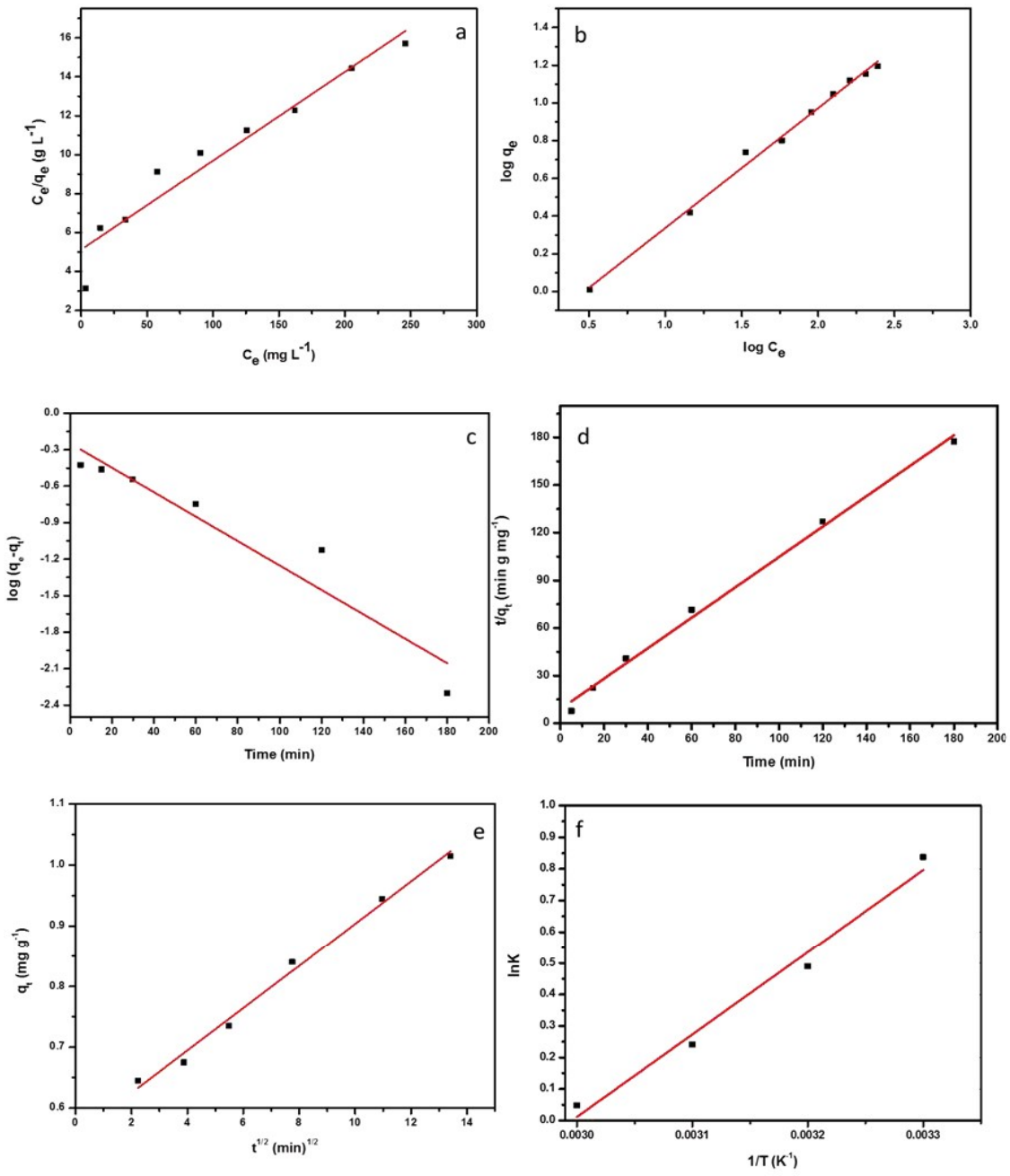


**Figure 6.18.** (a) Langmuir isotherm (b) Freundlich isotherm (c) Plot of psuedo first order kinetics(d)Plot of Pseudo second order kinetics (e) intra particle diffusion (f) Van't Hoff plot.(conditions: pH-2.0, adsorbent dosage- 0.2 g/30 mL)

**Table 6.6** Isotherm parameters involved in the biosorption mechanism

| Langmuir $\frac{C_e}{q_e} = \frac{1}{q_o b} + \frac{C_e}{q_o}$ | $q_o$(mg $g^{-1}$) | b(L $mg^{-1}$) | $R^2$ | $\chi^2$ | $R_L$ |
|---|---|---|---|---|---|
| | 22.22 | 0.0087 | 0.9315 | 0.0685 | 0.9199 |
| Freundlich $\log q_e = logK_F - \frac{1}{n} logC_e$ | $K_F$($mg^{1-1/n}L^{1/n}$) | n | $R^2$ | $\chi^2$ | |
| | 0.5058 | 1.5755 | 0.9935 | 0.0386 | |

**Table 6.7** Biosorption kinetics

| $C_o$(mg $L^{-1}$) | $q_e$ (mg $g^{-1}$) | $k_2$ (g $mg^{-1}$ $min^{-1}$) | $R^2$ | $k_1$ ($min^{-1}$) | $R_1^2$ | $k_{int}$ (mg $g^{-1}min^{-0.5}$) |
|---|---|---|---|---|---|---|
| 10 | 1.0446 | 0.0584 | 0.9943 | 0.0231 | 0.9031 | 0.034 |

**Table 6.8** Biosorption thermodynamics

| Temperature (Kelvin) | $\Delta G^0$ (kJ $mol^{-1}$) | $\Delta S^o$(J $mol^{-1}K^{-1}$) | $\Delta H^o$(kJ $mol^{-1}$) |
|---|---|---|---|
| 303 | -2.11 | -65.202 | -21.765 |
| 313 | -1.273 | | |
| 323 | -0.646 | | |
| 303 | -2.11 | | |

**(iv) Column studies**

**Effect of sample volume**

A higher volume of metal ion solution was tested with the developed biosorbent by performing small scale column studies. A 2.0 g of biosorbent was packed in a glass column of 30 cm length and 2 cm width up to a bed height of 3 cm.(Fig 6.19 a) A 50 mL volume of 5 mg $L^{-1}$ Cr(VI) was passed through the column and assessed periodically (10 mL portions) for the presence of Cr(VI) using UV visible spectrophotometry with diphenyl carbazide as the complexing agent.[12] A breakthrough volume was determined to be 150 mL and a sample volume of 150 mL could be treated quantitatively beyond which the saturation of active adsorption sites which decreased the metal ion adsorption.[33] (Fig 6.19c) At higher volumes, the swelling of clay results in expansion of the bed and reduces the adsorption efficiency.

**Regeneration of the Clay-Rhizobium biosorbent and application studies**

The reusability of clay-rhizobium biosorbent was tested using desorbing agents that were selected carefully not to inflict any damage to the biosorbent surface. The Cr(VI) adsorbed onto the biosorbent surface was eluted as sodium chromate using 10 mL of 1.5 mol $L^{-1}$ NaOH [34] (Fig 6.19d). Quantitative adsorption of chromium was achieved in the first two cycles and in the third cycle the adsorption was 78%, followed by 62% and 46% in the fourth and fifth cycles

respectively (Fig 6.19e). The eluted Cr(VI) was converted to Cr(III) (less toxic) and diluted to ppb levels to minimize direct disposal of higher levels of hexavalent chromium.

The effects of diverse ionic constituents were studied independently as well as in a mixture in the concentration range as reported earlier. [34] Accordingly, the interference studies were performed by preparing a synthetic mixture containing ions such as $Cu^{+2}$, $Pb^{+2}$, $Co^{+2}$, $Ni^{+2}$, $Fe^{+2}$, nitrate, chloride and sulphate at 100 mg $L^{-1}$ level using 5 mg $L^{-1}$ Cr(VI) solution. Due to the interference of sulphate and $Fe^{+2}$, reduction in Cr(VI) adsorption was observed and the formation of stable metal chloro complexes [$CoCl_4^{2-}$, $NiCl_4^{2-}$] also compete with hydrochromate ions thereby lowering the percentage adsorption of hexavalent chromium from aqueous phase.[34]

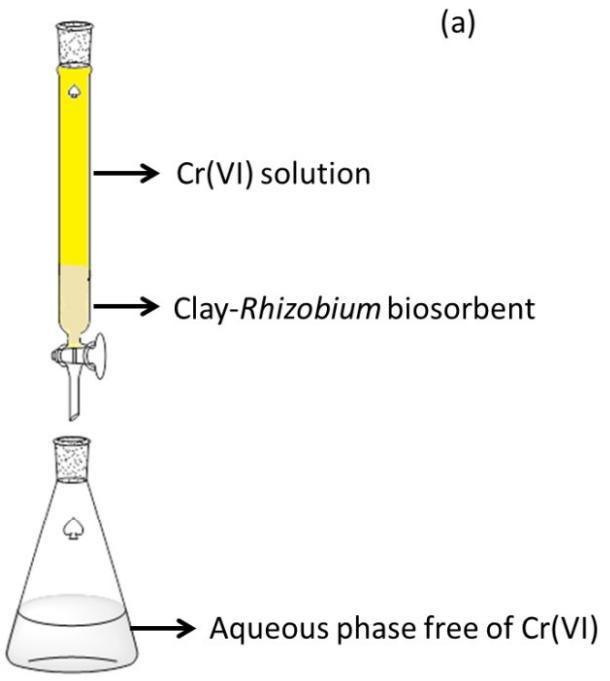

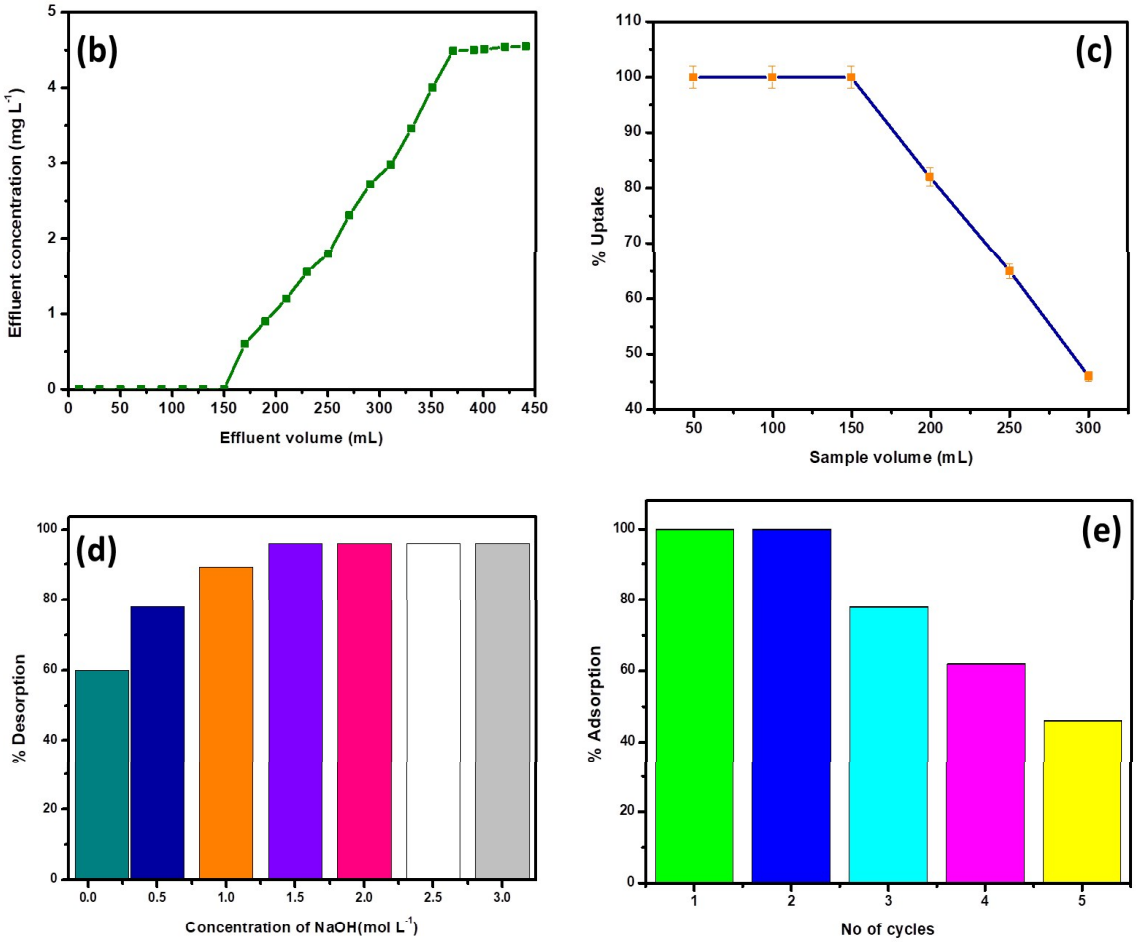


**Figure 6.19.** (a) Diagrammatic representation of Column setup for Cr(VI) treatment (b) Breakthrough curve (c) Effect of sample volume (conditions: pH-2.0, adsorbent dosage- 2.0 g , flow rate- 5 mL/min) (d) Effect of varied NaOH concentrations (e) Regeneration efficiency

### 6.2.4. Conclusions

The developed clay-*Rhizobium* biosorbent is environmental friendly and showed good efficacy in adsorbing Cr(VI) liquid phase. The adsorption followed pseudo second order kinetics and equilibrium is attained in 180 min with a Langmuir adsorption capacity of 22.22 mg $g^{-1}$. Protonated surface functional groups on the rhizobium cell surface and montmorillonite, promotes effective interaction with the hydrochromate ions from liquid phase. The thermodynamics of adsorption was observed to be less random, exothermic, and spontaneous with negative entropy ($\Delta S^o$ = -65.202 J $mol^{-1}K^{-1}$), enthalpy ($\Delta H^o$ = -21.705 kJ $mol^{-1}$ ) and free energy changes. The presence of Cr(VI) and trace Cr(III) were confirmed by XPS and confocal microscopy though Cr(VI) reduction is not instantaneous. The regeneration of the biosorbent using NaOH was effective up to two cycles from a sample volume of 150 mL was also validated in a synthetic mixture of diverse ions at 100 mg $L^{-1}$ concentration.

**References**


1. Sivakumaran, S.; Lockhart, P.J.; Jarvis, B.D.; .*Can. J.Microbiol.* **1997**, 43, 164-77.
2. Ehteshamul-haque, S.; Ghaffar, A., *J. Phytopathology*. **1993**, 138**,** 157—163.
3. Rebah F.B.; Prévost D.; Yezza, A;. Tyagi, R.D. *Bioresour Technol*. **2007,** 98, 3535-46.
4. Dodson, J.R.; Parker, H.L.; García, A.M.; Hicken, A.; Asemave, K.; Farmer, T.J.; He, H.; Clark, J.H.; Hunt, A.J, *Green Chem.* **2015,** 17, 1951-1965.
5. Lua, W.; Lia, J.; Sheng, Y.; Zhang, X.; You, J.; Chen, L. *J Colloid Interface Sci*. **2017**, 505, 1134-1146 .
6. Masheane, M.L.; Nthunya, L.N.; Malinga, S.P.; Nxumalo, E.N.; Mamba, B.B.; Mhlanga, S.D. *Sep. Purif. Technol.* **2017**, 184, 79-87.
7. Salam, M.A., *J. Mol. Liq* .**2017**, 233**,** 197-202.
8. Yan, F.F.; Wu, C.; Cheng, Y.Y.; He, Y.R.; Li , W.W.; Yu, H.Q..*Biochem. Eng. J.* **2013**, 77, 183– 189.
9. Tuzen, M.; Saygi, K,O.; Usta, B.; Soylak, M, *Bioresour Technol*. **2008**, 99, 1563–1570.
10. Loiret, F.G.; Ortega, G.; Kleiner, D.; Rodes, P.O.; Rodes, R.; Dong, Z. *J.Appl.Microbiol*. **2004**, 97, 504-511.
11. Chen, W.P.; Kuo, T.T. *Nucleic Acids Res*. **1993**, 21, 2260.
12. Sambrook, J. Russel, D.W. (Eds.). Molecular cloning- A laboratory manual. Cold Spring Harbor Laboratory Press, Cold Spring Harbor, 2001.
13. Tamas, E.; Mara, E.; Laslo, E.; Gyorgy, E.; Mathe, I.; Abraham, B;. Lanyi, S. *U.P.B. Sci. Bull.* **2010**, 72, 137-144.
14. Rincon, A.; Arenal, F.; González, I.; Manrique, E.; Lucas, M.M.; Pueyo, J.J. *Microb. Ecol.* 2008, 56, 223-233.
15. Parlayici, S.; Eskizeybek, V.; Avcı, A.; Pehlivan, E. *J Nanostruct Chem*. **2015,** 5, 255-263.
16. Sheehan, J.C.; Cruickshank, P.A.; Boshart, G.L. *J. Org. Chem*. **1961**, 26, 2525-2528.
17. Xiang, Y.; Mei, L.; Li, N.; Tong, A. *Anal. Chim. Acta*. **2007**, 581, 132–136.
18. Zhou, Y.; Zhang, J.; Zhang, L.; Zhang, Q.; Ma, T.; Niu, J. *Dyes. Pigm*. **2013**, 97, 148-154.

19. Kumar, A.S.K.; Jiang, S.J.; Tseng, W.L. *J. Mater. Chem. A.* **2015**, 3, 7044-7057.
20. Naumann, D. Infra-red spectroscopy in microbiology, Encyclopedia of Analytical Chemistry (ed. R. A. Meyers) 102–131.( John Wiley and Sons Ltd,2000).
21. Zhao, J.; Wang, J., *J. Phys. Chem. B.* **2015**, 119, 14831–14839.
22. Kumar, A.S.K.; Jiang, S.J.; Warcho, J.K. *ACS Omega.* **2017**, 2, 6187−6200.
23. Sathvika, T.; Manasi; Rajesh,V.; Rajesh, N. *Chem.Eng.J*. **2015**, 279, 38-46.
24. Zheng, W.; An, Q.; Lei, Z.; Xiao, Z.; Zhai, S.; Liu Q. *RSC Adv.* **2016,** 6**,** 104897-104910.
25. Reigh, G. & Connell, M. O. *J Bacteriol.* **1993,** 175, 94-102.
26. Bae, Y.S.; Yazaydın, A.O.; Snurr, R.Q. *Langmuir*, **2010**, 26, 5475–5483.
27. Yadav, S.K.; Mahapatra, S.S.; Yadav, M.K.; Dutta, P.K. *RSC Adv.* **2013,** 3**,** 23631-23637.
28. Anslyn. E.V.; Dougherty, D.A. Modern Physical Organic Chemistry, University Science Books, 603-604, (2005).
29. Lagergren, S. *K. Sven. Vetenskapsakad. Handl*. **1898**, 24, 1–39.
30. Ho, Y.S;. Mckay,G., *Water Res*. **2000**, 34, 735–742.
31. Fierro, V.; Torne-Fernandez, T.; Montane, D.; Celzard, A.; *Mesoporous Mater.* **2008**, 111, 276–284.
32. Sun, L.; Zhang, Y.; Ye, X.; Liu, H.; Zhang, H.; Wu, A.; Wu, Z., *ACS Sustainable Chem. Eng.*, **2017**, 5, 7700–7708.
33. Hasan, S.H.; Ranjan, D.; Talat, M.; *J. Hazard. Mater*. **2010**, 181,1134–1142.
34. Kumar, A.S.K.; Kalidhasan, S.; Rajesh, V.; Rajesh, N. *Ind.Eng. Chem. Res*. **2012**, 51, 58–69.
35. Zhao, Y.G.; Shen, H.Y.; Pan,S.H.; Hu,M.Q.; Xia,Q.H.; *J. Mater. Sci*. **2010**, *45*, 5291-5301.
36. Huang,Z.N.;Wanga,X.L.; Yanga, D.S.; *Water Science and Engineering***, 2015**, *8*, 226-232.
37. Dinda, D.; Gupta, A.; Saha, S.K.; *J. Mater. Chem. A*, **2013**,1, 11221-11228.
38. Dinker, M.K.; Kulkarni, P.S.; *New J. Chem.*, **2015**,39, 3687-3697.

39. Fang, J.;Gu,Z.;Gang,D.;Liu,C.;Ilton,E.S.;Deng,B; *Environ. Sci. Technol*. **2007**,41, 4748–4753.

40. Raaman,N.; Mahendran, B.; Jaganathan,C.; Sukumar, S.; Chandrasekaran,V.; *World. J.Microbiol.Biotechnol*. **2012**, 28, 627–636.

41. Sathvika, T.; Manasi ;Rajesh,V.; Rajesh, N.; *RSC Adv*., **2015**, 5, 107031-107044.

42. Sathvika, T.; Manasi ;Rajesh,V.; Rajesh, N.; *J. Environ. Chem. Eng*. **2016**, 4, 3193–3204.

43. Park,D.; Yun, Y.S.;Jo,J.H.;Park,J.M.; *Water Res*. **2005**, 39, 533–540.

44. Raylor,R.W.; Shen, J.S.; Bleam, W.F.; Shu-i tu ; *Clays. Clay. Miner*. **2000**, 48, 648–654.

45. Dong, H.; Elements, **2012**, 8, 113–118.

46. Boufait, M.; Amar, H.A.; *Desalination*, **2007**, 206, 300–310.

47. Ramsey,J.D.; McCreery,R.L.; *J. Electrochem. Soc*. **1999**, 146. 4076−4081.

48. Yu, B.; Xu, J.; Liu, J.-H.; Yang, S..T.; Luo, J.; Zhou, Q.; Wan, J.;Liao, R.; Wang, H.; Liu, Y., *J. Environ. Chem. Eng*. **2013**, 1,1044−1050.

49. Ho,Y.S.; *Carbon*. **2004**, 42, 2115–2116.

50. Sun,C.; Sun, L.;Sun,X.; *Ind. Eng. Chem. Res*. **2013**, 52, 14251–14260.

# Chapter – 7

## A co-operative endeavor by nitrifying bacteria, *Nitrosomonas* and Zirconium based Metal Organic Framework to remove hexavalent chromium

# A co-operative endeavor by nitrifying bacteria, *Nitrosomonas* and zirconium based metal organic framework to remove hexavalent chromium

## 7.1. Introduction

This chapter deals with the synthesis of *Nitrosomonas* modified metal organic framework (MOF). *Nitrosomonas* is a rod shaped gram negative chemolithotroph which derives its energy by converting ammonia to nitrite which is further transformed to nitrate by nitrite oxidizing bacteria known as nitrification.[1] *Nitrosomonas*, has potential applications in biotechnology such as bioremediation and degradation of halogenated aliphatic hydrocarbons and aromatic compounds.[2] The zirconium based MOFs are used widely in several potential applications in gas storage, drug delivery, sensing, catalysis, ion exchange, separation due to their tremendous aqueous, acid and thermal stabilities extremely high surface area, high porosity.[3,4] Uio-66 (University of Oslo) is a cubical framework $Zr_6O_4(OH)_4$ clusters and terephthalic acid ($H_2$bdc) as organic linker. [3] The remediation of Cr(VI) by MOFs reported in the recent times include using a composite of Uio-66 $NH_2$ and silica gel [5] and IL-MIL-100(Fe) is an ionic liquid and iron nano particle modified MOF developed by Nasrollahpur et al. could efficiently remediate Cr (VI). [6] However, there are no reports of microbe modified MOF synthesis and the current method developed elaborates the microwave assisted microbial-MOF synthesis and its application for the hexavalent chromium removal.

## 7. 2. Experimental section

### (i) Microwave synthesis of Uio-66

The Zirconium based metal organic framework was synthesized using microwave assisted method as reported in literature.[3] A 25mL volume of dimethylformamide solution taken in a beaker followed by the addition of a 1.0g of $ZrOCl_2$ (3.1mmol) , 0.515g of $H_2$bdc (3.1mmol), 6mL of acetic acid and 0.33mL of water and stirred for 15 min. The mixture was transferred to a 30mL glass vial and subjected to microwave irradiation in a microwave reactor at a temperature of 120$^oC$ with 15 min hold time. The solid was isolated from the mixture by centrifugation and soaked in DMF for 12 hours. Subsequently, the product was left in acetone for 24 hours and washed. The final product obtained was dried at 60$^oC$ and used for the adsorption of Cr(VI).

**(ii) Preparation of the biosorbent**

The *Nitrosomonas sp* was maintained in the following medium. A 1200 mL volume of distilled water was taken in a flask- I followed by the sequential addition of $(NH_4)_2\ SO_4$ (4.95 g), $KH_2PO_4$ (0.62 g), $MgSO_4\ .7H_2O$ (0.27 g), $CaCl_2.2H_2O$ (0.04g), $CuSO_4.5H_2O$ (0.2 mg) respectively. The solution was mixed thoroughly and autoclaved. $FeSO_4$ (0.5 mL, 30 mM in 50 mM EDTA at pH 7.0) was filter sterilized separately and added to the above mixture. In another conical flask (II) $KH_2PO_4$ (8.2 g) and $NaH_2PO_4$ (0.7 g) was dissolved in 300 mL autoclaved water and filter sterilized. The conical flask (III) medium consists of 0.6 g sodium carbonate dissolved in 12 mL of autoclaved water and filter sterilized. The contents of the three conical flasks were combined and divided into required aliquots for culturing the bacteria. The culture medium was incubated at 26$^oC$ in dark and bacterial growth was observed after 6-7 days [7] and the medium was centrifuged to obtain the bacterial pellet. A 1 g weight of the bacterial pellet was added to the reagents used in Uio-66 preparation, stirred for 15 min and synthesized using microwave irradiation as explained in the earlier section. The combinations of *Nitrosomonas* based biosorbents such as *Nitrosomonas*-cellulose, *Nitrosomonas*-clay, *Nitrosomona*s-MWCNTs were also prepared to compare the removal efficiency of hexavalent chromium. The above mentioned combinations were developed based on the method reported previously. [8,9]

**(iii) Adsorption studies**

The various parameters such as pH, adsorbent dosage, kinetics, isotherms and thermodynamics were optimized using batch adsorption studies. A 10 mL of 5 mg $L^{-1}$ of Cr(VI) solution was added to 0.1 g of the biosorbent and the pH of the medium was adjusted to 4.0. The homogenous mixing was performed in an orbital incubator shaker, for 180 min at a temperature of 30$^oC$ at a speed of 120 rpm. The chromium concentration in the aqueous phase was obtained using Ion chromatography [10] with the post column derivatization method using a UV-Vis detector at 540 nm. The mobile phase used was sodium carbonate and the post column reagent was prepared by dissolving diphenylcarbazide in methanol and sulphuric acid.

## 7. 3 Results and Discussion

### (i) Analytical Characterization of the biosorbent

The phase purity and crystallinity of the adsorbent material was established through the powder XRD patterns. The 2θ values of the high intensity peak for as synthesized Uio-66 and bacterial modified MOF (BMOF) were found to be 7.409$^{o}$ and 7.493$^{o}$ respectively. The nano crystallite size was calculated using the Debye-Scherrer formula $D_P = \frac{(0.94\ X\ \lambda)}{(\beta\ X\ Cos\theta)}$ where $D_p$ is the average crystallite size, λ is the wavelength, β is the line broadening at half maxima (FWHM), θ is Bragg's angle. The average crystallite sizes were found to be 33.9 nm for Uio-66 and 23.92 nm for BMOF and as shown in Fig 7.1a the purity of the as synthesized Uio-66 was in correlation with the simulated MOF. ,[11] The FTIR spectra (Fig.7.1b) of the as synthesized Uio-66 and the biosorbent before and after adsorption were recorded. The peak at 3399 cm$^{-1}$ in the biosorbent could be attributed to amine and hydroxyl groups from the microbe cell surface. The peak at 934 cm$^{-1}$ could be indexed to Cr=O bond indicating chromium adsorption onto the biosorbent surface. The peaks at 1578, 1392 cm$^{-1}$ indicate the presence of carboxylate ligand of MOF. The peaks 661 cm$^{-1}$ , 552 cm$^{-1}$ and 487 cm$^{-1}$ correspond to the stretching bands of Zr-$O_2$ and Zr-O, respectively. [12] Thermal stability of the MOF was ascertained through thermogravimetric analysis (TGA) as depicted in Fig 7.1c. The initial weight loss between 30$^{o}$C and 140$^{o}$C is attributed to the removal of moisture, carbon dioxide and trapped molecules of DMF in the MOF framework and the dehydroxylation process of Zr clusters occurred below 400$^{o}$C. The decomposition of organic linker was observed around 450$^{o}$C-600$^{o}$C. [3,12] The complexing agent diphenylcarbazide when added to the biosorbent after metal adsorption turned purple indicating the presence of Cr(VI) which was identified through the optical microscopy images (Fig 7.2).

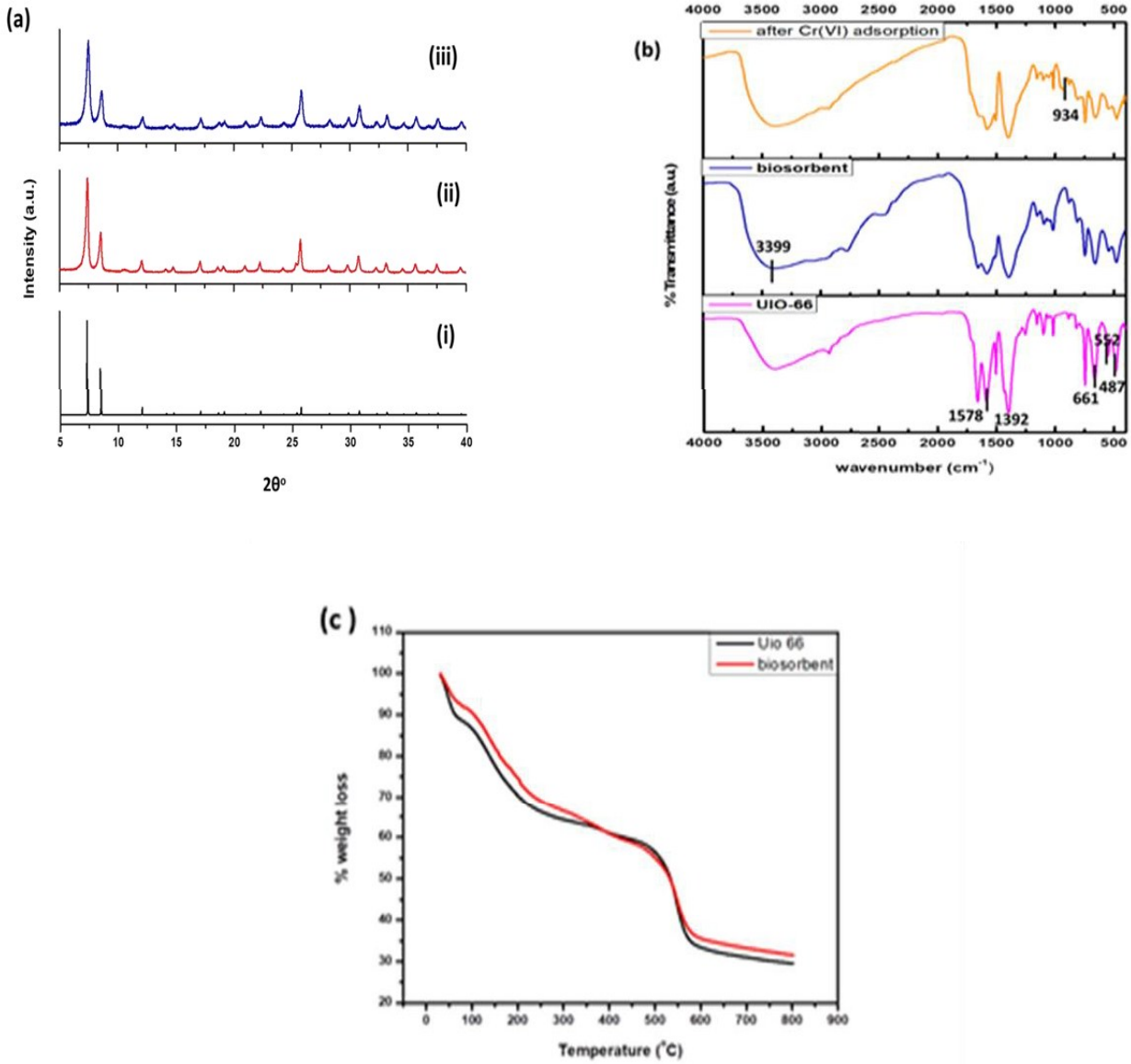


**Figure 7.1.** PXRD patterns of (a) (i) simulated Uio-66 (ii) as synthesized Uio-66 (iii) microbial modified Uio-66 (b) FTIR of Uio-66, BMOF and BMOF after Cr(VI) adsorption (c) TGA of the adsorbents.

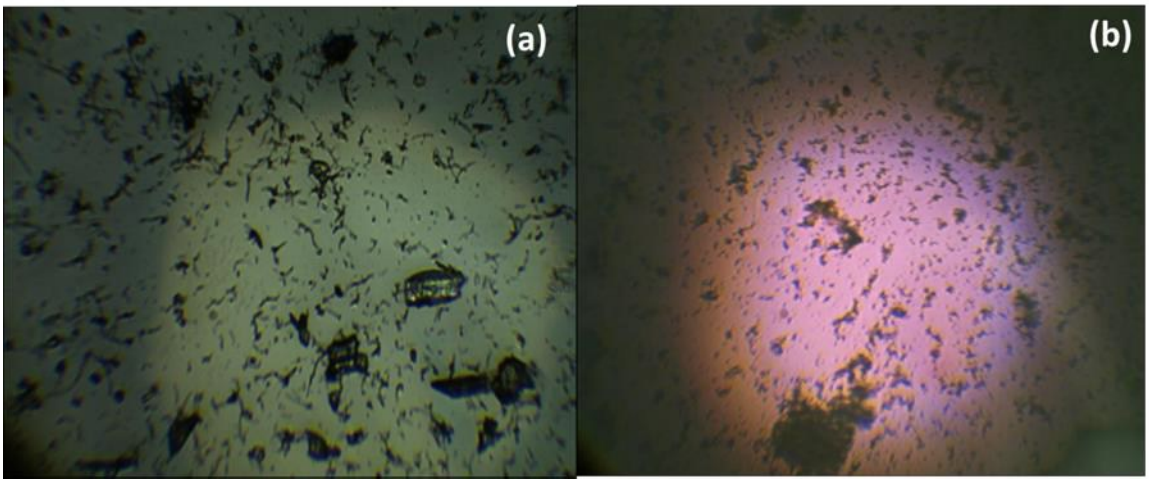


**Figure 7.2.** Optical images of the biosorbent before and after Cr(VI) adsorption under 20X objective.

The morphological characteristics of the adsorbent was obtained through the surface characterization such as FESEM and HRTEM techniques (Fig 7.3 and 7.4). The material synthesized was observed to be porous and the similar morphologies for MOF and BMOF indicate the structural features are not destroyed after microbe modification. The average particle size from the particle distribution curves of Zr-MOF and BMOF were found to be 54 nm and 39 nm as measured from the HRTEM images (Fig 7.4). The elemental mapping done using EDAX spectral analysis indicated the presence of Zr, Cl, C, O, N and Cr on the biosorbent surface (Fig 7.3). The XPS study reveals the oxidation state of chromium present on the biosorbent surface. The Fig 7.5a shows the survey scan spectra of the biosorbent after chromium adsorption and Fig 7.5b shows the high resolution spectra of chromium. The Cr 2p3/2 peak at 577 eV corresponds to Cr(III) and peak at 580 eV corresponds to Cr(VI) whereas the Cr2p1/2 peak at 587 nm is attributed to Cr(VI). The immediate reduction of Cr(VI) was not observed and the prolonged contact of the Cr(VI) with carbon in the biosorbent showed a pale green appearance on the surface indicating the presence of Cr(III). [8,11] The BET surface area and porosity were calculated using $N_2$ adsorption-desorption isotherms. The isotherms (Fig 7.6) obtained belongs to type IV isotherm [13] and the surface area of the as synthesized MOF was found to be 1232 $m^2 g^{-1}$ with a pore volume and pore diameter of 1.23 $cm^3 g^{-1}$ and 4.0052 nm respectively. The surface area of the bacteria modified MOF was found to be 921 $m^2 g^{-1}$ with a pore volume of 0.849 $cm^3 g^{-1}$. The

mean pore diameter of 3.6898 nm obtained from Barrett-Joyner-Halenda (BJH) plots (Fig 7.6) indicate the mesoporous nature of the adsorbent.

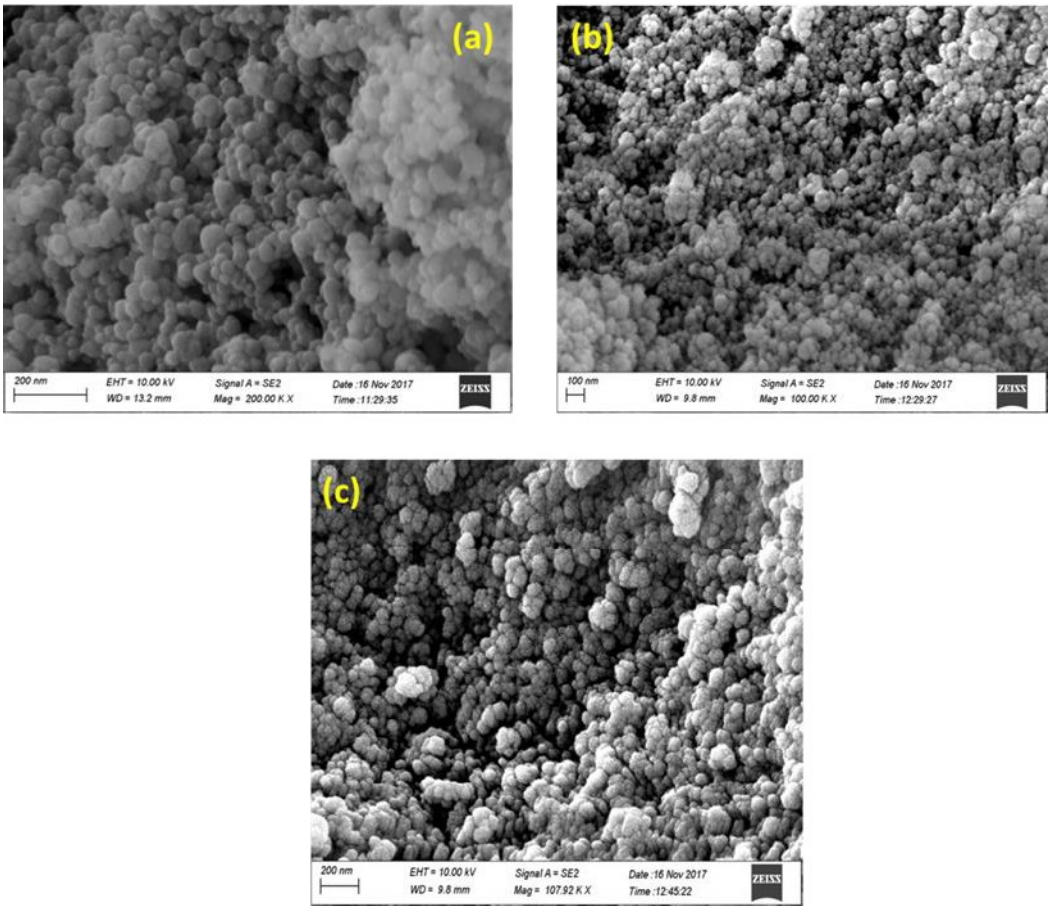

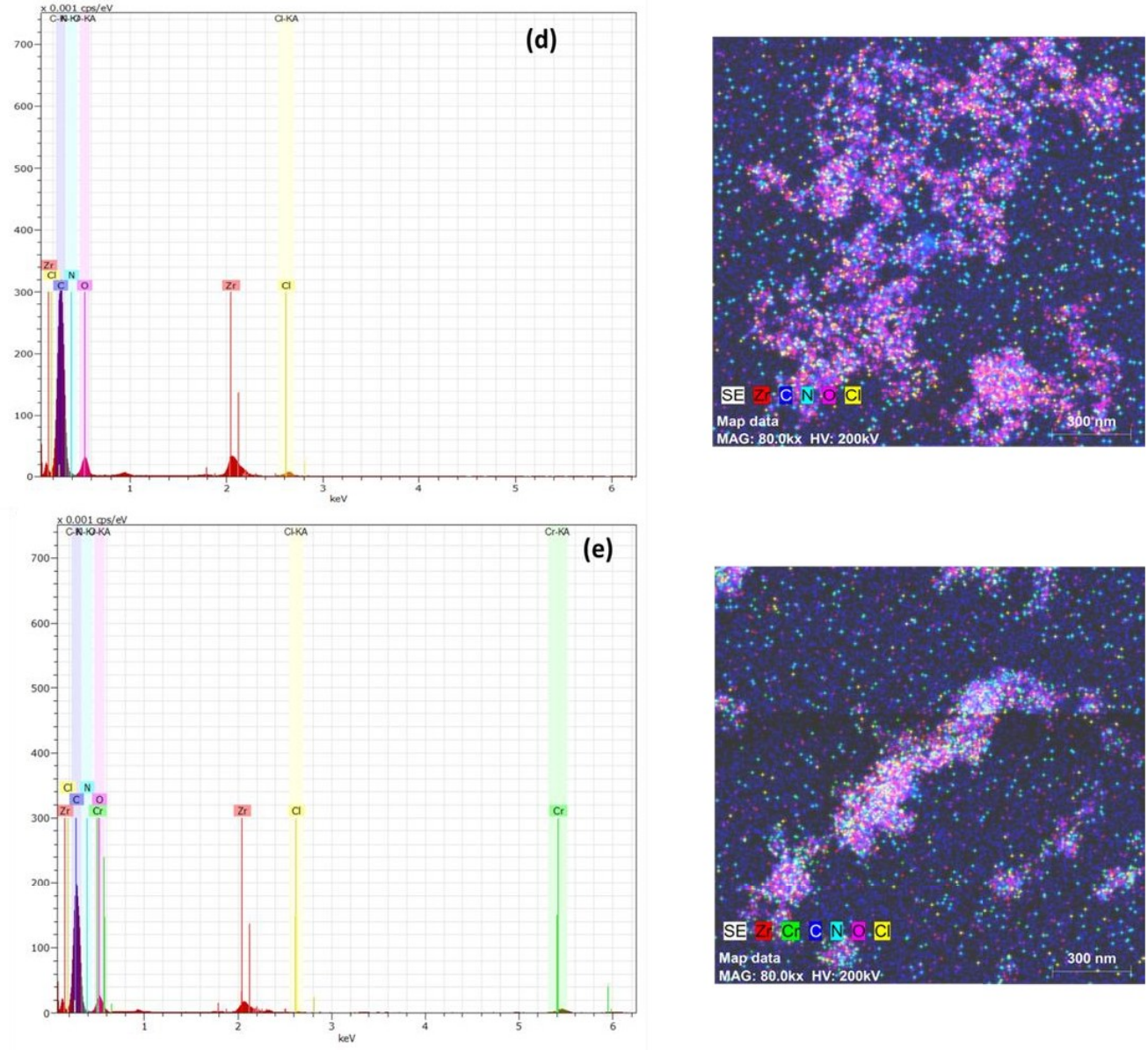


**Fig 7.3.** FESEM images of (a) as synthesized Uio-66 (b) BMOF (c) BMOF after Cr(VI) adsorption. EDAX spectra and elemental mapping of (d) the biosorbent before adsorption (e) biosorbent after Cr(VI) adsorption.

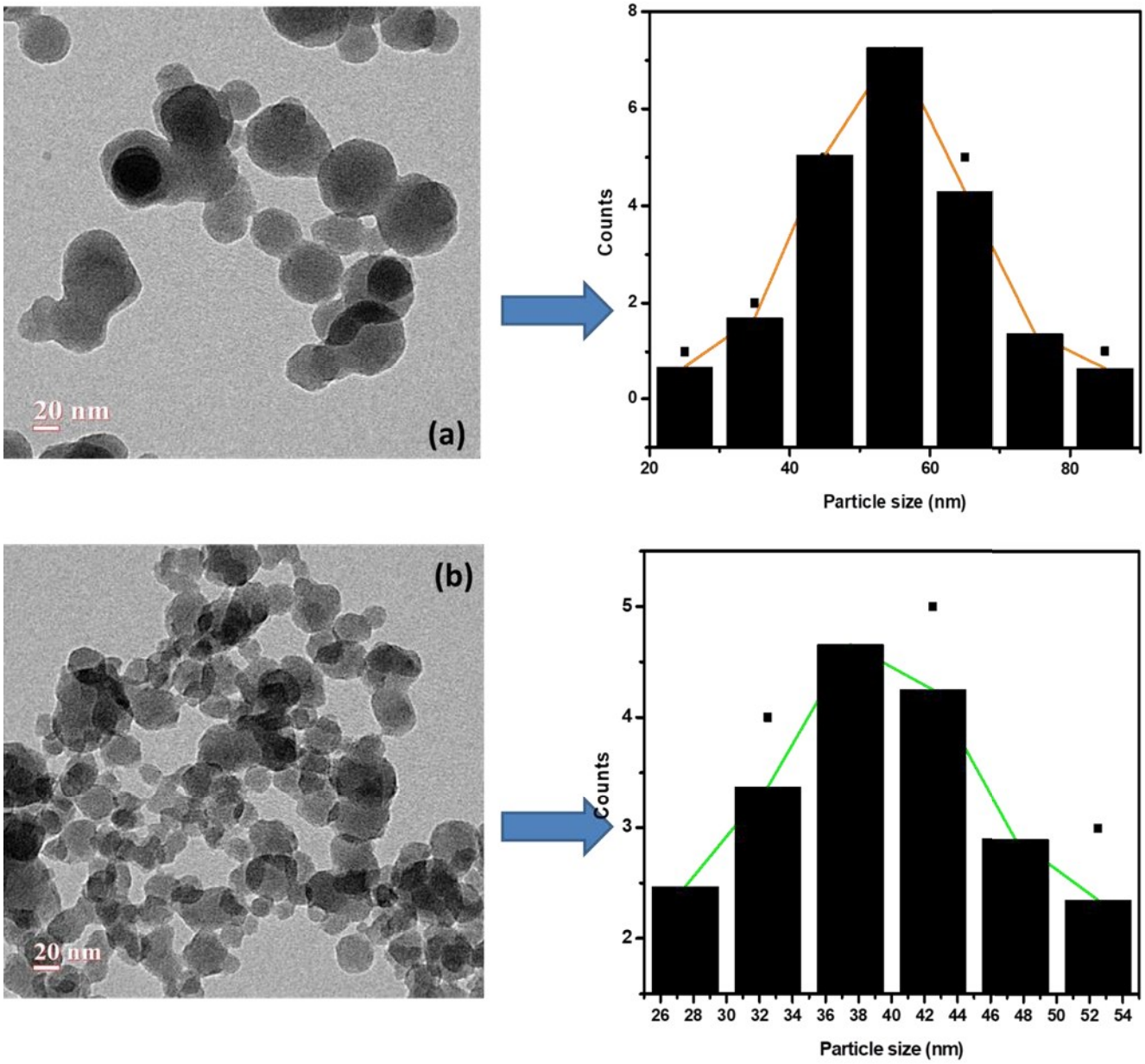


**Figure 7.4.** HRTEM images and particle size distribution curves of (a) as synthesized Uio-66 (b) microbial modified Uio-66

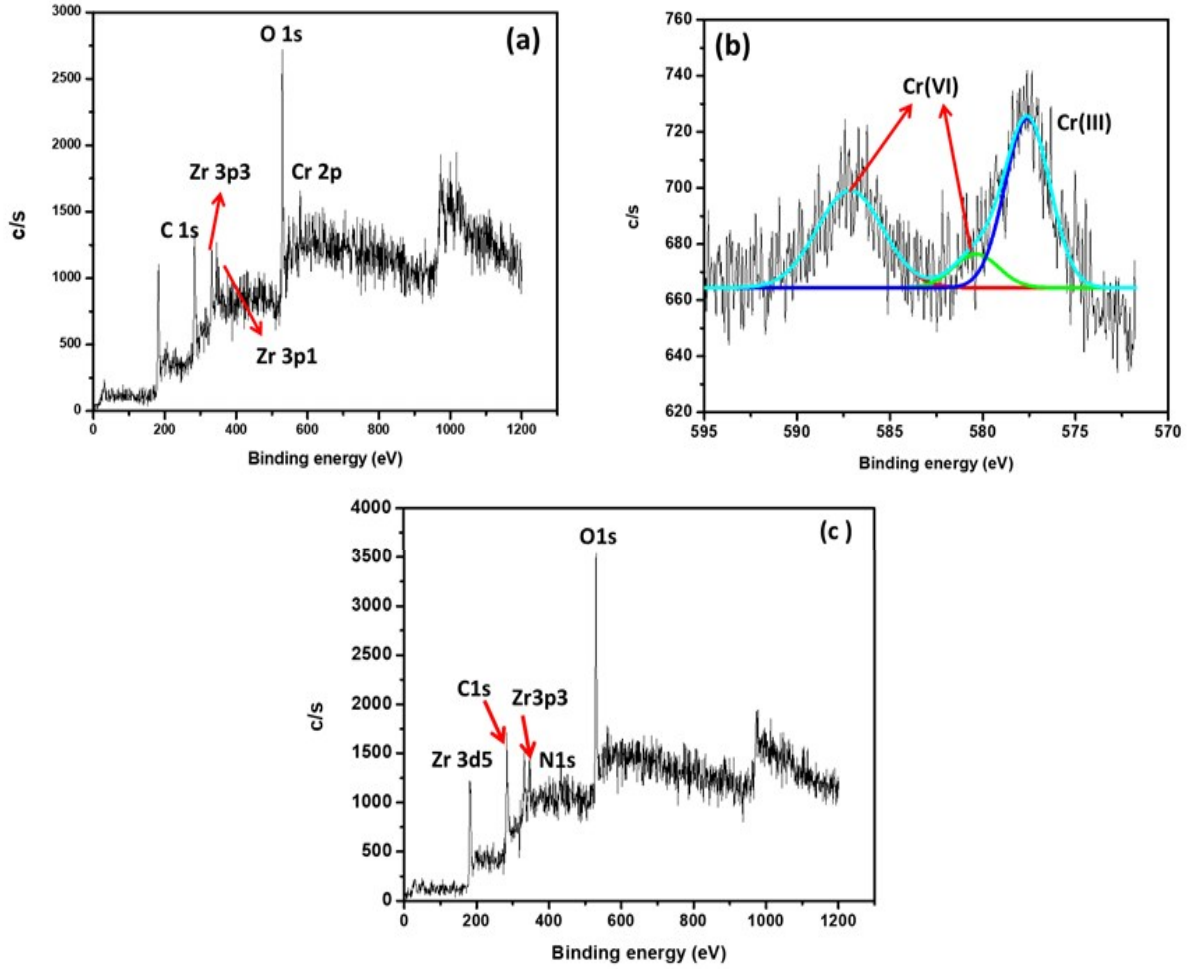


**Figure 7.5.** XPS spectra of (a) survey scan of the biosorbent (b) high resolution scan of chromium

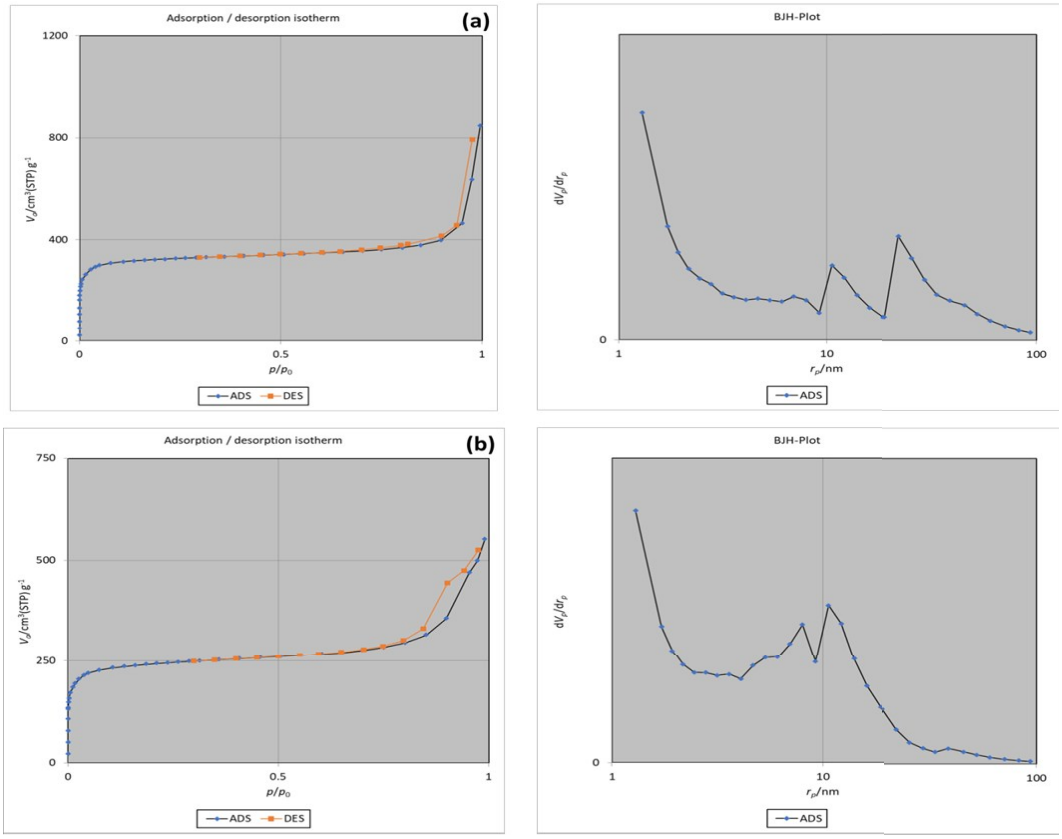


**Figure 7.6.** BET and BJH measurements for (a) as synthesized Uio-66 (b) the biosorbent

**(ii) Interaction mechanisms in biosorption**

The biosorption of metal ion is majorly influenced by pH and the isoelectric charge on the surface of the biosorbent. where the biosorbent surface becomes neutral. A 50 mL volume of 0.01 mol $L^{-1}$ NaCl was added to 0.15 g of the biosorbent and adjusted at various pH values ranging from 2.0-8.0 and allowed to homogenise for 24 hours in an orbital shaker at 28$^{o}$C. The final pH was measured after equilibration and a plot of initial pH against difference in initial and final pH (**Δ**pH) indicated that the surface of the biosorbent remains protonated at or below pH 4.0. (Fig 7.7a) The existence of varying ionic forms of hexavalent chromium is dependent on the pH of the medium. Hydrogen chromate ($HCrO_4^-$) and dichromate ($Cr_2O_7^{2-}$) exist in the pH range 2.0-4.0 whereas chromate ions ($CrO_4^{2-}$) predominate at higher pH values.[8] At pH 4.0, maximum adsorption (100%) of Cr(VI) was observed (Fig 7.7b) with a 10mL volume of 5 mg $L^{-1}$ Cr(VI) indicating the protonation of the functional groups such as amines, carboxyl and

hydroxyl groups present on the biosorbent surface and the electrostatic interactions with hydrogen chromate ions (Fig 7.8). At higher pH, decrease in the percentage adsorption was observed and this could be attributed to the deprotonation of functional groups on the surface of the biosorbent. The biosorbent surface provides sites for the metal ion to adsorb and hence adsorbent dosage is also a vital parameter in biosorption. Different weights of the biosorbent were taken ranging from 0.05 g to 0.6 g and the maximum adsorption occurred at 0.1 g beyond which the adsorption remained constant indicating the saturation of binding sites (Fig 7.7c).

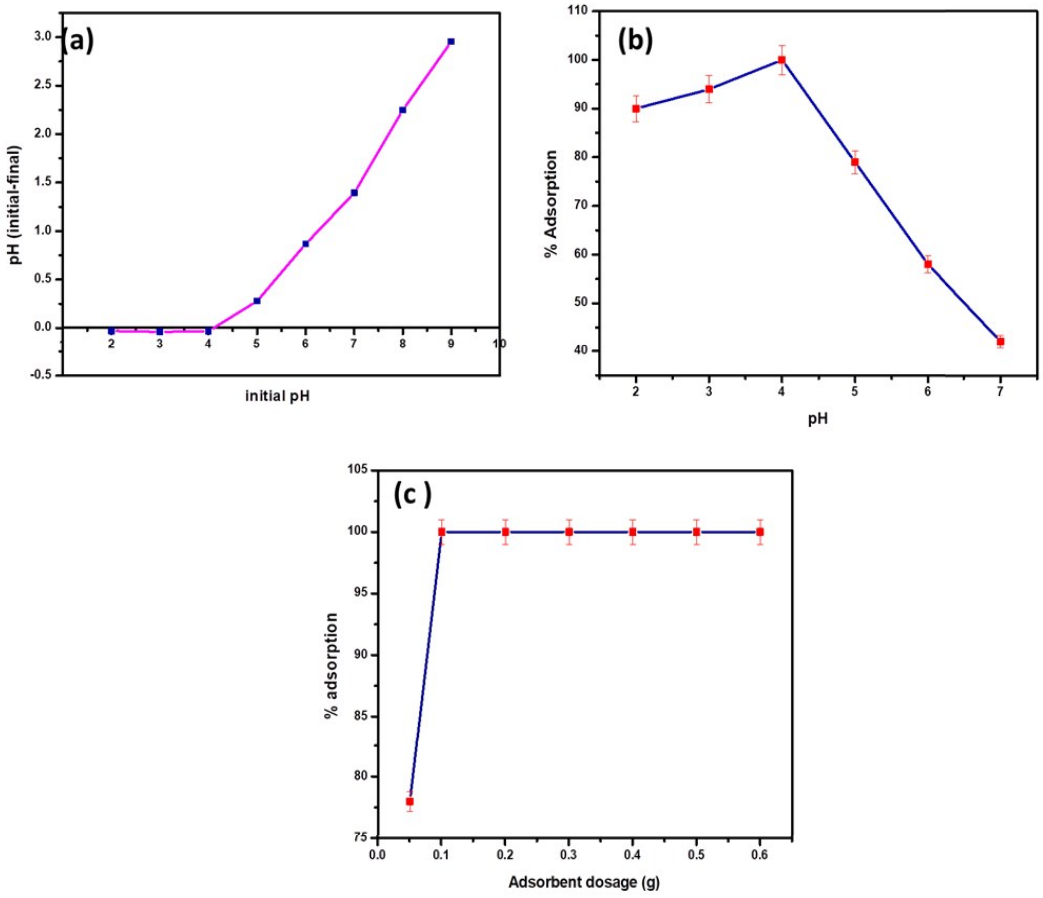


**Figure 7.7.** (a) Point of zero charge of the biosorbent for adsorption study (b) Effect of pH effect sorption (Conditions: weight of the adsorbent- 0.1 g, Cr(VI) concentration- 5 mg $L^{-1}$/10 mL) (c) Effect of adsorbent dosage (Conditions: pH-4.0, Cr(VI) concentration- 5 mg $L^{-1}$/10 mL)

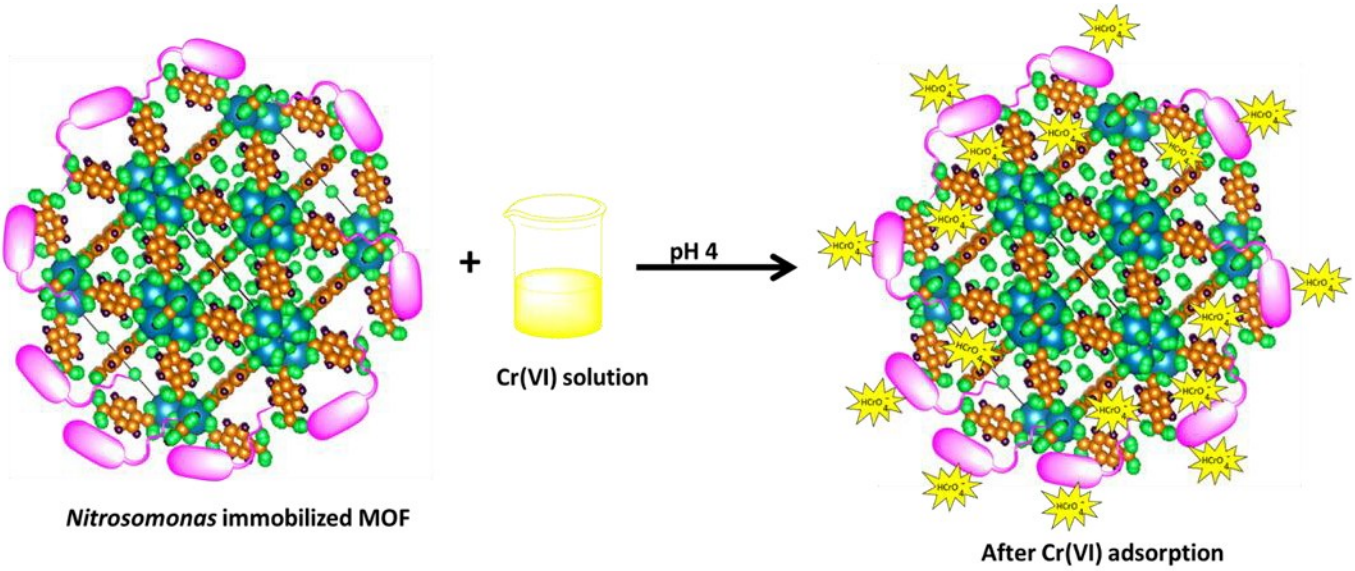


**Figure 7.8.** Illustration of plausible interaction mechanism of the biosorbent with Cr(VI) (pink rod shape represents microbe, Zr-blue, O-green, C-orange, H-violet, Cr(VI)- yellow)

**(iii) Equilibrium adsorption isotherms, kinetics and thermodynamic studies**

The mechanism of biosorption is well understood using isotherms that correlate the concentration of the metal ion in the liquid and solid phases at constant temperature. The most commonly used Langmuir and Freundlich [14] models were chosen for the isotherm studies (Fig 7.9a,b). The monolayer adsorption is well described by Langmuir model which is assumed to take place on homogenised biosorbent surface whereas the multilayer Freundlich model is on heterogeneous surface. From the data obtained (Table 7.1) it was observed that the biosorption follows Freundlich model with a high $R^2$ value of 0.925 and low $\chi^2$ value (0.131) and furthermore the sorption intensity (n) also is in the interval 1-10 indicating the suitability of the adsorption model. The *Nitrosomonas sp* as such has a Langmuir capacity of 8.98 mg $g^{-1}$ whereas as synthesized Uio-66 MOF has an adsorption capacity of 13.33 mg $g^{-1}$. The microbe modified MOF has a Langmuir adsorption capacity of 23.69 mg $g^{-1}$ with a low $R^2$ value of 0.87 and high $\chi^2$ value (0.262). The suitability and reversibility of the adsorption was verified by the dimensionless constant $R_L$ which lies below unity. [15] The adsorption capacity was compared against other matrices such as cellulose, clay and multiwalled carbon nanotubes. It was found

that the *Nitosomonas*-MOF combination could remove Cr(VI) with a higher adsorption capacity as compared to the other matrices (Table 7.2) .

**Table 7.1** Isotherm parameters for Cr(VI) adsorption

| **Langmuir** $\frac{C_e}{q_e} = \frac{1}{q_o b} + \frac{C_e}{q_o}$ | **$q_o$(mg $g^{-1}$)** | **b ($mg^{-1}$ L)** | **$R^2$** | **$\chi^2$** | **$R_L$** |
|---|---|---|---|---|---|
| | 23.69 | 0.0113 | 0.877 | 0.262 | 0.898 |
| **Freundlich** $\log q_e = \log K_F - \frac{1}{n} \log C_e$ | **$K_F$($mg^{1-1/n} g^{-1} L^{1/n}$)** | **n** | **$R^2$** | **$\chi^2$** | |
| | 1.166 | 2.136 | 0.9254 | 0.131 | |

**Table 7.2** Isotherm parameters for Cr(VI) adsorption

| **Developed adsorbents** | **pH** | **Langmuir adsorption capacities (mg $g^{-1}$)** |
|---|---|---|
| *Nitrosomonas*-Cellulose biosorbent | 3.0 | 17.3 |
| *Nitrosomonas*-Clay biosorbent | 2.0 | 20.5 |
| *Nitrosomonas*-CNTs biosorbent | 2.0 | 22.26 |
| Only *Nitrosomonas* | 4.0 | 8.98 |
| Only Uio-66 | 4.0 | 13.33 |
| *Nitrosomonas*-MOF biosorbent | 4.0 | 23.67 |

The kinetic models such as pseudo first order,[16] pseudo second order, [17] and intra particle diffusion[18] were used to evaluate the biosorption kinetics. A 0.1 g weight of the biosorbent was mixed with 10 mL of 10 mg $L^{-1}$ Cr(VI) at different time intervals ranging from 5 min to 180 min. Initially, with fast adsorption of Cr(VI) adsorption percentage was around 60% in 5 min followed by mass transfer and later a slower intra particle diffusion. A 100% metal uptake was achieved at 180 min and the data obtained from the plots (Fig 7.9c,d ) are presented in Table 7.3 . The well-known diffusion kinetic mechanisms hypothesized are (i) external mass transfer involving the transfer of Cr(VI) ions on the MOF-bacteria biosorbent surface and (ii) intra particle diffusion . The system followed pseudo second order kinetics with a high $R^2$ value of 0.994. The experimental as well as calculated $q_e$ values were found to be as 0.818 mg $g^{-1}$ and 0.865 mg $g^{-1}$ respectively. The relation between $q_t$ and $\sqrt{t}$ (Fig. 7.9e) is given by the Weber-Morris intra particle diffusion model and the obtained plot with a finite intercept accounts for the the impact of boundary layer mechanism towards the effective Cr(VI) uptake.

**Table 7.3** The kinetic parameters for the adsorption of Cr(VI)

| $C_o$ (mg $L^{-1}$) | $q_e$ (mg $g^{-1}$) | $k_2$ (g $mg^{-1}$ $min^{-1}$) | $R^2$ | $k_1$ ($min^{-1}$) | $R_1^2$ | $k_{int}$ (mg $g^{-1}$ $min^{-0.5}$) |
|---|---|---|---|---|---|---|
| 10 | 0.865 | 0.075 | 0.994 | 0.2805 | 0.878 | 0.04 |

The spontaneity and energetics of the adsorption process ascertained was explained through thermodynamic parameters such as enthalpy (ΔH), entropy (ΔS) and Gibbs free energy (ΔG) changes. The enthalpy and the entropy values were obtained from the plot of lnK against 1/T (Fig 7.9 f) where K is the equilibrium constant obtained from the ratio of the concentration of Cr(VI) in the solid and liquid phases. The overall free energy depends on the free energy involving the interaction between the MOF- *Nitrosomonas* before and after adsorption. The Gibbs free energy change is explained as follows:

$$\Delta G_r = \Delta G_{\text{MOF-Nitrosomonas surface}} + \Delta G_{\text{MOF-Nitrosomonas-Cr}} \qquad (7.1)$$

The reaction Gibbs free energy is related to the enthalpy and entropy changes as

$$\Delta G_r = \Delta H_{MOF\text{-}Nitrosomonas\ –Cr} - T\Delta S_{MOF\text{-}Nitrosomonas\text{-}Cr} \quad (7.2)$$

At equilibrium,

$$MOF\text{-}Nitrosomonas\text{-}Cr_{(solution)} \rightleftharpoons MOF\text{-}Nitrosomonas\text{-}Cr_{(surface)} \quad (7.3)$$

$$\Delta G_r = \Delta G_r{}^0 + RT\ln \frac{a_{MOF-Nitrosomonas-Cr]surface}}{a_{cMOF-Nitrosomonas-Cr]\,solution}} \quad (7.4)$$

In dilute solution activity (a) is directly proportional to concentration (C) of the Cr (VI) ion

$$\text{Therefore,} \quad \Delta G_r = \Delta G_r{}^0 + RT\ln \frac{[MOF-Nitrosomonas-Cr]_{surface}}{[MOF-Nitrosomonas-Cr]_{solution}} \quad (7.5)$$

The parameters obtained are tabulated in Table 7.4 where the negative free energy indicates the spontaneous nature of biosorption mechanism while the negative enthalpy and activation energy ($E_a = \Delta H^o_{ads}+RT$) values indicate that the system follows exothermic adsorption. The negative entropy values reveal the decreased randomness at the MOF-bacteria-solution interphase. The magnitude of enthalpy change lies between physisorption and chemisorption values (20-80 kJ $mol^{-1}$ ) and hence the system follows physico-chemical adsorption process. [8,9] The enthalpy – entropy compensation points to the fact that the biosorption process is enthalpically driven rather than favourable entropy.

**Table 7.4** Temperature variation studies during biosorption

| T (kelvin) | $\Delta G^o$ (kJ $mol^{-1}$) | $\Delta S^o$ (J $mol^{-1}$ $K^{-1}$) | $\Delta H^o$ (kJ $mol^{-1}$) | $E_a$ (kJ $mol^{-1}$) |
|---|---|---|---|---|
| 303 | -3.78 | -118.23 | -39.707 | -37.06 |
| 313 | -2.92 | | | |
| 323 | -1.51 | | | |
| 333 | -0.27 | | | |

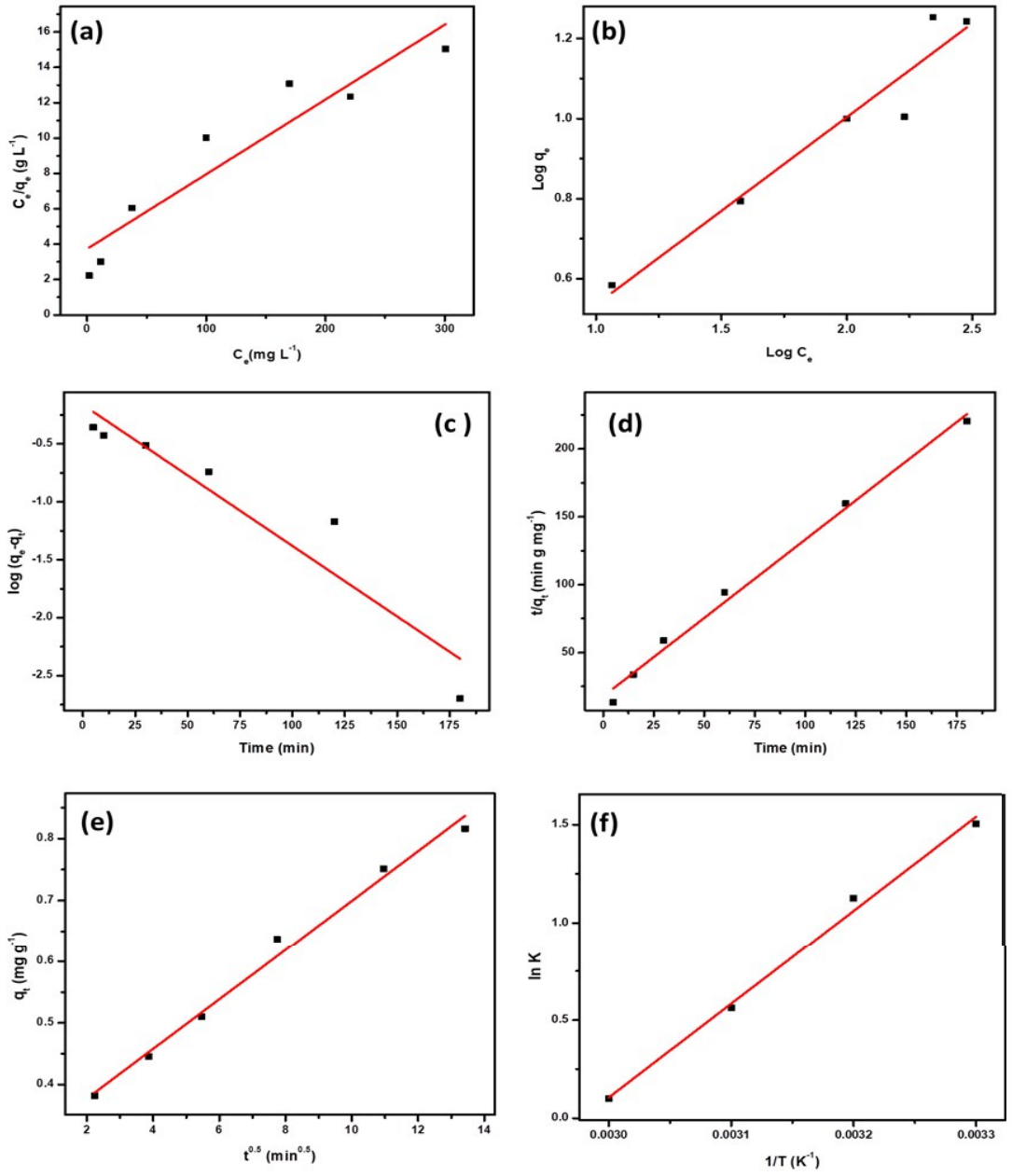


**Figure 7.9.** (a) Langmuir isotherm (b) Freundlich isotherm (c) Pseudo first order kinetics (d) Pseudo second order kinetics (e) Intra particular diffusion (f) lnK against 1/T (conditions: pH-4.0, adsorbent dosage- 0.1 g/10 mL)

**(iv) Lab scale column studies, Regeneration and Interference studies**

Column studies were performed using a glass column of dimensions 30 cm in length and 2 cm diameter. A 2.0 g weight of the biosorbent was prepared as a slurry in aqueous medium and packed in the column up to a bed height of 3 cm. A 50 mL volume of 5 mg $L^{-1}$ of Cr(VI) was loaded onto the column and checked intermittently (every 10 mL) for presence of Cr(VI) in the eluate. Another 50 mL volume of the metal ion solution was loaded on the column and the above procedure was repeated. A 200 mL volume of Cr(VI) was adsorbed effectively beyond which there was saturation of active adsorption sites (Fig 7.10a) on the biosorbent surface. [19]

The quality of an adsorbent is assessed through the regeneration capacity. The desorption of Cr(VI) is expected to be more facile under alkaline conditions. Accordingly, varying concentrations of NaOH (0.5-3.0 mol $L^{-1}$ ) were tried to desorb the chromium(VI) oxyanion. Quantitative desorption was achieved using 1.5 mol $L^{-1}$ NaOH (Fig 7.10b) as sodium chromate in the eluate. The percentage desorption decreased gradually to 76% and 56% after 4-5 cycles as shown in Fig 7.10c. The eluted Cr(VI) was converted to less toxic Cr(III) using suitable reducing agents to minimise the disposal of hexavalent chromium.

**(v) Application studies**

A synthetic waste water mixture was prepared by adding various cations ($Ni^{+2}$, $Mn^{+2}$, $Cu^{+2}$ , $Hg^{+2}$, $Fe^{+2}$, $Pb^{+2}$, $Co^{+2}$) and anions (chloride , nitrate, sulphate) at 100 mg $L^{-1}$ level to 5 mg $L^{-1}$ Cr(VI) solution. The interference of Mn(II) and Fe(II) was observed through the which caused the reduction of Cr(VI) and also the chloro complexes which are formed could compete with the hydrochromate ions affecting the adsorption efficiency. [20]

Certified reference material BCR-032, is a natural Moroccan phosphate rock that consists elements (mg $kg^{-1}$) such as As (9.5±0.5), Cd(20.8±0.7), B (22.6±2.2), Cr (257±16), Co (0.59±0.06), Hg (0.055±0.011), Cu (33.7±1.4), Ni (34.6±1.9), Mn (18.8±1.3), Ti (171±10),Ni (34.6±1.9), Zn (253±6) and V (153±7) respectively. A 1.0 g weight of the rock sample was digested using aqua regia for 10 min at 50$^{o}$C filtered and diluted to 100 mL. The total chromium concentration was verified through AAS at 357.8 nm. The total chromium was found to be 262

mg $kg^{-1}$ which was in close proximity with the Cr as certified in the rock sample. A 10 mL volume of the phosphate rock solution was taken and chromium was oxidised to Cr(VI) by adding NaOH and $H_2O_2$ . A 0.4 g of the BMOF biosorbent was added to 10 mL of phosphate rock solution and adjusted at pH 4.0 and agitated in an incubator shaker for 180 min. The Cr was absorbed completely and further 1.5 mol $L^{-1}$ NaOH could desorb 95% of Cr(VI) and was confirmed through AAS measurement

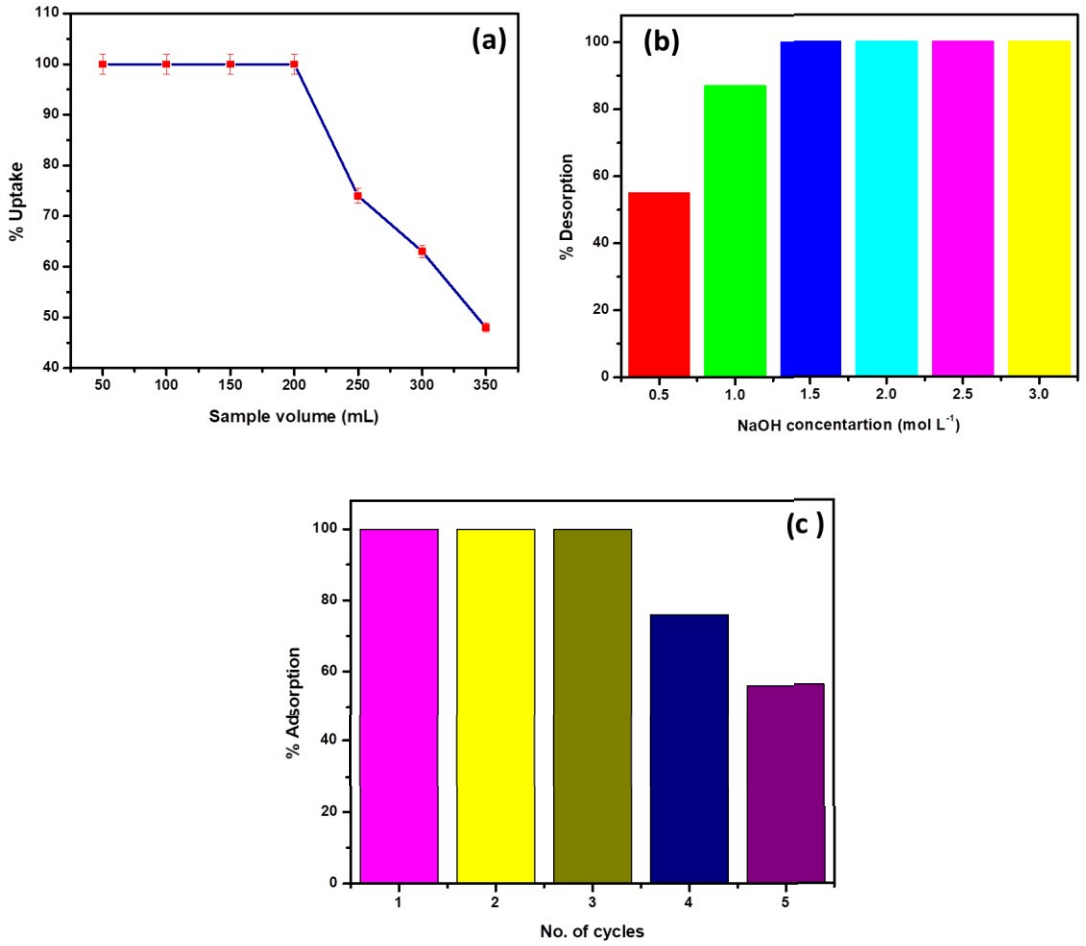


**Figure 7.10.** (a) Effect of sample volume (conditions: weight of adsorbent- 2.0 g, Cr(VI) concentration- 5 mg $L^{-1}$, pH- 4.0, flowrate- 5 mL $min^{-1}$) (b) Effect of desorbing agent on the biosorbent (c) Regeneration efficiency of the biosorbent

## 7.4. Conclusions

The proposed MOF - *Nitrosomonas* combination has highlighted the significant impact and convergence of biotechnology and a porous material to remove toxic hexavalent chromium. With the backing of sound analytical characterization techniques, the interaction of chromium with the biosorbent was well established. The porosity of metal organic framework in conjunction with the functional groups ($NH_2$, COOH, OH) on the bacterial cell surface augments the affinity between the hydrochromate anion and the biosorbent through electrostatic interaction mechanism. With a Langmuir adsorption capacity of 23.69 mg $g^{-1}$ and facile adsorption-desorption kinetics and favorable thermodynamics a removal efficiency of greater than 95% was achieved with this biosorbent. The proof of concept was validated in the removal of chromium in a certified rock phosphate sample with high efficiency. The reusability of the biosorbent was ascertained through the facile desorption using NaOH for three adsorption-desorption cycles. In principle, microbe modified MOF represents an interesting confluence of biotechnology and material science towards the development of sustainable methods for the removal of diverse pollutants from the environment.

**References**


1. Chapman, B.D.; Schleicher, M.; Beuger, A.; Gostomski, P.;. Thiele, J.H. *J Microbiol Methods*. **2006**, 65 , 96–106.
2. Chain,P.; Lamerdin,J.; Larimer, F.; Regala,W.; Lao,V.; Miriam L.; Hauser, L.; Hooper, A.; Klotz, M.; Norton, J.; Soto, L.S.; Arciero, D.; Hommes,N.; Whittaker, M.; Arp, D. *J. Bacteriol*, **2003**, 185, 2759–2773.
3. Taddei,M.; Dau, P.V.; Cohen, S.M.; Ranocchiari,M.; van Bokhoven,J.A.; Costantino, F.; Sabatini. S.; Vivani , R. *Dalton Trans*. **2015,** 44**,** 14019-14026.
4. Katz, M.J.; Brown, Z.J.; Colo´n,Y.J.; Siu, P.W.; Scheidt, K.A.; Snurr,R.Q.; Hupp, J.T.; Farha, O.K. . *Chem. Commun*., **2013**, 49, 9449.
5. El-Mehalmey, W.A.; Ibrahim, A.H.; Abugable, A.A; Hassan, M.H.; Haikal,R.R.; Karakalos, S.G.; Zakid, O.; Alkordi, M.H.; *J. Mater. Chem. A*, **2018**, 6,2742.
6. Nasrollahpour, A.; Moradi, S.E. *Microporous Mesoporous Mater*. **2017**, 243, 47-55.
7. Hovanec, T.A.; Delong, E.F. *Appl. Environ. Microbiol*. **1996**, 62, 2888–2896.
8. Sathvika, T.; Manasi; Rajesh,V.; Rajesh, N. *Chem.Eng.J*. **2015**, 279, 38-46
9. Sathvika, T.; Manasi; Rajesh,V.; Rajesh, N. *RSC Adv*. **2015**, 5, 107031-107044.
10. Arar, E.J.; Pfaff, J.D. *J. Chromatogr. A*.**1991**, 546, 335–340.
11. Luan, Y.; Qi, Y.; Gao, H.; Andriamitantso, R.S.; Zheng, N.; Wang, G. *J. Mater. Chem. A*, **2015**, 3, 17320.
12. Sadeghi,S.; Jafarzadeh, M.; Abbasi, A.R.; Daasbjerg, K. *New J.Chem*., **2017**, 41, 12014.
13. Wu, S.; Ge, Y.; Wang, Y.; Chen, X.; Li, F.; Xuan, H.; Li, X. 2017, doi.org/10.1080/09593330.2017.1344732
14. Sun, L.; Zhang, Y.; Ye, X.; Liu, H.; Zhang, H.; Wu, A.; Wu, Z. *ACS Sustainable Chem. Eng*., **2017**, 5, 7700–7708.
15. Sun, C.; Sun, L.; Sun, X.; *Ind. Eng. Chem. Res*. **2013**, 52, 14251–14260.
16. Lagergren, S. *K. Sven. Vetenskapsakad. Handl*.**1898**, 24, 1–39.
17. Ho, Y.S.; Mckay,G. *Water Res*. **2000**, 34, 735–742.
18. Yu, B.; Xu, J.; Liu, J.H.; Yang, S.T.; Luo, J.; Zhou, Q.; Wan, J.; Liao, R.; Wang, H.; Liu , Y. *J. Environ. Chem. Eng*. **2013**, 1, 1044−1050.

19. Sathvika, T.; Manasi; Rajesh,V.; Rajesh, N. *J. Environ. Chem. Eng*., **2016**, 4, 3193–3204.
20. Kumar, A.S.K.; Kalidhasan, S.; Rajesh, V.; Rajesh, N. *Ind.Eng. Chem. Res*. **2012**, 51, 58–69.

# Summary and conclusions

## 8.1. Summary and Conclusions

To combat the disadvantages of the chemically modified adsorbents there is a necessity to develop novel green methods such as microbe immobilized adsorbents for the sequestration of toxic hexavalent chromium. To accomplish this, biosorbents were developed using microbes such as *Saccharomyces cerevisiae*, *Aspergillus sp*, Arbuscular Mycorrhizal Fungal spores, *Rhizobium sp, Nitrosomonas sp* and immobilized in various supports such as cellulose, clay, carbon nanotubes and metal organic frameworks in different combinations.

The first method presented in the thesis provides an effective approach to immobilize yeast in a biodegradable cellulose polymeric support using microwave irradiation and bioremediation as a sustainable alternative to detoxify chromium. The conventional method for the preparation requires 3 hours for the immobilization of yeast. With a simple microwave oven, it requires just 200 sec for immobilizing yeast and shows a good adsorption capacity of 23.61 mg $g^{-1}$ for Cr(VI). In the range 10-30 mg $L^{-1}$ Cr(VI), yeast as such shows an average adsorption of 92.6 %, whereas glutaraldehyde cross linked cellulose immobilized with yeast gives a quantitative average adsorption value of 98.8 %. The adsorption of chromium with cellulose as such was found to be only 49.6 % and when yeast is immobilized within the biopolymer matrix the adsorption capacity of the cellulose is enhanced two fold thereby improving its metal uptake to great extent. Cr(VI) as well as Cr(III) could be removed at acidic and alkaline pH respectively. The biosorbent could be regenerated using 2.0 mol $L^{-1}$ sodium hydroxide. The negative free energy ($\Delta G$) and the enthalpy changes ($\Delta H$) confirm the spontaneous and exothermic aspects of the biosorption process. The $\Delta S$ values were also found to be negative and this shows the decreased randomness at the fungi immobilized biopolymer-solution interface. Among the various isotherms, Langmuir model gave a good fit the biosorption data with a high correlation coefficient and a statistically lower chi square value. Further, the uptake of Cr(VI) was also in accordance with the second order kinetic model. Furthermore, yeast and cellulose are non-toxic and hence this low cost blend adsorbent serves as a promising green option for chromium remediation. Quite optimistically, from the results obtained it can be concluded that this method would also enhance the potential of microwave chemistry in biosorbent preparation to detoxify various other pollutants.

The second method developed has highlighted the confluence of biotechnology and nano materials as an emerging area towards heavy metal remediation. The proposed methodology has illustrated the ability of yeast immobilized in oxidized multiwalled carbon nano tubes as effective adsorbent to sequester chromium in the +6 oxidation state. The biosorbent followed Langmuir isotherm with 31.6 mg $g^{-1}$ adsorption capacity respectively. The biosorption process was exothermic, spontaneous and pseudo second order model was effective in understanding the adsorption kinetics. The mechanism involves electrostatic interaction between the heavy metal ion and biosorbent surface. Characterization techniques confirmed the interaction of microbe and oxidized carbon nano tubes with Cr(VI). A good sample volume of synthetic waste water sample was treated in lab scale column studies which could tolerate up to 5 cycles of adsorption and desorption by regenerating the biosorbents using 1.0 mol $L^{-1}$sodium hydroxide. On an optimistic note, biotechnology and nanoscience complement each other by opening diverse possibilities in detoxifying the pollutants from industrial waste water.

The third method has illustrated the combined influence of fungi and sodium montmorillonite for the prospective removal of hexavalent chromium. The fungus was isolated from bread and the molecular biology techniques confirmed the genera to be *Aspergillus*. The use of clay as a support reinforces the interaction between the functional groups present in the cell wall of *Aspergillus* and chromium. The inorganic support imparts good stability thereby giving a high adsorption capacity of 45.72 mg $g^{-1}$. Second order model is more appropriate in describing the adsorption kinetics of chromium (VI). The thermodynamics of biosorption process indicates the spontaneous and exothermic interaction. The preliminary laboratory scale column tests have indicated the prospects of this biosorbent in the scale up operations to a higher sample volume. The ability of the biosorbent to treat industrial wastewater and the regeneration using sodium hydroxide highlights the convergence of chemistry and biotechnology in formulating sustainable solutions to address heavy metal contamination.

The *Aspergillus*- cellulose biosorbent was found to be effective for the removal of Cr(VI) both in batch and column studies with a good efficacy. The fungus immobilized in epichlorohydrin crosslinked cellulose yields a Langmuir adsorption capacity of 23.83 mg $g^{-1}$. An increase in bed height increased the adsorption capacity while an increase in flow rate and Cr(VI) concentration

reduces the adsorption efficiency. Pseudo second order model is appropriate for the thermodynamically spontaneous and exothermic adsorption process. Various column parameters were studied through the breakthrough curves and mathematical models such as Thomas, Yoon-Nelson, and BDST were applied to the system, of which BDST model was the best fit with a good adsorption capacity. The biosorbent efficiently removes Cr(VI) from synthetic waste water sample and certified industrial effluent sample. The regeneration of Cr (VI) was done using 1.5 mol $L^{-1}$ sodium hydroxide and the *Aspergillus*-cellulose combination has good ability to treat Cr(VI) contaminated waste water.

The chapter 5 involves an interesting application of fungal spores immobilized in clay for the metal removal. The isolation of Arbuscular Mycorrhizal Fungal spores is quite challenging as compared to the vegetative cells of microbes (yeast, *Aspergillus)*. Further, we found that the spores as such gave a low uptake efficiency for chromium. Yet, when it is immobilized in a suitable support such as clay there was an enhancement in the metal uptake. The developed AMF-clay biosorbent has the potential to adsorb Cr(VI) at pH 2.0-3.0 up to an extent of 78% at 5 mg $L^{-1}$ concentration. Langmuir adsorption capacity obtained was 11.185 mg $g^{-1}$ and the system kinetics followed pseudo second order by attaining equilibrium in 180 min. The immobilization of AMF spores in sodium montmorillonite enhanced the Langmuir adsorption capacity from 4.5 mg $g^{-1}$ to 11.185 mg $g^{-1}$. The exergonic system thermodynamics yields a negative entropy (-79.215 J $mol^{-1}$ $K^{-1}$) and enthalpy (-26.530 kJ $mol^{-1}$). The regeneration of the biosorbent using NaOH was facile and this AMF-clay combination would prove to be quite beneficial to adsorb hexavalent Cr from diverse matrices. However, compared to the vegetative cells of yeast or *Aspergillus* wherein there is more surface area, the AMF spores possess comparatively lesser adsorption capacity. The AMF-clay combination would certainly open the doors towards exploring other supports involving cellulose, silica or alumina as a practical approach for heavy metal remediation.

The next proposed methodology has illustrated the ability of nitrogen fixing bacteria, *Rhizobium* immobilized in oxidized multiwalled carbon nano tubes as effective adsorbent to sequester chromium in the +6 oxidation state. The microbe was isolated from soil and the microbiology and molecular biology techniques confirmed the genus to be *Rhizobium*. The biosorbent

followed Langmuir isotherm with 24.86 mg $g^{-1}$ adsorption capacity respectively. The biosorption process was exothermic, spontaneous and pseudo second order model was effective in understanding the adsorption kinetics. The mechanism involves electrostatic interaction between the heavy metal ion and biosorbent surface. Characterization techniques confirmed the interaction of microbe and oxidized carbon nano tubes with Cr(VI). A good sample volume of synthetic waste water sample was treated in lab scale column studies which could tolerate up to 4 cycles of adsorption and desorption by regenerating the biosorbents using 1.0 mol $L^{-1}$ sodium hydroxide.

The clay-Rhizobium biosorbent showed good efficacy in adsorbing Cr(VI) which is relatively economical, environmental friendly and easily degradable. The system followed pseudo second order kinetics attaining equilibrium in 180 min with a Langmuir adsorption capacity of 22.22 mg $g^{-1}$. The thermodynamics of adsorption was observed to be less random, exothermic, and spontaneous with negative entropy ($\Delta S^o$ = -65.202 J $mol^{-1}K^{-1}$ ) , enthalpy ($\Delta H^o$ = -21.705 kJ $mol^{-1}$ ) and free energy changes. The presence of Cr(VI) and Cr(III) are confirmed by XPS and confocal microscopy though Cr(VI) reduction is not instantaneous. The regeneration of the biosorbent using NaOH was up to two full cycles to a sample volume of 150 mL, promising the effective removal for Cr(VI).

The MOF - *Nitrosomonas* combination has highlighted the significant impact and convergence of biotechnology and a porous material to remove toxic hexavalent chromium. With the backing of sound analytical characterization techniques, the interaction of chromium with the biosorbent was well established. The porosity of metal organic framework in conjunction with the functional groups ($NH_2$, COOH, OH) on the bacterial cell surface augments the affinity between the hydrochromate anion and the biosorbent through electrostatic interaction mechanism. With a Langmuir adsorption capacity of 23.69 mg $g^{-1}$ and facile adsorption-desorption kinetics and favorable thermodynamics a removal efficiency of greater than 95% was achieved with this biosorbent. The proof of concept was validated in the removal of chromium in a certified rock phosphate sample with high efficiency. The reusability of the biosorbent was ascertained through the facile desorption using NaOH for three adsorption-desorption cycles. In principle, microbe modified MOF represents an interesting confluence of biotechnology and material science

towards the development of sustainable methods for the removal of diverse pollutants from the environment.

In the quest to develop the good biosorbents for removal of Cr(VI), the proposed four microbes in the work were immobilized in each of the four solid supports thereby developing a total of sixteen biosorbent combinations. Each of these possess their distinct merits with regard to the adsorption capacity, regeneration ability and scale up to larger volumes. The summary of all the developed methods is divided based on the individual microbe and its four combinations of solid supports and are tabulated in Tables 8.1- 8.4.

**8.2. Scope for future work**

The results obtained in this study offer many new and interesting possibilities for future research. Some of them are listed below:

- The developed biosorbents would open up the scope for the better selectivity and enhancement of the sequestration of chromium.
- The biosorbents developed would serve the effectiveness to adsorb the chromium in diverse industrial effluents.
- Larger volumes of metal contaminated waters could be treated by scaling up through various column modeling studies.
- With proper optimization of experimental variables, the biosorbents as a microbial consortia could also open up the possibility to sequester other toxic metal ions.

**Table 8.1.** Summary of the yeast immobilized biosorbents developed for Cr(VI) removal

| **Biosorbent** | **pH** | **Langmuir adsorption capacity (mg $g^{-1}$)** | **Kinetics** | **Thermodynamics** |
|---|---|---|---|---|
| *Saccharomyces cerevisiae*-cellulose | 2.5-3.0 | 23.61 | Pseudo second order | Exothermic, spontaneous, negative entropy |
| *Saccharomyces cerevisiae* -clay | 2.0 | 26.35 | Pseudo second order | Exothermic, spontaneous, negative entropy |
| *Saccharomyces cerevisiae* - MWCNTs | 2.0 | 31.6 | Pseudo second order | Exothermic, spontaneous, negative entropy |
| *Saccharomyces cerevisiae* - MOF | 4.0 | 34.53 | Pseudo second order | Exothermic, spontaneous, negative entropy |

**Table 8.2.** Summary of the *Aspergillus* immobilized biosorbents developed for Cr(VI) removal

| **Biosorbent** | **pH** | **Langmuir adsorption capacity (mg $g^{-1}$)** | **Kinetics** | **Thermodynamics** |
|---|---|---|---|---|
| *Aspergillus*-cellulose | 2.5-3.0 | 28.83 | Pseudo second order | Exothermic, spontaneous, negative entropy |
| *Aspergillus*-clay | 2.0 | 45.72 | Pseudo second order | Exothermic, spontaneous, negative entropy |
| *Aspergillus*-MWCNTs | 2.0 | 35.12 | Pseudo second order | Exothermic, spontaneous, negative entropy |
| *Aspergillus*-MOF | 4.0 | 40.8 | Pseudo second order | Exothermic, spontaneous, negative entropy |

**Table 8.3.** Summary of the *Rhizobium* immobilized biosorbents developed for Cr(VI) removal

| **Biosorbent** | **pH** | **Langmuir adsorption capacity (mg $g^{-1}$)** | **Kinetics** | **Thermodynamics** |
|---|---|---|---|---|
| *Rhizobium*-cellulose | 2.5-3.0 | 19.7 | Pseudo second order | Exothermic, spontaneous, negative entropy |
| *Rhizobium*-clay | 2.0 | 22.2 | Pseudo second order | Exothermic, spontaneous, negative entropy |
| *Rhizobium*-MWCNTs | 2.0 | 24.82 | Pseudo second order | Exothermic, spontaneous, negative entropy |
| *Rhizobium*-MOF | 4.0 | 26.31 | Pseudo second order | Exothermic, spontaneous, negative entropy |

**Table 8.4.** Summary of the *Nitrosomonas* immobilized biosorbents developed for Cr(VI) removal

| **Biosorbent** | **pH** | **Langmuir adsorption capacity (mg $g^{-1}$)** | **Kinetics** | **Thermodynamics** |
|---|---|---|---|---|
| *Nitrosomonas*-cellulose | 2.5-3.0 | 17.3 | Pseudo second order | Exothermic, spontaneous, negative entropy |
| *Nitrosomonas*-clay | 2.0 | 20.5 | Pseudo second order | Exothermic, spontaneous, negative entropy |
| *Nitrosomonas*-MWCNTs | 2.0 | 22.26 | Pseudo second order | Exothermic, spontaneous, negative entropy |
| *Nitrosomonas*-MOF | 4.0 | 23.67 | Pseudo second order | Exothermic, spontaneous, negative entropy |

# List of Publications

**Publications from the thesis work**

1. **T. Sathvika,** Manasi, Vidya Rajesh, N. Rajesh**, "**Microwave assisted immobilization of yeast in cellulose biopolymer as a green adsorbent for the sequestration of chromium." ***Chemical Engineering Journal*** , 279, 2015, 38 – 46.

2. **T. Sathvika,** Manasi, Vidya Rajesh, N. Rajesh, " Prospective application of *Aspergillus* sps. immobilized in sodium montmorillonite to remove toxic hexavalent chromium from waste water", ***RSC Advances***, 5, 2015, 107031 - 107044.

3. **T.Sathvika,** Manasi, Vidya Rajesh, N.Rajesh, "Adsorption of chromium supported with various column modelling studies through the synergistic influence of Aspergillus and cellulose", ***Journal of Environmental Chemical Engineering***, 4, 2016, 3193-3204.

4. **Talasila Sathvika**, Manasi Mudaliyar , Prof. Vidya Rajesh , Prof. Nagarathnam Rajesh**, "**Leveraging the potential of endomycorrhizal spores and montmorillonite for hexavalent chromium adsorption from aqueous phase", ***Chemistry Select***, 3, 2018, 2747-2755.

5**. T. Sathvika**, Amitesh Soni, Kriti Sharma, Malipeddi Praneeth, Manasi Mudaliyar, Vidya Rajesh and N. Rajesh, "Potential application of *Saccharomyces cerevisiae* and *Rhizobium* immobilized in multi walled carbon nanotubes to adsorb hexavalent chromium", ***Scientific Reports*** **(Nature publishing group)**, 8, 2018, 9862.

6. **T. Sathvika**, Smruthi Balaji, Mritunjai Chandra, Amitesh Soni, Vidya Rajesh and N. Rajesh, "A cooperative endeavor by zirconium based metal organic framework and a nitrifying bacteria, *Nitrosomomas* to remove hexavalent chromium". ***Chemical Engineering Journal***, 360, 2019, 879-889

7. **T. Sathvika,** Akhil Raj Kumar Saraswathi , Vidya Rajesh and N. Rajesh, Efficacy of Sodium Montmorillonite-*Rhizobium* combination as a prospective biosorbent to sequester hexavalent chromium. (under Review)

**Publications from other work**

8. B. ArunRaj, **T.Sathvika**, Vidya Rajesh, N.Rajesh, Removal of Europium from aqueous solution using *Saccharomyces cerevisiae* immobilized in glutaraldehyde cross-linked chitosan, ***Separation science and technology***, doi.org/10.1080/01496395.2018.1556303.

9. B.ArunRaj, **T.Sathvika**, Vidya Rajesh, N.Rajesh, Cellulose and *Saccharomyces cerevisiae* Embark To Recover Europium from Phosphor Powder, ***ACS Omega***, 2019, *4* (1), 940–952.

# Abstract presented in conferences

1**. T. Sathvika,** Vidya Rajesh, N. Rajesh, " A novel fungal biopolymer combination as an adsorbent for effective removal of hexavalent chromium ", International conference on Frontiers in Biological Sciences, NIT, Rourkela, 22$^{nd}$ - 24$^{th}$ January, 2015.

2. **T. Sathvika**, S. Akhil, Manasi, Vidya Rajesh, N. Rajesh, " A symbiotic nitrogen fixer immobilized in sodium montmorillonite for the effective sequestration of chromium from waste water", Nascent Development in Chemical Sciences - NDCS 2015, BITS, Pilani, Pilani Campus, Rajasthan, 16$^{th}$ - 18$^{th}$ October, 2015.

3. **T. Sathvika**, Manasi, Vidya Rajesh, N. Rajesh, "Rhizobium sps. immobilized in multi walled carbon nanotubes (MWCNT) for the effective adsorption of chromium", NFCFA, BITS, Pilani - Goa campus, 18$^{th}$ - 19$^{th}$ December, 2015.

4. **T. Sathvika**, S. Akhil, Manasi, Vidya Rajesh, N. Rajesh, " Nitrogen fixing bacteria (Rhizobium) immobilized in clay as a sustainable option for the removal of hexavalent chromium from waste water", ICMG, IISc, Bangalore, 17th Feb - 20th Feb, 2016.

5. **T. Sathvika**, Amitesh Soni, Kriti Sharma, Manasi, Vidya Rajesh, N. Rajesh, "Synergistic effect of nitrogen fixing bacteria immobilized in a carbonaceous material (MWCNT) for the sequestration of hexavalent chromium", 5th Symposium on advanced Biological Inorganic Chemistry, Kolkata, January 7$^{th}$ - 11$^{th}$, 2017.

6. **T.Sathvika**, Vidya Rajesh, N.Rajesh, "Yeast immobilized in carbon nanotubes for the effective removal of Cr(VI) from aqueous medium", Indian Analytical Science Congress, Kerala chapter, February, 8$^{th}$- 10$^{th}$ , 2018.

## BIOGRAPHY OF Prof. N. RAJESH

**Prof. N. Rajesh,** Department of Chemistry, Birla Institute of Technology and Science, Pilani, Hyderabad Campus, India obtained his Master's degree and Ph.D from Indian Institute of Technology (IIT), Madras, India. He is involved in teaching and research over the past 20 years. He is a fellow member of the Royal Society of Chemistry (FRSC) London. His research interests include development of greener sorbents for the effective detoxification of heavy metals and other pollutants from industrial effluents. He has several research publications in peer reviewed journals and is also an expert reviewer for various international journals. He has been recognized by Elsevier as an outstanding reviewer for 2017 for his reviewing contributions to the Journal of Hazardous Materials and Ultrasonics Sonochemistry. Currently, his group is engaged in the development of novel biopolymer, graphene and clay based sorbents for heavy metal remediation. He has research collaborations with Prof. Ranjit Koodali, Department of Chemistry, University of South Dakota, USA. He is a member of American Chemical Society (ACS), American Association for Advancement of Science (AAAS) and a life member of Chemical Research Society of India (CRSI), Association of Separation Scientists and Technologists (ASSET), India, Indian Council of Chemists and Indian Science Congress (ISC). He has successfully completed projects sponsored by UGC and DST, India.

## Biography of Prof. Vidya Rajesh

**Dr. Vidya Rajesh** is a Professor in the Department of Biological Sciences. She is also Associate Dean of Faculty Affairs of BITS, Pilani – Hyderabad Campus. Prof. Vidya Rajesh completed her M. Sc. in Microbiology from Nagpur University in the year 1995. She completed her M. E. in Biotechnology (2000) and Ph. D from BITS, Pilani – Pilani campus in the year 2007. The topic of her doctoral thesis was *"Studies on Sequence Diversity and Characterization of the Apical Membrane Antigen of Plasmodium in Indian Isolates".* Prof. Vidya Rajesh is an extremely dedicated and hard core team player with commitment to teaching and research. She has been actively involved and has gained 17 yrs of teaching, research and administrative experience during her tenure in various capacities at BITS. Her primary research interest is in the area of molecular genetics of human diseases. As a collaborative researcher with Prof. N. Rajesh of Department of Chemistry, her interest has expanded to microbe based heavy metal remediation. She has over 35 research publications and equal number of conference presentations. She has

completed three research projects as principal investigator and has an ongoing DST project as an investigator and co-investigator. She has extended her work by focusing on projects like Thyroid receptor mutations in Autism and analysis of urinary biomarkers in autistic patients. Prof. Vidya Rajesh is also part of other institutional projects like DST – FIST , DST – TBI and BITS-IOE at BITS, Pilani – Hyderabad campus.

**BIOGRAPHY OF Ms. SATHVIKA T.**

**Ms. Sathvika** completed her Master's (M.Sc.) in Analytical chemistry at Jawaharlal Nehru Technological University, Hyderabad India in 2011 and started her research career as Graduate Trainee at ARCI, Hyderabad India. She joined as a DST project fellow in the Department of Chemistry at BITS Pilani, Hyderabad campus, India. She is well versed in analytical procedures involving IC, GC, AAS, FTIR, HPLC and has good knowledge in microbiology and molecular biology techniques. She has good number of publications to her credit and has presented her work in several national and international conferences. She has been awarded the best poster award at ISAS Kerala chapter in the year 2018. Currently, her research interests focus on the immobilization of microbes in suitable matrices for the sequestration of chromium.

# Immobilization of Microorganisms in Suitable Matrices for the Sequestration of Chromium from Industrial Effluents

## THESIS

Submitted in partial fulfillment of

the requirements for the degree of

**DOCTOR OF PHILOSOPHY**

by

**SATHVIKA T**

**ID. No: 2013PHXF0406H**

Under the Supervision of

**Prof. N. RAJESH**

Department of Chemistry

&

**Prof. VIDYA RAJESH**

Department of Biological Sciences


**BIRLA INSTITUTE OF TECHNOLOGY AND SCIENCE, PILANI**

**Hyderabad Campus, Hyderabad, INDIA**

**2018**

## 8.1. Summary and Conclusions

To combat the disadvantages of the chemically modified adsorbents there is a necessity to develop novel green methods such as microbe immobilized adsorbents for the sequestration of toxic hexavalent chromium. To accomplish this, biosorbents were developed using microbes such as *Saccharomyces cerevisiae*, *Aspergillus sp*, Arbuscular Mycorrhizal Fungal spores, *Rhizobium sp, Nitrosomonas sp* and immobilized in various supports such as cellulose, clay, carbon nanotubes and metal organic frameworks in different combinations.

The first method presented in the thesis provides an effective approach to immobilize yeast in a biodegradable cellulose polymeric support using microwave irradiation and bioremediation as a sustainable alternative to detoxify chromium. The conventional method for the preparation requires 3 hours for the immobilization of yeast. With a simple microwave oven, it requires just 200 sec for immobilizing yeast and shows a good adsorption capacity of 23.61 mg $g^{-1}$ for Cr(VI). In the range 10-30 mg $L^{-1}$ Cr(VI), yeast as such shows an average adsorption of 92.6 %, whereas glutaraldehyde cross linked cellulose immobilized with yeast gives a quantitative average adsorption value of 98.8 %. The adsorption of chromium with cellulose as such was found to be only 49.6 % and when yeast is immobilized within the biopolymer matrix the adsorption capacity of the cellulose is enhanced two fold thereby improving its metal uptake to great extent. Cr(VI) as well as Cr(III) could be removed at acidic and alkaline pH respectively. The biosorbent could be regenerated using 2.0 mol $L^{-1}$ sodium hydroxide. The negative free energy ($\Delta G$) and the enthalpy changes ($\Delta H$) confirm the spontaneous and exothermic aspects of the biosorption process. The $\Delta S$ values were also found to be negative and this shows the decreased randomness at the fungi immobilized biopolymer-solution interface. Among the various isotherms, Langmuir model gave a good fit the biosorption data with a high correlation coefficient and a statistically lower chi square value. Further, the uptake of Cr(VI) was also in accordance with the second order kinetic model. Furthermore, yeast and cellulose are non-toxic and hence this low cost blend adsorbent serves as a promising green option for chromium remediation. Quite optimistically, from the results obtained it can be concluded that this method would also enhance the potential of microwave chemistry in biosorbent preparation to detoxify various other pollutants.

The second method developed has highlighted the confluence of biotechnology and nano materials as an emerging area towards heavy metal remediation. The proposed methodology has illustrated the ability of yeast immobilized in oxidized multiwalled carbon nano tubes as effective adsorbent to sequester chromium in the +6 oxidation state. The biosorbent followed Langmuir isotherm with 31.6 mg $g^{-1}$ adsorption capacity respectively. The biosorption process was exothermic, spontaneous and pseudo second order model was effective in understanding the adsorption kinetics. The mechanism involves electrostatic interaction between the heavy metal ion and biosorbent surface. Characterization techniques confirmed the interaction of microbe and oxidized carbon nano tubes with Cr(VI). A good sample volume of synthetic waste water sample was treated in lab scale column studies which could tolerate up to 5 cycles of adsorption and desorption by regenerating the biosorbents using 1.0 mol $L^{-1}$sodium hydroxide. On an optimistic note, biotechnology and nanoscience complement each other by opening diverse possibilities in detoxifying the pollutants from industrial waste water.

The third method has illustrated the combined influence of fungi and sodium montmorillonite for the prospective removal of hexavalent chromium. The fungus was isolated from bread and the molecular biology techniques confirmed the genera to be *Aspergillus*. The use of clay as a support reinforces the interaction between the functional groups present in the cell wall of *Aspergillus* and chromium. The inorganic support imparts good stability thereby giving a high adsorption capacity of 45.72 mg $g^{-1}$. Second order model is more appropriate in describing the adsorption kinetics of chromium (VI). The thermodynamics of biosorption process indicates the spontaneous and exothermic interaction. The preliminary laboratory scale column tests have indicated the prospects of this biosorbent in the scale up operations to a higher sample volume. The ability of the biosorbent to treat industrial wastewater and the regeneration using sodium hydroxide highlights the convergence of chemistry and biotechnology in formulating sustainable solutions to address heavy metal contamination.

The *Aspergillus*- cellulose biosorbent was found to be effective for the removal of Cr(VI) both in batch and column studies with a good efficacy. The fungus immobilized in epichlorohydrin crosslinked cellulose yields a Langmuir adsorption capacity of 23.83 mg $g^{-1}$. An increase in bed height increased the adsorption capacity while an increase in flow rate and Cr(VI) concentration

reduces the adsorption efficiency. Pseudo second order model is appropriate for the thermodynamically spontaneous and exothermic adsorption process. Various column parameters were studied through the breakthrough curves and mathematical models such as Thomas, Yoon-Nelson, and BDST were applied to the system, of which BDST model was the best fit with a good adsorption capacity. The biosorbent efficiently removes Cr(VI) from synthetic waste water sample and certified industrial effluent sample. The regeneration of Cr (VI) was done using 1.5 mol $L^{-1}$ sodium hydroxide and the *Aspergillus*-cellulose combination has good ability to treat Cr(VI) contaminated waste water.

The chapter 5 involves an interesting application of fungal spores immobilized in clay for the metal removal. The isolation of Arbuscular Mycorrhizal Fungal spores is quite challenging as compared to the vegetative cells of microbes (yeast, *Aspergillus).* Further, we found that the spores as such gave a low uptake efficiency for chromium. Yet, when it is immobilized in a suitable support such as clay there was an enhancement in the metal uptake. The developed AMF-clay biosorbent has the potential to adsorb Cr(VI) at pH 2.0-3.0 up to an extent of 78% at 5 mg $L^{-1}$ concentration. Langmuir adsorption capacity obtained was 11.185 mg $g^{-1}$ and the system kinetics followed pseudo second order by attaining equilibrium in 180 min. The immobilization of AMF spores in sodium montmorillonite enhanced the Langmuir adsorption capacity from 4.5 mg $g^{-1}$ to 11.185 mg $g^{-1}$. The exergonic system thermodynamics yields a negative entropy (-79.215 J $mol^{-1}$ $K^{-1}$) and enthalpy (-26.530 kJ $mol^{-1}$). The regeneration of the biosorbent using NaOH was facile and this AMF-clay combination would prove to be quite beneficial to adsorb hexavalent Cr from diverse matrices. However, compared to the vegetative cells of yeast or *Aspergillus* wherein there is more surface area, the AMF spores possess comparatively lesser adsorption capacity. The AMF-clay combination would certainly open the doors towards exploring other supports involving cellulose, silica or alumina as a practical approach for heavy metal remediation.

The next proposed methodology has illustrated the ability of nitrogen fixing bacteria, *Rhizobium* immobilized in oxidized multiwalled carbon nano tubes as effective adsorbent to sequester chromium in the +6 oxidation state. The microbe was isolated from soil and the microbiology and molecular biology techniques confirmed the genus to be *Rhizobium*. The biosorbent

followed Langmuir isotherm with 24.86 mg $g^{-1}$ adsorption capacity respectively. The biosorption process was exothermic, spontaneous and pseudo second order model was effective in understanding the adsorption kinetics. The mechanism involves electrostatic interaction between the heavy metal ion and biosorbent surface. Characterization techniques confirmed the interaction of microbe and oxidized carbon nano tubes with Cr(VI). A good sample volume of synthetic waste water sample was treated in lab scale column studies which could tolerate up to 4 cycles of adsorption and desorption by regenerating the biosorbents using 1.0 mol $L^{-1}$ sodium hydroxide.

The clay-Rhizobium biosorbent showed good efficacy in adsorbing Cr(VI) which is relatively economical, environmental friendly and easily degradable. The system followed pseudo second order kinetics attaining equilibrium in 180 min with a Langmuir adsorption capacity of 22.22 mg $g^{-1}$. The thermodynamics of adsorption was observed to be less random, exothermic, and spontaneous with negative entropy ($\Delta S^o$ = -65.202 J $mol^{-1}K^{-1}$ ) , enthalpy ($\Delta H^o$ = -21.705 kJ $mol^{-1}$ ) and free energy changes. The presence of Cr(VI) and Cr(III) are confirmed by XPS and confocal microscopy though Cr(VI) reduction is not instantaneous. The regeneration of the biosorbent using NaOH was up to two full cycles to a sample volume of 150 mL, promising the effective removal for Cr(VI).

The MOF - *Nitrosomonas* combination has highlighted the significant impact and convergence of biotechnology and a porous material to remove toxic hexavalent chromium. With the backing of sound analytical characterization techniques, the interaction of chromium with the biosorbent was well established. The porosity of metal organic framework in conjunction with the functional groups ($NH_2$, COOH, OH) on the bacterial cell surface augments the affinity between the hydrochromate anion and the biosorbent through electrostatic interaction mechanism. With a Langmuir adsorption capacity of 23.69 mg $g^{-1}$ and facile adsorption-desorption kinetics and favorable thermodynamics a removal efficiency of greater than 95% was achieved with this biosorbent. The proof of concept was validated in the removal of chromium in a certified rock phosphate sample with high efficiency. The reusability of the biosorbent was ascertained through the facile desorption using NaOH for three adsorption-desorption cycles. In principle, microbe modified MOF represents an interesting confluence of biotechnology and material science

towards the development of sustainable methods for the removal of diverse pollutants from the environment.

In the quest to develop the good biosorbents for removal of Cr(VI), the proposed four microbes in the work were immobilized in each of the four solid supports thereby developing a total of sixteen biosorbent combinations. Each of these possess their distinct merits with regard to the adsorption capacity, regeneration ability and scale up to larger volumes. The summary of all the developed methods is divided based on the individual microbe and its four combinations of solid supports and are tabulated in Tables 8.1- 8.4.

**8.2. Scope for future work**

The results obtained in this study offer many new and interesting possibilities for future research. Some of them are listed below:

- The developed biosorbents would open up the scope for the better selectivity and enhancement of the sequestration of chromium.
- The biosorbents developed would serve the effectiveness to adsorb the chromium in diverse industrial effluents.
- Larger volumes of metal contaminated waters could be treated by scaling up through various column modeling studies.
- With proper optimization of experimental variables, the biosorbents as a microbial consortia could also open up the possibility to sequester other toxic metal ions.

**Table 8.1.** Summary of the yeast immobilized biosorbents developed for Cr(VI) removal

| **Biosorbent** | **pH** | **Langmuir adsorption capacity (mg $g^{-1}$)** | **Kinetics** | **Thermodynamics** |
|---|---|---|---|---|
| *Saccharomyces cerevisiae*-cellulose | 2.5-3.0 | 23.61 | Pseudo second order | Exothermic, spontaneous, negative entropy |
| *Saccharomyces cerevisiae* -clay | 2.0 | 26.35 | Pseudo second order | Exothermic, spontaneous, negative entropy |
| *Saccharomyces cerevisiae* - MWCNTs | 2.0 | 31.6 | Pseudo second order | Exothermic, spontaneous, negative entropy |
| *Saccharomyces cerevisiae* - MOF | 4.0 | 34.53 | Pseudo second order | Exothermic, spontaneous, negative entropy |

**Table 8.2.** Summary of the *Aspergillus* immobilized biosorbents developed for Cr(VI) removal

| **Biosorbent** | **pH** | **Langmuir adsorption capacity (mg $g^{-1}$)** | **Kinetics** | **Thermodynamics** |
|---|---|---|---|---|
| *Aspergillus*-cellulose | 2.5-3.0 | 28.83 | Pseudo second order | Exothermic, spontaneous, negative entropy |
| *Aspergillus*-clay | 2.0 | 45.72 | Pseudo second order | Exothermic, spontaneous, negative entropy |
| *Aspergillus*-MWCNTs | 2.0 | 35.12 | Pseudo second order | Exothermic, spontaneous, negative entropy |
| *Aspergillus*-MOF | 4.0 | 40.8 | Pseudo second order | Exothermic, spontaneous, negative entropy |

**Table 8.3.** Summary of the *Rhizobium* immobilized biosorbents developed for Cr(VI) removal

| **Biosorbent** | **pH** | **Langmuir adsorption capacity (mg $g^{-1}$)** | **Kinetics** | **Thermodynamics** |
|---|---|---|---|---|
| *Rhizobium*-cellulose | 2.5-3.0 | 19.7 | Pseudo second order | Exothermic, spontaneous, negative entropy |
| *Rhizobium*-clay | 2.0 | 22.2 | Pseudo second order | Exothermic, spontaneous, negative entropy |
| *Rhizobium*-MWCNTs | 2.0 | 24.82 | Pseudo second order | Exothermic, spontaneous, negative entropy |
| *Rhizobium*-MOF | 4.0 | 26.31 | Pseudo second order | Exothermic, spontaneous, negative entropy |

**Table 8.4.** Summary of the *Nitrosomonas* immobilized biosorbents developed for Cr(VI) removal

| **Biosorbent** | **pH** | **Langmuir adsorption capacity (mg $g^{-1}$)** | **Kinetics** | **Thermodynamics** |
|---|---|---|---|---|
| *Nitrosomonas*-cellulose | 2.5-3.0 | 17.3 | Pseudo second order | Exothermic, spontaneous, negative entropy |
| *Nitrosomonas*-clay | 2.0 | 20.5 | Pseudo second order | Exothermic, spontaneous, negative entropy |
| *Nitrosomonas*-MWCNTs | 2.0 | 22.26 | Pseudo second order | Exothermic, spontaneous, negative entropy |
| *Nitrosomonas*-MOF | 4.0 | 23.67 | Pseudo second order | Exothermic, spontaneous, negative entropy |